# Characterization of a key signal transduction pathway involved in virulence regulation in *Pseudomonas aeruginosa*

by

## Anjali Y. Bhagirath

A Thesis submitted to the Faculty of Graduate Studies of

The University of Manitoba

In partial fulfillment of the requirements for the degree of

## Doctor of Philosophy

Department of Oral Biology

Faculty of Dentistry

University of Manitoba

Winnipeg, Manitoba, Canada

i

# ABSTRACT

*Pseudomonas aeruginosa* is the leading cause of morbidity and mortality in patients with chronic diseases, neutropenia and those with immunocompromise. Pulmonary infection with *P. aeruginosa* in patients with cystic fibrosis can result in respiratory failure and death.

The pathogenesis of *P. aeruginosa* involves a lifestyle change in the bacterium and depends on coordination between two-component regulatory systems, quorum sensing systems and signaling via small molecules such as bis-(3'-5')-cyclic dimeric guanosine monophosphate (c-di-GMP). Acute form of *P. aeruginosa* infection is characterized by motility and host-directed toxicity by Type Three Secretion System (T3SS). On the other hand, chronic infection is characterized by formation of biofilms. These biofilms are highly resistant to external stressors and play a role in bacterial persistence. RetS-GacS/A-PA1611-RsmA/Y/Z is a key regulatory pathway in *P. aeruginosa* that determines the bacterium's lifestyle choice. Previously, PA1611 a hybrid sensor kinase was identified as a new player in this pathway that functions independent of phosphorelay and influences biofilm formation and T3SS. However, the exact nature of its interaction, the regulation and the environmental signals that activate PA1611 are still unexplored.

In this study, using advanced molecular methods, the structural and mechanistic basis of the interaction between PA1611 and RetS is examined in *P. aeruginosa* PAO1. The histidine kinase A and histidine kinase-like ATPase domains of PA1611 are found to play crucial roles in the PA1611–RetS interaction and have been shown to exert profound effect on bacterial phenotypes. *cmpX* (PA1775) was identified as the regulator of PA1611. A *cmpX* knockout demonstrated higher biofilm formation, downregulation of the T3SS and elevated intracellular c-di-GMP levels. *cmpX* was also identified to exert its effects via both the RetS-GacS/A-PA1611-RsmA/Y/Z as well as via activated

c-di-GMP signaling.  Finally, mucin and anoxia were identified as activators of PA1611 expression as well as shown to facilitate biofilm formation in PAK strain of *P. aeruginosa*.

Collectively, these findings provide a significant and complex role for PA1611 in *P. aeruginosa* virulence. Understanding TCS function and the environmental signals that they respond to are key to controlling infections with *P. aeruginosa* and eventually improving disease outcomes.

## ACKNOWLEDGEMENTS

# DEDICATIONS

*To you…who I could not say good bye*

*God called you too soon, too young,*

*maybe you were needed more somewhere else*

*I will meet you again on the other side*

*Until then, this big empty black space of pain and guilt that's my place to be now*

*Forgive me, for I could not be there to hold you one last time*

## LIST OF MANUSCRIPT PUBLISHED OR IN PREPARATION

**Thesis relevant publications**

Bhagirath AY, Somayajula D, Li Y, Duan K. (2017) CmpX in *Pseudomonas aeruginosa* through the Gac/Rsm signaling pathway and by modulating c-di-GMP levels. The Journal of Membrane Biology DOI: 10.1007/s00232-017-9994-6

Bhagirath AY, Pydi SP, Li Y, Lin C, Kong W, Chelikani P, Duan K. (2017) Characterization of the direct interaction between hybrid sensor kinases PA1611 and RetS that controls biofilm formation and the type III secretion system in *Pseudomonas aeruginosa*. ACS Infectious Diseases; 3(2):162-175

Bhagirath AY, Li Y, Somayajula D, Dadashi M, Badr S, Duan K. (2016) Cystic fibrosis lung environment and *Pseudomonas aeruginosa* infection. BMC Pulmonary Medicine;16. (1):174

**Manuscripts in preparation**

Bhagirath AY, Patidar R, Kumar A, Duan K. Role of two component regulatory proteins in antimicrobial resistance of key gram-negative pathogens.

Bhagirath AY, Li Y, Duan K. Mucin and oxygen limitation activate PA1611 and facilitate biofilm formation in *P. aeruginosa* PAK.

**TABLE OF CONTENTS**

**Contents**        **Page number**

# LIST OF FIGURES

# LIST OF TABLES

# LIST OF COPYRIGHTED MATERIAL FOR WHICH PERMISSION WAS OBTAINED

**Chapter 1: Introduction**

**Cystic fibrosis lung environment and *Pseudomonas aeruginosa* infection**

Reprinted with permission from *BMC Pulmonary Medicine*, 2016. 16(1):174

BioMed Central Ltd.  (Creative Commons-CCBY) by Springer Nature

**Chapter 3: Characterization of the direct interaction between hybrid sensor kinases PA1611 and RetS that controls biofilm formation and the type III secretion system in *P. aeruginosa***

Reprinted with permission from *ACS Infectious diseases* 2017. 3(2):162-175.

©American Chemical Society

**Chapter 4: CmpX affects virulence in *P. aeruginosa* through the Gac/Rsm signaling pathway and by modulating c-di-GMP levels**

Reprinted with permission from the *Journal of membrane Biology,*

Oct 2017, DOI: 10.1007/s00232-017-9994-6. *License number-* 4293300368375, © by Springer Nature

# LIST OF ABBREVIATIONS

| | |
|---|---|
| Adenosine Triphosphate | ATP |
| Airway Surface Liquid Layer | ASL |
| 3-Amino-1,2,4-Triazole | 3-AT |
| Artificial Sputum Medium | ASM |
| Bacterial Two-Hybrid Assays | BTH |
| Bis-(3´-5´)-Cyclic Dimeric Guanosine Monophosphate | C-di-GMP |
| 2,2′-Bipyridyl | BIP |
| Cystic Fibrosis Inhibitory Factor | Cif |
| Colony Forming Units | CFU |
| Counts Per Second | Cps |
| Complementary DNA | cDNA |
| Cystic Fibrosis | CF |
| Cystic Fibrosis Transmembrane Conductance Regulator | CFTR |
| Cyclic Adenosine Monophosphate | cAMP |
| Diethylene Triamine Pentaacetic Acid | DTPA |
| Ethylenediaminetetraacetic Acid | EDTA |

| | |
|---|---|
| Ethylene Glycol-Bis (β-aminoethyl ether)-N,N,N',N'-Tetraacetic acid | EGTA |
| Glutathione | GSH |
| Granulocyte Macrophage Colony Stimulating Factor | GM-CSF |
| Green Fluorescent Protein | GFP |
| Histidine Kinase | HK |
| Histidyl-Aspartyl Phosphorelay | HAP |
| Histidine Phosphotransfer Protein | Hpt |
| 4-(2-Hydroxyethyl)-1-Piperazineethanesulfonic acid | HEPES |
| Hybrid Histidine Kinase | HHK |
| HisK–Adenylyl Cyclase-Methyl-Accepting Protein-Phosphatase | HAMP |
| Histidine Kinase-Like ATPase | HATPase |
| Interleukin-8 | IL-8 |
| Isopropyl β-D-1-Thiogalactopyranoside | IPTG |
| Lipopolysaccharide | LPS |
| Lysogeny Broth | LB |
| Major Histocompatibility Complex | MHC |
| Minimum Inhibitory Concentration | MIC |

Modified Artificial Cystic Fibrosis Sputum Media                    ASMDM

Multiple Cloning Site                    MCS

Multidrug Resistant                    MDR

Myeloid-Derived Suppressor Cells                    MDSCs

Neutrophil Extracellular Traps                    NETs

Nod-Like Receptors                    NLRs

NLR Family Apoptosis Inhibitory Protein                    NAIP

NLR Family Caspase Recruitment Domains Containing Protein 4                    NLRC4

Nitrate Reductase                    NR

Optical Density                    OD

Ortho-Nitrophenyl-β-Galactoside                    ONPG

Pathogen-Associated Molecular Patterns                    PAMPs

Polymorphonuclear Neutrophils                    PMNs

Polymerase Chain Reaction                    PCR

Polymorphonuclear Neutrophils                    PMN

Porcine Gastric Mucin                    PGM

Phosphate Buffered Saline                    PBS

| | |
|---|---|
| Pseudomonas Isolation Agar | PIA |
| Quantitative Real-Time Polymerase Chain Reaction | qPCR |
| Reactive Oxygen Species | ROS |
| Reverse-Transcriptase Polymerase Chain Reaction | RT-PCR |
| Resistance-Nodulation-Cell Division | RND |
| Response Regulator | RR |
| Relative Fluorescence Unit | RFU |
| Relative Luminescence Unit | RLU |
| RNA Polymerase | RNAP |
| Sensor Kinase | SK |
| Site Directed Mutagenesis | SDM |
| Signal Receiver Domain | REC |
| Sodium Dodecyl Sulfate Polyacrylamide Gel Electrophoresis | SDS-PAGE |
| Sputum Club Cell Secretory Proteins | CCSPs |
| Thiocyanate | $SCN^-$ |
| Toll-Like Receptor | TLR |
| Transmembrane | TM |

## 1.0 Introduction

### 1.1 *Pseudomonas aeruginosa* in chronic diseases

*Pseudomonas* spp. are gram-negative bacteria found ubiquitously within the environment. *Pseudomonas aeruginosa* is the most clinically significant member of this family. *P. aeruginosa* can cause life-threatening nosocomial infections in immunocompromised individuals and those with trauma and severe burns. It also a leading cause of infections in ventilator-associated pneumonia and Cystic fibrosis (CF). Hospital-acquired *P. aeruginosa* infections are now considered a worldwide healthcare issue as per the International Nosocomial Infection Control Consortium report in 2016 (Rosenthal et al., 2016). The rising incidence of multi-drug resistance among *P. aeruginosa* has added significantly to the global socio-economic burden. Treatment of *P. aeruginosa* can be challenging due to it's intrinsic resistant to a host of antimicrobials as well as the rapid acquisition of exogenous genes resulting in the emergence of multidrug-resistant forms (MDR). Antibiotic treatment also allows for selective expansion of specific resistant strains by substitution and acquisition of resistant genes, further complicating treatment (Vasse et al., 2017). The link between multi-drug resistance and pathogen virulence is now well established (Geisinger & Isberg, 2017). Thus, it is critical to understand the virulence mechanisms in *P. aeruginosa* to better inform new research and to design newer and more specific therapeutics.

### 1.1.1 Global virulence regulatory mechanisms in *P. aeruginosa*

The adaptability and versatility of *P. aeruginosa* is attributed to its genome. Compared with most other bacteria, Pseudomonas has a relatively large genome, ranging from 6.22 to 6.91 Mb (Silby et al., 2011). The genome of *P. aeruginosa* is described as having a 'core' genome containing a conserved set of genes common to the species making up 90% of the total, interspersed by

'regions of genomic plasticity' that contain genes unique to each strain (Mathee et al., 2008). When coupled with the high physiologic and functional diversity displayed by *P. aeruginosa*, it is possible that such a highly evolved genome of the *P. aeruginosa* genome arose from selective pressure for environmental adaptability. In *P. aeruginosa* PAO1 alone 521 genes are predicted to encode for regulatory proteins comprising nearly 10% of its genome (Stover et al., 2000), a significantly higher number than bacteria with smaller genomes.

At initial stages of host infection, the large array of virulence and intrinsic antibiotic resistance mechanisms mediate survival. After initial infection, *P. aeruginosa* are exposed to the host's inflammatory responses including oxidative stress followed by treatment with antibiotics. These induce the expression of different sets of genes enabling *P. aeruginosa* to adapt and switch to persistent and resistant phenotypes while becoming less virulent.

Infection by *P. aeruginosa* in a host is two-phased; An acute phase characterized by planktonic form, motility and toxin production and second, a more sessile chronic phase characterized by exopolysaccharide production and formation of "Biofilms." Biofilms are an important clinical concern due to their tenacious nature and resilience to external stressors. *P. aeruginosa* biofilms are detrimental in conditions where the host immune response is compromised and can lead to significant morbidity and mortality in such vulnerable hosts. The switch between acute forms and biofilm formation in *P. aeruginosa* involves genotypic and phenotypic changes in the bacterium such as increased antibiotic resistance, decreased metabolism, and slower growth rate, lack of motility, quorum sensing and overproduction of alginate.

The phenotypic changes in *P. aeruginosa* are subject to sensing extrinsic environment such as availability of nutrients, pH, temperature, antibiotic stress, etc. and mediating a suitable response via tightly regulated gene expression. The key mechanisms that regulate the response to an

2

external stressor mainly involve regulation by quorum sensing (QS), Two-component regulatory systems (TCS) and signaling via bis-(3'-5')-cyclic dimeric guanosine monophosphate (c-di-GMP). Though in isolation these systems indeed exert significant control over virulence in *P. aeruginosa,* an interplay of these factors is essential for the growth and survival under stressful conditions.

Quorum sensing in *P. aeruginosa* involves production and release of chemical signals outside the cells. When the external signal concentration reaches a threshold, transcriptional activation or repression of target genes is induced inside the cells (Fuqua et al., 1994). Diffusion rate and spatial distribution of signaling molecules are identified as key determinants to the mechanism of quorum sensing and therefore terms such as "diffusion sensing," "efficiency sensing" and "combinatorial quorum sensing" have been coined (Cornforth et al., 2014; Hense et al., 2007; Redfield, 2002). In *P. aeruginosa* the Las and Rhl systems lie at the center of QS circuitry and control several key physiological processes and virulence phenotypes (Schuster & Greenberg, 2006). Quinolone based signaling (PQS) is identified as the third mechanism for QS. PQS was initially described by Pesci and co-workers in 1999 as an antibacterial molecule, which caused dramatic induction of *lasB* in a *lasR* mutant of *P. aeruginosa* which could not be mimicked by homoserine lactones (HSLs). A fourth system was identified as an integrated quorum sensing system (IQS), shown to "integrate" environmental stress signals with other QS systems (J. Lee et al., 2013). IQS has been shown to be 2-(2-hydroxyphenyl)-thiazole-4-carbaldehyde encoded by non-ribosomal peptide synthase gene cluster *ambBCDE*. The emergence of IQS at least partially explains the quorum sensing mechanisms in clinical isolates with mutated LasI/R genes (Ciofu et al., 2010; L. R. Hoffman et al., 2009). These different quorum sensing pathways are organized in a hierarchy and serve to compensate in case one of them is switched off. The lasI/R system is

at the top which is activated by HSLs and further activates *rhlI/R* and lasI as a positive feedback loop (Ventre et al., 2003). LasI/R activates the *pqsABCD* operon to increase PQS biosynthesis. PQS, in turn, enhances the expression of the Rhl QS system. LasI/R was also shown to exert control over the IQS system (J. Lee et al., 2013).

Two-component regulatory systems (TCSs) in *P. aeruginosa* are key to sensing the external environment and facilitate bacterial survival in various microenvironments. *P. aeruginosa* exhibits considerable nutritional and metabolic versatility explaining the large set of signal transduction systems encoded by its genome. TCSs regulate a wide variety of cellular functions in Pseudomonas in response to environmental signals such as; pili production (PilG/PilH), nitrate metabolism (NarX/NarL), alginate production (AlgZ/AlgR), iron acquisition (PfeS/PfeR), phosphate regulation (Pho), adhesion (FleS/FleR), toxin secretion (GacS/GacA) and chemotaxis (CheA/CheY) (Ma et al., 1997; Rodrigue et al., 2000).

Bis-(3'-5')-cyclic dimeric guanosine monophosphate (c-di-GMP) has gained attention in recent years due to its key role in virulence regulation as well as its involvement in several other regulatory pathways in *P. aeruginosa*. The metabolism of c-di-GMP is regulated by the activity of Diguanylate Cyclases (DGCs) and Phosphodiesterases (PDEs). DGCs carry a conserved GGDEF domain and synthesize c-di-GMP from two molecules of GTP. PDEs degrade c-di-GMP. PDEs are classified into two families; those with an EAL domain degrade c-di-GMP to produce pGpGs, and proteins with an HD-GYP domain generate two molecules of GMP. C-di-GMP has been shown to play a key role in switch between planktonic to biofilm lifestyle (Ha & O'Toole, 2015; Valentini & Filloux, 2016) by regulating flagellar rotation (Baraquet & Harwood, 2013; Toutain et al., 2007), type IV pili retraction (Barken et al., 2008; Jin et al., 2011),

exopolysaccharide production (C. D. Boyd & O'Toole, 2012; M. Merighi et al., 2007), antimicrobial resistance (Petrova et al., 2017), and biofilm dispersal (An et al., 2010).

C-di-GMP signaling in *P. aeruginosa* mediates the switch between planktonic to biofilm states via the Gac/Rsm TCS (Moscoso et al., 2011; Moscoso et al., 2014). C-di-GMP signaling also intersects with the SagS pathway for the regulation of biofilm antimicrobial resistance (Petrova et al., 2017), and the Las-mediated quorum-sensing system for the control of biofilm formation and group motility (Ueda & Wood, 2009; Valentini & Filloux, 2016). **Figure 1** outlines the key virulence factors in *P. aeruginosa* and its regulatory genes (del Campo et al., 2005; Maselli et al., 2003; McCarthy, Mooij, Reen, Lesouhaitier, & O'Gara, 2014; Nixon et al., 2001; Zembrzuska-Sadkowska, Sneum, Ojeniyi, Heiden, & Hoiby, 1995; Zimakoff, Hoiby, Rosendal, & Guilbert, 1983). These networks represent a very broad but not isolated set of regulatory pathways to repress or activate distinct responses to external signals.
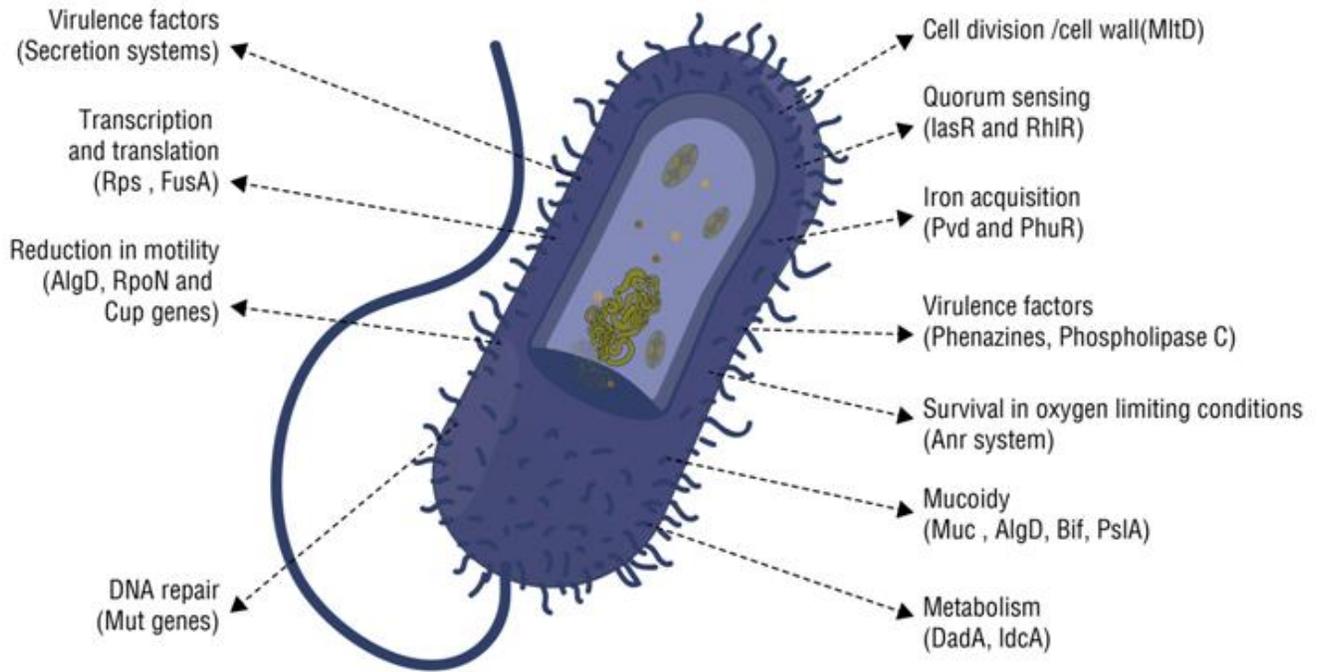
**Figure 1 Key features in *P. aeruginosa* relevant to survival and colonization.**

The expression of virulence genes in *P. aeruginosa* is controlled by extremely complex regulatory circuits and signaling systems. The diagram outlines key features relevant to its pathogenicity and survival in vivo.

## 1.1.2 Regulation of acute and chronic virulence factors in *P. aeruginosa*

*P. aeruginosa* infection is marked by two phases: a more aggressive acute phase and a sessile chronic phase. The acute phase of infection is frequently marked by high flagella and pili expression resulting in high motility as well as invasiveness, cytotoxicity and toxin production by Type III Secretion System (T3SS) (Sadikot et al., 2005) clinically evident as pneumonia and septicemia, leading to death within hours or days. However, upon encountering a suitable niche, a decision is made to switch towards a more "non-aggressive" lifestyle marked by exopolysaccharide production, biofilm formation, quorum-sensing and overcoming competition from other bacteria by Type Six Secretion System (T6SS).

T3SS, a hallmark of acute *P. aeruginosa* infection, are specialized needle-like secretion systems that facilitate the delivery (translocation) of bacterial effector proteins (ExoS, ExoT, ExoU, and ExoY) directly into the host cells. ExoS and ExoT inhibit phagocytosis by disrupting actin cytoskeletal rearrangement of the host cells (Barbieri & Sun, 2004). ExoU and ExoY are bi-functional cytotoxins with phospholipase and adenylate cyclase activities respectively (Sato & Frank, 2004). Studies have shown that T3SS expression is activated by host cell contact and growth in calcium-restricted conditions (Frank, 1997; Vallis et al., 1999).

T3SS is regulated by a master transcriptional regulator ExsA. ExsA belongs to the AraC /XylS - family which binds to a consensus sequence (TNAAAANA) centered ~15 base pairs upstream of the −35 RNA polymerase binding sites of T3SS genes (Diaz et al., 2011; Hovey & Frank, 1995). ExsA-dependent T3SS activation is coupled to secretion via a partner-switching mechanism involving ExsD (anti-activator), ExsC (anti-anti-activator), and ExsE (secreted regulator) (Brutinel et al., 2008; Diaz et al., 2011). Under non-inducing conditions, the T3SS expression is limited by inhibitory interactions between ExsA-ExsD and ExsC-ExsE proteins

(Yahr & Wolfgang, 2006). However, under inducing conditions, ExsE is secreted through the needle-like injectisome releasing ExsC to bind to ExsD and activating ExsA. ExsA then activates transcription of the ~40 genes associated with the T3SS (Urbanowski et al., 2007; Yahr & Wolfgang, 2006).

Other mechanisms for T3SS regulation include cAMP. cAMP acts an allosteric regulator of Vfr, which is required for exotoxin A, Type IV pilus motility and quorum sensing (Almblad et al., 2015; Marsden et al., 2016). Alteration of intracellular cAMP levels has also been shown to affect *vfr* levels which in turn regulates T3SS expression (Beatson et al., 2002). It has been further shown that elevated c-di-GMP levels inhibit cAMP levels downregulating *vfr* and T3SS expression (Almblad et al., 2015). Further, TCSs RetS, PA1611 and LadS have also been shown to reciprocally control T3SS expression by interaction with GacS/A TCS. GacS/A is a classical TCS of which, GacS functions as the sensor and GacA as the response regulator. Typically, under yet unknown environmental triggers GacS phosphorylates response-regulator GacA. Phosphorylation of GacA activates transcription of small RNAs RsmY and RsmZ. RsmY and RsmZ can sequester RNA binding regulator RsmA. RsmA belongs to the CsrA (carbon storage regulator) family of RNA binding proteins. Free RsmA binds directly to the 5' UTR of the *pslA* mRNA and represses translational initiation (Irie et al., 2010). RsmA also controls motility (Brencic & Lory, 2009)and Type IV pilus (Burrowes et al., 2006) in *P. aeruginosa*. An increased level of free RsmA is also required for optimal T3SS gene expression. Under yet unknown triggers for acute virulence conditions, RetS interacts with GacS directly and thus GacS is unable to phosphorylate GacA. This renders RsmA free to activate T3SS. Inversely under chronic infection conditions, RetS interacts with PA1611 (Bhagirath, Pydi, et al., 2017; Kong et al., 2013), allowing GacS to phosphorylate GacA, thus activating transcription of small

RNAs RsmY/Z to sequester RsmA, repress T3SS and activate chronic infection phase marked by biofilm formation. TCSs AlgR/FimS has also been shown to regulate the RsmAYZ post-transcriptional regulatory system to suppress the T3SS in mucoid *P. aeruginosa* isolates (Jones et al., 2010).

Alteration in motility is an important phenotypic change in *P. aeruginosa* in an acute-to-chronic switch. Motility plays a pivotal role in surface recognition-colonization and the spreading of bacteria across the surface. Early infection stages are marked by planktonic bacteria, utilizing a flagellum to swim, swarm, twitch and attach via bacterial adhesins, such as type IV pili and flagella. Once the bacteria are attached, combinations of specific surface-associated motilities, replication (clonal growth), and recruitment of additional planktonic bacteria leads to the formation of aggregates of bacteria called microcolonies, that can later lead to mature biofilm development. Swimming is identified as a more "individual-behavior" as opposed to swarming and twitching motility which are "group-behaviors." Swarming is a complex type of motility characterized by rapid and coordinated translocation of a bacterial population across a semi-solid surface (Fraser & Hughes, 1999; Harshey, 1994) which requires the release of rhamnolipids (RLs) (Deziel et al., 2003) and 3-(3-hydroxyalkanoyloxy) alkanoic acids (HAAs)(Köhler et al., 2000), which act as wetting agents and chemotactic stimuli. Twitching motility has been defined by Henrichsen (1972) as a kind of surface translocation that produces spreading zones and the colony edge exhibits varying micromorphological patterns. Cell movement in twitching motility is described as being "intermittent and jerky" and "predominantly single, although smaller aggregated movements occur". Components of the chemosensory *Che*IV cluster (Ferrández et al., 2002), including *pilJ* (Kearns et al., 2001) and the *chpA* (Whitchurch et al., 2004), as well as

an alteration in c-di-GMP levels (Kuchma et al., 2010; Kuchma et al., 2015) have been shown also play a central role in regulating surface behaviors of this microbe.

Production of exopolysaccharide matrix and formation of tenacious biofilms is the hallmark of *P. aeruginosa* chronic infection and colonization. Biofilm formation involves the convergence of several pathways and represents the most clinically challenging part of managing *P. aeruginosa* infection. Biofilm formation can be broadly described in three phases, initiation, maturation and dispersal. The complex biofilm structure represents the tight coordination between exopolysaccharide production (EPS), QS systems and the TCSs.

Las QS system has been shown to play a significant role in biofilm formation and maturation (D. G. Davies et al., 1998); however, the exact mechanism is still unclear. One of the proposed mechanisms is that LasR can bind to *psl* operon to activate its expression and thus facilitate biofilm formation (Gilbert et al., 2009). The Rhl system, on the other hand, has been shown to activate the *pel* operon  to form Pel polysaccharide biosynthesis to enhance biofilm formation (Sakuragi & Kolter, 2007).  Of the 60 TCSs found in the genome of *P. aeruginosa*, the GacS/GacA system has been shown to form a central pathway in biofilm formation (Parkins et al., 2001). The posttranscriptional regulator RsmA has been shown to negatively regulate the *psl* locus (*psl*A-L) to modulate biofilm levels (Kay et al., 2006; Pessi et al., 2002). RsmA also negatively controls the synthesis of C4-HSL and 3-oxo-C12-HSL and therefore controls the Las and Rhl systems effectively regulating biofilm formation (Reimmann et al., 1997). C-di-GMP has also emerged as a key regulator of biofilm formation. High intracellular levels of c-di-GMP have been shown to promote the biosynthesis of polysaccharides (alginate and Pel) by binding to PelD and Alg44 proteins (Massimo Merighi et al., 2007). Conversely, low levels of c-di-GMP

have been shown to promote bacterial dispersal and flagellar motility (Valentini & Filloux, 2016).

Though many aspects of chronic colonization by *P. aeruginosa* have been studied, others remain unanswered: How does *P. aeruginosa* overcome competition by other bacteria to gain predominance? Do the other inhabiting bacteria support or compete with *P. aeruginosa*? What is the role of biofilm dispersal in infection state and disease? In-Depth knowledge of *P. aeruginosa* colonization mechanisms is critical to answer these questions and inform new research.

### 1.1.3 Two-component regulatory systems in *P. aeruginosa*

During infection and colonization, microorganisms sense many environmental signals and process much of this information using two-component signal transduction systems. In response to external signals, TCSs regulate varied cellular functions to bring about internal adjustments in response to those stimuli. Signal transduction systems are found in all three kingdoms but are numerically variable depending upon the environmental diversity of the organisms.

Given their relevance in cell survival, it is not surprising that the highest number of TCSs were found in bacteria with largest interspecies variation, suggesting a correlation between their numbers to the variability in the existence of the microorganism. The largest number of TCSs in a single genome was found in *Cyanobacterium Synechocystis* PCC 6803. In Proteobacteria, the largest number of TCSs were found in *Escherichia coli*. Gram-positive bacteria *Bacillus subtilus* demonstrated about 70 TCSs (Koretke et al., 2000). It was also observed that free-living bacteria demonstrated greater numbers than specific-niche associated ones (Koretke et al., 2000).

The PAO1 genome sequence analysis has identified the presence of at least 130 genes encoding for TCSs (Rodrigue et al., 2000). Out of these at least 63 encoded for classical TCSs, 11 for atypical kinases devoid of an Hpt domain, and three are independent Hpt modules.

Typically, a signaling system consists of a Sensor Kinase [SK] with a conserved histidine residue [H box] also known as Histidine Kinase [HK] that senses external signals and transfers a phosphate molecule to the Response Regulator [RR] with conserved aspartate residue that then mediates a cellular response towards the external stimuli (**Figure 2A**). These are also known as histidyl-aspartyl phosphorelay (HAP) systems. Sometimes the RR harbors a DNA binding domain, which contributes directly to the control of gene expression or may even possess enzymatic activity (Galperin & Nikolskaya, 2007; Nikolskaya & Galperin, 2002; Tapparel et al., 2006). An additional step in this phosphotransfer process is added by an extra phosphoaspartate receiver (Rec) domain or a Histidine phosphotransfer protein (Hpt). The Hpt protein may be a part of the TCS (cognate) or an independent protein. Apart from the classical TCS where HK and RR domains are encoded in the same operon, sometimes they present either isolated as orphan HKs or along with intermediaries for phosphotransfer as the Hpt proteins (**Figure 2B**). The latter are known as Hybrid Histidine Kinase (HHK).
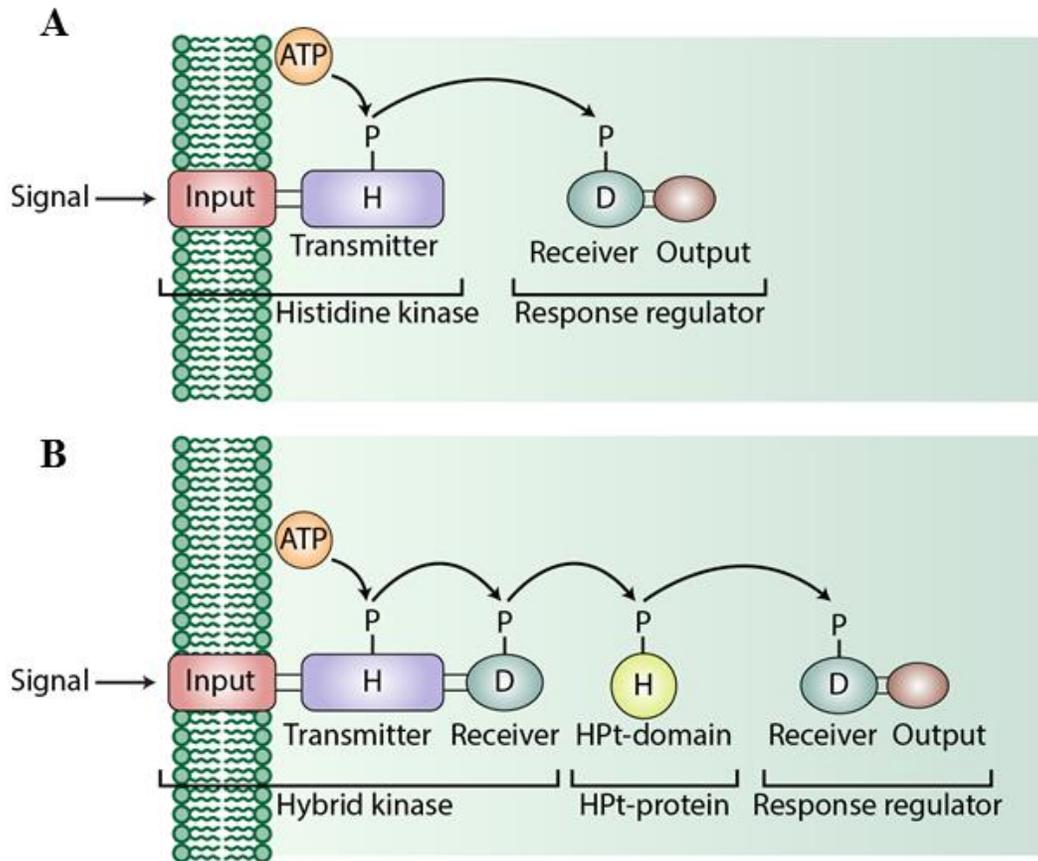
**Figure 2 Cartoon representation and basic features of the classical (A) and the hybrid histidine kinase (B) two-component signaling systems**. A signal perception by the input domain of histidine kinase induces autophosphorylation of the transmitter at a conserved His residue (H). The phosphate (P) is then relayed to a conserved Asp residue (D) that is localized at the receiver of the cognate response regulator. In the multistep, two-component signaling system, His-containing phosphotransfer (HPt) domain proteins serve as an intermediate between the hybrid kinase and the response regulator.

Phylogenetically, the RRs are more conserved as compared to the HKs. The transmembrane domains in the HKs of the TCSs may extend into the cytoplasm from cell membrane or be present completely in the cytoplasm where they can sense intra-cellular signals. A classic example of a cytoplasmic HK is NtrB-HK. NtrB is present in wide variety of species and senses intracellular nitrogen-dependent signals and regulates expression of nitrogen metabolic pathways. Recently, an extracellular sensor domain, termed Cache ($Ca^{2+}$ channels and chemotaxis receptors) or ESENS (extracellular sensing) also known as cyclases/histidine kinases associated sensing extracellular domains, was reported as a prokaryotic histidine kinase receptor. The proposed function for the Cache domain is the binding of small ligands, such as amino acids, sugars and organic acids (Mougel & Zhulin, 2001).

The RR domains though conserved can regulate diverse output domains. Phosphorylation of the RR initiates a cascade at the output domain which may respond by either binding to DNA or RNA. The DNA-binding motifs can be associated with varying output domain conformations including helix-turn-helix to winged helix domains.  The other output modules activated by RR include transcriptional control, enzymatic activity such as methylesterase, diguanylate cyclases, adenylate cyclases and serine/threonine kinases. HKs may function by either de-phosphorylating the response regulator or preventing the RR from de-phosphorylation (Zhu et al., 2000).

The division of domains in HHK for phosphotransfer provides for additional checkpoints for phosphorylation as well as may serve to integrate signals for a collective response. Recently, increasing number of reports have shown a non-phosphotransfer based signaling pathway in TCSs, which suggests complex signaling mechanisms.

TCSs regulate a wide variety of cellular functions in Pseudomonas in response to environmental signals and for the cell to function as a single unit, these signaling pathways must act in a combinatorial fashion to either promote or inhibit expression of certain gene products. Moreover, signaling systems of some organisms are too complex in their pathways suggesting that mechanisms other than phosphorelay mediated signal transduction might be at play.

### 1.1.4 Hybrid histidine kinase in two-component regulatory signaling

Classical TCSs are encoded on operons that include both the sensor kinase and response regulators. This reduces cross-talk and allows for co-expression of other proteins. Such is not the case with hybrid histidine kinase. Apart from participating in the phosphorelay, the Hpt protein is also capable of functioning as an independent protein and autophosphorylation. Often the term "HPt domain" has been used generically to describe any two-component histidine phosphotransfer domain including the dimerization domains such as those in EnvZ and Spo0B (Ohta & Newton, 2003) as well as monomeric structures such as those in CheA from salmonella (Morrison & Parkinson, 1994), ArcBC from *Escherichia coli* (Matsushika & Mizuno, 1998), and Ypd1 from the yeast (Xu et al., 2003). However, studies suggest that the monomeric and dimeric phosphotransfer domains are structurally quite distinct. These may often retain their Hpt function without specifically forming a part of any TCS (Mourey et al., 2001).

As much as 90% of the TCSs in eukaryotes use hybrid HK, but this is not the case in other kingdoms. In prokaryotes, only 20% of the characterized genomes encode hybrid kinases whereas in archae its only 1% (Schaller et al., 2011). Given the larger size of the eukaryotic cell, a multi-step phosphorelay seems logical to ensure that the phosphate is carried as the more stable phospho-histidine by the Hpt protein from the plasma membrane to the nucleus for

transcriptional regulation. Based on the modular organization in the phosphorelay it may be derived that phosphorylation at any level may lead to activation of the output domain. Interestingly, it has been observed that some of the hybrid HK may reverse the phosphotransfer thus dephosphorylating the RR (Pena-Sandoval et al., 2005).

Recent studies have highlighted interactions between the TCSs and other auxiliary proteins as a strategy to integrate signals in the regulation of TCS. Interestingly, more and more reports have emerged suggesting that TCS-TCS direct interaction may affect signaling states sometimes independent of the phosphorelay and at other times act as signal transducers for interacting proteins (Airola et al., 2010; Hsing & Silhavy, 1997; Matamouros et al., 2015). These reports suggest a clear correlation between structural properties, domain interaction, and signaling states. The complex nature of TCS function and interactions yet remain to be fully understood. Furthering the understanding into TCSs signaling is significant in developing ways to influence the overall cellular physiology of the organism.

### 1.1.5 Hybrid histidine kinase in virulence regulation in *P. aeruginosa*

Hybrid histidine kinases (HHKs) have recently emerged as a key sensing protein in *P. aeruginosa*. HHKs have been previously demonstrated to play a major role in stress adaptation, regulating virulence and mediating host-pathogen interactions in some yeast and mold models (Navarro-Arias et al., 2017). As compared to classical TCSs, HHKs present major advantages such as allowing for modularity or cross-talk between TCS components. The involvement of Hpt allows for additional checkpoints in the signaling pathway, and the multiple phosphorylation sites of the phosphorelay could provide more junction points for communicating with other signaling pathways. A comprehensive analysis of 156 complete microbial genomes demonstrated

that HHKs are at least 5-times more prevalent than identifiable Hpt sequences. This may be explained by the fact that the receiver domains have evolved to include diverse functions, some of which are independent of phosphorelay (Wise et al., 2010; Zhang & Shi, 2005).

HHK RetS (PA4856), has been shown to be a crucial sensor for controlling the expression of the T3SS, motility, inhibition of biofilm development and exopolysaccharide production (Laskowski et al., 2004). Similarly, HHK SagS (PA2824) was also found to be a negative regulator of biofilm formation (Goodman et al., 2004). On the other hand, the HHK LadS (PA3974) is known to function opposite to RetS (Goodman et al., 2004). Recent reports have shown that, LadS may function both by a phosphorelay-independent manner (Hsu et al., 2008) as well as via a phosphorelay (Chambonnier et al., 2016).

These studies shed light on the very complex signaling mechanisms of HHKs as well as their central role in regulating bacterial virulence. Several key elements in the signaling mechanisms of HHKs remain to be identified and characterized, including the environmental signals detected and the downstream target genes regulated by the pathways well as any involvement in cross-signaling. A detailed molecular mechanism on how HHKs function is necessary to inform further research and understand pathogenic mechanisms.

### 1.1.6 The GacA/GacS/RetS/PA1611-RsmA/Y/Z two-component regulatory pathway

At the center of the regulatory mechanisms in *P. aeruginosa* is the GacS/GacA-RsmA/Y/Z regulatory pathway where GacS functions as the sensor kinase, and GacA serves as the cognate response regulator **(Figure 3)**. Once GacS is autophosphorylated, the phosphorelay from GacS to GacA activates the production of small RNAs RsmY and RsmZ which are antagonists of the RNA-binding regulator RsmA. These small RNAs act by sequestering free RsmA. RsmA

regulates T3SS, motility, and biofilm formation post-transcriptionally in a dose-dependent manner. RsmA positively controls motility and the expression of genes in T3SS, a hallmark of acute infection, (Brencic & Lory, 2009) and negatively regulates biofilm formation, a characteristic of chronic infection (Goodman et al., 2004). The presence of unsequestered RsmA enables the expression of genes associated with acute infection and turns off genes involved in chronic infection. In contrast, the sequestration of functional RsmA in the presence of antagonists RsmY/Z enhances the production of Pel exopolysaccharides, biofilm formation and shuts off genes associated with acute infection (Brencic et al., 2009; Lapouge et al., 2008). The GacS/GacA-RsmA regulatory pathway thus serves as a switch, determining the acute or chronic state of the infection (Goodman et al., 2004).

Apart from the conventional TCSs, HHKs such as RetS, LadS, and PA1611 have been shown to play a major role in the GacA/GacS/RetS/PA1611-RsmA/Y/Z pathway. Although the stimuli or environmental signals remain unknown, once activated, RetS and LadS exert opposite effects on transcriptional regulator RsmA and reciprocally control the selection of acute or chronic infection state (P. Bielecki et al., 2013; Brencic & Lory, 2009; Chambonnier et al., 2016; Goodman et al., 2004; Lapouge et al., 2008). RetS forms a heterodimer with GacS thus blocking its phosphorelay activity (Goodman et al., 2009). Once GacS is blocked, downstream activation of the small RNAs stops, and consequently, the presence of free RsmA enables the selection of acute phase of infection over chronic phase. HHisK LadS also works through the GacS/GacA-RsmA pathway and favors chronic state. LadS functions through a phosphorelay cascade first from LadS to GacS then from GacS to GacA. Such a signal transduction results in activation of the production of the RsmY and RsmZ, (Chambonnier et al., 2016) which in turn sequester RsmA and hence favoring a sessile (biofilm) lifestyle. RetS has been shown to interact with the

PA1611, allowing the non-cognate GacS to phosphorylate its cognate response regulator and control important virulence factors  (Bhagirath, Pydi, et al., 2017; Kong et al., 2013).
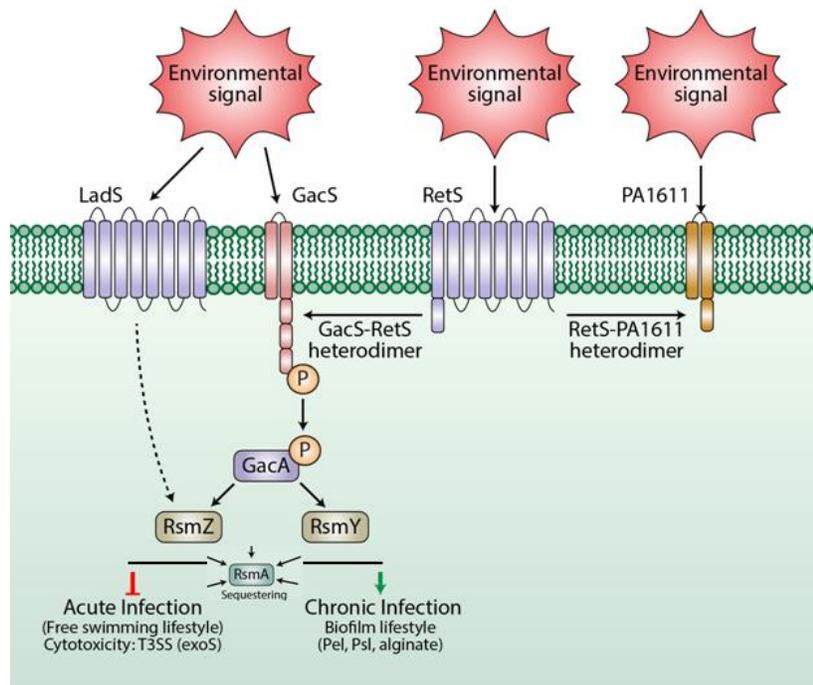
**Figure 3 GacA/GacS/LadS/RetS/PA1611-RsmA/Y/Z in *P. aeruginosa.*** The multicomponent signal transduction system made of the LadS, GacS/GacA, RetS and PA1611 form a multiple-input system in response to yet unknown environmental conditions. RetS blocks autophosphorylation of GacS by the formation of a heterodimer. LadS antagonizes the function of RetS by the formation of a phosphorelay based multicomponent signal transduction system. PA1611 interacts with RetS in a manner similar to GacS. The TCS GacS/GacA activates the production of two small non-coding RNAs, RsmY and RsmZ. These two sRNAs sequester the RNA-binding translational repressor RsmA and thus cause activation of the chronic phase of infection characterized by Pel exopolysaccharide production and T3SS repression (Goodman et al., 2004). Under yet unknown environmental signals favoring chronic infection, PA1611 is expressed and interacts with RetS (Bhagirath, Pydi, et al., 2017; Kong et al., 2013), leaving GacS to form homodimers and to phosphorylate GacA. Phosphorylated GacA, in turn, promotes the production of RsmY/Z which sequesters RsmA, causing the expression of genes associated with chronic infection. Note that the figure is for representation only and is not drawn to scale.

## 1.2 Cystic fibrosis

Cystic fibrosis (CF) is the most common life-threatening autosomal recessive genetic disease in Caucasians. The estimated incidence of CF is one in 2500–4000 within the Caucasian population and holds a prevalence of about 100,000 globally (J. C. Davies et al., 2014). Fortunately, the incidence rates for CF has been declining (Scotet et al., 2012) over the recent years. This is a result of neonatal screening and newer treatment modalities such as improved control of pulmonary infections and mucociliary clearance. CF lung disease is associated with dysregulation of host defense systems. This results in impaired host defenses to infecting pathogens. The imbalance between infection and host response leaves the host susceptible to colonization. Recent years have also seen an increase in disease complexity (Sawicki et al., 2013) with newer, more resistant pathogenic genetic variants of *P. aeruginosa* (Dewulf et al., 2015) emerging often. One common theme that gets less than deserved attention is the interplay of immediate environmental factors and the bacterial sensing mechanisms in shaping the bacterial virulence and thus determining the course of disease progression. It is now understood that bacterial sensing systems function in a highly complex manner in response to external environmental triggers and must be well studied to inform newer and more specific treatment approaches.

### 1.2.1 The pathophysiology of cystic fibrosis

CF is caused by mutations in the Cystic Fibrosis Transmembrane Conductance Regulator [CFTR] gene. Currently, more than 2000 mutations have been identified, of which 127 are confirmed as disease-causing (Sosnay et al., 2013). However, the molecular mechanisms underlying the strict transcriptional regulation of CFTRs remain poorly understood. CFTR/ABCC7 is a cyclic adenosine monophosphate (cAMP)-dependent member of the

adenosine triphosphate (ATP)-binding cassette transporter superfamily, found in the apical membrane of epithelial cells. It is the only member of the ATP-binding cassette protein family known to function as an ion channel rather than as an active transporter. CFTRs are expressed in many organs such as the kidneys, pancreas, intestine, heart, vas deferens and lungs (Crawford et al., 1991). CFTRs have been shown to perform a significant role in regulation of ; sodium channels (Ji et al., 2000; Nagel et al., 2001; Qadri et al., 2011), potassium (Leroy et al., 2006; Lu et al., 2006; Wang et al., 2013), outward rectifying chloride channels (Egan et al., 1995; Gabriel et al., 1993), calcium-activated chloride channels (Fischer et al., 2010; Hendrick et al., 2014), sodium bicarbonate (Borowitz, 2015; Xie et al., 2014) and aquaporin (Cheung et al., 2003) channels. Other CFTR functions include the regulation of vesicle trafficking, ATP release, and the expression of inflammatory epithelial mediators (Interleukin 8 and 10, and inducible nitric oxide synthase) (Clancy, 2016). These findings link the complex and diverse CFTR functions to CF lung disease.

Structurally, a CFTR is a membrane-bound glycoprotein of 1480 amino acid residue, with a molecular mass of 170,000. CFTR has a typical architecture of 12 transmembrane spanning helices arranged into two pseudo-symmetrical transmembrane domains and two nuclear-binding domains (NBDs) which bind and hydrolyze ATP and contain several highly conserved motifs (**Figure 4A**) (Bhagirath et al., 2016; Dalton et al., 2012; Dawson & Locher, 2006; Harris & Kirk, 2016; Mornon et al., 2009; Serohijos et al., 2008). These two NBDs, NBD1 and NBD2, can form a "head-to-tail" dimer, forming two composite binding sites for ATP at their interface. Between the two NBD units is a unique regulatory (R) domain which is made up of many charged amino acids (Molinski et al., 2015). The loss of a phenylalanine at position 508 in the CFTR gene is the most common mutation in CF and occurs in a highly conserved α-helical subdomain (495–565)

in NBD1(**Figure 4B**) (H. A. Lewis et al., 2005). Similarly, many of the other identified mutations have also been observed to occur in NBD1, while relatively few occur in NBD2.

In a non-mutated CFTR, gating has been shown to be tightly coupled with ATPase cycles through NBD dimerization. NBD dimerization then induces the formation of a transmembrane domain cavity that opens towards the extracellular side to allow for selective anion flow (**Figure 4C**) (Csanády et al., 2010; Hwang & Sheppard, 2009; Vergani et al., 2005). Deletion of phenylalanine at 508 (F508del) position in NBD1 leads to a CFTR trafficking defect. The current paradigm is not to view CFTR as just an ion channel, but a signaling system. It is hypothesized that if the cellular environment can be altered, the CFTR protein defect may be bypassed.

Owing to the complex function of CFTR, multiple physiological disorders arise in CF. Dysfunctional CFTR in the secretory epithelial cells results in obstructions in the lung airways and pancreatic ducts as a major pathological consequence. In CF airways, CFTR dysfunction instigates the accumulation of abnormally thick, sticky mucus in the respiratory tract, which hampers bacterial mucociliary clearance and allows the colonization of the airways by microbial pathogens (discussed further in the following sections). The most notable bacterial pathogens include *Pseudomonas aeruginosa*, *Staphylococcus aureus*, *Haemophilus influenzae* and *Burkholderia cepacia* complex, with *P. aeruginosa* causing the most predominant lung infection in CF. The dominant chronic inflammation is generated by the failure of microbial clearance and the creation of a toxic pro-inflammatory local microenvironment, which damages the lung and the innate immunity, further facilitating infections.
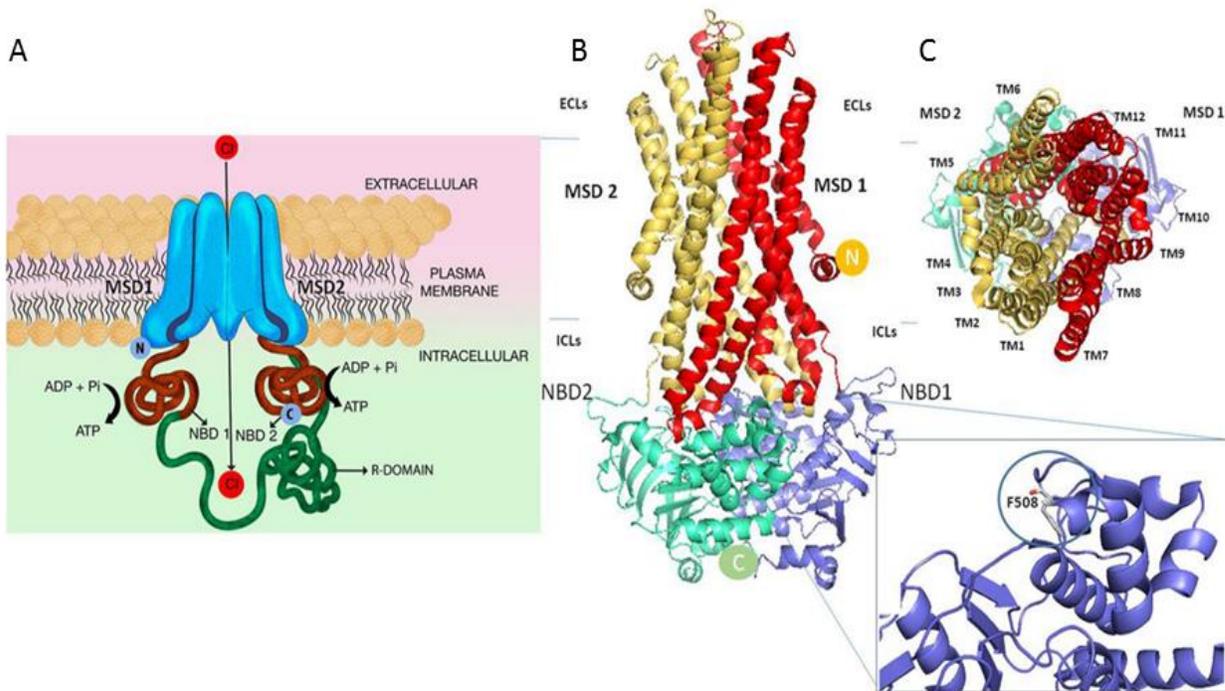
**Figure 4 Two-dimensional representation of CFTR channel and homology models**. **A.** A cartoon representation of CFTR. CFTR is composed of two membrane-spanning domains (MSDs), each linked through intracellular loops (ICLs) and extracellular loops (ECLs) (not shown here) to nucleotide binding domains (NBD1 and 2) (red). Unique to CFTR, NBD1 is connected to the MSD2 by a regulatory domain (R). **B.** The three-dimensional homology model for CFTR based on Sav1866 structure (2HYD)(Dalton et al., 2012; Serohijos et al., 2008). MSD1 contains transmembrane helices (TM) 1–6 and MSD2 contain TMs 7–12. The amino N-terminus and carboxyl-terminus are labeled respectively as N and C in yellow and shown circles. Insert shows F508A mutation in the NBD1 crystal structure (1XMI) seen in gray. **C.** CFTR is shown in its outward facing (extracellular) conformation.

Normally, airway epithelial cells can ingest the invading pathogens such as *P. aeruginosa,* followed by desquamation, thus protecting lungs from injury. In CF, however, it has been observed that CF epithelial cells phagocytose fewer cells of *P. aeruginosa* (Pier et al., 1997). It was initially suggested that CFTR is a cell-surface receptor for *P. aeruginosa* with an intact lipopolysaccharide [LPS] core (Pier et al., 1997). However, it was later shown that the internalization of *P. aeruginosa* in epithelial cells does not involve the chloride conductance channels but lipid rafts (Jolly et al., 2015). After *P. aeruginosa* enters cultured epithelial cells, the infected cells display plasma membrane blebs, while others show co-localization to acidic vacuoles (Jolly et al., 2015). Increased apoptosis has also been observed in such blebbing cells (Pier et al., 1997). It is hypothesized that the blebbing may be in response to *P. aeruginosa* LPS. Prolonged and repeated *Pseudomonas* LPS exposure in CF mice has been shown to result in abnormal and persistent immune response and significant structural changes in the lungs (Jolly et al., 2015). Airway acidification by the abnormal CFTR function has also been shown to be a major factor that initiates host defense abnormalities and microbial colonization (Shah et al., 2016). Yet the detailed mechanisms of the high susceptibility of the CF lung to bacterial infections are not completely clear. What becomes clear, however, is that CF lung pathogenesis begins with the altered lung environment triggered by the abnormal CFTR. A major outcome of changes in lung environment is a shift of the balance between surviving microorganisms that enter the lung and the host defense mechanisms, which eventually result in conditions that favor the survival of the invading microbes together with persistent yet ineffective immune responses.

## 1.2.2 The host internal environment in cystic fibrosis

The lung environment in CF is different from that of healthy individuals and undergoes significant alterations over the course of a patient's lifetime regarding disease progression,

microbial infections, and the lung microbiota. The lung environment dictates host-microbe interactions which shape the course of the disease. In the healthy respiratory system, the upper respiratory tract is colonized by microorganisms comprising the normal flora while the lower respiratory tract is relatively sterile due to the various host innate defenses. The presence of unique microbiota in the lower respiratory tracts of CF patients points to fundamental differences between the CF airways and those of the healthy individuals. It is thus important to understand the internal environment in the CF lung to decipher the host-pathogen interaction better.

**1.2.3 Airway anatomical complexity as a contributor to disease**

The human airway is highly compartmentalized, with the upper respiratory tract, consisting of the nose and the paranasal sinuses followed by the lower respiratory tract, which is further divided into conductive and respiratory zones. The sinuses in the upper respiratory tract have comparatively less airflow and are relatively isolated from antibiotic exposure and host immune responses. Their primary function is to provide resonance to sounds and produce mucus to facilitate bacterial clearance. The shape and size of the airways impact the overall flow and resistance of air passing through them. Airway morphology is essential to lung function and has been suggested to be an indicator of disease severity in patients with respiratory disease including CF (Montaudon et al., 2007). Understanding airway complexity is critical to understanding respiratory symptoms, developing ways to facilitate efficient delivery of inhaled medications and improve mucus clearance.

Studies from animal models suggest that CF patients present with abnormalities in the size and shape of the trachea from birth (Meyerholz et al., 2010). Pulmonary imaging of young children with CF indicates early structural defects, even in those with normal pulmonary function test results (Meyerholz et al., 2010). It has also been observed that the airways of infants and young

children with CF have thicker walls, with higher dilation than those of normal infants (Long et al., 2004; Meyerholz et al., 2010). The sinuses in CF form a very well-protected habitat given the complexity of the anatomy and the viscidity of mucus lining it thus, making them an excellent reservoir for chronic and relapsing lower respiratory infections. It has been reported that CF patients often present with chronic rhinosinusitis and the sinus microbiota in CF is often considered to be predictive of pulmonary disease. In the lower respiratory tract, the conductive zones produce mucus and facilitate bacterial clearance, leaving the alveoli free of bacteria. Mucus within the conductive zones is produced by sub-mucosal glands which occur at a frequency of about 1 per $mm^2$ in the trachea and go down to airway lumen diameters of 1-2 mm (**Figure 5A**). In healthy humans, sub-mucosal glands provide more than 95% of upper airway mucus. Each gland is composed of tubules that feed into a single collecting duct, which then narrows into a ciliated duct that is continuous with the airway surface (**Figure 5B**). Tubules are lined with mucous cells in their proximal regions and serous cells in the distal acini (B Meyrick et al., 1969; Widdicombe & Wine, 2015; Wine & Joo, 2004). Normal submucosal glands are made up of 60% serous and 40% mucous cells by volume. The serous cells secrete water, electrolytes, and a mixture of compounds with antimicrobial, anti-inflammatory and antioxidant properties, while mucous cells provide most of the mucins. Of relevance to CF, is the observation that within airways, CFTRs are most highly expressed in serous cells (Basbaum et al., 1990; Engelhardt et al., 1992; Barbara Meyrick & Reid, 1970). Secretion of water across these glands is driven predominantly by active secretion of chloride and bicarbonate as well as an increase in intracellular cAMP. Both cAMP and $Cl^-/HCO_3^-$ can be stimulated by a variety of agonists that elevate either cAMP, $Ca^{2+}$, or both, such as cholinergic agents and vasoactive

27

intestinal peptide (Ballard & Inglis, 2004; Ballard et al., 1999; Joo et al., 2002; Wine & Joo, 2004).

In tracheobronchial airways of animal models, it was observed that the inhibition of $Cl^-$ and $HCO_3^-$ secretion by bumetanide and dimethylamiloride in submucosal glands produces CF-like pathology, including production of thick dehydrated mucus and occlusion of gland ducts (Inglis et al., 1997; Trout et al., 1998). The mucus secretions from the submucosal glands in lower airways are also important for mucociliary clearance and provide major antimicrobial proteins involved in airway defense against bacteria. The abnormalities in CF lung secretions will be discussed in the next section. The CF respiratory tract is a highly diverse and complex ecosystem posing several challenges to inhabiting microorganisms in the process. These challenges include oxygen and nutrient limitation, antibiotics, competing microorganisms, changing lung pathophysiology and hyperactive immune response. In healthy individuals, while the upper airways present the anatomical component that may favor bacterial colonization, the lower airways present a more complex scenario of anatomical variations with other factors such as oxygen availability and exaggerated immune response to invading microbes. The CFTR defect in CF changes the airway environment and anatomical parameters in the lower airways. The CF lower airways host microorganisms, and pathogens that are usually absent in healthy individuals. The microorganisms which evolve in these conditions give rise to persisters (Fauvart et al., 2011; K. Lewis, 2010, 2012) and mutators (Ferroni et al., 2009; Hogardt & Heesemann, 2013; Oliver, 2010; Oliver & Mena, 2010; Warren et al., 2011) that are capable of long-term surviving and colonizing the otherwise harsh lung environment (López-Causapé et al., 2015).
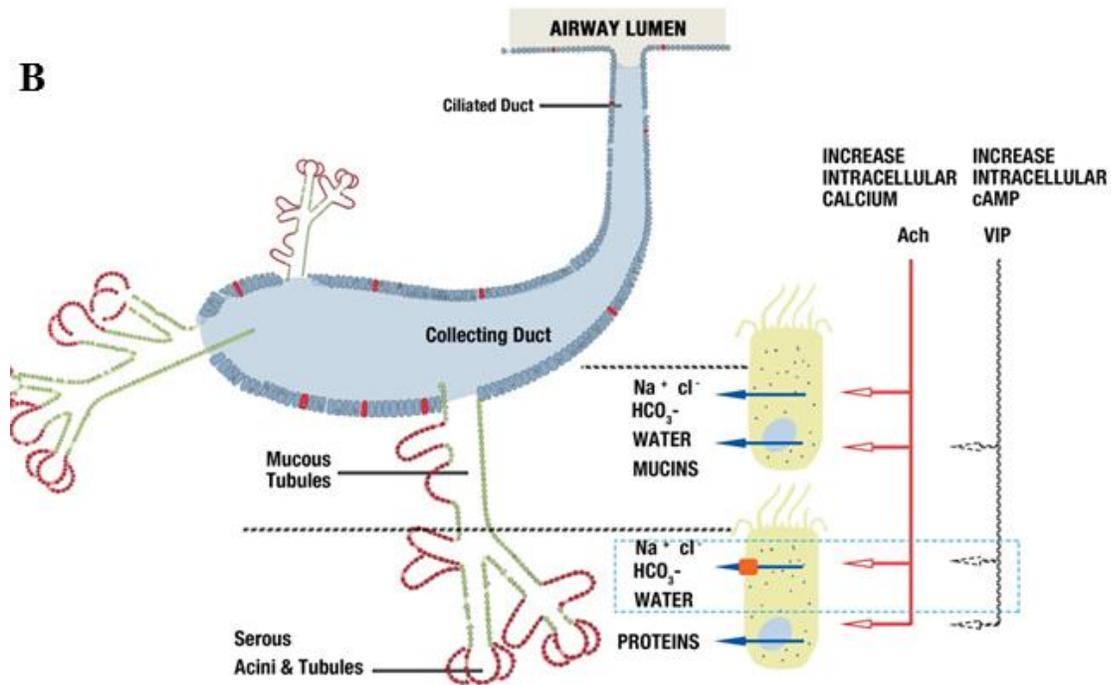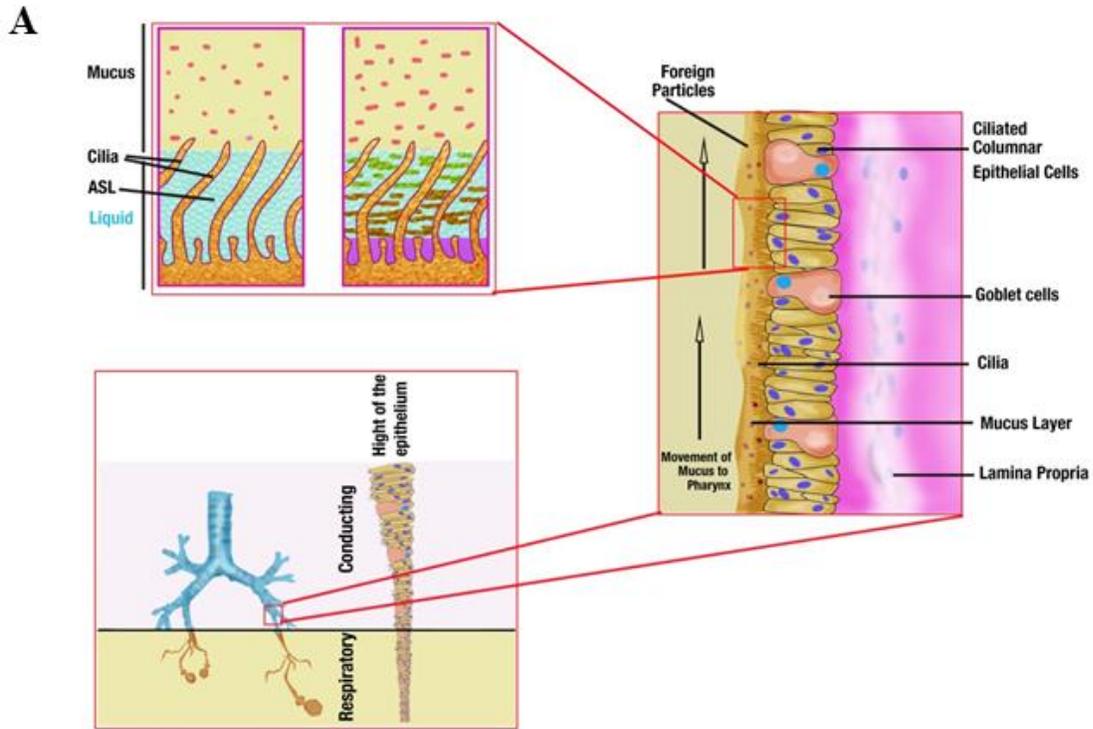
**Figure 5 Anatomical distribution of mucus-secreting cells in normal airways and pathological alterations in CF**. **A**. Mucus is secreted by submucosal glands in the conductive

zone and paranasal sinuses. The submucosal glands go on decreasing towards the lowest components of the respiratory zone. In healthy individuals, the cilia of the epithelial cells clear irritants and microorganisms, trapping them in the thin fluidic mucus and clearing by rhythmic ciliary beating upwards known as a mucus escalator. In CF, the airway surface liquid layer thins and the mucus comes in contact with cilia resulting in ciliary dyskinesis, causing poor clearance of bacteria which exacerbates inflammation. **B**. Schematic drawing of a single submucosal gland shows serous acini, mucous tubules, and collecting duct. Secretion of water across the epithelium of airway glands is driven predominantly by active secretion of chloride and bicarbonate. The CFTR-dependent water-secreting pathway is defective in CF. Figure adapted from previous publications (Engelhardt et al., 1992; Barbara Meyrick & Reid, 1970; Widdicombe & Wine, 2015; Wine & Joo, 2004).

It is plausible that the complex anatomical and physiological environments make CF lung a distinctive ecosystem with various niches that are eventually occupied by microorganisms. This is supported by the different microbiota observed in different parts of the airways (Boutin et al., 2015), and intrapulmonary spread of pathogens to previously unaffected niches (Fodor et al., 2012). The presence of active subpopulations of bacteria in particular areas of the airways is suggested to be potentially play a role in the pulmonary exacerbations in CF (Whelan & Surette, 2015).

### 1.2.4 Cystic fibrosis sputum

The mucociliary system consists of the cilia, the mucus layer covering the airway and the airway surface liquid (ASL) layer. This mucus layer is separated from the underlying ciliated epithelium by the liquid phase ASL. The mucus forms a trap for bacteria, viruses, as well as other particles and molecules inhaled during respiration, and the ciliary beating carries them back to the pharynx by forming a "mucus escalator" where they are normally swallowed or expelled. Mucus production is thus an innate defense mechanism, which protects airway surfaces against irritants and infecting microorganisms. Mucus composition and viscoelastic properties are good indicators of pulmonary health (Lamblin et al., 2001). Lamblin thus correctly reviewed mucus as "an interface between the environment and the *milieu interieur*."

In normal airways, if the ASL thins beyond a critical point, the surface epithelium converts from absorptive to secretory, though the exact mechanism is unclear. In CF, however, the defect in CFTR function leads to further absorption of isotonic liquid from ASL, leading to increasing in viscosity and decrease in thickness of the ASL. Thus, the gel-forming mucins that would otherwise float above the cilia are brought into close contact with the airway surface and attach

to it. The antimicrobials within these mucus plaques soon become ineffective and the invading microbes proliferate. The viscous mucous impairs ciliary beating, resulting in pulmonary ciliary dyskinesis, which results in the formation of mucous plaques. These mucus plaques, along with infecting microorganisms and resulting airway inflammation, lead to a decline in lung function. Conditions within the plaques, such as low $O_2$ tension, have been shown to contribute further to the airway colonization by pathogens such as *P. aeruginosa* and *Streptococcus* spp. (Huffnagle & Dickson, 2015; Quinn et al., 2014).

Normal mucus is about 95-98% water and 2-5% of mucins with other materials. Mucins form a part of the innate airway immunity and play a very critical role in CF disease progression and treatment outcomes but also remain one of the poorly understood aspects of CF. In CF, the mucin to water ratio is about 5–10 fold higher than normal, with mucus viscoelasticity $10^4$–$10^5$ fold greater than water at shear rates comparable to rubber (R. Boucher et al., 1988). Human airway mucins comprise a very broad family of high molecular weight glycoproteins. Structurally, mucins contain anywhere from one to several hundred carbohydrate chains attached to the peptide by O-glycosidic linkages between N-acetylgalactosamine and a hydroxylated amino acid. Very often, the carbohydrate chains are clustered in glycosylated domains. Apomucins, which correspond to their peptide part, are encoded by at least six different genes (MUC1, MUC2, MUC4, MUC5B, MUC5AC, and MUC7). However, the carbohydrate chains that cover these peptides are highly variable. Given the structural diversity of these carbohydrates as well as their location at airway surfaces, mucins may be involved in interactions with inhabiting microorganisms. The expression of at least two of these genes (MUC2 and MUC5AC) have been shown to be inducible by bacterial products, tobacco smoke and different cytokines (Lamblin et al., 2001).

The ASL in CF lungs of children has been shown to be abnormally acidic (Abou Alaiwa et al., 2014). Alaiwa *et al.* (Abou Alaiwa et al., 2014) found that in neonates with CF, nasal ASL (pH $5.2 \pm 0.3$) was more acidic than in non-CF neonates (pH $6.4 \pm 0.2$). Opinions vary about whether ASL pH remains abnormally acidic with age (McShane et al., 2003). In CF mouse model the decreased $HCO_3^-$ secretion due to CFTR defect and the unchecked $H^+$ secretion by the non-gastric $H^+/K^+$ adenosine triphosphatase (ATP12A) acidifies ASL (Shah et al., 2016). Experiments using CF primary airway epithelial cells stimulated with forskolin and 3-isobutyl-1-methylxanthine demonstrated that between $HCO_3^-$ and pH, it is the pH that affects the ASL viscosity more significantly (Tang et al., 2016). It was suggested that the decreased pH probably affected di-sulfide bonds in mucins, thus stabilizing them and resulting in increased viscosity. More importantly, the acidification of ASL impairs airway host defenses, allowing microorganisms to thrive in the CF lungs (Pezzulo et al., 2012; Shah et al., 2016).

Micro-rheological properties of CF sputum (Stigliani et al., 2016) have been investigated using several techniques such as; diffusion rates or behavior of a tracer (molecules, peptides, nanospheres and microspheres) using fluorescence recovery after photobleaching, dynamic light scattering, fluorescence correlation spectroscopy and single-particle tracking tracking experiments (Lai et al., 2009). These experiments and biochemical analyses have demonstrated that sputum microstructure is significantly altered by elevated mucin and extracellular DNA content. Apart from bacterial infection, the presence of airway proteases and airway remodeling, which occur as the disease progresses, may also affect mucus properties and further alter mucociliary transport and bring about pulmonary inflammation. As CF lung disease progresses, the sticky mucus formed generates microaerobic or even anaerobic settings within the normally aerobic environment (Worlitzsch et al., 2002). Such a lung environment of reduced oxygen level

contributes to the persistence of infection and decline of lung function (Borriello et al., 2004; Leeper-Woodford & Detmer, 1999).

Also, an important factor in CF pathophysiology, CF sputum has been a key source of information on lung microbiome and disease state. An in-depth analysis of CF lung environment and its role in bacterial pathophysiology may provide valuable insights into managing chronic lung infections and improving disease outcomes.

## 1.3 Study Rationale

*P. aeruginosa* is a key pathogenic bacterium in those with compromised immune system such as cystic fibrosis patients. The chronic colonization with *P. aeruginosa* is associated with significantly faster rate of lung function decline and respiratory failure which may prove fatal to CF patients. The chronic form of infection in *P. aeruginosa* involves the formation of robust biofilms in a vulnerable host which is resistant to external stressors such as antibiotic exposure or nutrient limitation. Management of such tenacious bacterial colonies takes a significant toll on the quality of life of the affected individual as well as poses a significant healthcare burden. Insight into its pathogenic mechanism is very critical to developing specific therapeutics. *P. aeruginosa* is endowed with many TCSs which allow it to sense its external environment and modulate its internal systems to respond to it. Two-component regulatory pathway such as GacS/GacA/LadS/RetS/PA1611-RsmA/Y/Z has emerged central to acute to chronic lifestyle transition in *P. aeruginosa*.

A hybrid sensor kinase PA1611, whose over-expression in *P. aeruginosa* PAO completely repressed T3SS expression, swarming motility, and promoted biofilm formation was identified previously (Kong et al., 2013). It was also shown that the regulation of T3SS and biofilm formation by PA1611 was independent of the phosphorelay. We also showed that PA1611 and

RetS interact. Given the key role of PA1611 in mediating chronic phenotypes in *P. aeruginosa,* it is possible that PA1611 may also play a role in survival and persistence during infection. Thus, to target specific virulence factors in *P. aeruginosa* such as antimicrobial resistance and host-directed toxicity, it is important to explore the environmental signals sensed by TCSs, the signal transduction mechanisms and explore their overall role in genetic regulation and pathogenesis.

## 1.4 Hypothesis

The RetS-PA1611-Gac-RsmA pathway is a key regulatory pathway in *P. aeruginosa*, which integrates environmental signals, including those in CF lung environment, through various mechanisms and mediates acute to chronic transition during *P. aeruginosa* infections.

## 1.5 Objectives

The three specific objectives of my project are:

## 1. Characterization of the direct interaction between hybrid sensor kinases PA1611 and RetS in *P. aeruginosa*

To obtain mechanistic insights into PA1611-RetS interaction, site-directed mutagenesis of the predicted residues involved in the interaction was performed as well as their functional roles in *Pseudomonas* phenotypes were characterized.

## 2. Characterize the role of *cmpX* in regulation of *P. aeruginosa* virulence

CmpX emerged as a regulator for PA1611. In this objective, *cmpX* was studied for its role in *P. aeruginosa* pathophysiology. I further analyzed the pathway by which *cmpX* mediates the observed effects.

**3. Identifying signals for PA1611 activation and biofilm formation in *P. aeruginosa***

PA1611 is important for acute-chronic infection transition in *Pseudomonas*, however, the exact cues it responds to are yet unknown. PA1611 was screened for triggers that it may respond to and the mechanistic pathway was explored.

**Chapter 2**

**2.0 General material and methods**

**2.1 Materials**

All routine culture media and additives were purchased either from Fisher Scientific (Toronto, ON, Canada) or Sigma Aldrich. Compounds: Orphenadrine (Cat # 75517), Compound 48/80 (Cat# C2313), Lauryl sulfobetaine (Cat # D0431), Methyltrioctylammonium chloride (Cat # 69485), Vancomycin (Cat # 1709007) , Tobramycin (Cat # T4014) and Josamycin (Cat # 59983) were purchased from Sigma Aldrich Co. (St. Louis, Mo.). Cyclic-di-GMP (Cat # ED0003) was purchased from KeraFast (Boston, MA). His dropout amino acid supplement was purchased from BD/Clontech (Cat. #630415). BacLight, Bacterial Viability Kit, (Cat#L7007) for microscopy was purchased from Invitrogen. For generating anaerobic conditions during growth, anaerobic gaspaks were purchased from BD (Cat# 260001 and Cat# 260680). All chemicals were of analytical grade and used without further purification.

For PCR cycling, LifePro Thermal Cycler purchased from Bioer Serves Life (Tokyo, Japan); for quantitative Real-Time PCR, PCR system was purchased from MBI Lab Equipment (Montreal, Canada); Imaging system: Fusion FX Vilber Lourmat was purchased from MBI Lab Equipment (Montreal, Canada) was used. For centrifugation purposes, Optima XE-90 ultracentrifuge purchased from Beckman Coulter (Hebron, US) was used. Electrophoresis system consisted of FB300 purchased from Fisher Science (Ottawa, Canada) and Electroporator: Electroporation Pak purchased from BTX Harvard Apparatus (Holliston, US).

## 2.1.1 Media for bacterial culture

Unless indicated otherwise, all *P. aeruginosa* and *E. coli* strains were cultured at 37 °C in Luria Bertani (LB) broth with vigorous shaking at 225 rpm. LB was used as T3SS non-inducing media; LB supplemented with 5 mM ethylene glycol tetra-acetic acid (EGTA) and 20 mM $MgCl_2$ was used as T3SS-inducing media (calcium-deplete).

**Luria-Bertani (LB) broth**: 10 g/L Tryptone, 5 g/L Yeast extract, NaCl 5 g/L(pH 7.0).

**NaCl-free LB broth (LB0)**: 10 g/L Tryptone, 5 g/L Yeast extract

**CAS (CAA) medium**: 5 g/L casamino acids; 1.18 g/L $K_2HPO_4*3H_2O$, 0.25 g/L, $MgSO_4*7H_2O$, 25 mM HEPES and 400 µM 2,2′-Bipyridyl(BIP) (pH 7.0).

**M9 Minimal media**: $Na_2HPO_4 \cdot 7H_2O$ 12.8g/L, $KH_2PO_4$ 3 g/L, NaCl 0.5 g/L, $NH_4Cl$ 1 g/L, glycerol to 0.2% (v/v) (pH to 7.4)

**10X M9 salts**: $Na_2HPO_4$-$2H_2O$ 75.2 g/L, $KH_2PO_4$ 30 g/L, NaCl 5 g/L, $NH_4Cl$ 5 g/L

**M9 Media additives for bacterial two hybrid assays**: Per preparation (67.5 ml)

Solution 1: 10 ml of 20% glucose (filter-sterilized), 5 ml of 20 mM adenine HCl (filter sterilized), 50 ml of 10× His dropout amino acid supplement

Solution 2: 0.5 ml of 1 M $MgSO_4$, 0.5 ml of 1 M Thiamine HCl, 0.5 ml of 10 mM $ZnSO_4$, 0.5 ml of 100 mM $CaCl_2$, 0.5 ml of 50 mM Isopropyl β-D-1-thiogalactopyranoside (IPTG)

Non-selective media for bacterial two hybrid assay: 7.5g/L Bacto agar, 50 ml of 10× M9 salts, M9 Media Additives (one preparation), 0.5 ml of 25 mg/ml chloramphenicol, 0.5 ml of 12.5 mg/ml tetracycline.

**Selective media for bacterial two hybrid assay**: 7.5g/L Bacto agar, 50 ml of 10× M9 salts, M9 Media Additives (one preparation), 0.5 ml of 25 mg/ml chloramphenicol, 0.5 ml of 12.5 mg/ml tetracycline, 2.5 ml of 1 M 3-AT (dissolved in DMSO)

**Double selective media for bacterial two hybrid assay**: 7.5g/L Bacto agar, 50 ml of 10× M9 salts, M9 Media Additives (one preparation), 0.5 ml of 25 mg/ml chloramphenicol, 0.5 ml of 12.5 mg/ml tetracycline, 2.5 ml of 1 M 3-AT (dissolved in DMSO), 0.5 ml of 12.5 mg/ml streptomycin.

**SOB media**: 2% Bacto-Tryptone, 0.5% Yeast extract, 10 mM NaCl, 2.5 mM KCl (pH 7.0) 10 mM $MgCl_2$ added before use.

**SOC media**: SOB media containing 20 mM glucose (pH 7.0).

Antibiotics, where necessary, were added at the following concentrations: for *E. coli*, chloramphenicol (Cm) 25 µg/ml, tetracycline (Tc) 12.5 µg/ml, kanamycin (Km) 50 µg/ml, and ampicillin (Ap) 100 µg/ml were used in LB media. For *P. aeruginosa*, Tc at 70 µg/ml in LB or 300 µg/ml in Pseudomonas isolation agar (PIA), carbenicillin (Cb) at 250 µg/ml in LB, and trimethoprim (Tmp) at 300 µg/ml in PIA was used.

### 2.1.2 Buffers

**PBS**: 137 mM NaCl, 2.7 mM KCl, 1.8 mM $KH_2PO_4$, 10 mM $Na_2HPO_4$.

Storage buffer: 50 mM Tris, 12.5 mM $MgCl_2.6H_2O$, pH 7.4, containing protease inhibitors

**TAE buffer** (Tris Acetate-EDTA): 4.84 g Tris, 2 ml 0.5 M $Na_2EDTA$ (pH 8.0), 1.1 ml glacial acetic acid, and water to make 1 liter.

**Agarose loading buffer**: 25 mg bromophenol blue, 3.3 ml 150 mM Tris, pH 7.6, 6 ml glycerol, 0.7 ml water to make 10 ml.

**1.5 M Tris**, pH 6.8 and 8.8.

**0.5 M Tris-HCl** (pH 6.8), 8% SDS, 60% glycerol, 80 µg/ml bromophenol blue, 8% β-mercaptoethanol.

### 2.2 Molecular biology techniques

### 2.2.1 Genomic DNA isolation

*P. aeruginosa* (PAO1) was inoculated in LB broth and incubated at 37°C with agitation at 225 rpm overnight. A 5 ml culture was centrifuged at 5,000×g for 10 minutes at room temperature. The supernatant was discarded. 100 µl TE buffer was added and the pellet was re-suspended completely via vortex, followed by the addition of 10 µl Lysozyme and incubated at 37°C for 10 minutes. After that, 100 µl BTL buffer and 20 µl Proteinase K Solution was added and mixed thoroughly, then incubated at 55°C in a shaking water bath. 5 µl RNase was added and the tube was inverted several times to mix. The tube was incubated at room temperature for 5 minutes, then centrifuged at 10,000×g for 2 minutes to pellet any undigested material. 220 µl BDL buffer was added after the supernatant was transferred to a new 1.5 ml microcentrifuge tube, to distribute the pellet. Followed by incubation at 65°C for 10 minutes, 220µl 100% ethanol was added and vortexed for 20 seconds at maximum speed. A HiBind DNA Mini Column was inserted into a 2 ml collection tube, and the entire sample was transferred to the column, followed by a centrifugation at 10,000×g for 1 minute. The column was then inserted into a new 2 ml collection tube and 500 µl of HBC buffer was added. After centrifugation, 700 µl DNA wash buffer was added and then centrifuged again. The wash step was repeated twice. The empty column was centrifuged at a maximum speed for 10 minutes to dry the column. The DNA was eluted by adding pre-warmed elution buffer 50 µl, and stored at -20°C.

### 2.2.2 Plasmid isolation

PrestoTM Mini Plasmid Kit (Geneaid) was used for plasmid isolation. Cultures were grown overnight in media supplemented with the appropriate antibiotic. 1.5 ml of the overnight culture was transferred into a centrifuge tube at room temperature, and then re-suspended in 200 µl PD1

buffer. 200 µl of lysis buffer PD2 was added, and the tube was gently mixed by inverting 10 times. 300 µl neutralization buffer PD3 was added within 5 minutes, and the solution was mixed by gently inverting10 times, followed by a 10 minutes centrifuge at 12,000×g to clarify the lysate. An PDH column was placed in a 2 ml Collection Tube, and the clarified supernatant was transferred to the column followed by centrifugation at 12,000×g for 1 minute. 600 µl of wash buffer was added into the column and centrifuged at 12,000×g for 1 minute. This step was repeated twice. After that, the filtrate was discarded, and the column was centrifuged to dry for 10min. 30-50 µl pre-warmed elution buffer was added to the column to purify the plasmid DNA followed by centrifugation to collect the eluted plasmid DNA. Plasmid was stored at -20°C.

### 2.2.3 Preparation of *P. aeruginosa* electrocompetent cells

*P. aeruginosa* cells were grown overnight in LB media at 37°C. The bacteria were collected and re-suspended in 1 ml 0.3 M sucrose and then centrifuged at 8000 rpm for 3 minutes at room temperature. The supernatant was discarded, and the wash step was repeated three times. Then, the cells were subjected to another wash with 1 ml 10% glycerol(Choi et al., 2006). The amount of 10% glycerol added was based on the concentration of competent cells, and 1 ml aliquots of the resulting solution were stored at -80°C.

### 2.2.4 Preparation of *E. coli* competent cells for chemical transformation

For chemical transformation, *E. coli* cells subjected to calcium cation induced competence which allows the cells to uptake DNA from the environment. A DH5α colony was transferred to a tube with 3 ml of LB medium. The culture was incubated for 12 hours at 37°C with agitation at 220 rpm. After that, the culture was transferred into 50 ml of LB broth. The cells were then grown until the optical density ($OD_{600}$) of 0.5. The cells were cooled for 10 minutes on ice, and then

centrifuged at 5000 rpm at 4°C for 10 minutes, and the pellet was gently re-suspended in 20 ml ice-cold 100 mM $CaCl_2$. The suspension was kept on ice for 10 minutes and centrifuged one more time. The pellet was gently re-suspended in 4 ml 100 mM $CaCl_2$ and kept on ice for 30 minutes. After the addition of 1 ml 80% glycerol, aliquots of 100 µl were transferred into 1.5 ml centrifuge tubes. The aliquots were frozen and stored at -80°C.

## 2.2.5 Preparation of *E. coli* electrocompetent cells

E. coli cells were grown in LB broth at 37°C overnight with agitation at 225 rpm. 100 ml of fresh LB broth was inoculated with 1 ml of inoculum from the overnight culture and incubated for 3 additional hours with agitation. 50 ml of the 3-hour culture was transferred to falcon tubes, and centrifuged at 4500 rpm for 7 minutes at 4°C. The cells were re-suspended in 25 ml of 10 mM HEPES and centrifuged again. The supernatant was discarded, and the process was repeated one more time. Then, the cells were washed again with 1 ml of 10% glycerol. The amount of 10% glycerol added was based on the concentration of competent cells. 100 µl aliquots were stored at -80°C.

## 2.2.6 Transformation

DH5α competent cells thawed on ice. 5 µl of ligation mix was added to it and gently mixed. After incubation on ice for 30 minutes, the mixture was heat-shocked for 20 seconds in a 42°C water bath, and then the tubes were placed on ice for 2 minutes for cold shocking. 950 µl of pre-warmed SOC medium was added into the tubes and the cells were cultured at 37°C for 1 hour with agitation at 225 rpm. 200-300 µl of transformation was spread on selective media and the plates were incubated overnight at 37°C.

**2.2.7 Electroporation**

As described previously by (Filloux & Ramos, 2014) for *P. aeruginosa* transformation electroporation cuvettes and centrifuge tubes were pre-chilled on ice. 100 µl of electroporation competent cells were thawed on ice and suspended well by gently flicking the tubes. 2-3 µl plasmid was added into the competent cells, mixed well, and the entire solution was transferred to the cuvette gently avoiding bubbles. Then, electroporation was carried out immediately by setting the electroporator to 2000 V. After that, 500 µl of 37°C pre-warmed SOC media was added into the cuvette and mixed well gently, then transferred to a centrifuge tube. The cells were cultured for about 1 hour at 37°C and were spread on selective media plates and cultured overnight. The remaining cells were stored at -80°C.

**2.2.8 Polymerase Chain Reaction (PCR)**

Polymerase chain reaction (PCR) is a molecular biology technique that utilize a thermos stable DNA polymerase enzyme to amplify a specific DNA sequence of interest. All PCR reactions were carried out in LifePro Thermal Cycler (Bioer Serves Life), with either *P. aeruginosa* genomic DNA or plasmid DNA as the template. The template denaturation was at 95°C, while annealing occurred at a ranged 55-65°C. Lastly, elongation was carried out at 72°C for 30 seconds per every 1 Kb of product. Ready PCR mix kit from Invitrogen (USA) was used to perform standard PCR and colony screening. Supplied as a 2× mixture of reaction buffer, Taq polymerase blend, dNTPs, electrophoresis tracking dye and a non-mutagenic EZ-Vision visualization dye was used. The size of the PCR products was analyzed and confirmed by agarose gel electrophoresis, which was used to separate the fragments from the template DNA, unincorporated nucleotides, polymerase and buffer salts as well. After PCR amplification, 1-2 µl of 10× DNA loading buffer

was added to the reaction mixtures containing the amplified fragments and loaded on to the premade gel with 3 µl molecular weight marker (GeneRuler[TM] 1Kb DNA ladder, Fermentas). The gel was run at 70 V for 70 minutes. Results were performed using imagine machine Vilber Lourmat Fusion FX7 imager (Montreal Biotech Inc.).

### 2.2.9 Construction of gene expression detecting systems

An integration vector CTX6.1 originating from plasmid mini-CTX-*lux* (Becher & Schweizer, 2000) was used to construct chromosomal fusion reporters. The plasmid has all the elements required for integration, the origin of replication, and a Tc-resistance marker. The pMS402 fragment containing the kanamycin-resistance marker, the MCS, and the promoter-*luxCDABE* reporter cassette was then isolated and ligated into CTX6.1. The plasmid construct was first transferred into *E. coli* SM10-λ (Simon et al., 1983) and *P. aeruginosa* reporter integration strain was generated using bi-parental mating as reported previously (Hoang et al., 1998). Gene expression in liquid cultures was examined as counts per second (cps) of light production using a Synergy H4 Multimode Microplate Reader (BioTek) using the *lux*-based reporter. Luminescence was measured every 30 min for 24 h. The bacterial growth was also monitored simultaneously by measuring $OD_{600}$ in the microplate reader.

### 2.2.10 Isolation of total RNA

Strains were inoculated from glycerol stocks into 2 mL LB medium and grown overnight at 37°C followed by sub-culturing in 5 mL LB medium and grown to mid-exponential phase. A 0.25 mL aliquot of the cell culture, corresponding to $5 \times 10^8$ cells, was added to 0.5 mL of RNeasy bacteria protect solution (Qiagen, Hilden, Germany). Total RNA was isolated according to the manufacturer's instructions. Residual DNA was eliminated by DNase treatment using 20 U of

RQ1 RNase-free DNase (Promega, Madison, WI). After removal of DNase, RNA was extracted and resuspended in 30 µl of RNase-free $H_2O$. The presence of residual DNA and the RNA quality was checked by formaldehyde/agarose gel electrophoresis.

## 2.2.11 Synthesis of cDNA and quantitative Real-Time PCR (qPCR)

cDNA was synthesized from 500ng of total RNA and a mixture of oligo dT and random primers using the Quanta qScript cDNA Synthesis kit (Quanta BioSciences, MD) as per the manufacturer's instructions. cDNA was stored at -20ºC and unused RNA was stored at -80ºC. As a quality control, RNAs were checked for the absence of genomic DNA contamination by quantitative real-time PCR with primers for the housekeeping gene *rpoD*.

qPCR was performed using SYBR select master mix (Invitrogen) on an Eco Illumina real-time detection system (Montreal Biotech). Reaction mixtures with a final volume of 20 µl consisted of 2 µl reverse transcribed cDNA, 5 pmol primers, 1x SYBR green containing dNTP mix and Taq polymerase. The reaction consisted of the following steps; an initial denaturation step of 2 min at 95ºC followed by 40 cycles of : 95ºC for 15 sec, annealing at 60ºC for 30 sec and extension at 72ºC for 30 sec and a final extension at 72ºC for 1 min. This was followed by the melt curve analysis. Melt curve analysis confirmed the presence of a single PCR product in each reaction. Gene expression fold-change was calculated using the ΔΔ Ct method. Ct values of each gene tested were normalized to the Ct values of the housekeeping gene *rpoD* (Park et al., 2013). Data are presented as percent change relative to gene expression in wild type PAO1.

## 2.3 Phenotypic characterization

## 2.3.1 Bacterial motility assay

Bacteria were assessed for swarming and swimming motility by a protocol described by Rashid and Kornberg (2000) (Bordi et al., 2010). The swarming motility assay medium consisted of 0.5% agar, 8 g/L nutrient broth, and 5 g/L glucose. For swimming motility assay, the medium consisted of 10 g/L tryptone, 5 g/L NaCl, and 0.3% agar. The medium for twitching motility assay consisted of LB broth solidified with 1% agar (Rashid & Kornberg, 2000).

For swimming and swarming motility assay, stationary-phase cells (3 µl; $2.0 \times 10^8$ cells/ml) were seeded onto the centers of 100 mm-diameter motility plates bacteria followed by incubation at 37 and 30 °C, respectively, for 12–14 h. The diameters of the migration front were measured after 12-14 h incubation. For twitching motility assay, stationary -phase cells were stab inoculated through a 1% agar plate and, were incubated overnight at 37°C, the zone of twitching motility between the agar and petri dish interface was visualized by staining with Coomassie brilliant blue. Photographs were taken with Vilber Lourmat Fusion FX7 imager.

### 2.3.2 ExoS secretion under T3SS inducing condition

Protein secretion measurements were performed as described previously with minor modifications.(Motley & Lory, 1999)  A single colony from Pseudomonas isolation agar plates was inoculated into 1.5 ml LB medium supplemented with antibiotics and grown overnight at 37°C. Overnight cultures were diluted at 2% concentration in fresh media containing 5 mM EGTA and 20 mM $MgCl_2$, incubate at  37$^o$C with shaking at 250 rpm for 6 h. Cells were pelleted from 5 ml of a bacterial culture by centrifugation at 12000 rpm for 5 min at 4 $^o$C.  The clarified supernatant was precipitated with 10% trichloroacetic acid for 1h on ice and centrifuged at 12,000 $\times$ g for 15min at 4°C, and the protein pellets were washed two times at $-20$°C with cold acetone. The pelleted protein was resuspended in 100 µl of PBS. 20 µl of the protein solution was

separated on a 12% SDS gel (Goodman et al., 2004) and visualized by Coomassie blue staining.

### 2.3.3 Measurement of biofilm formation

Biofilm formation was measured as described by O'Toole and Kolter (O'Toole & Kolter, 1998) with minor modifications. Cells from overnight cultures were inoculated at 1:100 dilutions in M9 medium supplemented with 0.2% glucose, 1 mM $MgSO_4$, and 0.5% casamino acids in 96-well polystyrene microtiter plates (Costar) and grown at 30 °C for 24 h. A 100 µl of crystal violet solution was added to each well and staining was allowed for 15 min prior to removal of liquid by aspiration. The wells were rinsed three times with distilled water, and the remaining crystal violet was dissolved in 200 µl of 95% ethanol. A 125 µl portion of this solution was then transferred to a new polystyrene microtiter plate, and absorbance was measured at 590 nm.(O'Toole & Kolter, 1998)

### 2.3.4 Metabolic phenotype arrays

Metabolic phenotype arrays of *P. aeruginosa* strains PAO1, ΔPA1775, ΔPA1611 were performed by commercially available, Biolog Phenotype MicroArrays (PM) (Biolog Inc., Harvard, CA, USA). Biolog PMs are 20, 96-well microtiter plates with each well containing defined medium with a unique metabolic substrate and tetrazolium dye as an indicator for cell respiration which is reduced by the action of dehydrogenases, yielding a purple formazan dye. PM1 to PM8 are metabolic panels containing various N, P, or S sources. Panels PM9 to PM20 measure sensitivity to salt, pH stress, antibiotics, antimetabolites, and other inhibitors. Two replicates were conducted for each strain. Incubation and recording of phenotypic data were performed with an OmniLog instrument at 490 nm (Bochner, 2009). A color change indicates that the cells are actively metabolizing a substrate in the well, while the lack of color change

implies that the cells are unable to utilize the substrate. The strains were incubated, and the 1920 phenotypes were recorded simultaneously four times each hour by the OmniLog instrument, which captured a digital image of the microarray and stored quantitative color change or turbidity values in a computer file. PM Kinetic Analysis software is then used to generate a mean growth kinetic phenotype curve. The mutant strain tracings are overlaid on the control strain tracings. A mean height difference threshold of 50 for metabolic panels and a difference threshold of 74 for sensitivity panels were used to consider the difference between the two growths as significant. The values observed above the threshold show phenotypes gained and those below it is the lost phenotypes.

## 2.3.5 Minimum Inhibitory Concentration (MIC) testing

Susceptibilities to antimicrobial agents were tested using broth microdilution method in Mueller-Hinton broth (Oxoid, Ltd., Basingstoke, Hampshire, United Kingdom) according to the CLSI guidelines (CLSI, 2012). Compounds for testing were purchased from Sigma Aldrich Co. (St. Louis, Mo.). PAO1, ΔPA1611 and ΔPA1775 were cultured and the inoculum volume for minimum inhibitory concentration testing was adjusted to a concentration of 5 x $10^5$ CFU/ml. *P. aeruginosa* PAO1 was used as the control strain in each run. The MIC was defined as the lowest antibiotic concentration that inhibited visible growth of the organism.

## 2.4 Statistical analysis

Statistical analysis was performed using either one-way analysis of variance (ANOVA) with Tukey or Dunnette post-hoc test from a minimum of three independent experiments to determine the statistical significance or an unpaired t-test where applicable. NS *p>0.05*, *$*p < 0.05$, $**p < 0.01$, $***p < 0.001$, $****p < 0.0001$.

**Chapter 3**

**Characterization of the direct interaction between hybrid sensor kinases PA1611 and RetS that controls biofilm formation and the type III secretion system in *Pseudomonas aeruginosa*.**

## 3.1 Rationale

Infection with *Pseudomonas aeruginosa* is the primary cause of morbidity and mortality in patients with cystic fibrosis (CF) (Govan et al., 2007; Sanders et al., 2010). Patients with CF acquire *P. aeruginosa* infection almost certainly, (Murray et al., 2007) and acute infection eventually becomes chronic. The two phases (acute and chronic) of infection differ remarkably in bacterial physiology, disease pathogenesis, treatment options, and outcomes. Acute *P. aeruginosa* infection is characterized by motility in the form of swimming, swarming and twitching as well as low alginate production, and toxic effector production *via* the Type Three Secretion System (T3SS), e.g., ExoS, ExoY, ExoT and ExoU. In contrast, chronic phase is characterized by elevated alginate production, lack of T3SS activity, and the formation of biofilms (Boles et al., 2005; Cullen & McClean, 2015). Cells in biofilms resemble those in the chronic stage of the disease. These cells are sedentary and surrounded by a matrix of exopolysaccharides (EPS) and extracellular DNA. Biofilms form protective niches for the residing pathogens against antibiotics and adverse environmental conditions, posing a great clinical challenge (P. Bielecki et al., 2013; Chambonnier et al., 2016).

The transition between an acute and chronic state in *P. aeruginosa* is achieved *via* highly complex signaling pathways. Under the conditions of either chronic or acute infection, a range of genes such as those affecting virulence is differentially regulated by a complex network of two-component regulatory systems (TCS). At the center of the signaling systems is the GacS/GacA-RsmA/Y/Z regulatory pathway where GacS functions as the sensor kinase, and GacA serves as the cognate response regulator. Once GacS is autophosphorylated, the phosphorelay from GacS to GacA activates the production of small RNAs RsmY and RsmZ which are antagonists of the RNA-binding regulator RsmA. These small RNAs act by sequestering free RsmA. RsmA

regulates T3SS, motility, and biofilm formation post-transcriptionally in a dose-dependent manner. RsmA positively controls motility and the expression of genes in T3SS, a hallmark of acute infection, (Brencic & Lory, 2009) and negatively regulates biofilm formation, a characteristic of chronic infection (Goodman et al., 2004). The presence of un-sequestered RsmA enables the expression of genes associated with acute infection and turns off genes involved in chronic infection. In contrast, the sequestration of functional RsmA in the presence of antagonists RsmY/Z enhances the production of Pel exopolysaccharides, biofilm formation and shuts off genes associated with acute infection (Brencic & Lory, 2009).

The GacS/GacA-RsmA regulatory pathway thus serves as a switch, determining the acute or chronic state of the infection (Goodman et al., 2004). Apart from the conventional TCSs, a group of hybrid sensor kinases functions as a multi-relay network that potentially integrates multiple signals into key regulatory pathways, sometimes through a non-phosphate relay process. These often seemingly independent TCS components act as auxiliary components to influence other typical TCSs. (Buelow & Raivio, 2010)

 Upstream of the GacS/GacA regulatory system are the Hybrid Histidine Kinase (HHisK) RetS and LadS. Although the stimuli or environmental signals remain unknown, once activated, RetS and LadS have opposite effect on RsmA and reciprocally control the selection of acute or chronic infection state (P. Bielecki et al., 2013; Brencic & Lory, 2009; Chambonnier et al., 2016; Goodman et al., 2004). RetS forms a heterodimer with GacS thus blocking its phosphorelay activity (Brencic et al., 2009; Goodman et al., 2009; Lapouge et al., 2008) Once GacS is blocked, downstream activation of the small RNAs stops, and consequently, the presence of free RsmA enables the selection of acute phase of infection over chronic phase. HHK LadS also works through the GacS/GacA-RsmA pathway and favors chronic state eventually. However, it does

not form heterodimers with either RetS or GacS. Instead, it functions through a genuine phosphorelay cascade first from LadS to GacS then from GacS to GacA. Such a signal transduction results in activation of the production of the RsmY and RsmZ, (Chambonnier et al., 2016) which in turn sequester RsmA and hence favoring a sessile (biofilm) lifestyle.

Previously, an HHK PA1611 was identified, whose over-expression in *P. aeruginosa* PAO completely repressed T3SS expression, swarming motility, and promoted biofilm formation (Kong et al., 2013). It was also showed that the regulation of T3SS and biofilm formation by PA1611 was independent of the phosphorelay (Kong et al., 2013). Like RetS and LadS, the functioning of PA1611 falls within the recently uncovered bacterial strategy of integrating multiple signals *via* direct interaction between TCSs (Piotr Bielecki et al., 2015; Gardner et al., 2015). Recently, reports have emerged suggesting that TCS-TCS direct interactions affect signaling states independent of phosphorelay and often act as signal integration pathways (Airola et al., 2010). To understand the complex signal transduction and bacterial pathogenesis, it is important to explore the correlation and structural basis of such direct interactions between these sensor kinases.

In this objective, I investigated the structural and mechanistic basis of the interaction between PA1611 and RetS. First, the residues critical in PA1611 and RetS interaction were identified by molecular modeling and site-directed mutational analyses, followed by functional studies in *P. aeruginosa*. It is observed that, despite the non-involvement of phosphotransfer, the histidine kinase (HisK) domain and the histidine kinase-like ATPase domains are critical in the TCS interaction which determines bacterial lifestyle selection during infection and colonization and provides a new target for controlling bacterial infection.

## 3.2. Material and methods

### 3.2.1 Bacterial strains and plasmids

Table **3.2.1** lists the bacterial strains and plasmids used in this study. Unless otherwise stated, *P. aeruginosa* and *Escherichia coli* were grown routinely in Luria Bertani (LB) media at 37 °C. LB was used as T3SS non-inducing media; LB supplemented with 5 mM ethylene glycol tetra-acetic acid (EGTA) and 20 mM MgCl$_2$ was used as T3SS-inducing media (calcium-deplete). Antibiotics, where necessary, were added at the following concentrations: for *E. coli*, chloramphenicol (Cm) 25 µg/ml, tetracycline (Tc) 12.5 µg/ml, kanamycin (Km) 50 µg/ml, and ampicillin (Ap) 100 µg/ml were used in LB media. For *P. aeruginosa*, Tc at 70 µg/ml in LB or 300 µg/ml in Pseudomonas isolation agar (PIA), carbenicillin (Cb) at 250 µg/ml in LB, and trimethoprim (Tmp) at 300 µg/ml in PIA was used.

**Table 3.2.1 Bacterial strains and plasmids used in this study**

| Strain or plasmid | Relevant characteristics | Source |
|---|---|---|
| *E. coli* | | |
| SM10-λ *pir* | Mobilizing strain, RP4 integrated into the chromosome; Kn$^r$ | (Simon et al., 1983) |
| XL1-Blue | *recA1 endA1 gyrA96 thi-1 hsdR17 supE44 relA1 lac [F´ proAB lacIq ZΔM15 Tn10 (Tet$^r$)].* | Invitrogen |
| XL1-BlueMRF'-Kan$^H$ | Host strain for propagating pBT and pTRG recombinants; *Δ(mcrA)183 Δ(mcrCB-hsdSMR-mrr)173 endA1 supE44 thi-1 recA1 gyrA96 relA1 lac [F´proAB lacIq Z ΔM15 Tn5 (Kn$^r$)]* | Agilent |
| XL1-BlueMRF'-Kan$^R$ | BacterioMatch II two-hybrid system reporter strain; *Δ(mcrA)183 Δ(mcrCB- hsdSMR-mrr) 173 endA1 supE44 thi-1 recA1 gyrA96 relA1 lac [F´laqIq HIS3 aadA (Kn$^r$)]* | Agilent |
| BN469 | *E. coli* Beta-galactosidase assay strain harboring a test promoter–*lacZ* fusion to detect lambda cI-dependent protein-protein interactions. | Dr. Simon Dove |
| *P. aeruginosa* | | |
| PAO1 | Wild-type *P. aeruginosa* | This lab |
| PA(ΔPA1611) | PA1611 Knockout mutant of PAO1 | This lab |
| PA(ΔRetS) | PARetS Knockout mutant of PAO1 | This lab |

| PA(ΔgacA) | gacA knockout mutant of PAO1; Gm$^r$ | This lab |
|---|---|---|
| Plasmids | | |
| CTX6.1 | Integration plasmid origins of plasmid mini-CTX-lux; Tc$^r$ | This lab |
| pAK1900 | *E. coli-P. aeruginosa* shuttle cloning vector carrying P*lac* upstream of MCS; Ap$^r$ ;Cb$^r$ | This lab |
| pBT | p15A origin of replication, lac-UV5 promoter, λ cI open reading frame; Cm$^r$ | Agilent |
| pTRG | ColE1 origin of replication, *lpp* promoter, *lac*-UV5 promoter, RNAPα open reading frame; Tc$^r$ | Agilent |
| PBT-LGF[2] | Interaction control plasmid encoding the dimerization domain (40 amino acid residues) of the Gal[4] transcriptional activator protein; Cm$^r$ | Agilent |
| pTRG-GAl1[P] | Interaction control plasmid encoding a domain (90 amino acid residues) of the mutant form of the Gal11 protein; Tc$^r$ | Agilent |
| pAK1611 | pAK1900 with a 2024 bp fragment of *PA1611* between *Sal*I and *Hind*III; Ap$^r$, Cb$^r$ | This study |
| pAKRetS | pAK1900 with a 2829 bp fragment of *PA1611* between *Hind*III and *Xba*I; Apr, Cb$^r$ | This study |
| pAK*gacA* | pAK1900 with a 644 bp fragment of *gacA* between *Hind*III and *Xba*I; Apr, Cb$^r$ | This study |
| CTX-*exoS* | Integration plasmid, CTX6.1 with a fragment of pKD- | This Lab |

| | | |
|---|---|---|
| | *exoS* containing *exoS* promoter region and *luxCDABE* gene; Kn$^r$, Tmp$^r$ , Tc$^r$ | |
| CTX-*rsmZ* | Integration plasmid, CTX6.1 with a fragment of pKD-*rsmZ* containing *rsmZ* promoter region and *luxCDABE* gene; Kn$^r$, Tmp$^r$, Tc$^r$ | This lab |
| pKD-*rsmZ* | pMS402 containing *rsmZ* promoter region; Kn$^r$, Tmp$^r$ | This lab |
| pBT-*1611* | pBT with a PA1611 subclone encoding from amino acid residue 202 to 505; Cm$^r$ | This study |
| pTRG-*retS* | pTRG with a *retS* subclone encoding for amino acid residue 393 to 652; Tc$^r$ | This study |
| pMS402 | Expression reporter plasmid carrying the promoterless *luxCDABE* gene; Kn$^r$,Tmp$^r$ | (Duan et al., 2003) |
| pEX18Tc | oriT$^+$ sacB$^+$ gene replacement vector with multiple-cloning site from pUC18; Tc$^r$ | (Hoang et al., 1998) |
| CTX-*exoS* | Integration plasmid, CTX6.1 with a fragment of pKD-*exoS* containing *exoS* promoter region and *luxCDABE* gene; Kn$^r$, Tmp$^r$ , Tc$^r$ | This Lab |
| CTX-*rsmY* | Integration plasmid, CTX6.1 with a fragment of pKD-*rsmZ* containing *rsmZ* promoter region and *luxCDABE* gene; Kn$^r$, Tmp$^r$, Tc$^r$ | This lab |

**3.2.2 Sequence retrieval, domain analysis, molecular modeling, and protein–protein docking**

All the amino acid sequences were retrieved from the NCBI database, and multiple sequence alignment was performed using Clustal W 2.1 multiple sequence program. Homology models were obtained using the Swiss Model (Benkert et al., 2011). The final structural prediction was selected by taking the lowest energy model as determined by a low-resolution Rosetta energy function. As there is no crystal structure available for PA1611 (681 amino acid (aa) residues), to gain insight into its structure, an *in-silico* analysis of its sequence was performed. Amino acid sequences of RetS (942 aa) and PA1611 were obtained from NCBI **(Figure 6).** The domains within PA1611, RetS, and GacS were identified using SMART database. Homology-based modeling of PA1611 and RetS was carried out to predict its three-dimensional (3D) structure. Molecular models of the crucial kinase and phosphatase domains of these two proteins were built as follows: Conserved domains on the proteins were predicted using NCBI conserved domain (CDD) search database. The molecular models of RetS from aa residues 393 to 652 and of PA1611 from 202 to 505 that harbor the conserved domains were generated based on the crystal structure of the C-terminal part of tyrosine kinase (DivL) from *Caulobacter crescentus* CB15 (PDB ID: 4ew8) as the template using Swiss Model (Benkert et al., 2011).

The final structural prediction was selected by taking the lowest energy model as determined by a low-resolution Rosetta energy function. The backbone conformation of the modeled structure was estimated by analyzing phi (F) and psi (ψ) torsion angles using Rampage (Lovell et al., 2003). Protein–protein interactions between RetS and PA1611 models were then predicted using ZDOCK server (Pierce et al., 2011) following the previously published protocols (Chakraborty et al., 2013). The protein complexes were analyzed, and the images were generated using PyMOL **(**Schrödinger**).**

## A

**Interaction modeled**

202 — 505

13 35 167 186 191   243   265   330   378   494   515   628   651

TM TM | HAMP | HisKA | HATPase_c | REC | **PA1611**

11 33 168 187 191   243   283   348   395   511   665   781   817   913   925

TM TM | HAMP | HisKA | HATPase_c | REC | HPT | **GacS**

393 — 652

7 26 189 211 218 240 250 272 305 327 337 359 366 388   414   479   526   640   657   776   807   923   942

TM TM TM TM TM TM TM | HisKA | HATPase_c | REC | REC | **RetS**

## B

```
                    1         10        20        30        40        50        60
PA1611   AIGQLISAREEAEQANRAKSDALAMMSHELRTPMNGVLGMLQLLETTEQTREQAEYTALATESTEHLLK
GacS     ~~~~~~~~~~~~~~EEASRIKSEFLANMSHEIRTPLNGILGFTNLLQKSELSPRQQDYLTTIQKSAESLLG

                    70        80        90        100       110       120       130
PA1611   VINDILDFSRIERGALELECIPFNLLELVQGSALVFQHSAQQRGLALELQIQAGLENIEVCGDPTRIRQ
GacS     IINEILDFSKIEAGKLVLENLPFNLRDLIQDALTMLAPAAHEKQLELVSLVYRDTP~IQLQGDPQRLKQ

                    140       150       160       170       180       190       200
PA1611   ILVNLLGNALKFTEEGAIHLSLEWQALDHDVLWLTCAVHDSGIGISPERLEHMFDAFQQADSSISRRYG
GacS     ILTNLVGNAIKFTQGGTVAVRAMLEDESDDRAQLRISVQDTGIGLSEEDQQALFKAFSQADNSLSRQAG

                    210       220       230       240       250       260       270
PA1611   GTGLGLAIARTLAERMGGTLQAESKEGSGSTFT~~~~~~~~~~~~~~~~~~~
GacS     GTGLGLVISKRLIEQMGGEIGVDSTPGEGAEF~WISLSLPKSRDDNE
```

## C

**PA1611**                                    **RetS**

General/Pre-Pro/Proline Favoured   General/Pre-Pro/Proline Allowed
Glycine Favoured   Glycine Allowed

58

**Figure 6 Amino acid sequence analysis and Ramachandran plot of PA1611 and RetS molecular models. A.** PA1611, GacS and RetS domain organization. The domain architectures were constructed by individually comparing the protein sequences against the SMART 4.0 and the Pfam30.0 databases. The figure is not drawn to scale. **B.** Sequence alignment between PA1611 and GacS. Alignment was performed on ExPASy and image generated from Maestro Biolumine (Schrödinger). Homologous amino acid residues are in grey. The secondary structure is depicted below the sequence alignment. The helices are shown in red and the beta sheets in blue. **C.** Ramachandran plots of PA1611 and RetS obtained using Rampage. As described in the methods, most of the amino acids are within the favored (dark blue) and allowed regions (light blue). The glycine favored (orange) and glycine allowed (light pink) are also shown. Only around 1% or four residues in each model are in the disallowed regions. In PA1611 model these are Q296, I374, H404, and W418; and in RetS model these amino acids are Q413, L445, S627, and L601.

### 3.2.3 Generation of PA1611 mutants and PA1611 expression in the mutants

Site-directed mutagenesis of PA1611 in bacterial two-hybrid (BTH) bait plasmid and pAK1611, and pAKRetS *Pseudomonas* expression vector was performed by using the QuikChange II protocol (Agilent Technologies, United Kingdom), according to the manufacturer's guidelines. **Table 3.2.3** lists the primers used in mutagenesis protocol.

**Table 3.2.3 Primers used in the study**

| Primer | Sequence (5'-3') |
| --- | --- |
| pBT-1611-F | GTAGCGGCCGCACAGGCGGTCGAGGCGATC |
| pBT-1611-R | GCTGAATTCGGCGGCCTGCTGCCGGTG |
| PA1611-F | GTAGTCGACGAAGGAGAAGAACCATG |
| PA1611-R | GCTAAGCTTGGCGAACAGATGTTCACT |
| pETSUMO PA1611-F | TCACAGGCGGTCGAGGCGATC |
| pETSUMO PA1611-R | TCAGGCGGCCTGCTGCCGGTG |
| pTRG-retS-F | GTAGCGGCCGCACTGATCCAGCAGCTCAAC |
| pTRG-retS-R | GATGAATTCGTCGAGGTCGGCGGTGGG |
| 1611F269A-F | CGGGCGAAGTCCGACGCCCTGGCGATGATGAG |
| 1611F269A-R | CTCATCATCGCCAGGGCGTCGGACTTCGCCCG |
| 1611M272A-F | CCGACTTCCTGGCGGCGATGAGCCACGAGC |
| 1611M272A-R | GCTCGTGGCTCATCGCCGCCAGGAAGTCGG |
| 1611E276A-F | ATGATGAGCCACGCGCTTCGCACGCCG |
| 1611E276A-R | CGGGGTGCGAAGCGCGTGGCTCATCAT |
| 1611T279A-F | CCACGAGCTTCGCGCCCCGATGAACGG |
| 1611T279A-R | CCGTTCATCGGGGCGCGAAGCTCGTGG |
| 1611S310A-F | GGTGTTCGGTGGCCTCGGTGGCCAG |
| 1611S310A-R | CTGGCCACCGAGGCCACCGAACACC |
| 1611Q444A-F | GTTCGACGCCTTCCAGGCAGCGGATTCGTCGATT |
| 1611Q444A-R | AATCGACGAATCCGCTGCCTGGAAGGCGTCGAAC |

| | |
|---|---|
| 1611Y453A-F | GATTTCCCGGCGCGCCGGCGGCACCGGG |
| 1611Y453A-R | CCCGGTGCCGCCGGCGCGCCGGGAAATC |
| 1611F269Y-F | GCTCATCATCGCCAGATAGTCGGACTTCGCCC |
| 1611F269Y-R | GGGCGAAGTCCGACTATCTGGCGATGATGAGC |
| 1611M272C-F | GAAGCTCGTGGCTCATGCACGCCAGGAAGTCGGAC |
| 1611M272C-R | GTCCGACTTCCTGGCGTGCATGAGCCACGAGCTTC |
| 1611E276D-F | CATCGGGGTGCGAAGATCGTGGCTCATCATC |
| 1611E276D-R | GATGATGAGCCACGATCTTCGCACCCCGATG |
| 1611T279V-F | CGCCGTTCATCGGGACGCGAAGCTCGTGGC |
| 1611T279V-R | GCCACGAGCTTCGCGTCCCGATGAACGGCG |
| 1611T279S-F | GTTCATCGGGCTGCGAAGCTCGTGGCTC |
| 1611T279S-R | GAGCCACGAGCTTCGCAGCCCGATGAAC |
| 1611S310T-F | GGTGTTCGGTGGTCTCGGTGGCCAG |
| 1611S310T-R | CTGGCCACCGAGACCAACCGAACACC |
| 1611Q444N-F | GAAATCGACGAATCCGCATTCTGGAAGGCGTCGA |
| 1611Q444N-R | TGTTCGACGCCTTCCAGAATGCGGATTCGTCGATT |
| 1611Y453F-F | TGCCGCCGAAGCGCCGGGAAATCG |
| 1611Y453F-R | CGATTTCCCGGCGCTTCGGCGGCA |
| 1611K316A-F | GAATGTCGTTGATGACCGCCAGCAGGTGTTCGGTGG |
| 1611K316A-R | CCACCGAACACCTGCTGGCGGTCATCAACGACATTC |
| 1611A463T-F | CCAGGGTCCTGGTGATCGCCAGGCC |
| 1611A463T-R | GGCCTGGCGATCACCAGGACCCTGG |
| pAKRetS- F | TGCTCTAGACCACGGCCACTTGGCTAT |

| | |
|---|---|
| pAKRetS- R | TATAAGCTT CGAATAGCCGCGTGCGGTT |
| pAKGacA-F | TGCTCTAGATGCGCGACGAGGT |
| pAKGacA-R | CCCAAGCTTCTACAGGTAGCGAGG |
| RetS R509A F | GATCAGCTCGATGGCCTGCTGCTCGGCC |
| RetS R509AR | GGCCGAGCAGCAGGCCATCGAGCTGATC |
| RetS E511A F | TGAAGCTGATCAGCGCGATGCGCTGCTGC |
| RetS E511A R | GCAGCAGCGCATCGCGCTGATCAGCTTCA |
| RetS Q517A F | CGGCACCTGCGGCGCGGTGAAGCTGATC |
| RetS Q517A R | GATCAGCTTCACCGCGCCGCAGGTGCCG |
| RetS E547A F | GGATCTCGCCTTCCGCGGTCTGCTTGAAC |
| RetS E547A R | GTTCAAGCAGACCGCGGAAGGCGAGATCC |
| RetS R567A F | CTGCACGGCGATGGCCAGGCGTGGCGTC |
| RetS R567A R | GACGCCACGCCTGGCCATCGCCGTGCAG |
| RetS Q624A F | GCTGCTGCCGGACGCGATGCCGAACTCC |
| RetS Q624A R | GGAGTTCGGCATCGCGTCCGGCAGCAGC |
| RetS R509K F | GAAGCTGATCAGCTCGATCTTCTGCTGCTCGGCCTT |
| RetS R509K R | TCAAGGCCGAGCAGCAGAAGATCGAGCTGATCAG |
| RetS E511D F | GGTGAAGCTGATCAGATCGATGCGCTGCTGC |
| RetS E511D R | GCAGCAGCGCATCGATCTGATCAGCTTCACC |
| RetS Q517N F | CGCGGCACCTGCGGATTGGTGAAGCTGATCA |
| RetS Q517N R | TGATCAGCTTCACCAATCCGCAGGTGCCGCG |
| RetS E547D F | CAGGATCTCGCCTTCATCGGTCTGCTTGAAC |
| RetS E547D R | GTTCAAGCAGACCGATGAAGGCGAGATCCTG |

| RetS R567K F | GTCCTGCACGGCGATCTTCAGGCGTGGCGTCTC |
|---|---|
| RetS R567K R | GAGACGCCACGCCTGAAGATCGCCGTGCAGGAC |
| RetS Q624N F | TGGCTGCTGCCGGAATTGATGCCGAACTCCC |
| RetS Q624N R | GGGAGTTCGGCATCAATTCCGGCAGCAGCCA |

F-Forward primer; R-Reverse primer

### 3.2.4 Site-directed mutagenesis (SDM)

The template consisted of the plasmid with the insert into which the point mutations were to be introduced. The reaction mix consisted of 2.5 pmoles/µl of forward and reverse primers, 10mM of dNTPs, fusion polymerase buffer, high fidelity fusion polymerase 100ng template. The cycling conditions included 1.30 seconds at 98°C, 18 cycles of; 10 s at 98°C, 1 min at 60°C, 1 min/1 kb template at 72◦C and a final extension at 72°C at 10 mins. This was followed by a DpnI digest of the reaction mix to digest any methylated DNA or template DNA. The reaction mix was then cleaned up and transformed into *E. coli*. The mutants were selected from appropriate antibiotic-supplemented LB plates. All mutants were then further confirmed by sequencing (MICB—University of Manitoba). All plasmids were introduced in *E. coli* by a chemical transformation method, whereas plasmids were introduced in *P. aeruginosa* by electroporation.

### 3.2.5 Protein expression and visualization

All plasmids were introduced in *E. coli* by a chemical transformation method, whereas plasmids were introduced in *P. aeruginosa* by electroporation. Mutant fragments of PA1611 were introduced in the pETSUMO expression vector (Invitrogen) by TA cloning for protein expression analysis. PA1611 wild type and mutant were inoculated in 100 ml of LB with 50 µg/ml kanamycin and 1% glucose. The culture was grown for six hours to $OD_{600}$ of 04-0.6. IPTG to a final concentration of 1 mM to the cultures. After induction, cultures were centrifuged at 5000 X g in a microcentrifuge for 10 minutes, and the supernatant was discarded. The cell pellet was resuspended in sonication buffer. The expressed PA1611 protein was analyzed on 12% sodium dodecyl sulfate (SDS)-PAGE. The positive control used was the pETSUMO/CAT control vector. The molecular weight of CAT fusion protein is approximately 39 kDa. The

negative control was the total protein from BL21 (DE3) cells containing empty vector under inducing conditions. The expressed proteins were analyzed on 12% sodium dodecyl sulfate (SDS)-PAGE.

**3.2.6 Bacterial two-hybrid assays**

Plasmids for Bacterial two-hybrid (BTH) assays were constructed using the BacterioMatch II Two-Hybrid System Vector Kit (Agilent Technologies, USA). PA1611 encoding aa residues 202 to 505 was cloned at the 3′ end of the gene encoding λ repressor protein (λcI, 237 aa residues), containing the amino-terminal DNA-binding domain and the carboxyl-terminal dimerization domain on pBT vector. Amino acid residues of RetS from 393 to 652 were cloned at the 3′ end of the gene encoding a subunit RNA polymerase (RNAP) (248 amino acids) domain on pTRG vector. **Table 3.2.3** lists the primers used. These constructs were then co-transformed into BN469 for β-galactosidase assay (Dove & Hochschild, 2004). BN469 was a kind gift from Dr. Simon Dove. For BTH complementation assays, recombinant pBT and pTRG carrying the PA1611 (202–505) and *retS* (393–652) were used in various combinations to co-transform into BN469 cells. The transformants were plated onto LB–X-Gal–IPTG medium containing appropriate antibiotics and incubated at 30 °C for 24 to 36 h. Efficiencies of interactions between different proteins were quantified by measuring the β-galactosidase activity in liquid cultures as described previously (Dove & Hochschild, 2004; Karna et al., 2010). For β-galactosidase assay, Individual colonies from the transformation plates were inoculated into 3 mL of LB containing the appropriate antibiotics and 0.5 mM IPTG for 14-16h. Thirty microliters of overnight culture was inoculated into 3 mL of LB supplemented with antibiotics and IPTG at the same concentration used for the overnight culture until $OD_{600}$ of 0.3-0.7. The cultures were placed on ice for 20 min before $OD_{600}$ was recorded. To permeabilize cells, 800 μl of Z-buffer (Dove &

Hochschild, 2004) and 30 µl of 0.1% SDS solution were added to 200 µl of bacterial suspension. Chloroform (60 µl) was then added to the suspension. The tubes were vortexed for 6 s and incubated at 28 °C for 10 min. The reaction was started by adding 200 µl of 0.4% o-nitrophenol-β-galactoside (ONPG) in Z buffer (without β-mercaptoethanol). The reaction was stopped by adding 0.5 ml of a 1 M $Na_2CO_3$ solution. $OD_{420}$ and $OD_{550}$ were then recorded. One unit of β-galactosidase activity corresponds to the hydrolyzation of 1 nmol of ONPG per min at 28 °C. The positive controls used were pTRGGAl1[P] and pBT-LGF2. Empty vectors pBT and PTRG were used as negative controls. For BTH assay using colony forming units counting on double selective media, as per Agilent protocol, derivatives of pBT and pTRG were co-transformed into *E. coli* XL1-BlueMRF' Kan[r] cells and selected on selective screening plates and the positive colonies were verified by patching on dual selective screening plates according to the manufacturer's instructions.The non-selective medium consisted of M9 minimal media agar plates supplemented with 12.5 µg/ml tetracycline, 25 µg/ml chloramphenicol, and 50 µg/ml kanamycin. The selective screening media consisted of M9 minimal media agar plates supplemented with 12.5 µg/ml tetracycline, 25 µg/ml chloramphenicol, and 50 µg/ml kanamycin and (5 mM 3-AT). The double selective medium tests for activation of the second reporter gene, *aadA*, encoding streptomycin resistance. To assay for transcriptional activation of the *aadA* reporter, cells from a putative positive colonies from a selective screening medium (5mM 3-AT) plate were patched onto a dual selective screening medium plate. As indicators of growth on the dual selective screening medium, patches of positive control cotransformants (pBT-LGF2 + pTRG-Gal11[P], taken from a selective screening medium plate) and negative control cotransformants (e.g., recombinant pBT + pTRG empty vector, taken from a nonselective screening medium plate) were included (Agilent, USA).

## 3.3 Results

### 3.3.1 Molecular modeling of PA1611-RetS interaction and identification of key amino acid residues

To investigate the structural basis of the interaction between PA1611 and RetS and to elucidate the amino acids involved in this interaction, an approach of sequence analysis, molecular modeling, and model-guided mutagenesis was followed. A comprehensive bioinformatics analysis of PA1611, RetS, and GacS revealed sequence homology and conserved features that are unique to the respective families. Using Lalign (Expasy), 55% similarity between full-length PA1611 and GacS was identified using the Smith-Waterman algorithm and BL50 substitution matrix (**Figure 6A**). PA1611 contains two transmembrane (TM) domains as predicted by the TMpred server, an HisK–Adenylyl Cyclase-Methyl-Accepting Protein phosphatase (HAMP) domain, Histidine Kinases A (HisKA), histidine kinase-like ATPase (HATPase) and a signal receiver (REC) domain present in tandem, similar to GacS with the exception of the absence of an Hpt domain in PA1611. RetS has seven TM regions, an HisKA (dimerization/phosphoacceptor) domain, an HATPase domain, and two signal receiver domains. The crystal structure is available only for the N-terminal region of this protein from residues P44 to E185, which does not harbor the important functional domains. Therefore, the HisKA domain and the HATPase domains of RetS from 393 to 652 amino acids were modeled. A homology-based molecular model of PA1611 from residues 202 to 505 that harbors the HAMP, HisKA and HATPase domains was constructed using Swiss model (**Figure 7A**). The Ramachandran plots for the predicted models were obtained from RAMPAGE (**Figure 7B**). RetS and PA1611 showed around 25% and 30% sequence identity with the template(s). QMEAN Z-score is provided by Swiss-Model to evaluate the quality of the

generated molecular models. QMEAN Z-score provides an estimate of the 'degree of nativeness' of the structural features observed in a model and the experimental structures (Benkert et al., 2011). Average QMEAN Z-scores for X-ray diffraction, NMR, and EM structures are −0.58, −1.19 and −2.00 respectively (Benkert et al., 2011). The generated models of RetS and PA1611 showed QMEAN Z-Score values of -1.728 and -2.256 respectively, which are acceptable values for homology-based molecular models (Benkert et al., 2011). The quality of the RetS and PA1611 molecular models were further analyzed by Ramachandran plot, which showed only around 1% residues in the outlier region in both models. The generated molecular models of the PA1611 and RetS were docked using the ZDOCK program (**Figure 7B**). Docking simulations between PA1611 and RetS revealed a series of H-bonding and hydrophobic interactions. **Table 3.3.1** lists the predicted intermolecular interactions between the two proteins and the amino acids involved. A total of seven residues, F269, M272, E276, T279, S310, Q444, and Y453 in PA1611 and corresponding six residues, R509, E511, Q517, E547, R567, and Q624 in RetS were predicted to be involved in the interaction. These amino acids were then targeted for site-directed mutagenesis in the respective proteins. Two types of mutations were made at each position. First, mutations were made to a smaller and aliphatic amino acid, A (alanine), with the expectation that this substitution will have a minimal effect on protein folding but will give insights into the function of the residue being replaced. Second, mutations were made with structurally and functionally similar amino acid residue substitution such as F (phenylalanine) to Y (tyrosine) or T (threonine) to S (serine). The mutants generated were characterized by their effect on interaction and function. As negative controls, two other point mutations were made as well. One-point mutation A463T was made in PA1611 distal to the predicted PA1611-RetS interaction region and another mutation K316A located close but not within the interaction region.
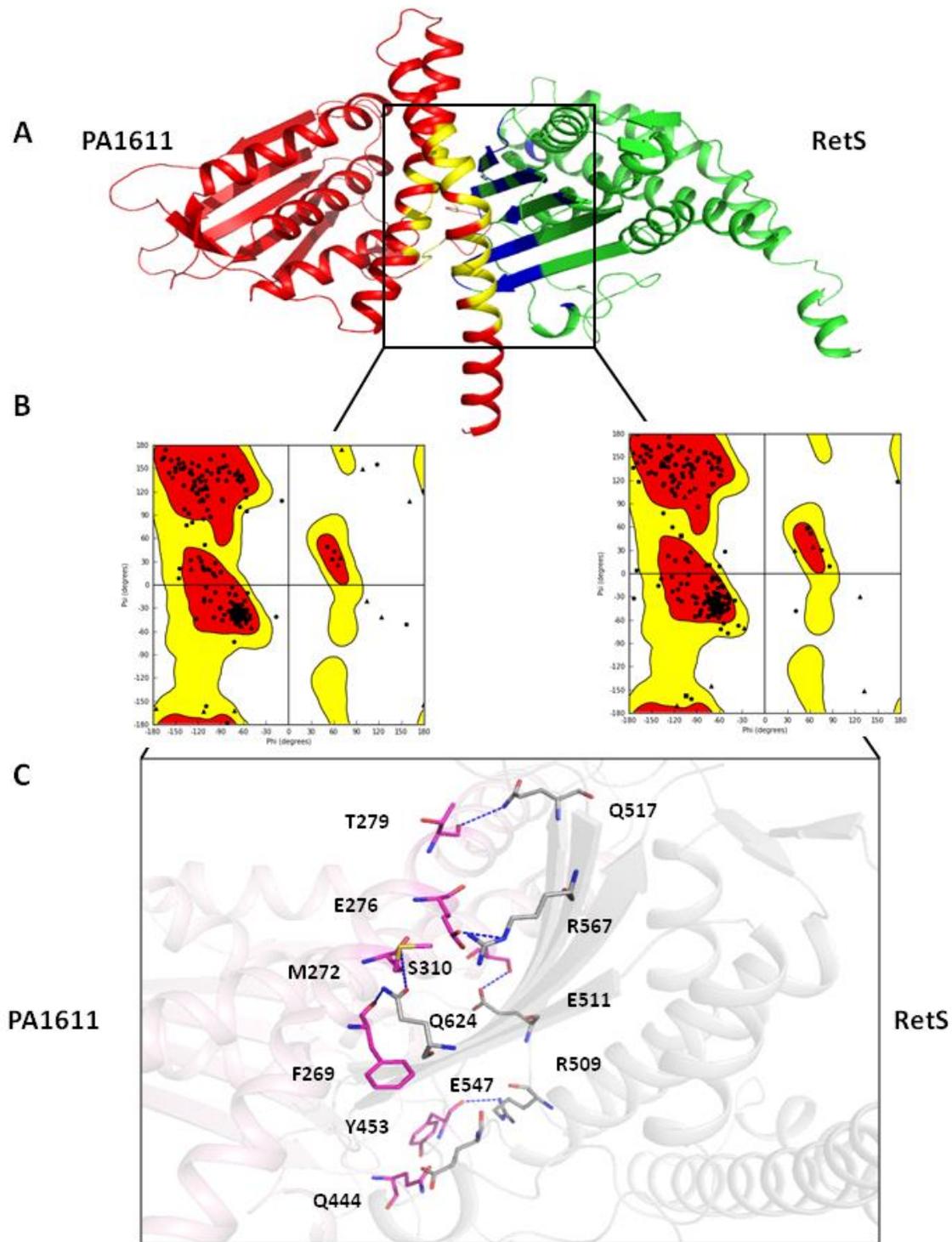
**Figure 7 Homology-based model for RetS and PA1611 structures predicted using Swiss model. A.** Three-dimensional molecular model representation of PA1611 (red) from 205 to 505

residues and RetS (green) from amino acid residues 393 to 652. The respective models are docked using ZDOCK program, and the visual images for the same were generated in PyMol. The regions predicted to interact between the proteins are shown in blue and yellow, respectively. **B.** The intermolecular interactions between the two proteins and the amino acids involved are shown. A total of seven residues F269, M272, E276, T279, S310, Q444, and Y453 in PA1611 (pink) and six residues R509, E511, Q517, E547, R567, and Q624 in RetS (gray) are predicted to be involved in the interaction. The visual images of the structures were generated in PyMOL.

**Table 3.3.1 List of predicted amino acid residues involved in the PA1611 and RetS interaction.**

| PA1611: Predicted residue (Residue atoms) | RetS: Residue interacting with PA1611(Residue atoms) | Functionally/Structurally conserved residue |
|---|---|---|
| F269(O-backbone) | Q624 (NE1) | Y |
| M272(SD) | Q624(OE1) | C |
| E276(OE2) | R567(NE) | D |
| T279(O-backbone) | Q517(NE2) | S, V |
| S310(OG) | E511(OE2) | T |
| Q444(NE2) | E547(OE2) | N |
| Y453(O-backbone) | R509(NH1) | F |

### 3.3.2 Assessment of the interactions between non-cognate HisKA–HisKA domains in PA1611 and RetS using bacterial two-hybrid assay

To characterize the interaction between PA1611 and RetS, Bacterial Two-Hybrid (BTH) bait vector pBT containing PA1611 (202–505) was tested for interaction with prey vector pTRG containing RetS (393–652). We used a β-galactosidase activity assay (Dove & Hochschild, 2004) to identify for positive interactions. The activity levels for each of the interactions are shown in **Figure 8A**. Amino acid residues at 269, 276, 279, and 444 in PA1611 were shown to be significant in PA1611–RetS interaction, while M272, S310, and Y453 seemed not to have a significant role. F269, when substituted with A, weakened the interaction and this was reversible by substitution with a structurally similar residue Y. E276 demonstrated similar results and the interaction strength was fully restored upon substitution with D. T279, however, was not fully reversible upon substitution with either V or S. Q444 mutants demonstrated distinct effects. Both Q444A and Q444N appear to alter the strength of the interaction significantly in this assay. We further performed the PA1611-RetS interaction assay by BacterioMatch Two-Hybrid system (Agilent Technologies, United Kingdom) by counting colony forming units (CFU) on double selective medium, according to the manufacturer's guidelines (**Figure 9**). The observed trend remained like that with the β-galactosidase assay except Q444A which was not significantly different from the wild type in the BTH CFU counting assay. To confirm whether the obtained results were due to the changed interaction and not due to a difference in the levels of protein expression, the DNA fragments containing the wild type and mutated PA1611 were then cloned in a pETSUMO expression vector and the expressed proteins isolated and analyzed by SDS-PAGE. No difference in protein levels was observed between pETSUMO containing wild-type PA1611 and pETSUMO containing PA1611 with any of the seven-point mutations (**Figure 8B**).

**A**
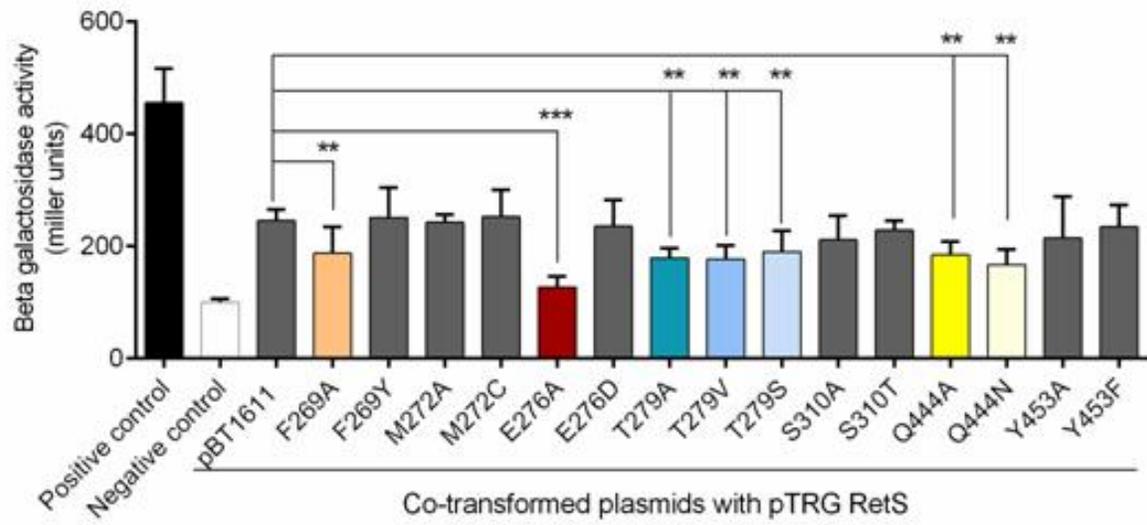


**B**
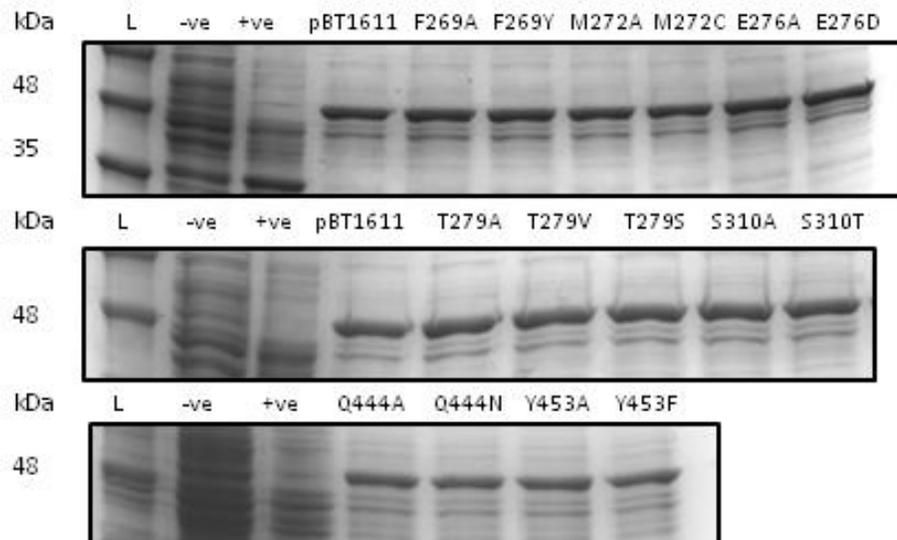
**Figure 8 Bacterial two-hybrid analysis for PA1611 and RetS interaction. A.** Interactions between PA1611 and RetS were quantified in BN469 using a β-galactosidase assay and mean Miller units of at least three independent measurements are presented. Empty vectors pBT and pTRG in BN469 was used as negative control. pBTLGF2 and pTRGGal1$^P$ in BN469 were used as positive control. Data were analyzed using one-way ANOVA with Dunnette post-hoc test, NS $p > 0.05$, *$p < 0.05$, **$p < 0.01$ and ***$p < 0.001$, ****$p < 0.0001$. pBT1611 represents the wild-type PA1611 in pBT vector co-transformed with non-mutated RetS in PTRG vector. The substitution mutants in PA1611 in pBT vector co-transformed with wild-type RetS have been represented as the single-lettered amino acid residue at the respective position followed by the amino acid it has been substituted with (e.g., F269A, F269Y…). The mutant groups demonstrating a significant role in interaction have been color-coded: F269 (Orange), E276 (Reds), T279 (Blues) Q444 (Yellows). The wild-type PA1611 and the mutants that demonstrated the effect on interaction like the wild-type pBT 1611 have been colored gray. **B.** SDS-PAGE analysis for PA1611 tagged with 6xHis in pETSUMO (46KDa). Lane L (Blue elf protein ladder), negative control (-ve) is the total protein from BL21(DE3) cells containing empty vector under inducing conditions, BL21 cells containing pETSUMO/CAT control vector is shown as the positive control (+ve). The molecular weight of CAT fusion protein is approximately 39 kDa. A sample of 10 μg of total protein was loaded in each lane for 12 % SDS-PAGE analysis, followed by staining with Coomassie blue.

**A**
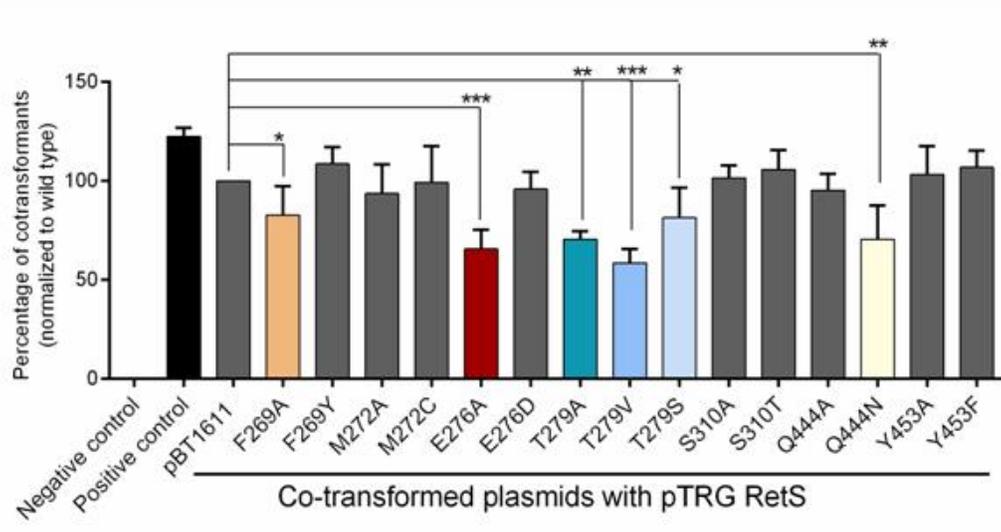


**B**
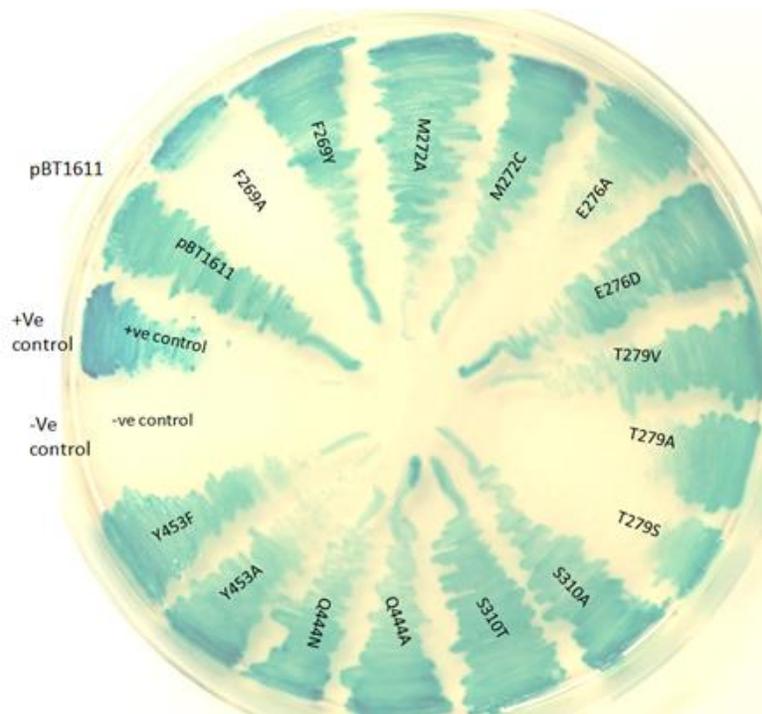
**Figure 9 PA1611-RetS interaction analyzed by the bacteriomatch two-hybrid system. A.** The BacterioMatch II two-hybrid system (Agilent, USA) was used to detect protein–protein interactions of different pairs of PA1611/RetS proteins, as described in the "Materials and Methods." Co-transformation with pBT-LGF2 and pTRG-Gal1$^P$ served as a positive control while co-transformation with pBT and pTRG as a negative control. The ratios were normalized against pBT1611(wild-type PA1611)-pTRGRetS. Data were analyzed using one-way ANOVA with Dunnette post-hoc test, NS $p> 0.05$, $*p < 0.05$, $**p < 0.01$ and $***p < 0.001$, $****p < 0.0001$. WT represents PA1611 wild-type in pBT vector co-transformed with wild type RetS in PTRG vector. The substitution mutants in PA1611 in pBT vector co-transformed with wild-type RetS have been represented as the single lettered amino acid residue at the respective position followed by the amino acid it has been substituted with (e.g., F269A and F269Y). The mutant groups demonstrating a significant role in interaction have been color-coded: F269 (Orange), E276 (Reds), T279 (Blues) Q444 (Yellows). **B.** The growth of BN469 on double selective medium (M9 minimal media agar plates supplemented with 12.5 µg/ml tetracycline, 25 µg/ml chloramphenicol, and 50 µg/ml kanamycin +5 mM 3-AT + Strep+ X-gal) to visualize protein–protein interactions.

### 3.3.3 HisKA and HATPase domains in PA1611 are important for PA1611 function

To verify whether these predicted residues were important in the functioning of PA1611 *in vivo* and whether they could affect the PA1611–RetS interaction in *P. aeruginosa*, we cloned the full-length PA1611 with and without the point mutations at the aforementioned positions in the expression vector pAK1900. These constructs were then introduced into a PA1611 knockout strain PA(ΔPA1611) containing *luxCDABE* reporter fused to the *exoS* promoter on the chromosome, and the promoter activity of *exoS* was tested. The PA(ΔPA1611) strain containing pAK1611 (the wild-type PA1611) was used as a control. Bacterial growth was monitored at the same time. The normalized *exoS* promoter activities over time in the wild-type and mutated pAK1611 are presented in **Figure 10** The time-course of *exoS* promoter activity suggested significant differences at the 6h time point in the majority of the mutants, therefore, the *exoS* expression and T3SS protein secretion were analyzed in detail at this time-point in the mutants.

As shown in **Figure 11A**, PA1611 mutants, F269A, E276A, T279A, and Q444N showed significantly higher *exoS* promoter activity as compared with the wild-type pAK1611. Conservative substitutions F269Y and E276D, as well as Q444A mutants, showed phenotypes similar to the wild-type pAK1611. Change in *exoS* promoter activity at much lesser magnitude was observed for substitutions at positions M272, S310, and Y453 (**Figure 10**) Interestingly, F269A increased the *exoS* promoter activity by 50-fold as compared with the wild-type PA1611 and this effect was reversed with the conservative substitution F269Y. Similarly, E276A mutant also increased the *exoS* promoter activity by 100-fold, and this effect was fully reversed with the conservative E276D substitution. Similar to what was observed with the BTH assay, T279 and Q444 demonstrated interesting results in these functional experiments. T279A increased *exoS* promoter activity by approximately 70-fold as compared with the wild-type pAK1611. T279 was

never fully rescued upon substitution with either V or S. The Q444N substitution increased the *exoS* promoter activity by about 30-fold as compared with the wild-type pAK1611. The negative controls, K316A and A463T, situated around the proposed region of interaction, demonstrated no significant difference in *exoS* promoter activity as compared with the wild type (**Figure 12**). The changes in *exoS* promoter activity were confirmed by measuring the secreted ExoS protein in culture supernatants at 6 h (**Figure 11B**). A positive correlation between the *exoS* promoter activity and ExoS protein secretion was observable.

To further analyze the phenotypical effect of the mutations, all the PA1611 mutants were then analyzed for swimming and swarming motility. These motilities were assessed by measuring the diameters of the migration front after 12-14 h incubation. **Figure 13** shows the swarming (top rows) and swimming (bottom rows) motility for PAO, PA($\Delta$PA1611), pAK1611 and the mutants. There was a complete loss of motility for $\Delta$PA1611 carrying pAK1611. There was a significant increase in swimming and swarming motility for F269A, E276A, and T279A. As expected, the motilities were reversed to the level of the wild-type PA1611 in F269Y and E276D, while no reversal was observed for T279S, T279V, and Q444N (**Figure 13A**). Less significant differences in swimming and swarming assays were observed for M272, S310, and Y453 mutants (Fig. S5). The results obtained for the substitution mutants in were in line with the *exoS* promoter activity results. Next, to define the effect of the mutations on biofilm formation, we performed a static crystal violet biofilm assay. A statistically significant decrease in biofilm formation was observed for F269A, E276A, T279A, T279V and T279S ($p<0.001$) (**Figure 13B**). The biofilm formation was restored to the wild-type levels in F269Y and E276D. Similar to the effect on *exoS* expression, biofilm formation of Q444N showed a significant difference. The mutant formed significantly less biofilm than the wild-type PA1611 ($p<0.05$). No significant difference in

biofilm formation was observed for the other mutants. The negative control mutants K316A and A463T showed no significant changes in motilities as compared with the wild-type PA1611 except that a slight increase in swarming motility was observed with A463T (**Figure 14**).
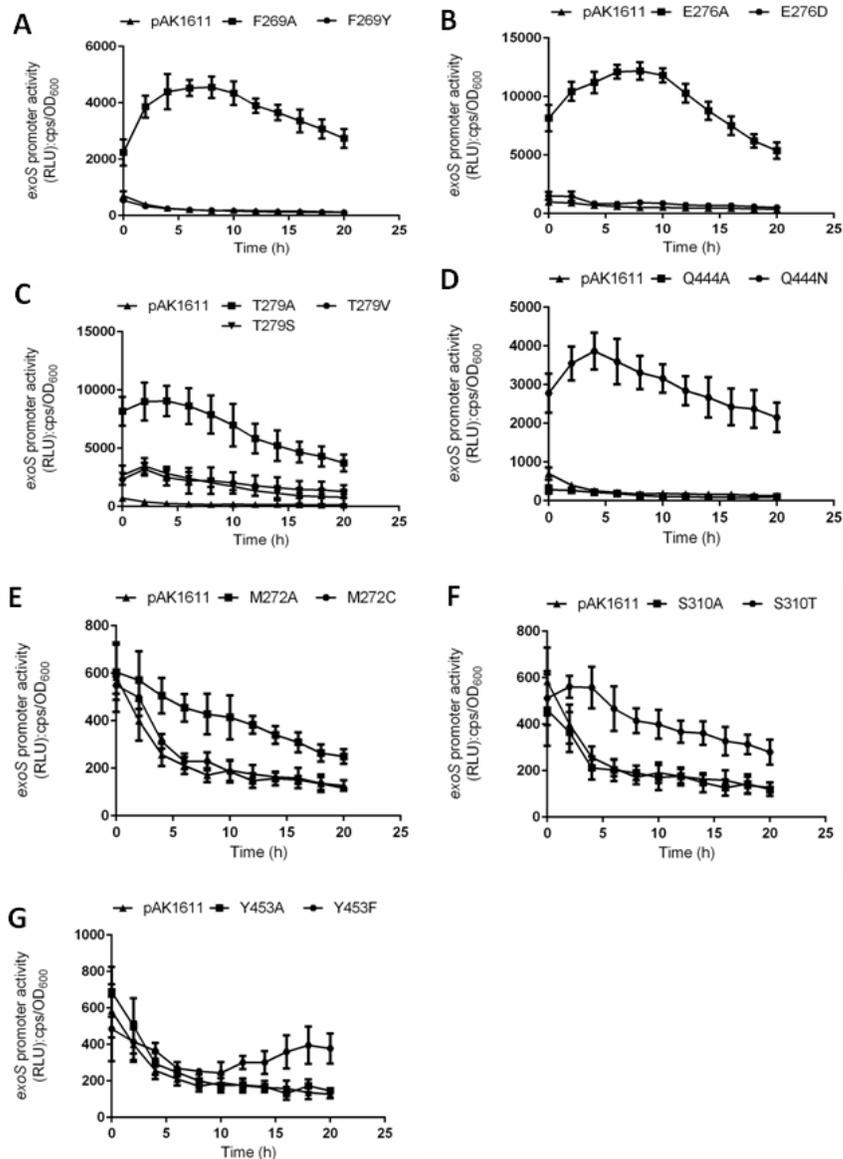
**Figure 10 The promoter activity of *exoS* in wild type and mutant PA1611 in PA(ΔPA1611).**
All experiments were done in a Δ PA1611 background containing plasmid pAK1611, carrying the wild-type (pAK1611) or the PA1611 point mutations, under T3SS inducing condition (LB+EGTA). Strain PA(ΔPA1611) (pAK1611) is used as a control and is labeled as pAK1611 here. **(A-G)** The *exoS* promoter activity in pAK1611 and mutants: F269 **(A)**; E276 **(B)**; T279 **(C)**; Q444 **(D)**; M272 **(E)**; S310 **(F)**; and Y453 **(G)**. The results represent the average of triplicate experiments, and the error bars indicate standard deviation.
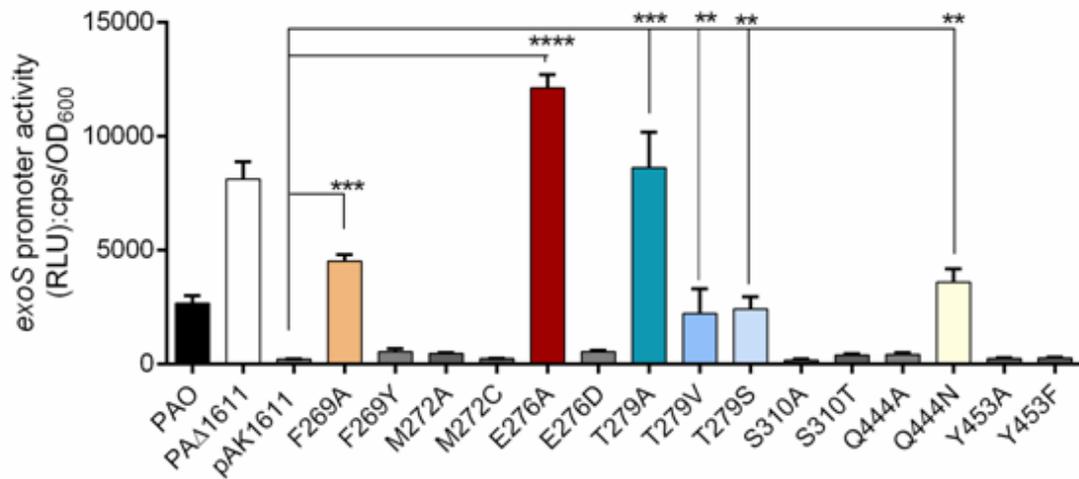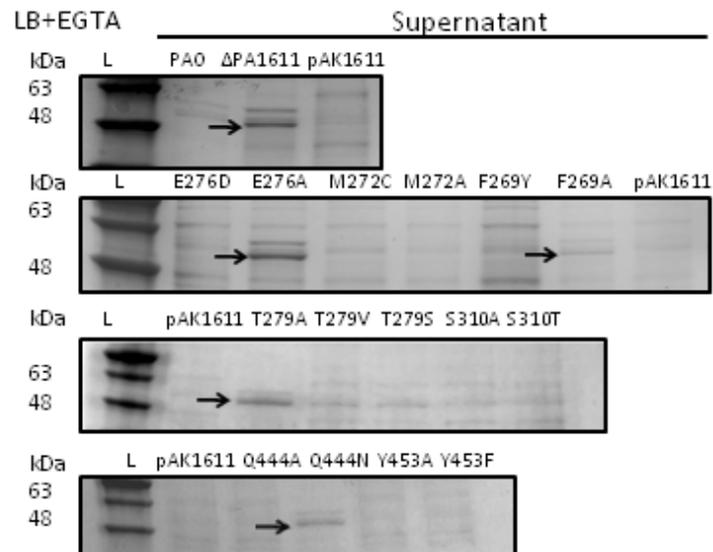
**Figure 11 *exoS* promoter activity and ExoS protein secretion in wild-type PA1611 and its substitution mutants.** These experiments were done in a PA(ΔPA1611) background using the plasmid pAK1611 carrying the wild-type or the various PA1611 mutants. The wild-type is used as the control and is labeled here as pAK1611 **A.** The *exoS* promoter activity at 6 h is normalized

to growth and shown in relative luminescence unit (RLU): cps (counts per second)/$OD_{600}$. The values shown are an average of three independent experiments. Data were analyzed by multiple comparisons using one-way ANOVA with Dunnette post-hoc test, NS $p > 0.05$, *$p < 0.05$, **$p <$ 0.01 and ***$p < 0.001$, ****$p < 0.0001$. The mutant groups demonstrating a significant role in interaction have been color coded. **B.** Secreted ExoS protein at 6 h under T3SS inducing conditions (LB+EGTA). Secreted ExoS protein in the culture supernatants was analyzed by 12 % SDS-PAGE followed by staining with Coomassie blue. Shown here are L-protein ladder, PAO, PA(ΔPA1611), wild-type control PA(ΔPA1611)(pAK1611) (shown as pAK1611) ) and the other mutants are shown in the respective amino acid at its position number followed by substituted amino acid in single letter The location of the ExoS bands (49 kDa) is indicated by arrows.
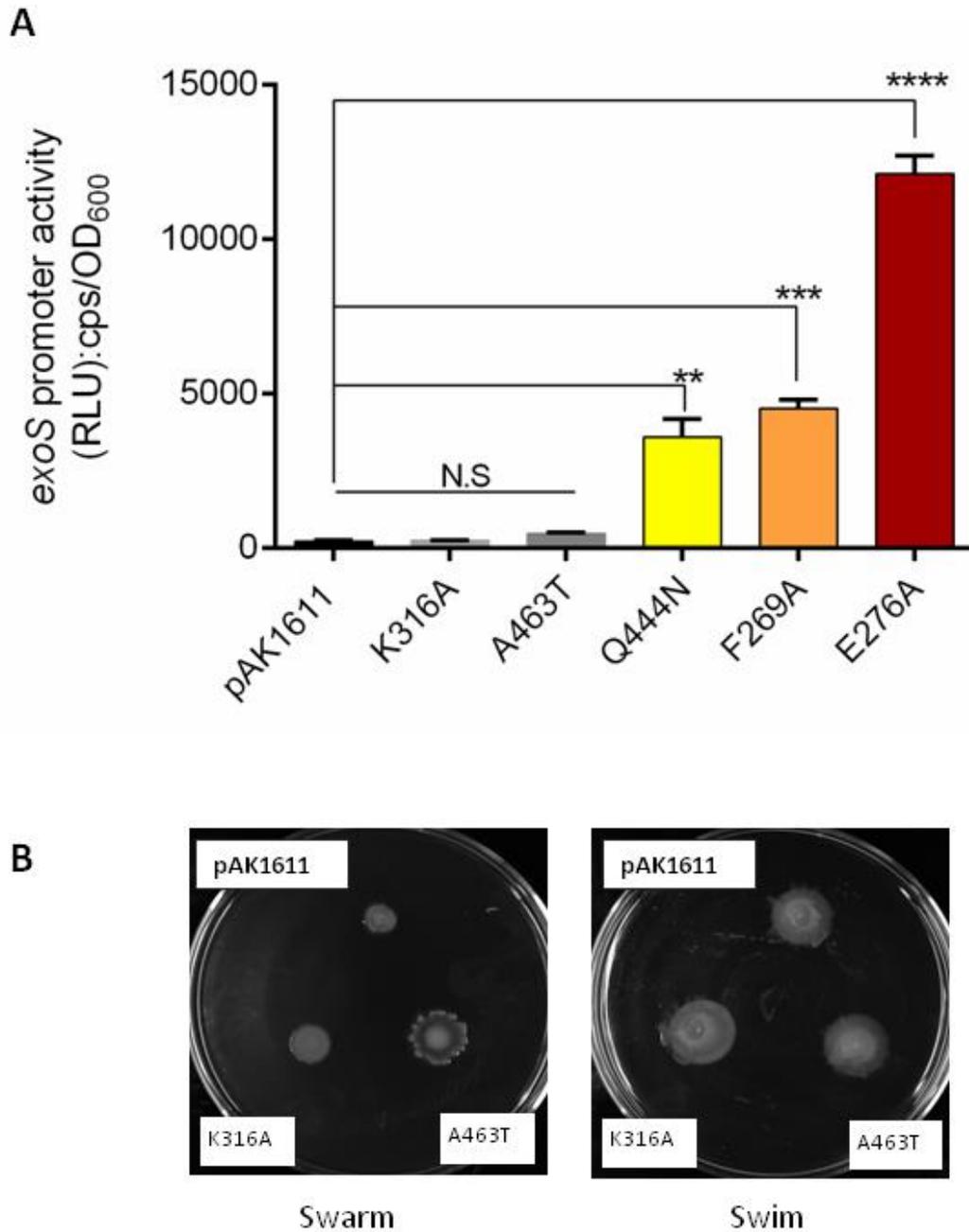
**Figure 12 Effect of PA1611 amino acid substitutions close and distal to predicted PA1611-RetS interaction region.** The experiments were done in PA(ΔPA1611) harboring plasmid pAK1611, carrying the wild-type (pAK1611) or the PA1611 point mutations. Strain PA(ΔPA1611) (pAK1611) is used as a control and is labeled as pAK1611 here. **A.** *exoS*

promoter activity at 6 h in pAK1611, K316A, A463T, Q444N, F269A, E276A. B. Effect of motility on the K316 and A463 substitution mutations. The results represent the average of triplicate experiments, and the error bars indicate standard deviations. Data were analyzed using one-way ANOVA with Dunnette post-hoc test, NS $p > 0.05$, $*p < 0.05$, $**p < 0.01$, and $***p < 0.001$, $****p < 0.0001$.
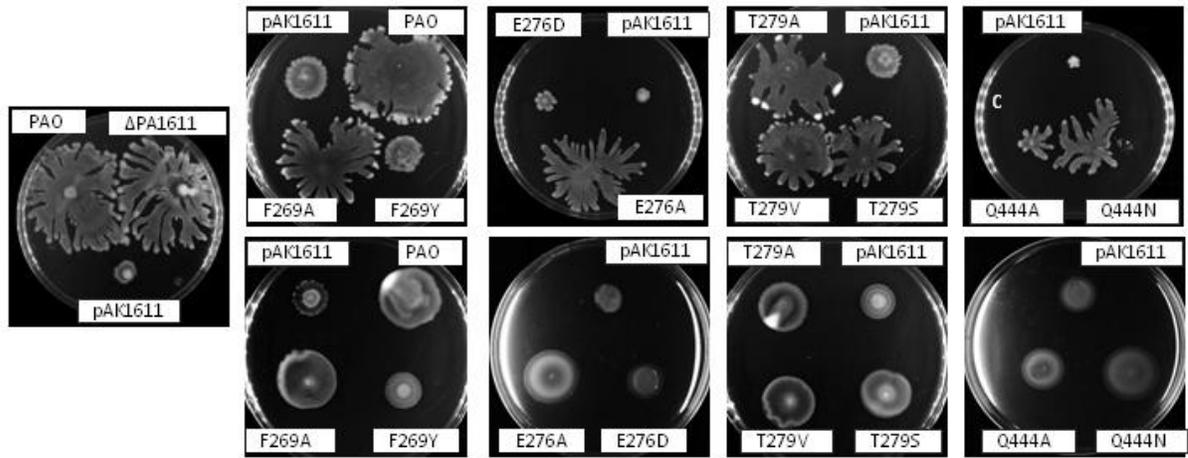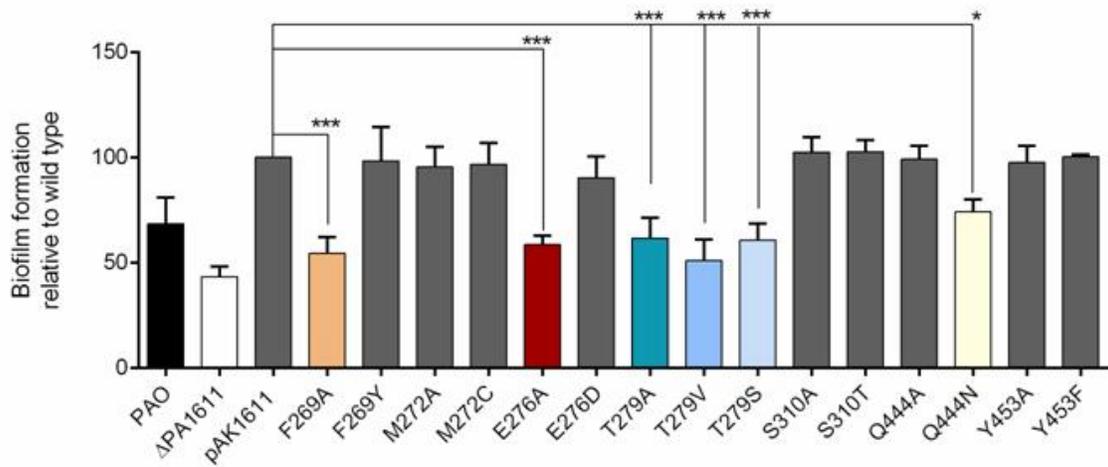
**Figure 13 Influence of substitutions in PA1611 on motility and biofilm formation.** These experiments were done in a PA(ΔPA1611) background using the plasmid pAK1611 carrying the wild-type (labeled as pAK1611) or the various PA1611 mutants. **A.** The effect of substitutions at F269, E276, T279, and Q444 on swarming (top row) and swimming (bottom row) are shown. The experiments were repeated at least three times, and similar results were observed. **B.** Biofilm formation of the PA1611 mutants compared with that of the wild type. Data are shown as the percentage of the wild-type. Data was analyzed using one-way ANOVA with Dunnette post-hoc test, NS $p > 0.05$, *$p < 0.05$, **$p < 0.01$ and ***$p < 0.001$, ****$p < 0.0001$. Error bars indicate standard deviations.
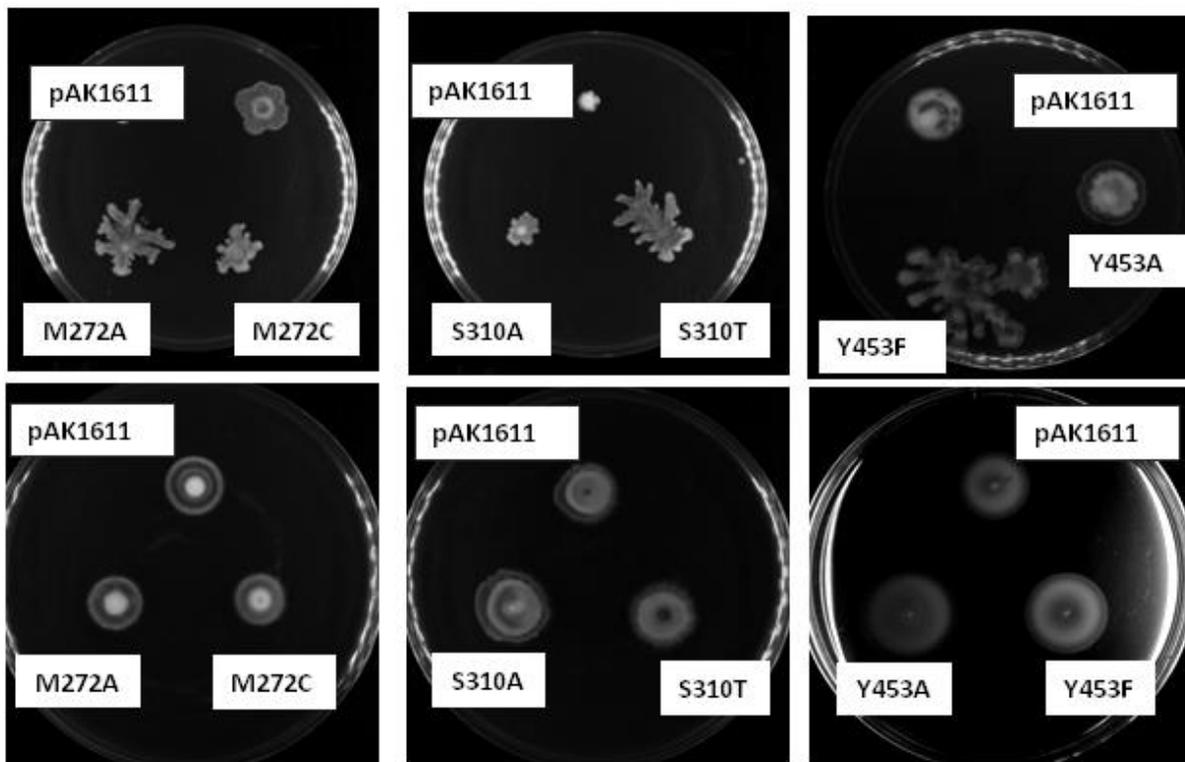
**Figure 14 Influence of PA1611 mutants on swarming and swimming motility**. Effect of substitutions at M272, S310, and Y453 on swarming (top row) and swimming motility (bottom rows), compared with the wild-type PA(ΔPA1611) (pAK1611), shown here as pAK1611.

**3.3.4 Changes observed for PA1611 point mutants were caused through the GacS/GacA-Rsm signaling pathway**

We have previously shown that PA1611 regulation works through the Gac-RsmA system (Kong et al., 2013). The effect of *gacA* deletion on *exoS* promoter activity is shown in **Figure 15**. To confirm that the mutations in PA1611 only affected its function *via* the Gac-RsmA pathway, we tested the mutants carried on pAK1900 in a *gacA*-deletion (Δ*gacA*) background. The *exoS* promoter activity was compared in the Δ*gacA* strain containing thee *exoS-luxCDABE* reporter on its chromosome. Because E276 substitutions in PA1611 demonstrated a significant effect in the phenotypic assays and the effect was fully reversible with a functionally similar residue, we chose E276 as a representative for this part of the experiment. *exoS* promoter activity was measured respectively in Δ*gacA* containing pAK1611(wild-type PA1611), E276A, and E276D. The results indicate that the presence or absence of mutations in PA1611 did not affect *exoS* promoter activity in the Δ*gacA* background (**Figure 16A**). In agreement with this result, swarming assay showed similar outcomes (**Figure 16B**). All these results confirm that PA1611 exerts its regulation on target genes through the GacS/GacA-Rsm pathway.

It has been shown that the GacS/GacA signal transduction system works exclusively through its control over the transcription of the regulatory small RNAs, RsmY and RsmZ. (Brencic et al., 2009) The impact of the mutations in PA1611 on *rsmZ* expression levels was further measured using the *lux*-based reporters. Once again E276A and E276D were selected as representative mutants in this experiment. The strain PA(ΔPA1611) (pAK1611) containing the wild-type pAK1611 is labeled as pAK1611 for simplicity. CTX-*rsmZ* reporter fusion was integrated onto the chromosomes of the test strains to measure the promoter activity of *rsmZ*. As shown in **Figure 16C**, higher *rsmZ* promoter activity was observed in pAK1611 as compared with E276A and

E276D. The *rsmZ* promoter activity for E276D reverted, but not to the levels of the wild-type control. The difference between E276D and the wild type is unexpected. Collectively, our results confirmed that PA1611 functions through the GacS/GacA-Rsm pathway and indicated that the phenotypic impact of the PA1611 point mutants was probably enacted by this signaling pathway.
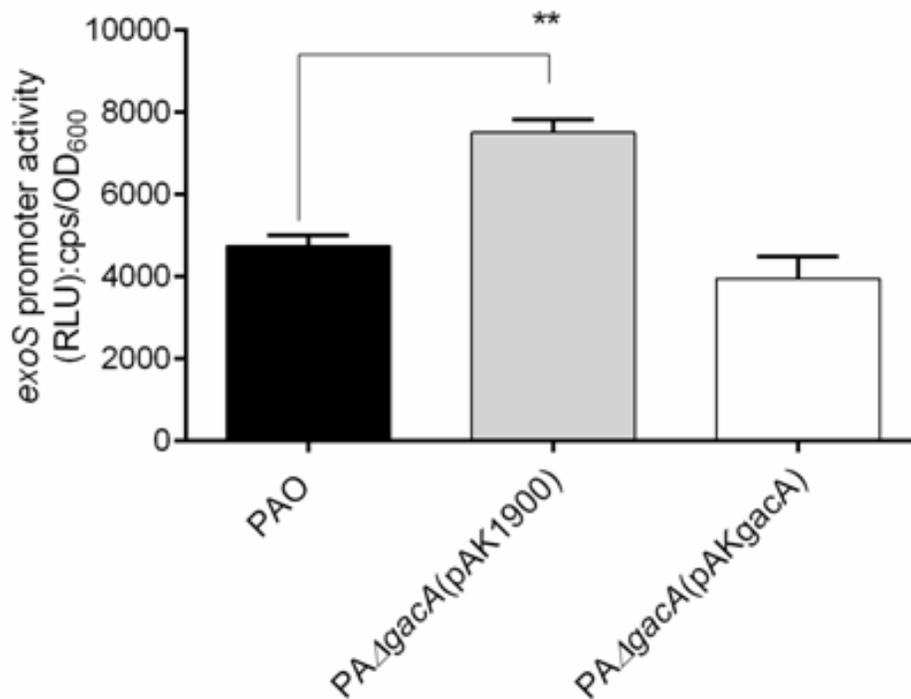
**Figure 15 *exoS* promoter activity in PAO, *gacA* deletion and the complementation strain.** A CTX-*exoS* reporter fusion integrated on the chromosome was used to measure the *exoS* promoter activity under T3SS inducing condition (LB+EGTA). This experiment was performed in PAO, pAK1900 in *gacA* deletion background (shown here as pAK1900) and *gacA* complementation strain (shown here as pAK*gacA*). The results represent the average values of triplicate experiments at 6 h, and the error bars indicate standard deviations. Data were analyzed using one-way ANOVA with Dunnette post-hoc test, NS $p > 0.05$, *$p < 0.05$, **$p < 0.01$, and ***$p < 0.001$, ****$p < 0.0001$.
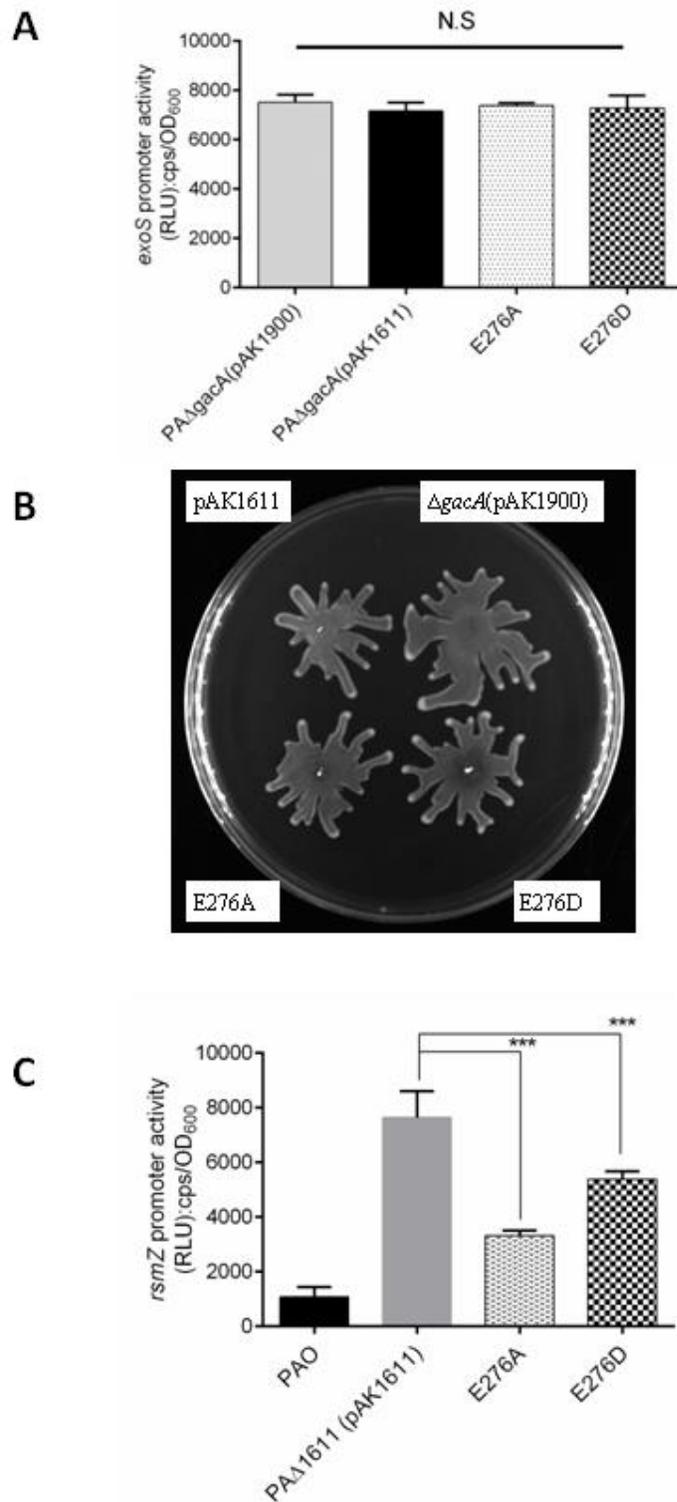
**Figure 16 Effect of substitutions at E276 on *exoS* and *rsmZ* promoter activity in a *gacA* and *PA1611* mutant background respectively. A.** *exoS* promoter activity at 6 h. N.S indicates the

statistically non-significant difference. **B.** Swarming motility of wild-type pAK1611, E276A and E276D in *gacA* deletion strain. **C.** *rsmZ* promoter activity at 6 h in PA(ΔPA1611) (pAK1611) and E276 mutants. PA(ΔPA1611) (pAK1611) is used as the control and is shown here as pAK1611. Data shown are an average of three independent experiments. Error bars indicate standard deviations. Note the *rsmZ* activity was not measured in *gacA* knockout background. Data were analyzed using one-way ANOVA with Dunnette post-hoc test, NS *p > 0.05, *p <* 0.05, ***p < 0.01 and ****p < 0.001, *****p < 0.0001

**3.3.5 Corresponding residues in the HisKA and HATPase domains of RetS are important for PA1611-RetS interaction**

To further test the PA1611-RetS interaction model and verify the residues in RetS that are important in RetS-PA1611 interaction, we performed amino acid residue substitutions for RetS similar to those for PA1611. The residues at all six positions on RetS predicted to interact with PA1611 according to the molecular model were first changed to smaller and aliphatic amino acid A and then to functionally and/or structurally similar residues (**Table 3.3.1**). Thus, similar to the PA1611 experiments described above, we cloned full-length *retS* in pAK1900 in PA(ΔRetS), which is referred to as pAKRetS from here onwards. We performed site-directed mutagenesis at six positions in *retS* in the pAKRetS plasmid. Similar to PA1611, *exoS* promoter activity for RetS and its mutants was measured over time and normalized to bacterial growth. With pAKRetS as the control, a significant increase in *exoS* promoter activity was observable at 6 h for R509A, E547D, R567A and Q624A (**Figure 17A**). At least two-fold increase in *exoS* promoter activity was observed for Q624A and 1.5-fold for R567A mutant which was predicted to interact with E276 and F269 in PA1611 respectively. This effect dissipated upon replacement with conservative substitutions at both positions, Q624N and R567K respectively. Such a result is significant considering PA1611 was not overexpressed in the experimental condition; any change to RetS is expected to decrease its functionality. These results further support the critical role of F269 and E276 in PA1611-RetS interaction as the model predicted. The *exoS* expression was increased significantly in E547D. This outcome was similar to that observed in Q444N, coinciding the model prediction that E547 in RetS interacts with Q444 in PA1611. An increase in *exoS* promoter activity was observed for R509A, and a reversal to wild-type level was observed for the compensatory mutation, R509K (**Figure 17A**).   We also performed a T3SS protein

93

secretion assay to confirm these findings. An increase in secreted ExoS was observed for R567A and Q624A (**Figure 17B**). This effect was reversed upon conservative replacements with R567K and Q624N. No significant difference in the secreted ExoS levels was observed for R509A, R509K, E511A, E511D, Q517A, Q517D, E547A, and E547D.

The RetS mutants R567A and Q624A also showed a decrease in biofilm formation as compared with wild-type pAKRetS (**Figure 17C**). The effect was reversed in R567K and Q624N. No significant change in biofilm formation assay was observed for the other assayed mutants.

To rule out that, besides RetS-PA1611 interaction, these mutations in RetS also affected GacS-RetS interaction, we analyzed the effect of these RetS mutants on *exoS* promoter activity in PA(ΔPA1611) background. Wild-type RetS and R567 and Q624 mutants were expressed on a plasmid and *exoS* activity were measured. No statistically significant difference was observable between PA(ΔPA1611) (pAKRetS) (wild-type RetS, labeled as pAKRetS) and R567A or R567K (**Figure 18**). A similar result was obtained for the comparison between the wild-type RetS and Q624A or Q624N. These results indicated that, in the absence of PA1611, the residue substitutions in RetS did not affect *exoS* expression, suggesting the effect observed previously was most likely a result of changed interaction with PA1611.

**A**

**B**

LB+EGTA — Supernatant

**C**
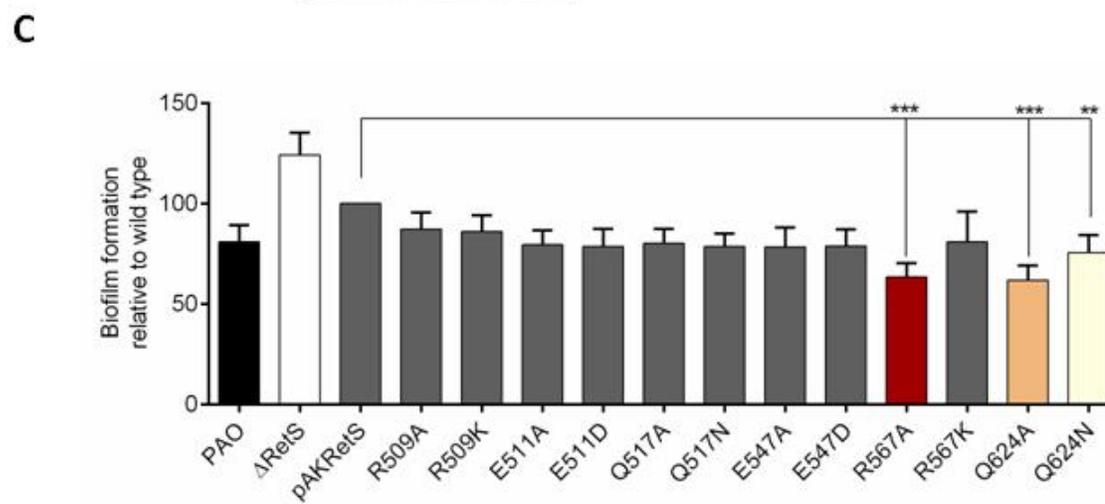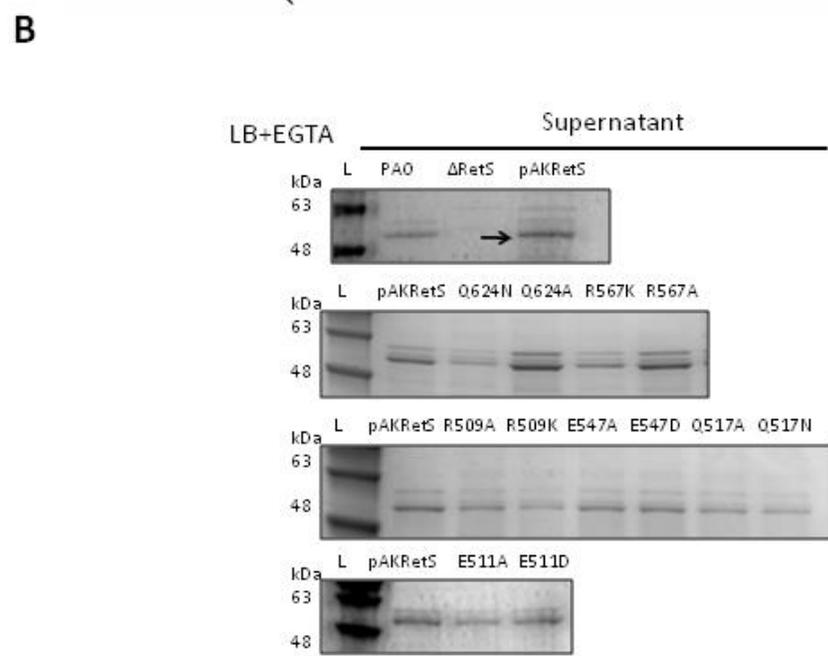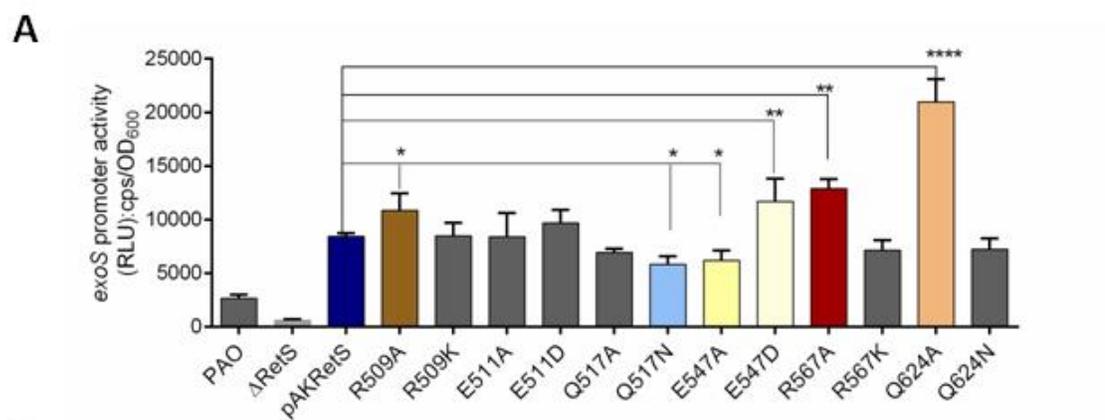
**Figure 17 *exoS* promoter activity, ExoS protein secretion and biofilm formation in  wild type and mutant RetS in PA(ΔRetS).** These experiments were carried out in PA(ΔRetS) using the plasmid pAKRetS, carrying the wild type (shown as pAKRetS) or the various RetS mutants. The mutant groups demonstrating a significant role in interaction have been color-coded corresponding to residues for PA1611 as described before: F269 (Orange), E276 (Reds), T279 (Blues) Q444 (Yellows), Y453 (Browns). Data was analyzed using one-way ANOVA with Dunnette post-hoc test, NS $p > 0.05$, $*p < 0.05$, $**p < 0.01$ and $***p < 0.001$, $****p < 0.0001$. Error bars indicate standard deviations. **A.** The *exoS* promoter activity at 6 h. **B.** ExoS secretion at 6 h under T3SS inducing conditions (LB+EGTA). The location of the ExoS bands (49 kDa) is indicated by arrows. **C.** Biofilm formation of the mutants compared with that of the wild-type pAKRetS control. Data are shown as the percentage of the wild-type. Statistical comparisons were made between mutant and non-mutated pAK1611strains.
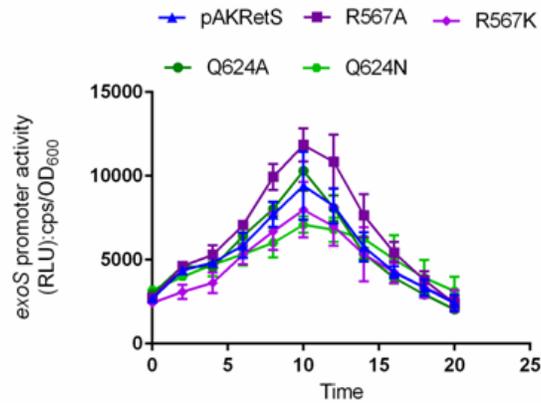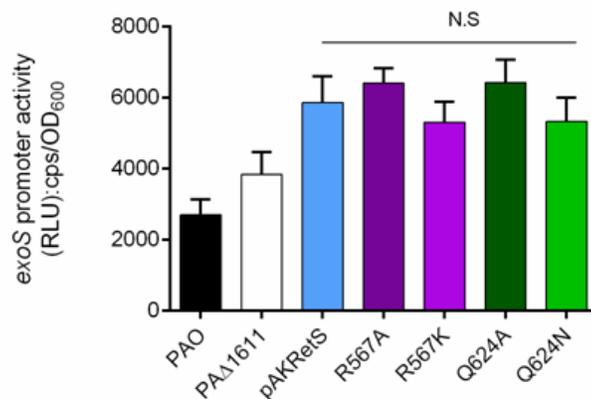
**Figure 18 The promoter activity of *exoS* in wild-type and mutant RetS in PA(ΔRetS).** All experiments were done in a ΔRetS background using a plasmid pAKRetS, carrying the wild-type (pAKRetS) or the pAKRetS containing mutations. CTX-*exoS* reporter fusion integrated on the chromosome was used to measure the *exoS* promoter activity under T3SS inducing conditions (LB+EGTA). Strain PA(ΔRetS) (pAKRetS) is used as a control and is labeled as pAKRetS here. (**A-F**) The promoter activity of *exoS* in pAKRetS wild-type and mutants: R567 (**A**); Q624 (**B**); E547 (**C**); R509 (**D**); E511 (**E**); and Q517 (**F**). The results represent the average of triplicate experiments, and the error bars indicate standard deviations.

**3.4 Discussion**

**3.4.1 Residues in the conserved HisKA and HATPase domains in PA1611 are key to RetS-PA1611 direct interaction**

*P. aeruginosa* is a ubiquitous gram-negative bacterium, capable of growing in various conditions, even in distilled water (Favero et al., 1971). Its adaptability is attributable to the complex and extensive gene regulation, as well as intricate signaling mechanisms. Though a single TCS may function independently in several different ways, the interaction between TCSs can be described as Boolean operators with an analogy to neural networks, as was first noted in *E. coli.* (Gronlund, 2004; Hellingwerf et al., 1995) The direct interaction between cognate and non-cognate TCS proteins is a recently uncovered strategy that bacteria use to integrate multiple signals (Gardner et al., 2015). The proteins involved may also affect the RRs to either protect from de-phosphorylation or cause de-phosphorylation (Mitchell et al., 2015) and function as negative or positive regulators of the partner TCS. Hybrid HKs are an important group that facilitates signal integration (Huynh et al., 2015; Koretke et al., 2000; Norsworthy & Visick, 2015). HHK RetS controls GacS by forming a heterodimer between their H1 domains. Such an interaction between RetS and GacS prevents GacS from phosphorylating GacA. GacS when phosphorylated activates transcription of small RNAs RsmY and RsmZ. RsmY and RsmZ can sequester transcriptional regulator RsmA to mediate chronic phase of infection characterized by the formation of biofilms. It has been shown previously that PA1611 may interact with RetS directly, however, the exact nature of this interaction, residues involved, and the physiological effects were unknown. The study forms one of few reports that show key regulatory proteins may exert control via direct and specific interaction with other non-cognate protein. It has been shown here that PA1611 interacts with RetS in a similar manner to RetS-GacS interaction, by forming a

heterodimer between their HisK domains. The molecular analyses were guided by extensive bioinformatics analysis. Based on domain similarity between PA1611 and GacS, it was hypothesized that the interaction between PA1611 and RetS could be similar in mechanism to RetS/GacS. Though a partial structure is available for RetS, (Jing et al., 2010; Vincent et al., 2010) it falls outside of the predicted interaction zone. PA1611 and RetS were modeled based on homology followed by molecular docking to identify residues critical in interaction. These were followed by BTH assay to examine the effect of mutations for the specific residues on interaction in *E. coli.* Results from BTH assay identified four key residues in the conserved HisKA and HATPase domains in PA1611, namely, F269, E276, T279, and Q444 that demonstrated a significant effect on the interaction. The effect of these mutations on the PA1611 function was confirmed in *P. aeruginosa*.

The effects of mutations at F269 and E276 were fully restored upon substitution with structurally and functionally similar residues and could be explained as such. PA1611 residues T279 and Q444 demonstrated some interesting results however which could not be explained simply by having affected PA1611-RetS interaction.

We used the molecular model of PA1611-RetS to interpret the functional results of T279 and Q444 mutations (**Figure 19A**). The PA1611 molecular model shows T279 to be present in the α-helix of HisKA of PA1611. The backbone carbonyl atom of T279 interacts with the amino group side chain of the Q517 present at 3.4Å, in the loop region of RetS (**Figure 19B**).
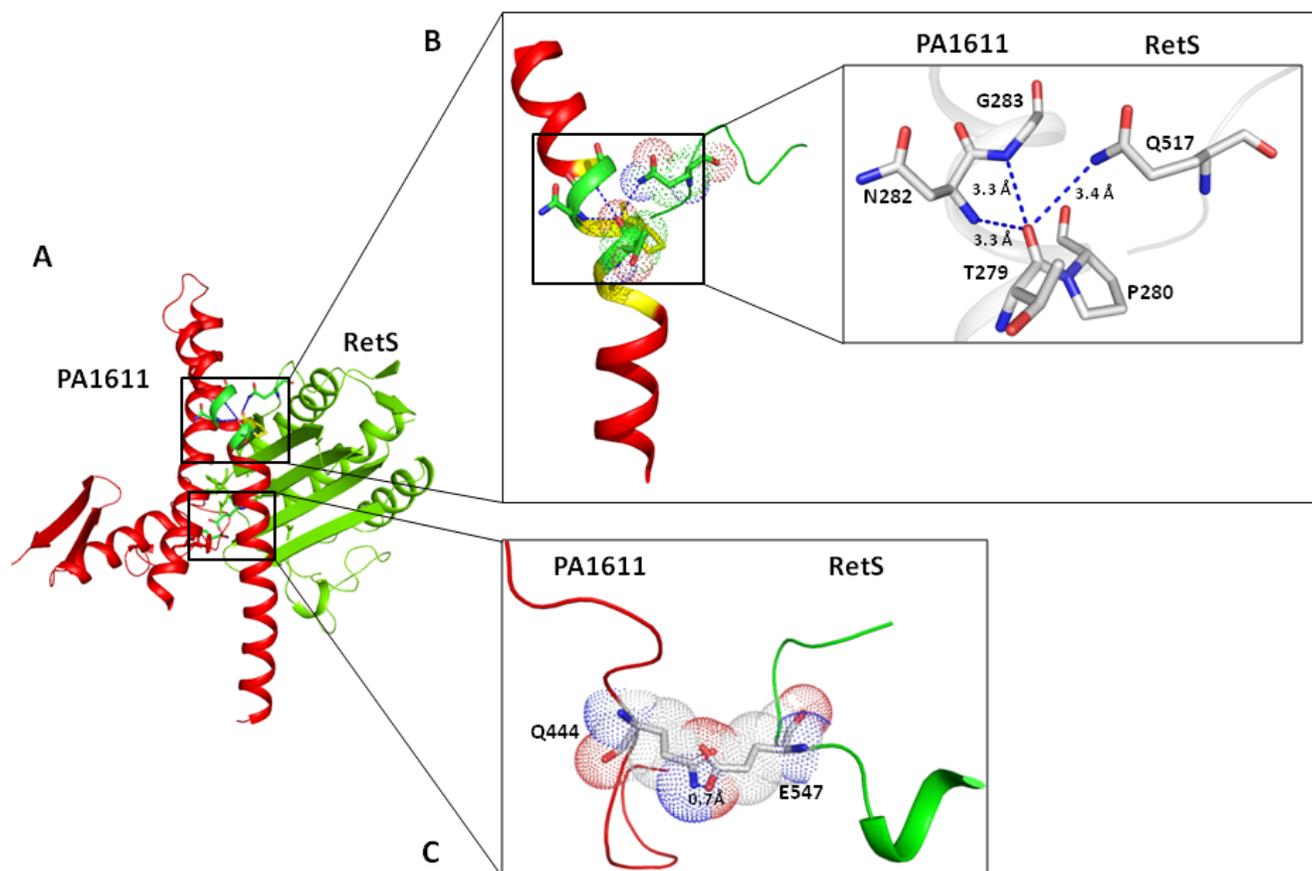
**Figure 19 Predicted inter-molecule interactions of PA1611 amino acids T279 and Q444 with RetS. A.** The image represents different segments of PA1611 (red) and RetS (green) complex with interactions required for the function of the protein(s). **B.** The interactions between T279 in PA1611 and Q517 in RetS represented as dotted spheres. The inset shows hydrogen bond interactions between the backbone carbonyl group (red) of T279 with backbone amino group (blue) of N282 and G283 within PA1611 and with a side chain amino group of Q517 in RetS. The blue dashes represent the bond length (Å). **C.** An ionic interaction (0.7 Å) between Q444 in PA1611 with E547 in RetS represented in dotted spheres.

Interestingly, the α-helix of HisKA in PA1611 is kinked next to T279 due to P280. As a well-observed phenomenon in membrane proteins, this proline induced kink causes unusual α-helix backbone interactions in this region (**Figure 19B inset**). It is speculated that any changes to the local structure as in the case of T279 mutants causes a non-functional PA1611. This suggests that T279 performs a crucial structure-function role in PA1611 rather than necessarily playing a significant role in interacting with RetS. Unlike T279, Q444 is present in the loop region of the HATPase domain of PA1611 and is found to be 0.7Å in proximity of E547 also in the HATPase domain of RetS (**Figure 19C**). Interestingly, the charge of the amino acid does not seem to be important as both Q444A in PA1611, and E547A in RetS are functional. Rather, it seems that the size of the amino acid and hence the degree of interaction might play a role, as both Q444N and E547D loose function. However, this does not completely explain why Q444A and E547A are functional. As both Q444 and E547 are present in the flexible loop regions which are highly dynamic, it is very difficult to predict the exact 3D conformation of the loops, and hence the orientation of the amino acids in the loops, and their function in the two interacting proteins by our molecular model.

The signals from PA1611 are presumably integrated into the RetS pathway, not at the level of cross-phosphorylation of a shared response regulator, but instead, by the formation of a heteromeric complex. The involvement of multiple hybrid HisKs such as RetS, LadS, and PA1611 in the GacA/S-Rsm regulatory pathway in *P. aeruginosa* is unique. Unlike the conventional two-component regulatory system where a signal is received by the sensor kinase and transferred to a response regulator which in turn acts on the target genes, this multicomponent system could receive multiple signals through various sensors and transfer the message through the same GacS-RsmA pathway. In this system, signal transduction involves both direct protein-

protein interaction, i.e. RetS-GacS and RetS-PA1611 and genuine phosphorelay, i.e. LadS-GacS. This may reflect a domain-specific evolution to facilitate the integration of stimuli in this bacterium.

This work dissects the interaction between PA1611 and RetS proteins in *P. aeruginosa*. A novel hybrid sensor kinase interaction model in an important regulatory pathway that controls virulence and lifestyle choice is described in this study. The mechanics of this interaction should help to understand the complex bacterial TCS signal transduction.

Interestingly, evidence has emerged in the recent past suggests that TCS–TCS direct interactions may sometimes be independent of the phosphorelay and at other times acting as signal transducers for interacting proteins (Airola, Watts, & Crane, 2010; Hsing & Silhavy, 1997; Matamouros, Hager, & Miller, 2015; Meena, Kaur, & Mondal, 2010; Muzamal, Gomez, Kapadia, & Golemi-Kotra, 2014). Hybrid HisKs can function alone or in conjunction with diverse cognate and non-cognate partners to form signaling complexes. (P. Bielecki et al., 2015; Firon et al., 2013; Gendrin et al., 2015; He et al., 2006; Reisinger, Huntwork, Viollier, & Ryan, 2007) Some of the HKs may also have lost their catalytic kinase activity during evolution and only retained their ability to participate in dimerization for signal transduction.

The cooperative interaction between membrane-anchored sensory proteins via dimerization of homologous domains is probably a driving force for signal interaction and amplification. Understanding such interactions may serve as a basis for developing new antimicrobial therapeutics by intervening TCS pathways.

**3.4.2 Results of impact on PA1611-RetS interaction in *P. aeruginosa* PAO1 can significantly influence virulence phenotypes and is mediated by the GacA/GacS-RetS-PA1611-RsmA/Y/Z pathway**

Previously, it has been shown that, when PA1611 was knocked out, the T3SS activity was increased as compared with that in the wild-type PAO1, and the T3SS activity was repressed upon PA1611 over-expression (Kong et al., 2013). Residues located within the HisKA and HATPase domains in PA1611, namely, F269, E276, T279, and Q444 demonstrated a significant effect on the PA1611-RetS interaction. However, it remained to be determined if they had any functional relevance and hence their effect in *P. aeruginosa* virulence was examined. In this study, substitution mutations in PA1611 and RetS showed that PA1611-RetS interaction had immense physiological relevance in influencing *P. aeruginosa* phenotypes. T3SS activity for point mutant E276A was higher than the wild-type pAK1611 in both PAO1 and PA1611 knockout, indicating a much-weakened interaction between RetS and PA1611. Furthermore, PA1611 substituted residues at T279 and Q444 could not be in fully restored to wild type levels in functional experiments suggesting that the effect at these residues affected more than just PA1611-RetS interaction.

Confirming the PA1611-RetS interaction model, mutations of the corresponding residues on the partner RetS caused similar changes observed in the PA1611 mutants. Given that the *exoS* promoter activity levels were comparable in PAO1 and PA(ΔRetS)(pAKRetS), significant differences were observable between wild-type and RetS mutants for the examined phenotypes. Because changes to RetS are normally expected to decrease its functionality, these results

confirmed that in fact, a physical interaction between the HisK domains in both PA1611 and RetS are significant in lifestyle switch in *P. aeruginosa*.

Direct protein-protein interaction as having significant effects on bacterial phenotypes has been described in very few instances, and most studies have been performed in *E. coli*. Previously it has been shown that *E. coli* nucleoid-associated H-NS protein interacts with the Hha protein, to regulate the expression of the toxin α-hemolysin (Nieto et al., 2002). Studies using high throughput protein-protein interaction mapping using bacterial two-hybrid assays identified functional dependencies among components involved in cellular processes, including envelope integrity, flagellum assembly and protein quality control in *E. coli* (Rajagopala et al., 2014). Availability of such studies is highly limited in *P. aeruginosa*. This study adds to the very limited pool of available knowledge on direct protein-protein interaction in *P. aeruginosa* and its relevance in mediating *P. aeruginosa* phenotypes.

Study of protein-protein interactions is increasingly becoming a key aspect of systems biology. Protein assembly, protein-protein interaction networks are highly dependent on noncovalent contacts between the residue side chains of interacting partners. It has been shown that more than 80% of proteins act in complexes and not alone (Berggård et al., 2007) and those proteins involved in the same or similar cellular processes are often found to physically interacting with each other (Von Mering et al., 2002). Uncovering the interactions of proteins is central to inform current understanding of the biochemistry of the cell as well as identification of new and specific drug targets.

**Chapter 4**

**CmpX affects virulence in *Pseudomonas aeruginosa* through the Gac/Rsm signaling pathway and by modulating c-di-GMP levels**

**4.1 Rationale**

Under the conditions that favor either acute or chronic infection, a range of virulence genes are regulated by two-component regulatory systems (TCSs), the second messenger bis-(3´-5´)-cyclic dimeric guanosine monophosphate (c-di-GMP) (V. T. Lee et al., 2007; Moscoso et al., 2011) and cell density-dependent quorum sensing (QS) systems such as the LasR/I and RhlR/I. PA1611-RetS-GacS/GacA-RsmA/Y/Z is a key TC regulatory pathway involved in virulence regulation during the switch between acute and chronic infection phases. PA1611 and RetS are hybrid histidine kinase (HHK) (Chambonnier et al., 2016; Kong et al., 2013) and GacS/GacA is a classical TCS. Under chronic infection conditions, PA1611 binds to RetS (Bhagirath, Pydi, et al., 2017); GacS phosphorylates GacA and activates production of small RNAs, *rsmY* and *rsmZ* (Goodman et al., 2004). RsmY and RsmZ bind and sequester transcriptional regulator RsmA (PA0905) in a titration-dependent manner to render it unavailable to activate downstream target genes. RsmA has been shown to post-translationally regulate T3SS, Type IV pili, motility and biofilm formation in a dose-dependent manner (Brencic & Lory, 2009). Signaling through small molecules such as c-di-GMP is another important mechanism for virulence regulation in *P. aeruginosa* (Romling et al., 2013). C-di-GMP is a second messenger used by *P. aeruginosa* and many other bacteria to regulate the expression of genes associated with flagellar motility, Type IV pili, and biofilm initiation. Previous studies have shown that, when free swimming *P. aeruginosa* cells attach to a solid surface, intracellular levels of c-di-GMP increase (Ha & O'Toole, 2015), however, the exact cues that are sensed are yet unknown. The two distinct mechanisms of TCS regulation and signaling via c-di-GMP intersect at several levels. Earlier, it has been shown that a diguanylate cyclase (c-di-GMP synthetase) encoding *wspR* is involved in the switch between T3SS to T6SS via RetS. A *retS* knockout in PAO1 demonstrated elevated c-di-GMP levels (Moscoso et al., 2011). It was also shown that small RNAs RsmY and RsmZ are

necessary for this c-di-GMP related response (Moscoso et al., 2011). Previously, we have identified that a transposon inserted in *cmpX* activated the expression of PA1611 (Kong et al., 2013). In this study, we constructed a *cmpX* deletion (ΔPA1775) mutant and characterized its role in virulence regulation in *P. aeruginosa* PAO1. To confirm the role of *cmpX* in GacS/GacA-RsmA/Y/Z pathway, we studied the effects of the *cmpX* mutant on the promoter activities of T3SS effector *exoS* and small RNA *rsmY*, as well on motility and biofilm formation. Further, to see if c-di-GMP was involved in *cmpX* mediated regulation we evaluated the effect of a *cmpX* knockout on *cdrA* and *wspR* expression levels as an indirect measure of intracellular c-di-GMP levels. Finally, we examine the effect of *cmpX* knockout on PAO1 by phenotype microarrays. We also demonstrate that two key regulatory genes *sigX* and *oprF* in *Pseudomonas* are downregulated in a *cmpX* knockout. Results indicate that *cmpX* affects both PA1611-RetS-GacS/GacA-RsmA/Y/Z and SigX-OprF pathways.

## 4.2 Materials and methods

### 4.2.1 Bacterial strains and plasmids

Bacterial strains and plasmids in this study are described in **Table 4.2.1**. *P. aeruginosa* and *Escherichia coli* were routinely grown on LB agar or in LB broth at 37°C unless otherwise specified. LB was used as a T3SS non-inducing medium and LB supplemented with 5 mM EGTA and 20 mM MgCl$_2$ as a T3SS inducing medium (calcium-depleted). Antibiotics were used at the following concentrations: for *P. aeruginosa*, tetracycline (Tc) at 70 µg/ml in LB or 300 µg/ml in Pseudomonas Isolation Agar (PIA), carbenicillin (Cb) at 250 µg/ml in LB and trimethoprim (Tmp) at 300 µg/ml in LB; for *E. coli*, kanamycin (Kn) at 50 µg/ml, ampicillin (Ap) at 100 µg/ml in LB.

**Table 4.2.1 Bacterial strains and plasmids used in this study.**

| Strain or plasmid | Relevant characteristics | Source |
|---|---|---|
| *E. coli* | | |
| SM10-λ *pir* | Mobilizing strain, RP4 integrated into the chromosome; Kn$^r$ | (Simon et al., 1983) |
| XL1-Blue | *recA1 endA1 gyrA96 thi-1 hsdR17 supE44 relA1 lac [F´ proAB lacIq ZΔM15 Tn10 (Tet$^r$)].* | Invitrogen |
| *P. aeruginosa* | | |
| PAO1 | Wild-type *P. aeruginosa* | This lab |
| PA(ΔPA1775) | PA1775 Knockout mutant of PAO1 | This lab |
| Plasmids | | |
| CTX6.1 | Integration plasmid origins of plasmid mini-CTX-lux; Tc$^r$ | This lab |
| pAK1900 | *E. coli-P. aeruginosa* shuttle cloning vector carrying P*lac* upstream of MCS; Ap$^r$; Cb$^r$ | This lab |
| CTX-*exoS* | Integration plasmid, CTX6.1 with a fragment of pKD-*exoS* containing *exoS* promoter region and *luxCDABE* gene; Kn$^r$, Tmp$^r$, Tc$^r$ | This Lab |
| CTX-*rsmZ* | Integration plasmid, CTX6.1 with a fragment of pKD-*rsmZ* containing *rsmZ* promoter region and *luxCDABE* gene; Kn$^r$, Tmp$^r$, Tc$^r$ | This lab |
| pKD-*rsmZ* | pMS402 containing *rsmZ* promoter region; Kn$^r$, Tmp$^r$ | This lab |

| | | |
|---|---|---|
| pMS402 | Expression reporter plasmid carrying the promoterless *luxCDABE* gene; Kn$^r$,Tmp$^r$ | (Duan et al., 2003) |
| pMS402$_{gfp}$ | Expression reporter plasmid carrying the promoterless *gfp* gene; Kn$^r$,Tmp$^r$ | This study |
| pEX18Tc | oriT$^+$ sacB$^+$ gene replacement vector with multiple-cloning site from pUC18; Tc$^r$ | (Hoang et al., 1998) |
| pAK-1775 | pAK1900 with a 1289 bp fragment of PA1775 between SphI and HindIII; Ap$^r$, Cb$^r$ | This Lab |
| CTX-*exoS* | Integration plasmid, CTX6.1 with a fragment of pKD-*exoS* containing *exoS* promoter region and *luxCDABE* gene; Kn$^r$, Tmp$^r$, Tc$^r$ | This Lab |
| CTX-*rsmY* | Integration plasmid, CTX6.1 with a fragment of pKD-*rsmZ* containing *rsmZ* promoter region and *luxCDABE* gene; Kn$^r$, Tmp$^r$, Tc$^r$ | This lab |
| pKD-*cdrA* | The pMS402 plasmid containing the *cdrA* promoter region and *luxCDABE* reporter cassette; Kn$^r$, Tmp$^r$ | This lab |
| pMS402-*sigX*$_{gfp}$ | The pMS402 plasmid containing the *SigX* promoter region and *gfp* reporter gene; Kn$^r$, Tmp$^r$ | This lab |
| pMS402-*oprF*$_{gfp}$ | The pMS402 plasmid containing the *oprF* promoter region and *gfp* reporter gene; Kn$^r$, Tmp$^r$ | This lab |

**4.2.2 Amino acid sequence and domain analysis of conserved membrane protein PA1775 (*cmpX*)**

All the amino acid sequences were retrieved from the NCBI database, and multiple sequence alignment was performed using Clustal W 2.1 multiple sequence program. Homology models were obtained using the Swiss Model.(Benkert et al., 2011) The final structural prediction was selected by taking the lowest energy model as determined by a low-resolution Rosetta energy function.

CmpX domain architectures were constructed by individually comparing the protein sequences against the SMART 4.0 and the Pfam30.0 databases. **Figure 20A** shows the domain organization of *cmpX* from *P. aeruginosa* PAO1. *cmpX* is a small membrane protein of 274 amino acids, constituted of five transmembrane helices as predicted by TMHMM server v.2.0 (Krogh et al., 2001). The conserved MscS domain is predicted to be between 168-271 amino acids (aa) (Interpro, EMBL). **Figure 20B** shows the ClustalX alignment (Larkin et al., 2007), for the region of highest conservation between CmpX (PAO1) and MscS from *E. coli* (Booth & Louis, 1999; Kloda & Martinac, 2001; Levina et al., 1999).

A
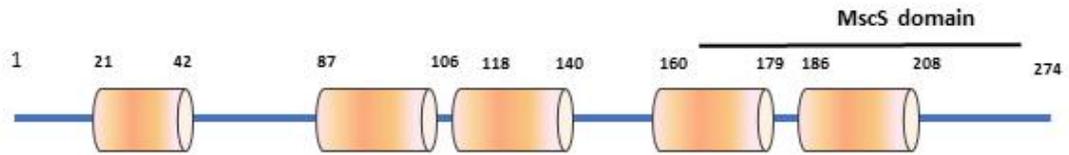


B



**Figure 20 PA1775 domain organization, sequence alignment and homology model. A.** PA1775 domain organization. The domain architectures were constructed by individually comparing the protein sequences against the SMART 4.0 and the Pfam30.0 databases. The figure is not drawn to scale. **B.** Sequence alignment between *cmpX* (PAO1) and MscS (*E. coli*). Alignment was performed on ExPASy.

**4.2.3 Construction of gene expression detecting systems**

The plasmid pMS402 carrying a promoterless *luxCDABE* reporter gene cluster was used to construct promoter-*luxCDABE* reporter fusions as described previously. For measuring the promoter activity of *sigX* and *oprF,* plasmid pMS402 carrying a promoterless *gfp* gene was used to construct promoter-*gfp* fusions. Promoter regions of *exoS*, *rsmY, SigX, OprF* and *cdrA* were PCR-amplified using high-fidelity Pfu DNA polymerase (Fermentas). The promoter regions were cloned into the BamHI–XhoI site upstream of the *lux/gfp* gene(s) on pMS402. Cloned promoter sequences were confirmed by DNA sequencing. Primers used are listed in **Table 4.2.2**.

**Table 4.2.2 Primers used in the study**

| Primer | Sequence (5'-3') |
|---|---|
| PA1775QS1-F | GCGGAATTCAACCGCACCATGTATCTC |
| PA1775QA1-R | TCAGGATCCGTTCACTCAGCCTTGTCA |
| PA1775QS2-F | TCAGGATCCCCGGGAGAGATAATGGAC |
| PA1775QA2-R | GCGAAGCTTTGACATGGACGAGCCAAC |
| pAK-PA1775-F | TAAGCATGCATCCGTTCGAAGAGTCCC |
| pAK-PA1775-R | GACAAGCTTAGACGTTGAACAGCGTGC |
| *rpoD*-F | CCTGATGAAGGCGGTGGAC |
| *rpoD*-R | GATGCGGATGGTGCGTGC |
| *oprF*-F | CAGTACCCGTCCACTTCCAC |
| *oprF*-R | TTCACGCGACCACCTTCTAC |
| *sigX*-F | AATTGATGCGGCGTTACCA |
| *sigX*-R | CCAGGTAGCGGGCACAGA |
| *wspR*-F | GCGGTCATGGTACTGCTTGT |
| *wspR*-R | CCGTCGGCTTGATCTGGTTG |
| pKD-*cdrA*-F | TTACTCGAGCTATCTGCGTGGCGCACGTCAG |

| | |
|---|---|
| pKD-*cdrA*-R | GTAGGATCCGGAAGGTTCCTTGGCGGCAGCG |
| pKD-*rsmY*-F | ATCTCGAGCAGTTCCTGGAGCTGGA |
| pKD-*rsmY*-R | GTCGGATCCTCTATCCTGACATCCG |
| pMS402-*sigX*-F | TTACTCGAGTCCTGGCGCAACTGGTGA |
| pMS402-*sigX*-R | GTAGGATCCGTGAGATCAGGCCAGTCAT |
| pMS402-*oprF*-F | TTACTCGAGGACGTGGCTGCTCTGCAGG |
| pMS402-*oprF*-R | GTAGGATCCCCGTTAAATCCCCATCTTG |
| *wspR*-F | GCGGTCATGGTACTGCTTGT |
| *wspR*-R | CCGTCGGCTTGATCTGGTTG |

F-Forward; R-Reverse

The reporter plasmid pKD-*cdrA,* pMS402-*sigX*$_{gfp}$ and pMS402-*oprF*$_{gfp}$ were transformed into *P. aeruginosa* respectively by electroporation. Besides the plasmid-based reporter system, an integration plasmid CTX6.1 originating from plasmid mini-CTX-*lux* (Becher & Schweizer, 2000) was used to construct chromosomal fusion reporters for *exoS* and *rsmY* as described earlier. These *lux* and *gfp*-based reporters were cultured overnight followed by dilution into fresh medium to an optical density at 600 nm (OD$_{600}$) of 0.2 and cultivated for an additional 3 h before use as inoculants. The cultures were inoculated into 96-well black (Fluorescence) or white (luminescence) plates with the transparent bottom in triplicates in a ratio of 5 µl of inoculum to 95 µl of fresh medium. 50 µl of filter-sterilized mineral oil (Sigma Aldrich) was added on top to prevent evaporation during the assay. Both luminescence (counts per second, cps) and fluorescence from promoter-*gfp* reporter fusions (excitation wavelength of 490 nm and an emission of 510 nm) were measured every 30 min for 24 h in a Synergy H4 Multimode Microplate Reader (BioTek). Bacterial growth (OD$_{600}$) was measured simultaneously. The gene expression was proportional to the level of light production. The level of gene expression was normalized to bacterial growth and is presented as relative luminescence units (RLU), calculated as cps/OD$_{600}$ or Relative fluorescence unit (RFU) calculated as RFU/OD$_{600}$. Strains carrying the empty vector pMS402$_{gfp}$ were measured for background levels corrections. All the data presented in this manuscript are means of three independent biological replicates.

### 4.2.4 Gene knockout and complementation

For the construction of *cmpX* (PA1775) gene knockout mutant, fragment upstream to PA1775 was amplified using Primer PA1775QS1 paired with PA1775QA1, and the downstream fragment was amplified using PA1775QS2 paired with PA1775QA2. The sequences of these primers are listed in **Table 4.2.2**. The two fragments were ligated into a pEX18Tc vector to obtain the

pEX18-PA1775. The $\varOmega$ fragment obtained from pHP45$\varOmega$ with streptomycin resistance gene was inserted in the middle of the two amplified PA1775 fragments. Gene knockout mutant was obtained using the tri-parental mating procedure in which the strain carrying the helper plasmid pRK2013 was used together with the donor and recipient (Ditta et al., 1980). The resulting mutant was verified by PCR. Here and elsewhere in the manuscript, *cmpX* refers to PA1775 as well as a *cmpX* knockout refers to ΔPA1775 and vice-versa. ΔPA1775 in PAO1 (PA (ΔPA1775)) has been shown as ΔPA1775.

The multi-copy-number *E. coli–P. aeruginosa* shuttle vector pAK-1900 (Poole et al., 1993) was used for complementation of PA1775 into ΔPA1775 (ΔPA1775 (pAK-PA1775)). Full-length PA1775 was PCR-amplified. The primers used are listed in Table 2. The PCR products were digested with SphI and HindIII and then cloned into pAK-1900 under control of a T7 promoter. The cloned PA1775 sequence was confirmed by DNA sequencing. The constructed plasmid was then transformed into *P. aeruginosa* by electroporation.

### 4.2.5 Metabolic phenotype array and confirmation assays

Phenotype microarrays were performed as described previously. To confirm the results of PM analysis, some of the key findings were subsequently investigated by performing independent studies. Thus, susceptibilities to antimicrobial agents were tested using broth microdilution method in Mueller-Hinton broth (Oxoid, Ltd., Basingstoke, Hampshire, United Kingdom) according to the CLSI guidelines (CLSI, 2012). Tested compounds were purchased from Sigma Aldrich Co. (St. Louis, Mo.). PAO1 and ΔPA1775 were cultured, and the inoculum volume for minimum inhibitory concentration (MIC) testing was adjusted to a concentration of $5 \times 10^5$

CFU/ml. *P. aeruginosa* PAO1 was used as the control strain in each run. The MIC was defined as the lowest antibiotic concentration that inhibited visible growth of the organism.

## 4.3 Results

### 4.3.1 Role of *cmpX* (PA1775) in virulence and biofilm formation

We have previously demonstrated that PA1611 can bind to RetS and allows for activated transcription of RsmY and RsmZ and represses T3SS (Bhagirath, Pydi, et al., 2017; Kong et al., 2013). The yet uncharacterized gene PA1775 (*cmpX*) has emerged as a regulator for PA1611 expression since a *cmpX* transposon insertion mutant showed activated expression of PA1611 (Kong et al., 2013). To understand the role of *cmpX*, we constructed a *cmpX* knockout mutant in PAO1, ΔPA1775, as well as a complementation strain, ΔPA1775 (pAK-PA1775). We examined the effect of *cmpX* deletion on T3SS effector *exoS* and on small RNAs RsmY/Z (**Figure 21**). As shown in **Figure 21A**, the *exoS* promoter activity in the *cmpX* knockout strain was at least 2-fold lower than in PAO1 under T3SS inducing conditions. The *exoS* expression level in the mutant was reverted to the wild type level upon complementation. Similarly, the effect of the *cmpX* on biofilm formation was tested. As seen in **Figure 21B** ΔPA1775 formed 1.5-fold higher biofilm than its wild type control ($p < 0.01$). This was reversible to wild type levels in ΔPA1775 (pAK-PA1775). Biofilm formation in *Pseudomonas* involves tight control over the transcription of the regulatory small RNAs, *rsmY,* and *rsmZ*. The impact of the *cmpX* knockout in PAO1 on levels of RsmY and RsmZ was further measured using the *lux*-based reporters. Here RsmY was used a representative. As shown in **Figure 21C**, a 4-fold higher *rsmY* promoter activity was observed in ΔPA1775 as compared with wild type PAO1. This was also reversible upon complementation with PA1775 on the plasmid.
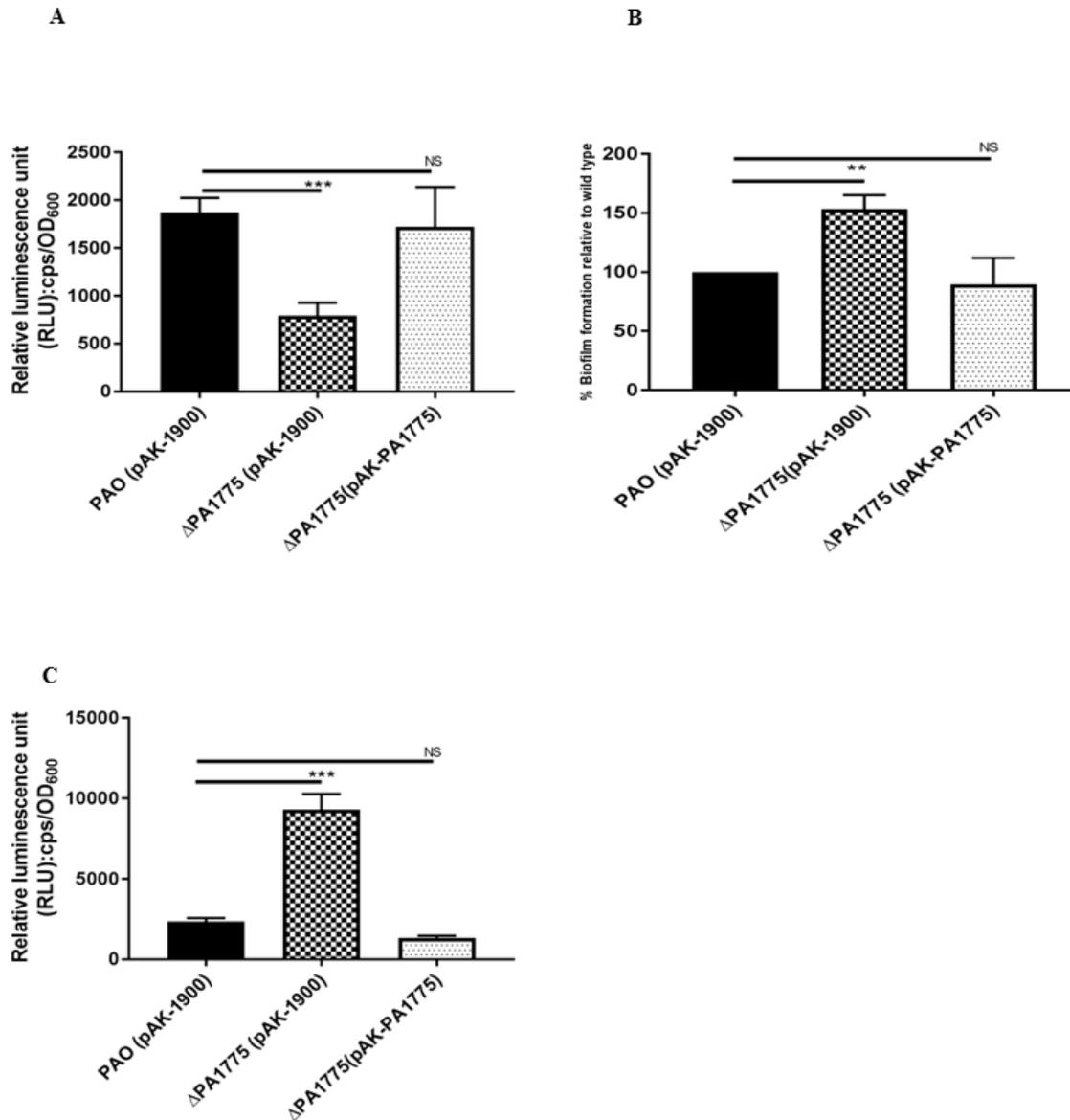
**Figure 21 Effect of a *cmpX* knockout on virulence and biofilm formation**. **A.** *exoS* promoter activity at 12 h. **B.** Biofilm formation of the ΔPA1775 and a ΔPA1775 (pAK-PA1775) complementation strain as compared with that of the wild type PAO1. Data are shown as the percent change relative to PAO1. **C.** *rsmY* promoter activity at 12h. A CTX-*exoS* and CTX-*rsmY* reporter fusion integrated to the chromosome was used to measure the *exoS* and *rsmY* promoter

activity respectively. CTX-*exoS* promoter activity was measured under T3SS inducing conditions. These experiments were done in wild type PAO1, ΔPA1775 and ΔPA1775 background containing the expression plasmid pAK-PA1775 carrying the full-length PA1775 in the expression vector pAK-1900 (ΔPA1775 (pAK-PA1775)). PAO1 and ΔPA1775 contain empty vector pAK-1900. PAO1 is used as the control. The *exoS* promoter activity at 12 h is normalized to growth and shown in relative luminescence unit (RLU): cps (counts per second)/$OD_{600}$. The values shown are an average of three independent experiments. Data were analyzed using one-way ANOVA with Dunnett post-hoc test. NS $p > 0.05$, **$p < 0.01$, ***$p < 0.001$, and ****$p < 0.0001$. Error bars indicate standard deviations.

**4.3.2 Role of *cmpX* (PA1775) in motility in *P. aeruginosa***

The acute phase of *P. aeruginosa* is characterized by high motility and is regulated by GacA/S TCS (K. Li et al., 2017). RsmA also regulates *exoS* expression and positively regulates motility (Heurlier et al., 2004). Thus, to further analyze the phenotypical effect of *cmpX* on motility, ΔPA1775 was analyzed for swimming, swarming and twitching motility (**Figure 22**). These motilities were assessed by measuring the diameters of the migration front after 12−14 h of incubation. As compared to wild type PAO1, ΔPA1775 demonstrated reduced swarming ($p <$ 0.01) and twitching ($p < 0.001$) motility as shown in **Figure 22A** and **C**. No significant difference in swimming motility was visible (**Figure 22B**).
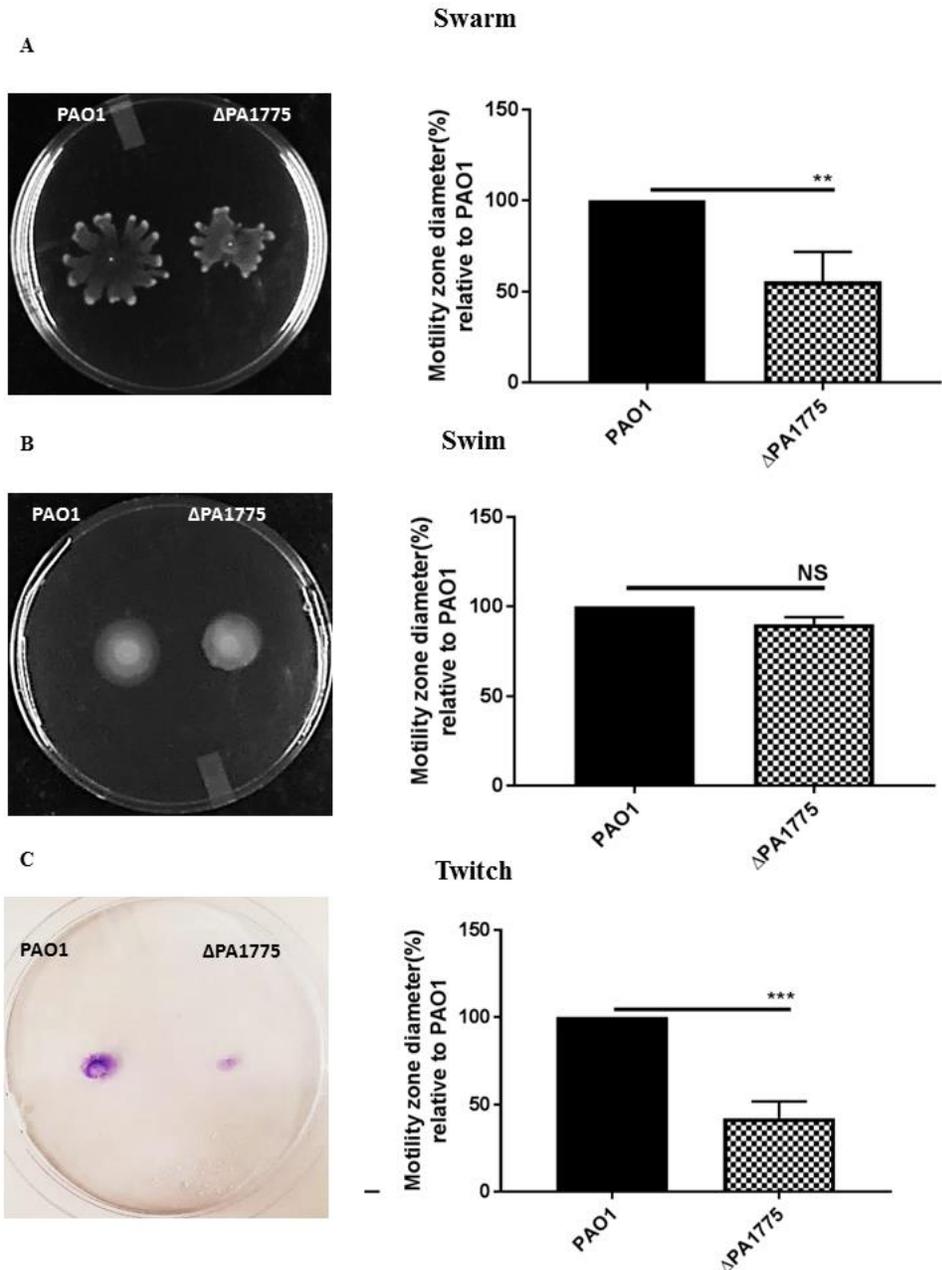
**Figure 22 Effect of a *cmpX* knockout on motility**. The effect of *cmpX* knockout on swarming **(A)**, swimming **(B)** and twitching **(C)** motility is shown. The diameter of the zone of motility expressed in percentages relative to the wild type PAO1. The experiments were repeated at least three times, and similar results were observed. NS $p> 0.05$, $**p < 0.01$ and $***p < 0.001$. Error bars indicate standard deviations.

### 4.3.3 CmpX is involved in signaling via c-di-GMP

Though, our results for the role of *cmpX* in virulence and biofilm formation were in alignment with the PA1611-RetS-GacS/GacA-RsmA/Y/Z pathway and could be explained as such; an alternative pathway that has been increasingly shown to regulate virulence and bacterial phenotypes involves signaling by c-di-GMP. Thus, to confirm if the observed phenotypes could be a result of altered c-di-GMP levels, we tested *cdrA* promoter activity within a *cmpX* knockout and wild type PAO1. Previously, *cdrA* promoter activity levels have been shown to faithfully reflect the fluctuations in intracellular c-di-GMP levels (Bouffartigues et al., 2015; Rybtke et al., 2012); hence, we measured *cdrA* levels to indirectly quantify c-di-GMP levels in ΔPA1775. Quantifications were performed in triplicates, and the data at 12h is presented in **Figure 23A** as relative luminescence units (RLUs). To avoid conditional changes in *cdrA* levels the growth conditions for PAO1 and ΔPA1775 were kept the same. ΔPA1775 demonstrated 2-fold higher levels of *cdrA* promoter activity than in the wild type PAO1 ($p < 0.001$), indicating a clear effect of *cmpX* on intracellular c-di-GMP levels.

A chemosensory-like surface-sensing system *wspR* encodes c-di-GMP synthase (Guvener & Harwood, 2007), and has been shown to be involved in modulation of c-di-GMP levels and switch between T3SS to T6SS (Moscoso et al., 2011) by control of Pel synthesis. Thus, we wanted to examine if the observed increase in c-di-GMP levels could be attributable to *wspR* activation. We examined the transcript levels of *wspR* in the *cmpX* knockout mutant. Primers for qPCR are listed in **Table 4.2.2.** As seen in **Figure 23B**, the *cmpX* knockout mutant demonstrates 1.7-fold higher expression as compared to that in the wild type PAO1, suggesting that the increased c-di-GMP levels in the *cmpX* knockout mutant may have at least partially resulted from the activated *wspR* expression.
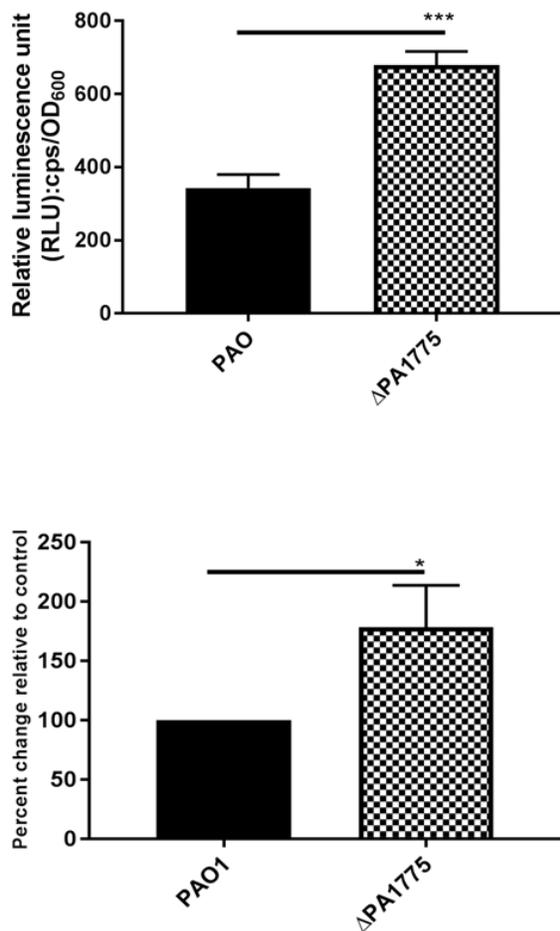
**Figure 23 CmpX is involved in signaling via c-di-GMP**. **A** *cdrA* promoter activity in PAO1 and ΔPA1775. The promoter region for *cdrA* was cloned into the pMS402 upstream of the *lux* genes. The resultant plasmid pKD-*cdrA* was transformed into *P. aeruginosa* respectively by electroporation. The wild type PAO1 is used as the control. *cdrA* promoter activity at 12 h is normalized to growth and shown in relative luminescence unit (RLU): cps (counts per second)/$OD_{600}$. **B** mRNA expression of *wspR* was normalized to the housekeeping gene *rpoD* in PAO1 and ΔPA1775. Data are presented as percent change relative to PAO1. The values shown are an average of three independent experiments. Data were analyzed using unpaired t-test. The error bars indicate standard deviations. $*p < 0.05$, $**p < 0.01$ and $***p < 0.001$

**4.3.4 The extracytoplasmic function sigma factor *sigX* and outer membrane porin, *oprF* are down-regulated in *cmpX* knockout mutant**

On the *P. aeruginosa* genome, *cmpX* is located immediately upstream of *sigX* and *oprF* genes. Outer membrane porin OprF has been shown to be involved in cell survival and in maintaining cell wall integrity (Rawling et al., 1998; Woodruff & Hancock, 1989). Extracytoplasmic function sigma factor *sigX* has also been shown to be involved in virulence regulation, fatty acid biosynthesis and maintaining membrane homeostasis (Brinkman et al., 1999). Both *oprF* and sigX knockout mutants demonstrated downregulation of *cmpX*, activation of small RNAs and elevated c-di-GMP levels by activation of diguanylate cyclase adcA (PA4843) and PA1181(Bouffartigues et al., 2012; Bouffartigues et al., 2015; Brinkman et al., 1999). Based on the genomic location, we wondered if *cmpX* had an effect on *sigX* and *oprF* which could contribute to the elevation in c-di-GMP levels. Thus, the effect of *cmpX* knockout on *sigX* and *oprF* were investigated by using qPCR. The expression levels of *oprF* and *sigX* in ΔPA1775 were compared with those in wild type PAO1. As seen in Fig. 4, the expression of *sigX* and *oprF* (**Figure 24A**) was decreased by 3-fold and 2.3-fold respectively in the *cmpX* mutant. We further confirmed this result by measuring promoter activity of *sigX* and *oprF* in the ΔPA1775 strain, and similar results were obtained (**Figure 24B** and **4C**). These results suggest that *cmpX* affects *sigX* and *oprF,* which could consequently influence intracellular c-di-GMP levels and affect virulence factors in *P. aeruginosa*.
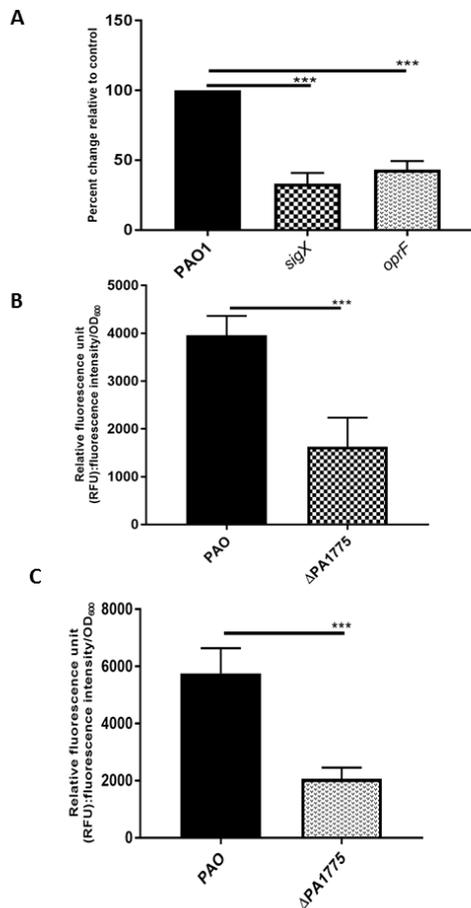
**Figure 24 Effect of a *cmpX* knockout on *sigX* and *oprF* gene expression. A.** mRNA expression for sigX and oprF were normalized to the housekeeping gene *rpoD* in PAO1 and ΔPA1775 respectively. Data are presented as percent change relative to PAO1. *sigX* **(B)** *and oprF* **(C)** promoter activity in PAO1 and ΔPA1775. The promoter region for *sigX* and *oprF* was cloned into the pMS402 upstream of the *gfp* gene. The resultant plasmid pMS402-*sigX*$_{gfp}$ and pMS402-*oprF*$_{gfp}$ were transformed into *P. aeruginosa* respectively by electroporation. The wild type PAO1 is used as the control. *sigX* and *oprF* promoter activity at 12 h are normalized to growth and shown in Relative fluorescence unit (RFU) calculated as RFU/OD$_{600}$. Strains carrying the empty vector pMS402$_{gfp}$ were measured for background levels corrections. Data were analyzed using unpaired t-test. $**p < 0.01$ and $***p < 0.001$

**4.3.5 PA1775 promoter activity during growth in PAO1, Biolog phenotype microarrays, and validation**

PA1775 has been annotated as a putative conserved cytoplasmic membrane protein in the genome database (Winsor et al., 2016). To investigate its potential roles, the expression profile of *cmpX* and the metabolic profiles of the *cmpX* knockout mutant were examined using PA1775 expression reporter and Biolog phenotype microarrays respectively.

The CTX−PA1775 reporter fusion was integrated into the chromosome of PAO1, and PA1775 promoter activity was monitored over an extended period of growth. **Figure 25** shows PA1775 promoter activity over 70 h with growth monitored simultaneously. PA1775 demonstrated an increased promoter activity during the early log phase of growth followed by a second surge during the late stationary phase, suggesting it responds to signals present in these growth phases and may be cell density dependent. Biolog phenotype microarrays have been used to facilitate the characterization of unknown genes (Johnson et al., 2008). Despite the preliminary experiments showing a significant role of *cmpX* in controlling phenotypes in *P. aeruginosa*, the function of CmpX has been relatively unexplored. Hence, we used PM technology to study the potential function of CmpX in *P. aeruginosa*. **Table 4.3.5** outlines the phenotypes lost and gained in a PA1775 knockout strain. To confirm the results obtained through the PMs some of the key findings were subsequently verified (**Table 4.3.6**). The results confirmed that the *cmpX* mutants demonstrated greater sensitivity to membrane detergents, environmental toxins such as potassium tellurite, cell wall synthesis inhibitor and protein synthesis inhibitors such as tobramycin. Highest difference in sensitivity for the *cmpX* mutant was observed for tobramycin (0.3 µg/ml), vancomycin (150 µg/ml), potassium tellurite (4 µg/ml) and methyltrioctylammonium chloride (3 µg/ml).

126
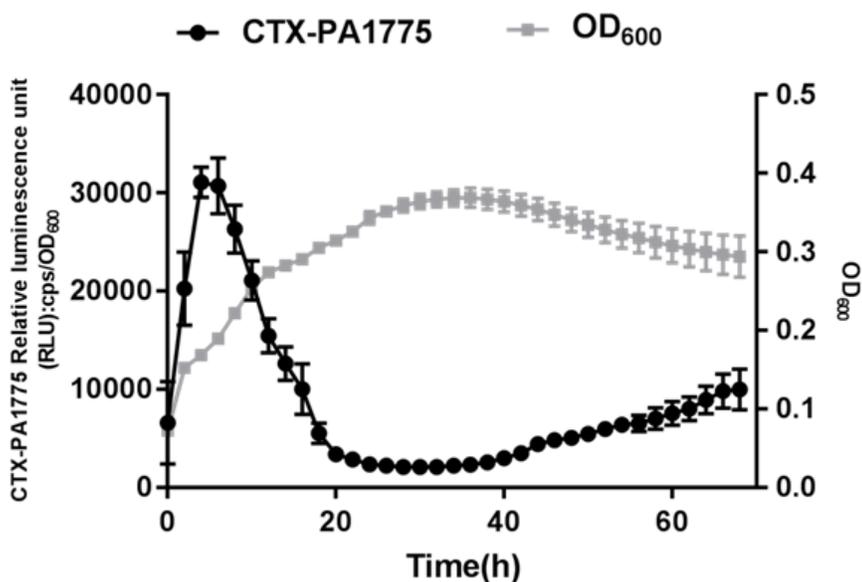
**Figure 25    PA1775 promoter activity during growth in PAO1 over time.**  CTX-PA1775 reporter fusion integrated to the chromosome was used to measure the PA1775 promoter activity (solid line). Bacterial growth was monitored simultaneously and ($OD_{600}$) is shown in grey dotted line. The PA1775 promoter activity is normalized to growth and shown as relative luminescence unit (RLU): cps (counts per second)/$OD_{600}$. The values shown are average of three independent experiments. The error bars indicate standard deviations.

**Table 4.3.5 Summary of gained and lost phenotypes for *P. aeruginosa cmpX* knockout mutants.**

| Index | Compound | Metabolic values | Function |
|---|---|---|---|
| **Phenotypes lost** | | | |
| 1 | Orphenadrine | -146 | Anti-cholinergic |
| 2 | D,L-Propanolol | -113 | Beta-adrenergic blocker |
| 3 | Compound 48/80 | -101 | Cyclic AMP phosphodiesterase inhibitor |
| 4 | Methyltrioctylammonium chloride | -106 | Membrane, detergent, cationic |
| 5 | Dodecyltrimethyl ammonium bromide | -74 | Membrane, detergent, cationic |
| 6 | N-Dodecyl-N,N-dimethyl-3-ammonio-1-propanesulfonate) Lauryl sulfobetaine | -287 | Membrane, detergent, zwitterionic |
| 7 | Lysine-Tryptophan | -94 | N-Source, peptide |
| 8 | L-Asparagine | -53 | Nutritional supplement |
| 9 | Blasticidin S | -194 | Protein synthesis |
| 10 | Tobramycin | -221 | Protein synthesis, 30S |

| | | | ribosomal subunit, aminoglycoside |
|---|---|---|---|
| 11 | Josamycin | -136 | Protein synthesis, 50S ribosomal subunit, macrolide |

| | Compound | PAO1 | ΔPA1775 |
|---|---|---|---|
| 12 | D, L-Thioctic acid | -250 | Reducing agent |
| 13 | Potassium tellurite | -742 | Toxic anion |
| 14 | Vancomycin | -87 | Cell wall synthesis inhibitor |
| **Phenotypes gained** | | | |
| 15 | L-Aspartic acid | 67 | C-Source, amino acid |
| 16 | L-Glutamic acid | 54 | C-Source, amino acid |

The table shows the phenotypes gained or lost by *cmpX* mutants as compared to wild type PAO1. Phenotype microarrays were performed by the commercially available Biolog PM, and data were analyzed by the OmniLog® V. 1.5 comparison module, and the average height parameters were used for data analysis with standard thresholds for detection. The metabolic distance threshold was set at 50, and the sensitivity threshold was set at 74.

| | | |
|---|---|---|
| Tobramycin | 2 µg/ml | 0.3 µg/ml |
| Vancomycin | 300 µg/ml | 150 µg/ml |
| Orphendrine | 800 µg/ml | 600 µg/ml |
| Compound 48/80 | 10 µg/ml | 8 µg/ml |
| Lauryl sufobetaine | 3 mg/ml | 2.5 mg/ml |
| Methyltrioctylammonium chloride | 6 µg/ml | 3 µg/ml |
| Potassium tellurite | 10 µg/ml | 4 µg/ml |

**Table 4.3.6 Confirmed phenotypes for *cmpX***

The table shows MIC for *cmpX* knockout (ΔPA1775) and its wild type control PAO1. MIC was

defined as the lowest antibiotic concentration that inhibited visible growth of the organism

**4.4 Discussion**

**4.4.1 CmpX affects phenotypes in *P. aeruginosa* PAO1 via GacA/GacS-RetS-PA1611-RsmA/Y/Z pathway**

In the search for regulators of PA1611, a whole genome transposon mutagenesis was performed. A transposon mutant of *cmpX* (PA1775) demonstrated activation of PA1611 in *P. aeruginosa* PAO1(Kong et al., 2013). However, the role of *cmpX* and the exact mechanism by which *cmpX* participates in virulence regulation in *P. aeruginosa* is yet unknown. In this study, an investigation into the role of *cmpX* in virulence regulation and PA1611-RetS-GacS/GacA-RsmA/Y/Z pathway in *P. aeruginosa* has been explored (Bhagirath, Somayajula, et al., 2017).

CmpX falls into the category of highly conserved small membrane protein of 274 amino acids (aa). A domain analysis of CmpX shows a conserved, mechanosensor of small conductance (MscS) domain. However, when aligned with MscS, a small mechanosensor in *E. coli*, *cmpX* demonstrates a unique organization (**Figure 20**). The pore (TM3) domain is quite different (30 residues upstream of the gate), the hinge is not obvious, and the cage (C-term) domain does not align well, suggesting that the cage is also different. E104 sitting in the pore constriction instead of L105 in MscS means that the channel should be strictly cationic (Na/K), whereas MscSs are more anionic. Gene promoter assays for PA1775 identified dual expression peaks during growth. One, during early log phase and later during the late stationary phase. During early log phase when c-di-GMP levels are low the transcription of *cmpX* is much higher, whereas, during stationary phase, the c-di-GMP levels increase and *cmpX* transcription declines. After biofilm matures, *P. aeruginosa* cells are released in a controlled manner back to a planktonic mode of growth. For this, a well-established nitrosative stress model has been postulated (Webb et al., 2003; Yoon et al., 2002). Upon addition of Sodium Nitroprusside (SNP) to biofilms, intracellular

131

c-di-GMP levels in cells were shown to be decreased by ~45 to 47% (Barraud et al., 2009) and resulted in the dispersal of cells. Thus, a biofilm dispersion model may explain the activation of *cmpX* in the stationary phase.

PA1611 is an HHK, which senses yet unknown environmental cues to regulate biofilm formation. A PA1611 knockout in PAO1 demonstrated increased T3SS effector secretion and decreased biofilm formation by direct interaction with RetS (Bhagirath, Pydi, et al., 2017). The *cmpX* knockout mutant demonstrated decreased expression of T3SS effector ExoS and increased expression of *rsmY*, as well as enhanced biofilm formation. These results agree with the previously proposed role of *cmpX* in affecting PA1611 (Kong et al., 2013).

A *cmpX* transposon mutant activated PA1611. An activated PA1611 can bind to RetS (Bhagirath et al., 2017) and lead to elevated exopolysaccharide production and biofilm formation (Kong. et al., 2013). Exopolysaccharide production in *P. aeruginosa* involves activation of *pel* genes and both RetS and c-di-GMP have been shown to converge on Pel regulon. Motility assays demonstrated that only swarming and twitching motility was affected in the *cmpX* knockout mutant; whereas, swimming motility did not exhibit any difference. The reduction of swarming but not swimming is intriguing, yet consistent with a previous observation (Zheng, Tsuji, Opoku-Temeng, & Sintim, 2016). The difference may lie in differential regulation for these two motility patterns. Swimming and swarming do share some common features but are remarkably different in other aspects. Swarming is a group behavior that involves rapid and coordinated group movement across a hydrated semi-solid surface often typified by solar flare appearances. Swimming motility, on the other hand, is a mode of individual bacterial movement in a liquid environment (<0.3% agar) powered by rotating flagella. The effect of *cmpX* on swarming but not swimming may underline its role in regulating bacterial group behavior. Taken together these

findings suggest that *cmpX* may have a more complex function and functions by activating PA1611 in the GacS/A-RsmA/Y/Z pathway.

## 4.4.2 CmpX may be the intersection for signals by c-di-GMP signaling and the GacA/GacS-RetS-PA1611-RsmA/Y/Z pathway

High levels of c-di-GMP have been shown to affect T3SS negatively and increase polysaccharide production by activation of *pel* system and thus enhance biofilm formation (Borlee et al., 2010; Guvener & Harwood, 2007; Hickman et al., 2005; Moscoso et al., 2011; Starkey et al., 2009). A *cmpX* mutant demonstrated activation of *wspR*. WspR encodes a c-di-GMP synthase. Previously it has been shown that a *retS* mutant activated *wspR* and enhanced intracellular c-di-GMP levels to facilitate biofilm formation (Moscoso et al., 2011). Earlier, it has been shown that a *retS* knockout mutant demonstrated elevated c-di-GMP levels by activation of *wspR* (Moscoso et al., 2011). We have previously shown that the phenotype of a PA1611 overexpression strain was similar to that of *retS* knockout (Kong et al., 2013). Thus, in this study, it was examined if the effect of *cmpX* on virulence and biofilm formation could, be a combined result of elevated c-di-GMP and its effect on the GacA/GacS-RetS-PA1611-RsmA/Y/Z pathway.

Expression of *cdrA* encoding for an adhesin in *P. aeruginosa* was previously shown to be highly co-relatable to changes in the levels of intracellular c-di-GMP (Rybtke et al., 2012). As compared to PAO1, the *cmpX* knockout demonstrated an increase in *cdrA* promoter activity, suggesting elevated c-di-GMP levels in the mutant. *wspR,* a c-di-GMP synthase associated with the RetS/GacS signaling cascade was found to be elevated in a *cmpX* mutant, which may explain the elevated c-di-GMP levels in ΔPA1775. *wspR* when overexpressed caused an increase in

biofilm formation by activation of *pel* genes whereas *wspR* mutant demonstrated loss of cytotoxicity and reduced biofilm formation (Kulasakara et al., 2006; Moscoso et al., 2011).

Transcription of *oprF* and *sigX* was significantly decreased in the *cmpX* mutant. *cmpX* is the last gene in the *cmaX-crfX-cmpX* operon and is located upstream of the sigma factor *sigX* and the major outer membrane porin gene *oprF* on the *P. aeruginosa* genome. *cmpX* encodes an AlgU binding site, a *sigX* consensus sequence in its promoter region as well as one of the promoters for *oprF* in the *cmpX-sigX* intergenic region. The other promoters for *oprF* have been identified in the *sigX-oprF* intergenic region (controls > 80% transcription) and in *sigX* itself (Bouffartigues et al., 2012; Brinkman et al., 1999). Previous studies have shown that a *sigX* mutant demonstrated reduced transcription of *oprF*, reduced virulence, motility and enhanced biofilm formation (Gicquel et al., 2013). OprF is involved in the rhamnolipid production (Fito-Boncompte et al., 2011), biofilm development and resistance to antibiotics such as cephalosporins (Bratu et al., 2007). An *oprF* mutant demonstrated elevated levels of c-di-GMP (Bouffartigues et al., 2015), and reduction in T3SS effectors (ExoT and ExoS) as well as decreased production of pyocyanin, lectin PA-1, exotoxin A (Fito-Boncompte et al., 2011). An *oprF* knockout resulted in activation of *pel* genes as well as PA4843 and PA1181 genes of the *sigX* regulon both of which encode c-di-GMP synthase (Bouffartigues et al., 2015). Considering the complex relationship between intracellular c-di-GMP levels and several other regulatory networks including the GacS/GacA-RsmA/Y/Z (Moscoso et al., 2011) and OprF (Bouffartigues et al., 2015) pathways, the effect of *cmpX* knockout on c-di-GMP levels could be a combined one; although, the exact role of *cmpX* in *oprF* regulation needs further investigation (**Figure 26**).
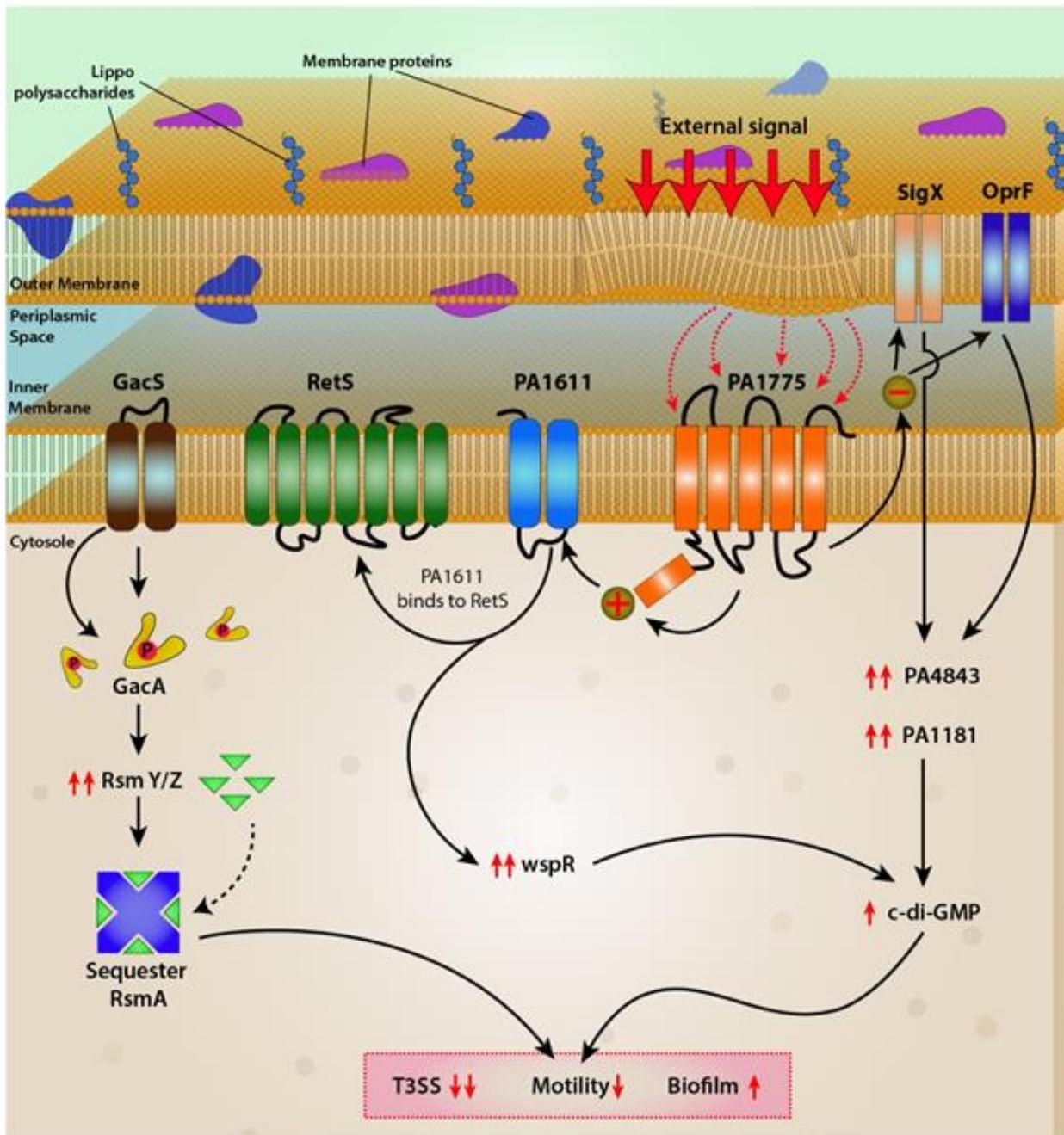
**Figure 26 Proposed role for *cmpX* in c-di-GMP regulation and PA1611-RetS-GacS/A-RsmA/Y/Z pathway.** CmpX (PA1775), a putative small mechanosensor, senses changes in the bacterial membrane. In response to external signals such as those in chronic infections (e.g.

increased cell density), *cmpX* has been shown to activate PA1611 (Kong et al., 2013). Activated

PA1611 has been shown to bind to RetS (Bhagirath, Pydi, et al., 2017). RetS mediates acute

phase of infection by binding to GacS. Once RetS is unavailable, GacS can phosphorylate

response regulator GacA and activate transcription of small RNAs RsmY/RsmZ which sequester

post-transcriptional regulator RsmA. It has been shown that RetS mutant activated c-di-GMP

synthase WspR (Moscoso et al., 2011), which in turn increases intracellular levels of c-di-GMP.

A *cmpX* mutant demonstrates decreased activity of *sigX* and *oprF*. An *oprF* and *sigX* mutant

have been shown to activate c-di-GMP synthases PA4853 and PA1181 further contributing to

increased c-di-GMP levels (Bouffartigues et al., 2015). All these factors together enhance

biofilm formation, downregulate T3SS and motility. The cartoon is for representation only and is

not drawn to scale.

Upon comparing the metabolic and sensitivity capabilities of a *cmpX* mutant to wild type PAO1, *cmpX* knockout demonstrated increased sensitivity to membrane detergents such as lauryl sulfobetaine, and antibiotics such as vancomycin and tobramycin, suggesting that *cmpX* may play a role in the cell membrane function or structure. Interestingly, *cmpX* knockout also demonstrated increased sensitivity to potassium tellurite an environmental toxin. Tellurite in the environment is a result of metalloid pollution. It is highly toxic to most bacteria and was understood in fact as an antimicrobial agent (Fleming & Young, 1940). It was recently shown that tellurite is capable of inducing c-di-GMP levels in *P. aeruginosa*. When c-di-GMP levels were artificially reduced, *P. aeruginosa* demonstrated increased sensitivity to this toxic metalloid (Chua et al., 2015).

*P. aeruginosa* colonizes and grows in the host in the form of biofilms by undergoing a specific transition from planktonic to sessile state. This process involves sensing its environment and regulation of virulence factors. The transition of *Pseudomonas* from planktonic to attached cells during infection is profoundly complex. Bacteria in biofilms are physiologically very different from their planktonic counterparts, including antimicrobial resistance profiles (Bhagirath et al., 2016; Dubois-Brissonnet et al., 2016); but the developmental process remains to be understood. C-di-GMP levels in planktonic bacteria (< 30 pmol) are much lesser than those in biofilms (75-110 pmol) (Basu Roy & Sauer, 2014). Collectively, these findings of affected phenotypes in a *cmpX* mutant support previous studies and suggest that *cmpX* may have a more complex function. Further studies are needed to elucidate its roles in complete details.

**Chapter 5**

**Mucin and oxygen limitation activate PA1611 to facilitate biofilm formation in**

*Pseudomonas aeruginosa*

**5.1 Rationale**

Pseudomonads have been shown to be able to form biofilms in virtually any environment conducive to growth. This is attributable to nutritional versatility of *P. aeruginosa* as well as its abilities to regulate its genes through several sensing mechanisms such as quorum sensing (QS), two-component regulatory systems and signaling by bis-(3'-5')-cyclic dimeric guanosine monophosphate (c-di-GMP), which facilitate bacterial adaptation to different niches and survival. Clinical isolates obtained from CF patients demonstrate an enhanced ability to form biofilms as well as exhibit distinct genetic differences from their environmental counterparts (Grosso-Becerra et al., 2014). CF sputum also demonstrates presence of quorum sensing molecules and their levels are co relatable with clinical stage of CF lung disease  (Barr et al., 2015). CF lungs present a unique niche, with hyper viscous mucus layer, impaired ciliary clearance, oxygen and nutrient limitation and antibiotic stress. Contrary to limiting bacterial survival, presentation of such conditions leads to the selection of competent strains by mutations and gene acquisition also known as the "hyper-mutator" strains, which are robust in colonization and resistance against external stressors.

Mucus in airways is predominantly composed of mucin glycoproteins. Mucins exist as secreted and cell-associated glycoproteins. Secreted, gel-forming mucins are mainly responsible for the viscoelastic property of mucus, which is crucial for effective mucociliary clearance. Cell-associated mucins shield the epithelial surface from pathogens through their extracellular domains and regulate intracellular signaling through their cytoplasmic regions (Lillehoj et al., 2013). *P. aeruginosa* has been shown to attach to the mucin and form biofilms (Landry et al., 2006). The hyper viscous mucus, apart from impairing mucociliary clearance and bacterial clogging, also present a problem of oxygen limitation and formation of the hypoxic gradients in

the mucus plugs (Lambiase et al., 2010). Low oxygen environment has been shown to facilitate bacterial adherence by creating a calcium imbalance in the bacterial cell and facilitate biofilm formation (S. Gupta et al., 2016). Further, a large proportion of anaerobic bacteria have been isolated from sputum of CF patients as compared to non-CF controls (Tunney et al., 2008). Mucins have also been shown to activate *P. aeruginosa* biofilm formation (Landry et al., 2006); Furthermore oxygen limitation activates type three secretion system (T3SS) and effector secretion mediated by *anr* pathway activation (O'Callaghan et al., 2011). In CF lungs both these conditions present together, however a combined effect on the phenotype of *P. aeruginosa* has never been fully investigated.

It has been previously shown that the role of PA1611 in RetS-GacS/A-RsmA-Y/Z system is key to biofilm formation in *P. aeruginosa* (Bhagirath, Pydi, et al., 2017; Kong et al., 2013). RetS and PA1611 are hybrid histidine kinases whereas GacS/A is a classical TCS. The exact environmental cues that activate these TCSs are yet unknown. RetS has been shown to suppress *pel* genes that encode for polysaccharide components of the biofilm. GacS, when activated, phosphorylates GacA and activates transcription of small RNAs RsmY and RsmZ. RsmZ and RsmY bind to posttranscriptional activator RsmA. RsmA has been shown to control motility, Type IV pili and T3SS in a titration dependent manner. T3SS is a needle-like injectisome which is used to secrete toxic effectors (ExoS, Y, T, U) in host cells resulting in cell damage and death. T3SS is a hallmark of acute infection phase. Once RsmA is sequestered, genes for biofilm formation are activated.

In this objective, the expression of PA1611 was characterized in clinical isolates as well as environmental isolates such as PAK. Using quantitative real-time PCR, it is shown that PA1611 knockout mutants demonstrated low c-di-GMP levels. Low c-di-GMP is associated with

activation of T3SS and high motility in *P. aeruginosa* (McCarthy et al., 2017). Previously intracellular *cdrA* expression levels have been shown to faithfully reflect c-di-GMP levels and hence has been used as a measure to quantify c-di-GMP levels indirectly (Rybtke et al., 2012). Clinical isolates of *P. aeruginosa* were found to demonstrate a high level of *cdrA* promoter activity as compared to PAO1.

Further, it is shown that PA1611 responds to oxygen limitation and mucin. Though when studied independently, oxygen limitation and mucin have opposite effects on acute virulence factors in *P. aeruginosa* such as T3SS, when combined, they facilitated biofilm formation in *P. aeruginosa*. It is also shown that this combined effect was mediated through the central PA1611-GacS/A-RetS-RsmA-Y/Z pathway. Given the complex nature of signaling pathways in *P. aeruginosa*, deciphering these intersecting pathways is key to understanding pathogenesis and designing new and effective therapies to control infection.

## 5.2 Material and methods

### 5.2.1 Bacterial strains and plasmids

Bacterial strains and plasmids used in this thesis are listed in **Table 5.2.1**. Primers used in the study are listed in **Table 5.2.2**. *Escherichia coli* strain DH5α was used for all cloning procedures, and *E. coli* strain *Sm10λpir* for conjugative DNA transfer. For fluorescence studies, the M9 minimal medium was used. The completely sequenced *P. aeruginosa* strain PAK was used as reference strain. *P. aeruginosa* clinical isolates from PA082-096 were a kind gift from Dr. Ayush Kumar at the University of Manitoba. p*cdrA*$_{gfp}$ was a kind gift from Dr. Morten Rybtke at the Costerton biofilm center, University of Copenhagen.

**Table 5.2.1 Bacterial strains and plasmids used in this study.**

| Strain or plasmid | Relevant characteristics | Source |
|---|---|---|
| *E. coli* | | |
| SM10-λ *pir* | Mobilizing strain, RP4 integrated into the chromosome; Kn$^r$ | (Simon et al., 1983) |
| XL1-Blue | *recA1 endA1 gyrA96 thi-1 hsdR17 supE44 relA1 lac [F´ proAB lacIq ZΔM15 Tn10 (Tet$^r$)].* | Invitrogen |
| *P. aeruginosa* | | |
| PAO1 | Wild-type *P. aeruginosa* | This lab |
| PAK | Environmental strain of *P. aeruginosa* | This lab |
| PA082-96 | CF clinical isolates | Dr. Ayush Kumar |
| P9 | Strain of *P. aeruginosa* | This lab |
| P11 | Strain of *P. aeruginosa* | This lab |
| PA(ΔPA1611) | PA1611 Knockout mutant of PAO1 | This lab |
| Plasmids | | |
| CTX6.1 | Integration plasmid origins of plasmid mini-CTX-lux; Tc$^r$ | This lab |
| pAK1900 | *E. coli-P. aeruginosa* shuttle cloning vector carrying P*lac* upstream of MCS; Ap$^r$; Cb$^r$ | This lab |
| p*cdrA$_{gfp}$*$^C$ | pUCP22Not-P*cdrA*-RBSII-*gfp*(Mut3)-T$_0$-T$_1$, Amp$^r$ Gm$^r$ | Dr. Morten Rybtke |
| pAK1611 | pAK1900 with a 2024 bp fragment of *PA1611* between *Sal*I and *Hind*III; Ap$^r$, Cb$^r$ | This study |

| | | |
|---|---|---|
| CTX-*exoS* | Integration plasmid, CTX6.1 with a fragment of pKD-*exoS* containing *exoS* promoter region and *luxCDABE* gene; Kn[r], Tmp[r] , Tc[r] | This Lab |
| CTX-*rsmZ* | Integration plasmid, CTX6.1 with a fragment of pKD-*rsmZ* containing *rsmZ* promoter region and *luxCDABE* gene; Kn[r], Tmp[r], Tc[r] | This lab |
| pKD-*rsmZ* | pMS402 containing *rsmZ* promoter region; Kn[r], Tmp[r] | This lab |
| pMS402 | Expression reporter plasmid carrying the promoterless *luxCDABE* gene; Kn[r],Tmp[r] | (Duan et al., 2003) |
| pMS402*gfp* | Expression reporter plasmid carrying the promoterless *gfp* gene; Kn[r],Tmp[r] | This study |
| pEX18Tc | oriT[+] sacB[+] gene replacement vector with multiple-cloning site from pUC18; Tc[r] | (Hoang et al., 1998) |
| CTX-*exoS* | Integration plasmid, CTX6.1 with a fragment of pKD-*exoS* containing *exoS* promoter region and *luxCDABE* gene; Kn[r], Tmp[r] , Tc[r] | This Lab |
| CTX-*rsmY* | Integration plasmid, CTX6.1 with a fragment of pKD-*rsmZ* containing *rsmZ* promoter region and *luxCDABE* gene; Kn[r], Tmp[r], Tc[r] | This lab |
| pKD-*cdrA* | The pMS402 plasmid containing the *cdrA* promoter region and *luxCDABE* reporter cassette; Kn[r], Tmp[r] | This lab |

**Table 5.2.2 Primers used in this study.**

| Primer | Sequence (5'-3') |
|---|---|
| PA1611-F | GTAGTCGACGAAGGAGAAGAACCATG |
| PA1611-R | GCTAAGCTTGGCGAACAGATGTTCACT |
| *rpoD*-F | CCTGATGAAGGCGGTGGAC |
| *rpoD*-R | GATGCGGATGGTGCGTGC |
| *oprF*-F | CAGTACCCGTCCACTTCCAC |
| *oprF*-R | TTCACGCGACCACCTTCTAC |
| *sigX*-F | AATTGATGCGGCGTTACCA |
| *sigX*-R | CCAGGTAGCGGGCACAGA |
| *wspR*-F | GCGGTCATGGTACTGCTTGT |
| *wspR*-R | CCGTCGGCTTGATCTGGTTG |
| pKD-*rsmY*-F | ATCTCGAGCAGTTCCTGGAGCTGGA |
| pKD-*rsmY*-R | GTCGGATCCTCTATCCTGACATCCG |
| pMS402-*sigX*-F | TTACTCGAGTCCTGGCGCAACTGGTGA |
| pMS402-*sigX*-R | GTAGGATCCGTGAGATCAGGCCAGTCAT |
| pMS402-*oprF*-F | TTACTCGAGGACGTGGCTGCTCTGCAGG |

| | |
|---|---|
| pMS402-*oprF*-R | GTAGGATCCCCGTTAAATCCCCATCTTG |
| *wspR*-F | GCGGTCATGGTACTGCTTGT |
| *wspR*-R | CCGTCGGCTTGATCTGGTTG |
| *Arr*-F | TCCTACGACGAACGGTTCCA |
| *Arr*-R | CACCTCGACCGGAAACCTTG |
| *anr*-F | TCGCTGACCGTGGAAGACAT |
| *anr*-R | AAAGGATCACCCTGGCGGAA |
| *rsmA*-F | GTGACGGTACTGGGTGTCAAA |
| *rsmA*-R | GGTGTACGGCGACTTCCTT |
| *cdrA*-F | TACGCTCAAGTACCGGCAGA |
| *cdrA*-R | GCTGTTGGCCTCGAGAATCC |
| *rhlR*-F | GCGTTGCATGATCGAGTTGC |
| *rhlR*-R | CCGGGTTGGACATCAGCATC |

F-Forward primer; R-Reverse primer

### 5.2.2 Mucin preparation

Mucin was prepared as per a protocol described previously (Flynn et al., 2016). Add 30g/L mucin (Sigma type III) was added to MilliQ $H_2O$ and autoclaved this was labeled "A mucin." "A mucin" was dialyzed for 1 hr at room temperature in a 13 kDa molecular weight cutoff membrane and overnight at 4 °C in MilliQ $H_2O$ and was labeled "AD mucin". The dialyzed mucin was clarified by centrifugation at 30,000 RPM for 5 min. The pellet at the bottom was collected using a sterile syringe and labeled as "ADC mucin." ADC mucin was further passaged through a 0.45 μm Millipore syringe filter to sterilize and isolate soluble intact glycoproteins.

### 5.2.3 Media mimicking artificial sputum/Modified artificial CF sputum media (ASMDM)

ASMDM was prepared as described previously (Fung et al., 2010; Sriramulu et al., 2005). First Artificial Sputum Medium (ASM) was prepared with 10 g/L mucin from pig stomach mucosa (PGM; Sigma), 4 g/L DNA (Fluka), 5.9 mg Diethylene Triamine Pentaacetic Acid (DTPA) (Sigma), 5 g NaCl and 2.2 g KCl was added to 700 ml dd $H_2O$ followed by stirring for 5 min, and homogenization to dissolve the mucin and DNA. This was followed by 110 $^{\circ}$C for 15 minutes. After the media has cooled down to room temperature, 5 ml egg yolk emulsion (phosphatidylcholine as a source of lecithin) (Oxoid) and 5 g casamino acids per 1 l water (pH 7. 0) and 1 g/L BSA (Sigma) was added. Prior to all experiments sterility of media was confirmed by culturing media on an LB plate as well as for growth studies a blank media was kept as negative control.

### 5.2.4 Culture under anaerobic conditions

For anaerobic studies *P. aeruginosa* PAO1 and PAK strains were cultured overnight at 37°C in an anaerobic chamber (BD Gaspak) in M9 medium supplemented with 100mM $KNO_3$ at 225

rpm with or without 1% mucin. BD Gaspaks Indicators were used as measure of anaerobicity (<1% oxygen) as per manufacturer's recommendations.

### 5.2.5 Isolation of total RNA from anaerobic cultures

Aerobic controls strains were inoculated from glycerol stocks into 2 mL LB medium and grown overnight at 37°C followed by sub-culturing in 5 mL LB medium and grown to mid-exponential phase. A 0.25 mL aliquot of the cell culture, corresponding to $5 \times 10^8$ cells, was added to 0.5 mL of RNeasy bacteria protect solution (Qiagen, Hilden, Germany). For anaerobic controls strains were cultured overnight at 37°C in media supplemented with 100mM $KNO_3$ with anaerobic indicator. RNA Protect (Qiagen) was used as RNA stabilizing agent in cultured cells. Total RNA was isolated according to the manufacturer's instructions. Residual DNA was eliminated by DNase treatment using 20 U of RQ1 RNase-free DNase (Promega, Madison, WI). After removal of DNase, RNA was extracted and resuspended in 30 μl of RNase-free $H_2O$. The presence of residual DNA and the RNA quality was checked by formaldehyde/agarose gel electrophoresis.

### 5.2.6 Live/dead staining and microscopy of biofilms

To examine effect of anaerobic environment on biofilm formation we performed a coverslip-based biofilm formation assay. 22 mm × 22 mm polyvinyl plastic coverslips (Fisherbrand, cat #12-541B) were placed (vertical or at 45 degrees) in each well of a six-well cell culture plate (Corning Costar, cat # 3516). Plates with coverslips were then UV-sterilized in a tissue culture hood for at least 2 h. Overnight cultures of PAK strain were inoculated at 1:100 dilutions in M9 medium supplemented with 0.2% glucose. For anaerobic growth, M9 medium with 0.2% glucose was supplemented with 100mM $KNO_3$. To harvest the biofilm, the media was aspirated off and the coverslips were washed twice with sterile water. Biofilms on coverslips were then stained

with BacLight Live/Dead cellular viability kit (Invitrogen), for 10 min at room temperature. Excess dye was removed and biofilms were washed with sterile water and visualized using Nikon Ti elements inverted Microscope (Nikon Inc., Melville, NY) using a 40× lens. Cells stained red with Propidium iodide (PPI; non-viable cells) and green with SYTO9 (viable cells) in ten random fields of view per sample.

### 5.2.7 Siderophore quantitation assay

**Pyoverdine production**: Production of pyoverdine was quantified as described previously (Sánchez et al., 2002). Briefly, bacterial strains were grown at 37°C overnight in the M9 minimal medium. At this time, bacteria were pelleted by centrifugation, and the amount of pyoverdine was measured by fluorescence emission, by exciting the supernatants at 400 nm and measuring the emission at 460 nm. Each experiment was performed in triplicate.

**Pyochelin estimation:** For quantitation of pyochelin one ml cell-free supernatant, one ml each of 0.5 N HCl, nitrite molybdate reagent and 1N NaOH were mixed, and the final volume was made to 5 ml with distilled water. Absorbance was recorded at 510 nm (R. K. Gupta et al., 2011).

**5.3 Results**

**5.3.1 A PA1611 knockout strain in *P. aeruginosa* PAO1 survived Iron limiting conditions better and showed increased expression of genes associated with c-di-GMP breakdown.**

PA1611 is key to biofilm formation in *P. aeruginosa* but was expressed at very low levels under tested laboratory conditions (Data not shown). Therefore, Biolog Phenotype Microarray (PM) analysis was performed for wild type PAO1 and a PA1611 knockout PA(ΔPA1611) (represented as ΔPA1611) to characterize its metabolic or physiological role in *P. aeruginosa* PAO1. **Table 5.3.1** outlines the phenotypes lost and gained in ΔPA1611. Some of the findings were subsequently confirmed by independent assays. ΔPA1611 demonstrated sensitivity to sodium salicylate in PM assays, however, this could not be validated in independent assay **Figure 27A.** PM also suggested a gain in phenotype associated with iron limiting conditions (2,2 BIP)**.** This was subsequently validated and is shown in **Figure 27B**. A chromosomal *lux*-PA1611 tagged reporter was subsequently used to examine gene promoter activity in PAO1, however, the levels detected were very low. To determine the regulatory genes that may be affected in a PA1611 knockout mutant a qPCR analysis was performed. Genes such as *arr* (PA2818), encoding for c-di-GMP phosphodiesterase ($p<0.001$), *rsmA* ($p<0.01$) and *anr* (PA1544) ($p<0.05$) were significantly upregulated **Figure 28**. ΔPA1611 demonstrated significantly lower *cdrA* promoter activity as compared to PAO1($p<0.01$). This observation is in alignment with the observation of increase in the *arr* transcript levels in a ΔPA1611.

**Table 5.3.1 Summary of gained and lost phenotypes for *P. aeruginosa* PA1611 knockout mutants.**

| Index | Compound | Metabolic values | Function |
|---|---|---|---|
| **Phenotypes lost** | | | |
| 1 | Sodium Salicylate | -89 | biofilm inhibitor, anti-capsule agent, chelator, prostaglandin synthetase inhibitor, mar inducer |
| **Phenotypes gained** | | | |
| 1 | L-Leucine | 68 | C-Source, amino acid |
| 2 | 2,2`- Dipyridyl | 77 | chelator, lipophilic |
| 3 | Dichlofluanid | 107 | fungicide, phenylsulphamide |
| 4 | L-Leucine | 62 | N-Source, amino acid |
| 5 | L-Arginine | 57 | N-Source, amino acid |
| 6 | Glycine | 55 | N-Source, amino acid |
| 7 | Histamine | 70 | N-Source, other |
| 8 | Putrescine | 53 | N-Source, other |
| 9 | Gly-Gly-Leu | 88 | N-Source, peptide |
| 10 | Ile-Val | 84 | N-Source, peptide |
| 11 | Gly-Gly-Phe | 84 | N-Source, peptide |

| 12 | Glu-Val | 76 | N-Source, peptide |
|----|---------|-----|-------------------|
| 13 | β-Ala-His | 74 | N-Source, peptide |
| 14 | Gly-His | 73 | N-Source, peptide |
| 15 | Val-Ser | 72 | N-Source, peptide |
| 16 | Gly-Thr | 71 | N-Source, peptide |
| 17 | Gly-Gly-Gly | 68 | N-Source, peptide |
| 18 | Asp-Gln | 64 | N-Source, peptide |
| 19 | Ser-Glu | 60 | N-Source, peptide |
| 20 | Asp-Ala | 59 | N-Source, peptide |
| 21 | Gly-Gly-Ile | 59 | N-Source, peptide |
| 22 | Thr-Asp | 55 | N-Source, peptide |
| 23 | Pro-Ser | 54 | N-Source, peptide |
| 24 | Ser-Asp | 53 | N-Source, peptide |
| 25 | Chlorodinitrobenzene | 99 | Oxidizes sulfhydryls, depletes glutathione |

The table shows the phenotypes gained or lost by PA1611 knockout mutants as compared to wild type PAO1. Phenotype microarrays were performed by the commercially available Biolog PM, and data was analyzed by the OmniLog® V. 1.5 comparison module, and the average height parameters were used for data analysis with standard thresholds for detection. The metabolic distance threshold was set at 50, and the sensitivity threshold was set at 74.
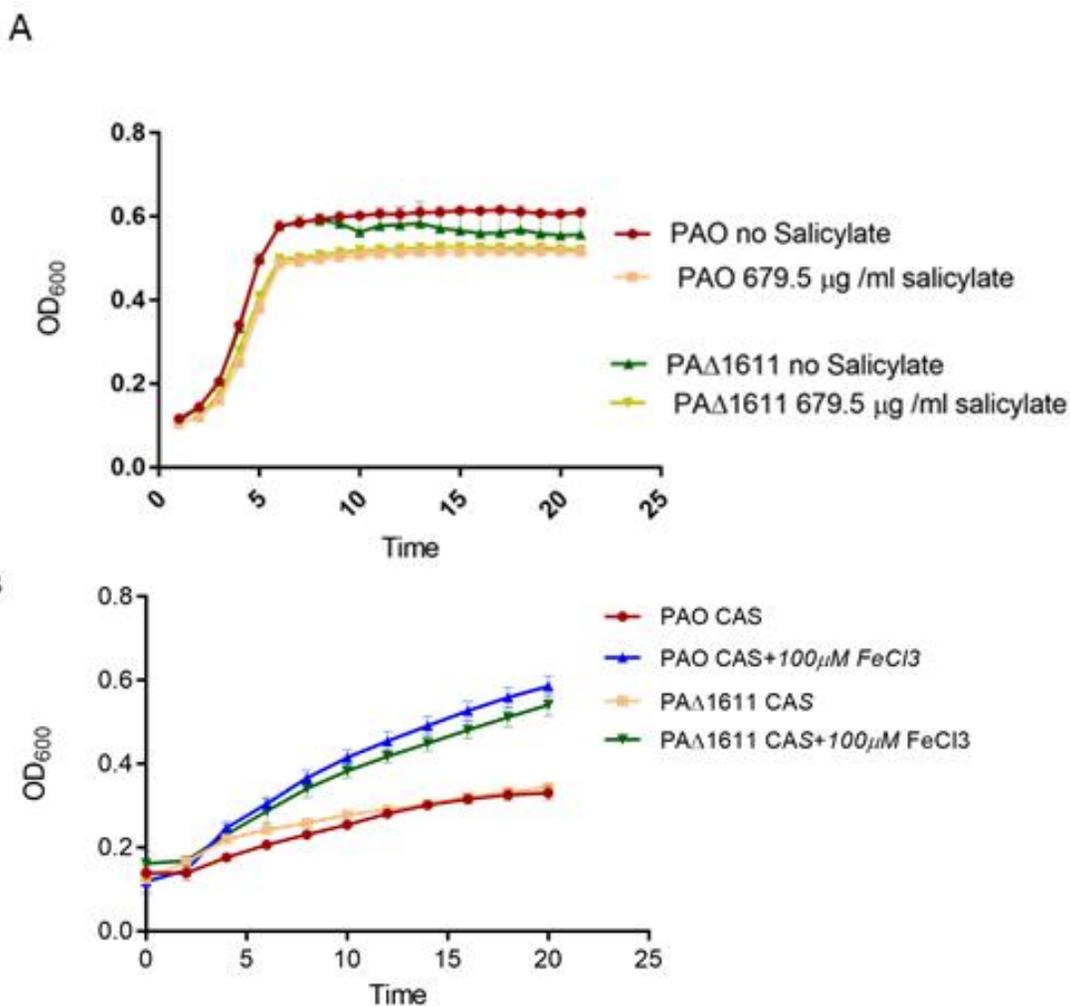
**Figure 27 Growth curves in the presence of sodium salicylate and iron restricted conditions. A.** Growth curves of *P. aeruginosa* PAO1 and ΔPA1611 in the presence of 679.5μg/ml of Sodium Salicylate. **B**. Growth of *P. aeruginosa* PAO1 and ΔPA1611 in presence of 2,2 BIP in CAS medium. Overnight cultures of wild type PAO1 and ΔPA1611 were inoculated into fresh medium in 96 well plate, and cell growth was measured by using optical density at 600 nm at indicated time points. The curves represent triplicates of three independent experiments. Error bars show the standard deviation.
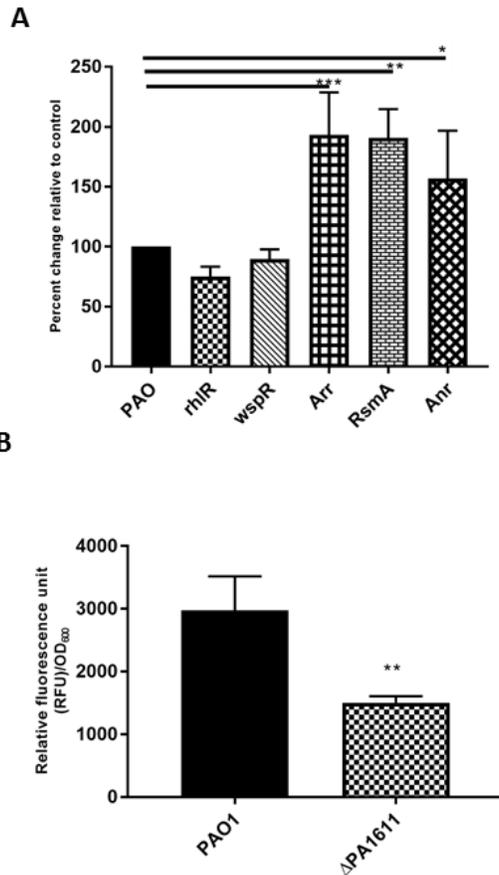
**Figure 28 Effect of PA1611 knockout on key regulatory genes in a PAO1 background. (A) mRNA expression (B) *cdrA* promoter activity in ΔPA1611 as compared to PAO1.** mRNA expression for analyzed genes was normalized to the housekeeping gene *rpoD*. Data are presented as percent change relative to control. A *cdrA*$_\text{gfp}$ chromosomally integrated strain of PAO1 and ΔPA1611 were compared for *cdrA* promoter activity. *cdrA* promoter activity at 12 h is normalized to growth and shown in relative fluorescence unit (RFU)/OD$_{600}$. The values represent an average of three independent experiments. Data were analyzed using unpaired t-test and one-way ANOVA. NS $p > 0.05$, *$p < 0.05$ **$p < 0.01$, and ***$p < 0.001$. Error bars indicate standard deviations.

## 5.3.2 PA1611 is well expressed in clinical isolates

A PA1611 knockout strain demonstrates significant phenotypic differences from the wild type. However, it is expressed at very low levels in *P. aeruginosa* PAO1. Given the crucial role of PA1611 in *P. aeruginosa* pathophysiology, we wanted to investigate if this expression has any clinical relevance. Thus *P. aeruginosa* clinical isolates were obtained to study expression levels of PA1611. *P. aeruginosa* CF isolates PA082-PA096 were kindly provided by Dr. Ayush Kumar at the University of Manitoba and were obtained from SickKids hospital (Toronto, Canada). PA1611 was tagged with a *luxCDABE* reporter as described before. We also included *P.aeruginosa* environmental strain PAK in this assay. As compared to other strains, these clinical isolates (PA082-PA096), as well as the PAK strain, demonstrated significantly higher expression of PA1611 ($p<0.0001$)(**Figure 29**). Expression levels of two-component regulatory proteins have been shown to be correlatable with antimicrobial resistance (L. Li et al., 2016; Yang et al., 2012). Thus, we wanted to see if expression levels of PA1611 in different strains can be associated with specific antimicrobial resistance, these clinical isolates were tested for MIC to common antimicrobial drugs. The MIC profiles for tested isolates are presented in **Table 5.3.3.** However, PA1611 gene expression could not be correlated to antimicrobial resistance profiles. The sub-inhibitory concentration of antibiotics such as tobramycin and ciprofloxacin did not show any significant change in expression of PA1611 as compared to that of controls.
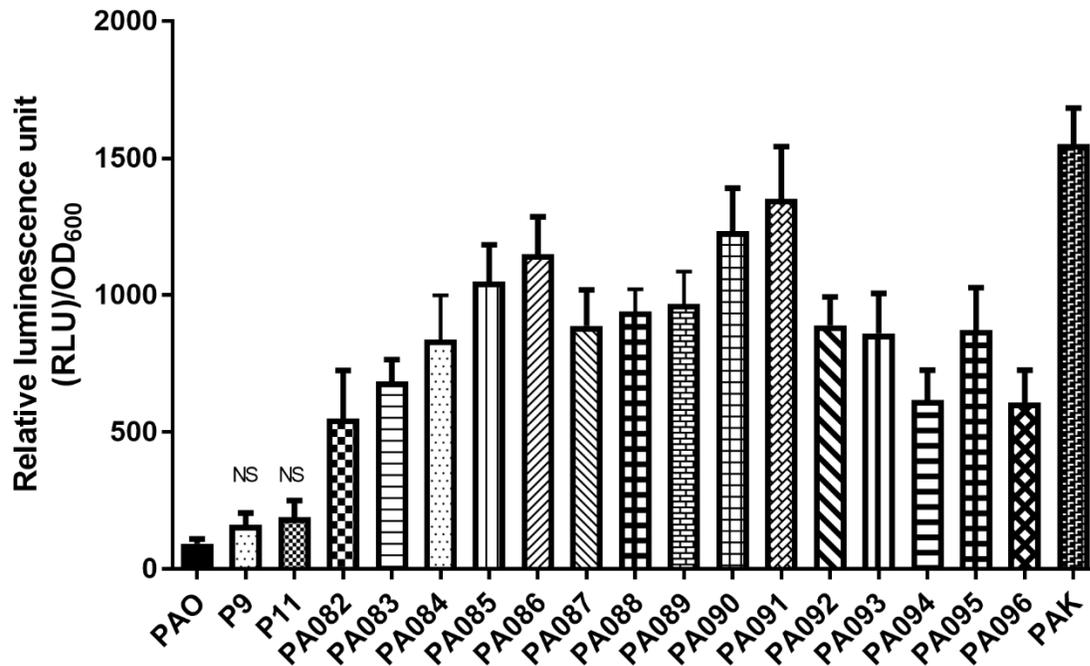
**Figure 29 PA1611 promoter activity in clinical isolates at 12h**. A CTX-PA1611 reporter fusion integrated to the chromosome was used to measure the PA1611 promoter activity. Bacterial growth was monitored simultaneously ($OD_{600}$). The promoter activity at 12 h is normalized to growth and shown as relative luminescence unit (RLU)/$OD_{600}$. The values shown are an average of three independent experiments. The error bars indicate standard deviations. All clinical isolates (PA082-PA096 and PAK) showed a significant increase in PA1611 promoter activity (***) as compared to PAO1. Data were analyzed using one-way ANOVA with Dunnett post-hoc test. NS $p > 0.05$, **$p < 0.01$ and ***$p < 0.001$.

**Table 5.3.3 MIC for tested clinical isolates**

| Antibiotics ((µg/ml) | Tobramycin | Amikacin | Ciprofloxacin | Levofloxacin | Ceftazidime | Meropenem | Cefazolin |
|---|---|---|---|---|---|---|---|
| PA 082 | 64 | >64 | 1 | 0.5 | 32 | 1 | >64 |
| PA083 | >64 | >64 | 4 | 2 | 1 | <0.125 | >64 |
| PA 084 | >64 | >64 | 1 | 1 | >64 | 0.125 | 32 |
| PA 085 | 32 | >64 | 0.5 | 0.5 | 2 | <0.125 | >64 |
| PA 086 | >64 | >64 | 8 | 4 | 4 | 4 | >64 |
| PA 087 | >64 | 4 | 32 | 16 | 8 | 32 | >64 |
| PA 088 | >64 | >64 | 8 | 4 | 32 | <0.125 | >64 |
| PA 089 | >64 | 8 | 0.125 | 0.25 | >64 | 4 | >64 |
| PA 090 | >64 | >64 | 4 | 2 | 1 | <0.125 | >64 |
| PA 091 | 32 | >64 | 2 | 1 | 8 | 8 | >64 |
| PA 092 | 64 | >64 | 0.5 | 1 | 16 | 1 | >64 |
| PA 093 | 8 | 64 | 8 | 8 | 4 | 1 | >64 |
| PA 094 | 64 | 64 | 4 | 4 | >64 | 1 | >64 |
| PA 095 | 64 | >64 | 4 | 2 | >64 | 32 | >64 |
| PA 096 | 32 | 32 | 4 | 4 | 4 | 1 | >64 |
| PAK | 8 | 32 | 1 | 0.5 | 2 | 1 | 8 |

The table shows MIC for tested clinical isolates. MIC was defined as the lowest antibiotic

concentration that inhibited visible growth of the organism.

### 5.3.3 Expression of T3SS effector *exoS* is decreased in artificial media mimicking CF sputum

Since PA1611 was well expressed in PAK strain and the clinical isolates, we hypothesized that it could respond to some clinical and environmental signal. *P. aeruginosa* is a ubiquitous organism and simulating triggers in the environment is too complex, and hence well identified signals in CF lung environment was used to examine for effect on expression of PA1611. The use of CF-patient sputum is impractical if not complex due to factors such as inter-patient variability, sterility of the sample, the presence of highly resistant yeasts and antibiotic use. Recently standardized media mimicking CF sputa have been formulated and have provided significant insights into Pseudomonas behavior in vivo. For this part of the study, PAK strain was used as its genome sequence is well known and PA1611 is well expressed. Thus, we constructed a CTX−*exoS* and *CTX−PA1611* reporter fusion which was integrated into the chromosome of PAK strain. PA1611 and *exoS* promoter activity was monitored over an extended period of growth. As shown in **Figure 30** no significant difference in PA1611 promoter activity was observable between LB and ASDM. We also examined the effect of ASMDM upon T3SS effector *exoS*. As shown in **Figure 31A** a significant decrease in promoter activity for *exoS* was observable in ASMDM as compared to that in LB media. ASMDM is a complex media of several components and to examine the specific component of ASMDM which was causing this effect, we examined *exoS* promoter activity in ASMDM media by removing one component at a time. A significant increase in *exoS* promoter activity was observable only in ASMDM devoid of mucin. Thus, we added 1% mucin into LB media to observe the gene expression while monitoring the growth simultaneously. *exoS* promoter activity was significantly decreased in presence of 1% mucin (**Figure 31B**).
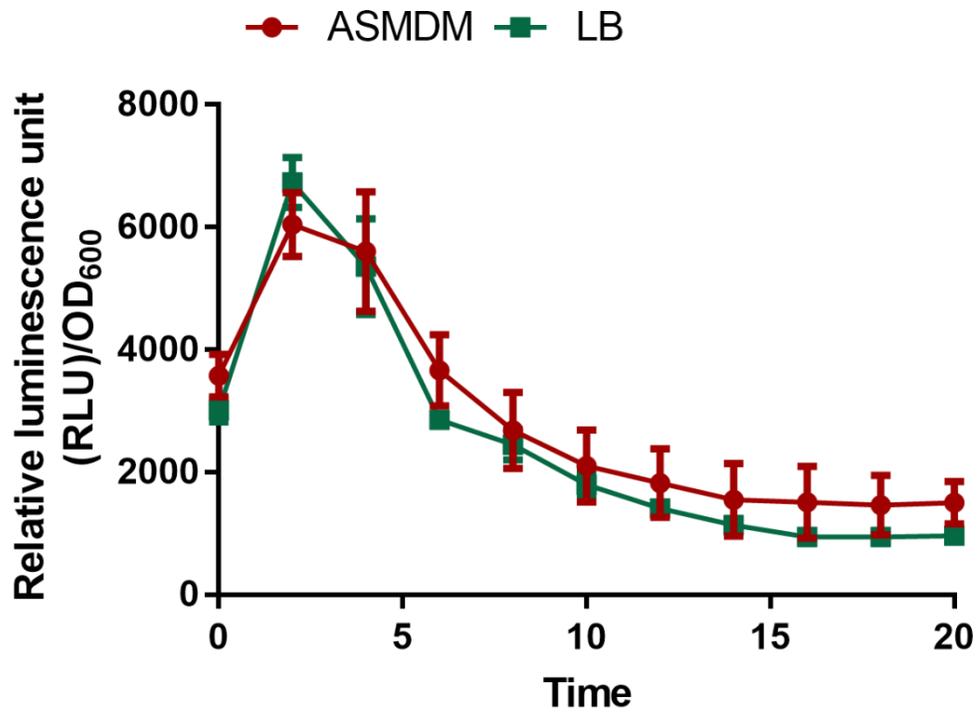
**Figure 30 PA1611 promoter activity normalized to growth over time in ASMDM and LB in**
*P. aeruginosa* **PAK strain.** A CTX-PA1611 reporter fusion integrated to the chromosome was
used to measure the PA1611 promoter activity in ASMDM medium (Red) and LB (Green).
Bacterial growth was monitored simultaneously ($OD_{600}$). The PA1611 promoter activity is
normalized to growth and shown as relative luminescence unit (RLU)/$OD_{600}$. The values shown
are an average of three independent experiments. The error bars indicate standard deviations.
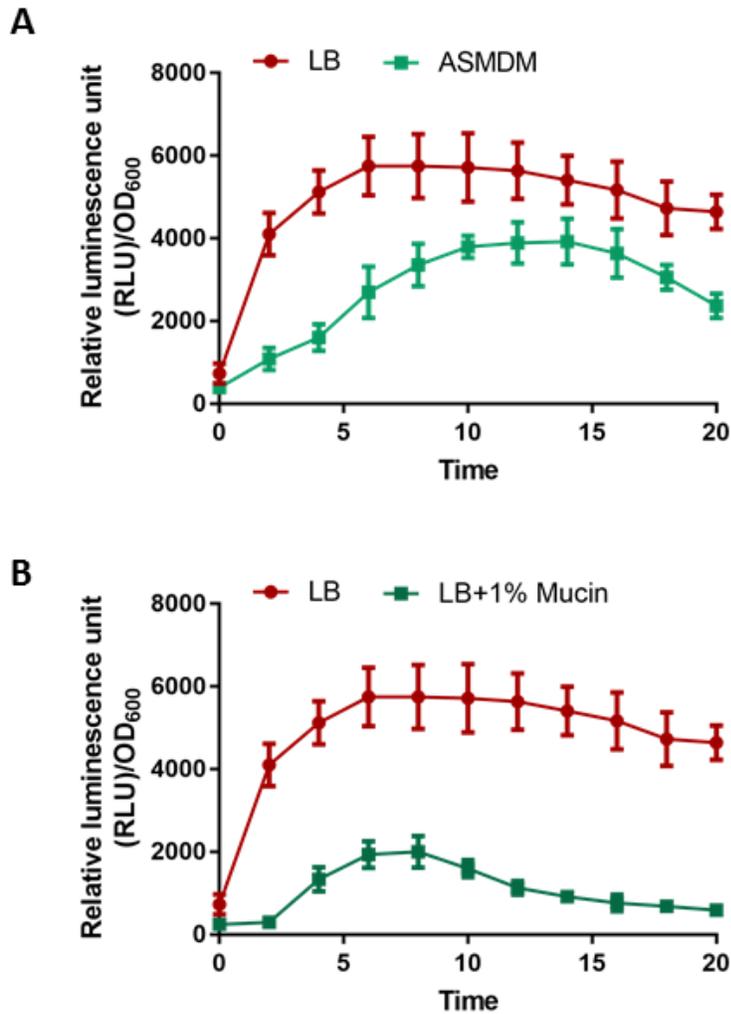
**Figure 31 *exoS* promoter activity normalized to growth over time in *P. aeruginosa* PAK strain.** A CTX-*exoS* reporter fusion integrated to the chromosome was used to measure the *exoS* promoter activity in LB and ASMDM (**A**) and LB compared to LB supplemented with 1% mucin (**B**). Bacterial growth was monitored simultaneously ($OD_{600}$). The *exoS* promoter activity is normalized to growth and shown as relative luminescence unit (RLU)/$OD_{600}$. The values shown are an average of three independent experiments. The error bars indicate standard deviations.

## 5.3.4 Mucin activates PA1611, small RNAs and biofilm formation in *P. aeruginosa* PAK

Cystic fibrosis lung disease is characterized by a deficient mucus barrier, mucus hyper-production as well as defective mucociliary clearance. A major component of mucus is mucin. Mucin is heavily glycosylated, with a protein backbone and is a key component of airway mucus. Because of its structure, mucin is known to serve as a carbon source of infecting pathogens including *P. aeruginosa* (Alrahman & Yoon, 2017). Such an association is a major contributing factor to establish airway infection. However, the genes involved in sensing mucin remain elusive.

Mucin is a dominant component of ASMDM. Though PA1611 promoter activity was not significantly increased in ASMDM, *exoS* promoter activity was lower, and we have previously shown that PA1611 and *exoS* are reciprocally expressed. Thus, we monitored the PA1611 gene expression in mucin containing media over time. A significant increase in promoter activity of PA1611 was observable in the presence of mucin. **Figure 32A** shows growth normalized promoter activity of PA1611 at 12h. Activation of PA1611 is associated with an increase in biofilm formation, and hence biofilm formation was examined using a crystal violet staining assay in the presence of mucin keeping a non-mucin control. Again, a significant increase in biofilm formation was observed (**Figure 32B**). Biofilm formation in *Pseudomonas* involves tight control over the transcription of the regulatory small RNAs, *rsmY,* and *rsmZ* and transcriptional regulator RsmA. Thus, to examine if activated biofilm was mediated through GacA/GacS/RetS/PA1611-RsmA/Y/Z pathway, the promoter activity of transcriptional regulator RsmA and small RNAs were measured in presence of mucin. For small RNAs, *rsmY* was used as representative. A significant decrease in *rsmA* promoter activity and increase in *rsmY* promoter activity was observed (**Figure 32C** and **D**). Further, it was observed that the biofilm quality is more compact and robust as compared to without mucin **(Figure 32E)**. This agrees with some

previous studies (Haley et al., 2012; Landry et al., 2006). The results of this experiment suggested that mucin related increase in biofilm formation is at least in part mediated by the GacA/GacS/RetS/PA1611-RsmA/Y/Z pathway.

**A**



**B**

Biofilm formation



**C**



**D**



**E**



No Mucin
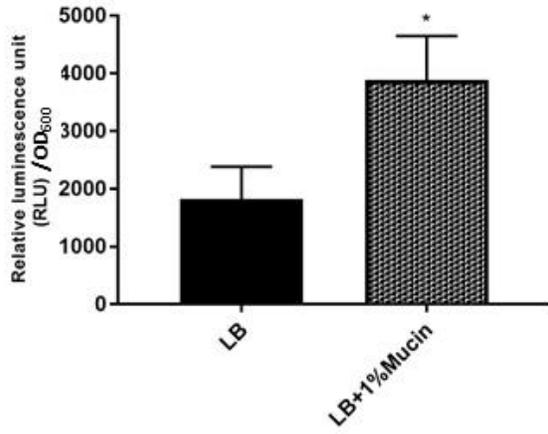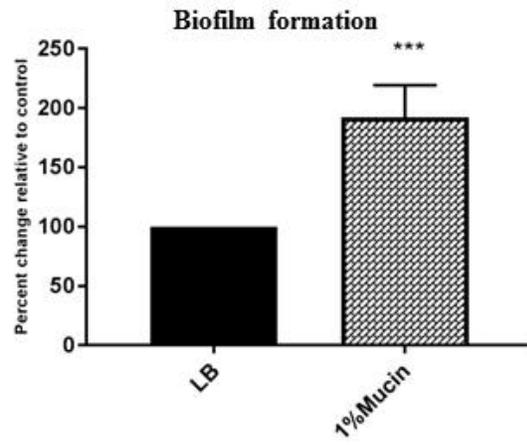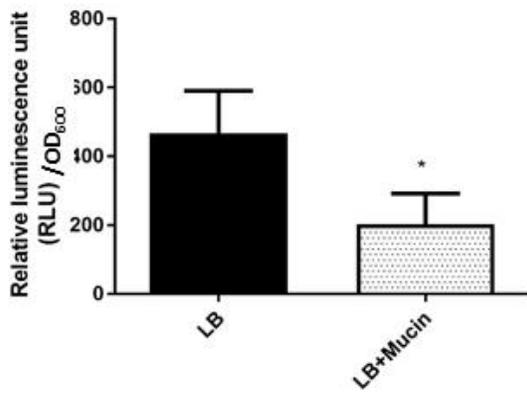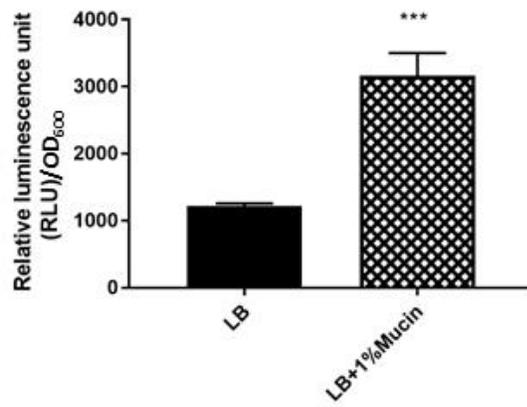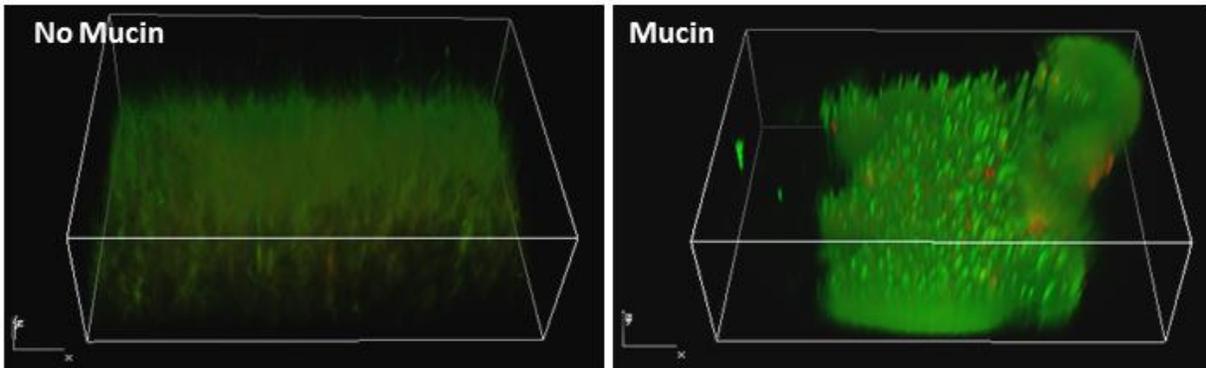
Mucin

**Figure 32 Role of mucin in the GacA/GacS/RetS/PA1611-RsmA/Y/Z pathway. A.** PA1611

promoter activity at 12h in mucin (LB with 1% mucin) and non-mucin containing (LB) media.

**B.** Biofilm formation in the presence of mucin as compared to non-mucin control. Data are

shown as the percent change relative to non-mucin control. **C** *rsmA* promoter activity at 12h. **D**.

*rsmY* promoter activity at 12h. **E.** A live/dead assay for biofilm visualization in the presence of

1% mucin (right) as compared to non-mucin (left) control in a M9 medium with 0.2% glucose.

Live cells are stained with to SYTO-9 (green), and dead cells are stained with Propidium iodide

(red). The top views are projected from a stack of 50 images taken at 1 μm intervals for a total of

50 μm. Experiments were repeated three times and representative images, processed at the same

magnification, are shown. A CTX-PA1611, CTX-*rsmA* and CTX-*rsmA* reporter fusion integrated

to the chromosome was used to measure the PA1611, *rsmA* and *rsmY* promoter activity

respectively in PAK strain. The *rsmA* and *rsmY* promoter activity at 12 h is normalized to growth

and shown in relative luminescence unit (RLU): cps (counts per second)/$OD_{600}$. The values

shown are an average of three independent experiments. Data were analyzed using unpaired t-

test. NS $p > 0.05$, **$p < 0.01$, ***$p < 0.001$, and ****$p < 0.0001$. Error bars indicate standard

deviations.

## 5.3.5 PA1611 is activated in response to oxygen limitation

Lungs of CF patients are characterized by areas of low oxygen tension. This is caused by lung function impairment, poor mucus clearance, and bacterial colonization. The metabolic behavior of colonizing microorganisms is complex within CF airway mucus. One aspect of the biofilm mode of growth of *P. aeruginosa* in such areas in CF airways is growth via anaerobic respiration. (D. J. Hassett et al., 2009; Schobert & Jahn, 2010). Though *P. aeruginosa* prefers oxygen respiration for growth, it is well adapted to survive under oxygen-limited to anaerobic conditions. Under oxygen-limited conditions, *P. aeruginosa* can utilize nitrate or nitrite by a process known as denitrification. CF airway secretions are a rich source of $NO_3$, $NO_2$ and arginine are present in CF airway secretions (250 to µmol/L to 1000 µmol/L) (Lucas R. Hoffman et al., 2010). Thus, to examine if PA1611 may be responsive to oxygen limitation and to better understand its role in forming biofilm *in vivo* we performed a quantitative real-time PCR analysis for PA1611 expression in PAK strain under anaerobic conditions as compared to under aerobic conditions. PAK strains were cultured in aerobic and anaerobic conditions for 12 h at 37$^{\textbf{o}}$C followed by RNA isolation for measuring PA1611 expression levels. Anaerobic cultures of PAK were supplemented with 100mM $KNO_3$ and were kept in anaerobic chambers (BD Gaspak) with indicators as per manufacturer's instruction (oxygen levels <1%). PA1611 transcript levels were increased at least 1.7-fold under anaerobic conditions as compared to aerobic controls (**Figure 33**).
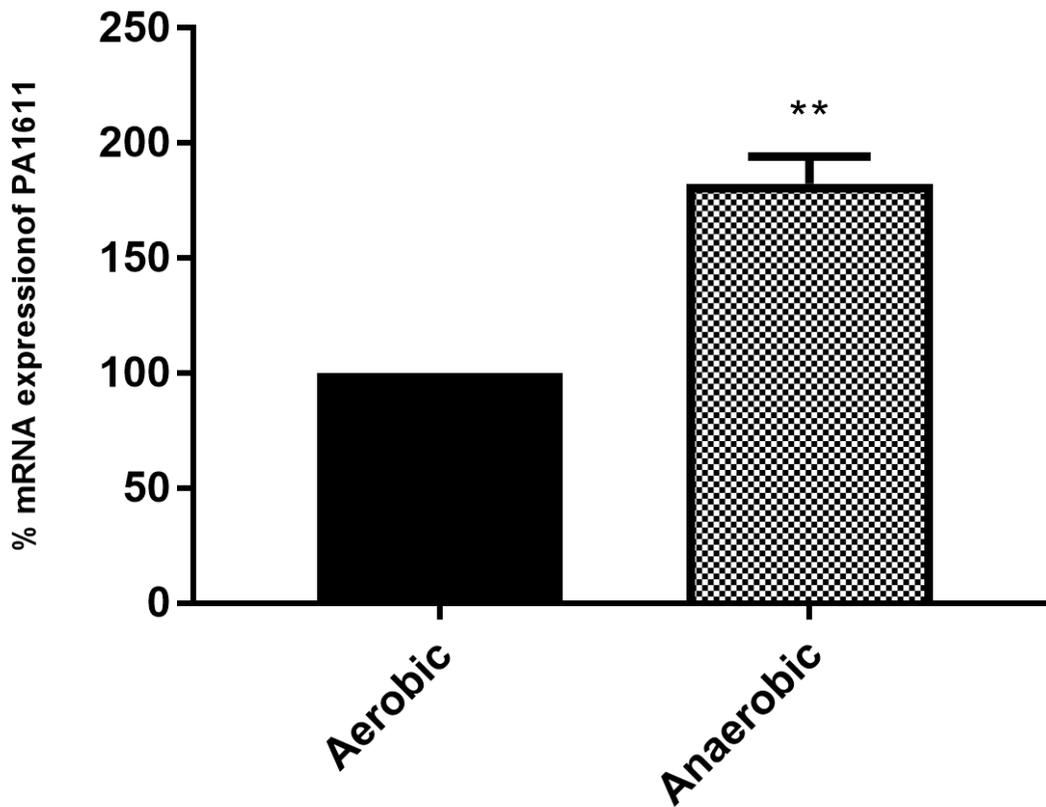
**Figure 33 PA1611 is activated in response to oxygen limitation.** mRNA expression for PA1611 was normalized to the housekeeping gene *rpoD* in PAK under aerobic and anaerobic conditions after 12h of culturing. Data are presented as percent change relative to the aerobic control. The values shown are an average of three independent experiments. Data were analyzed using unpaired t-test with $**p < 0.01$ considered significant. Error bars indicate standard deviations.

## 5.3.6 Oxygen limitation activates biofilm formation in *P. aeruginosa*

Given the activation of PA1611 under anaerobic conditions, we wondered if there was an effect on biofilm formation under similar conditions. To examine the effect of anaerobic environment on biofilm formation we performed a quantitative crystal violet assay and a coverslip-based biofilm formation assay to visualize biofilm structure under anaerobic conditions as described previously. Overnight cultures of PAK strain were inoculated at 1:100 dilutions in the M9 medium supplemented with 0.2% glucose for aerobic and M9 medium supplemented with 0.2% glucose and 100mM $KNO_3$ for anaerobic culture. For the quantitative assay, biofilms were stained with crystal violet and solubilized in 100% ethanol followed by recording the absorbance at 595nm. For visualizing biofilms, the coverslips with biofilms were washed and stained with Baclight live-dead viability stain. Cells stained red with Propidium iodide (PPI; non-viable cells) and green with SYTO9 (viable cells) in ten random fields of view per sample. After 24h, as shown in the figure, biofilm formation was enhanced under anaerobic conditions (**Figure 34A**) and was observed to be at least 2-fold higher ($p<0.001$) than aerobic controls. We further confirmed this with coverslip-based biofilm formation assay using live/dead assay. Anaerobic biofilms demonstrate the formation of mat-like tight colonies whereas aerobic biofilms demonstrate the formation of microcolonies. As shown in the **Figure 34B** PAK strain under the anaerobic conditions demonstrates thick and robust biofilm formation.
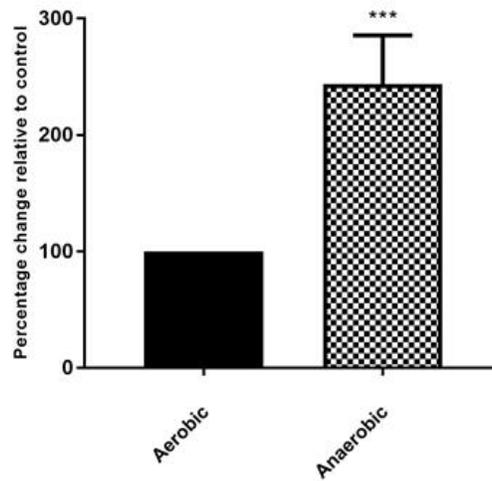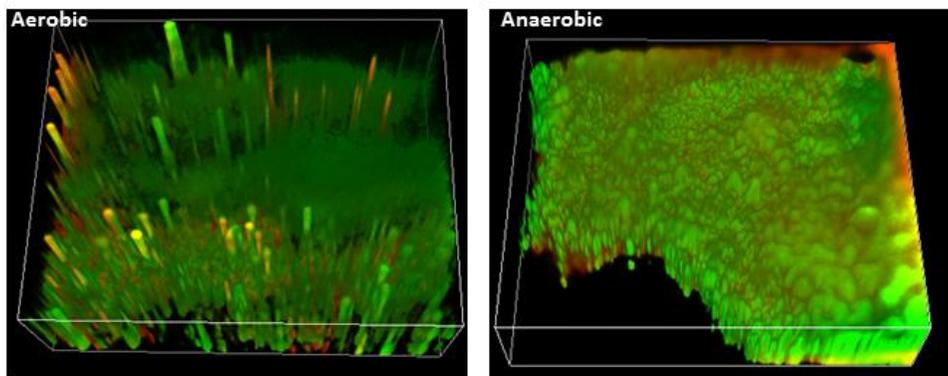
**Figure 34 Biofilm formation is activated in response to oxygen limitation. A.** Quantitative crystal violet-based biofilm formation assay under aerobic and anaerobic conditions. Data are shown as the percent change relative to aerobic control. **B.** A live/dead assay for biofilm under anaerobic conditions (right) as compared to aerobic (left) control in M9 medium. Live cells are stained with SYTO-9 (green), and dead cells are stained with Propidium iodide (red). The top views are projected from a stack of 50 images taken at 1 μm intervals for a total of 50 μm.

Experiments were repeated three times, and representative images, processed at the same magnification are shown. M9 medium supplemented with 0.2% glucose was used for aerobic control and M9 medium supplemented with 0.2% glucose and 100mM $KNO_3$ was used for anaerobic culturing. The values shown are an average of three independent experiments. Data were analyzed using unpaired t-test. ***$p < 0.001$. Error bars indicate standard deviations.

**5.3.7 PA1611 is activated in response to Iron limitation in PAK strain.**

Dysregulation of iron homeostasis is a common feature of cystic fibrosis and is key to biofilm formation in *P. aeruginosa*. Iron is an essential yet a scarce nutrient for bacterial survival in the host environment. *P. aeruginosa* undergoes intense competition for iron with the host as well as other colonizing microorganisms. Under iron-limiting conditions, *P. aeruginosa* secretes siderophores such as pyoverdine and pyochelin, to scavenge iron. High iron levels have been shown to promote biofilm formation (Berlutti et al., 2005). PA1611 knockout in PAO1 demonstrated better survival as compared to wild type in previous experiments. Thus, we wanted to test if iron or iron limitation may serve as a signal for PA1611 activation. We tested the PA1611 promoter activity in the PAK strain in an iron-free CAS media. 2,2′-Bipyridyl (BIP) was added at 400 μM as iron restricted condition and CAS media with 100 μM $FeCl_3$ was used as Iron replete media. M9 minimal media was used as a control. PAO1 did not demonstrate any change in promoter activity under iron limited conditions. As shown in the **Figure 35A**, PA1611 in PAK strain demonstrates increased activity in iron-restricted CAS media as compared to CAS with $FeCl_3$ as well as M9 control. To evaluate if PA1611 may have a role in Iron sequestration, a siderophore estimation assay was performed in the PAO1 strain. PAO, PA(ΔPA1611), and PA(pAK1611) were grown overnight in the presence of 100 mM iron at 37°C. The extracellular medium was separated from the cells by centrifugation. Pyoverdine concentration in the supernatant was determined by monitoring the by fluorescence emission, by exciting the supernatants at 400 nm and measuring the emission at 460 nm (Sánchez et al., 2002). For quantitation of pyochelin one ml cell-free supernatant, one ml each of 0.5 N HCl, nitrite molybdate reagent and 1N NaOH were mixed, and the final volume was made to 5 ml of distilled

water. Absorbance was taken at 510 nm (R. K. Gupta et al., 2011). As shown in **Figure 35B** as compared to wild type PAO1, PA(ΔPA1611) produced significantly lower quantities of pyoverdine and pyochelin, however, an overexpression strain produced at least 1.5-fold higher pyochelin and 1.3-fold higher pyoverdine. These results suggest that PA1611 may have a role in sequestering or Iron binding to facilitate biofilm formation under conditions in which it is activated.

A
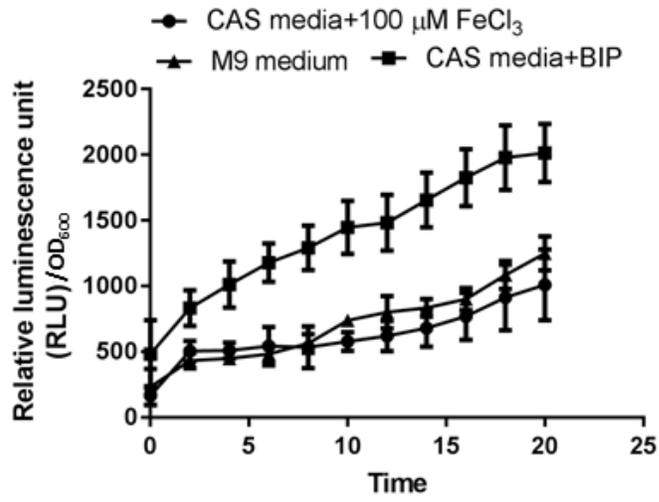


B
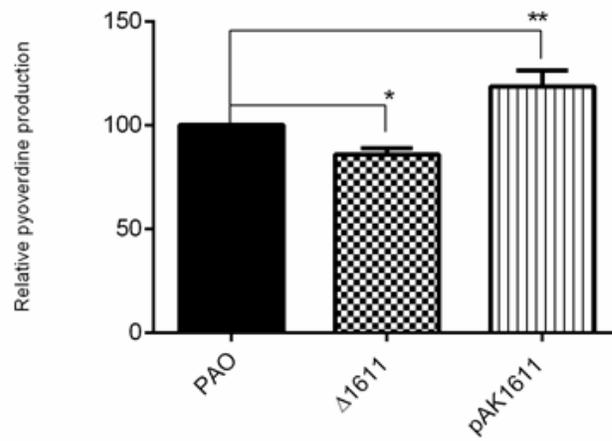


D
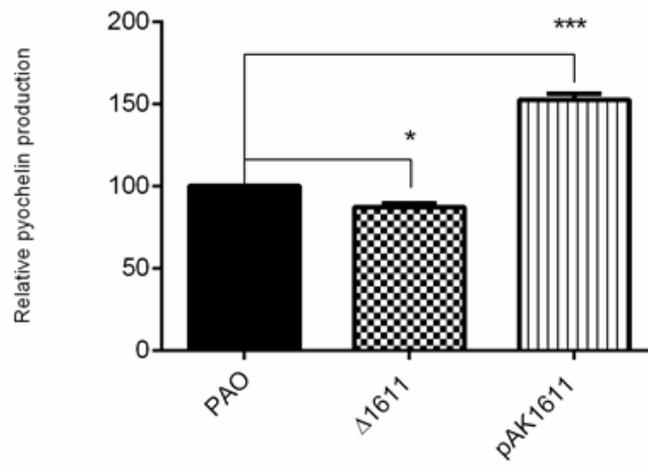
**Figure 35 PA1611 is activated in response to iron limitation**. **A.** PA1611 promoter activity in PAK strain over time in Iron-free CAS media. 2,2′-Bipyridyl (BIP) was added at 400 μM as iron restricted condition and CAS media with 100 μM was used as iron replete media. M9 minimal media was used as a control. **B.** Siderophore production assay for PA1611. PAO, PA(ΔPA1611), and PA(pAK1611) strains were grown overnight in the presence of 100 mM iron at 37°C. The extracellular medium was separated from the cells by centrifugation. Pyoverdine concentration in the supernatant was determined by monitoring the by fluorescence emission, by exciting the supernatants at 400 nm and measuring the emission at 460 nm. For quantitation of pyochelin one ml cell-free supernatant, one ml each of 0.5 N HCl, nitrite molybdate reagent and 1N NaOH were mixed and the final volume was made to 5 ml of distilled water. Absorbance was taken at 510 nm. PAO was used as a control for the siderophore estimation experiments. Data are presented as percent change relative to control. The values shown are an average of three independent experiments. Data were analyzed using one-way ANOVA. NS $p > 0.05$ and $**p < 0.01$. Error bars indicate standard deviations.

**5.3.8 Mucin and oxygen limitation together facilitate biofilm formation in *P. aeruginosa* via the GacA/GacS-RetS-PA1611-RsmA/Y/Z pathway**

CF airway environment is complex. Mucin and oxygen are key components in CF airway which modulate the behavior of colonizing microorganisms. PA1611 has demonstrated activation under both conditions in this study. We also observed that the expression of T3SS effector *exoS* decreased in mucin but was activated under oxygen-limited conditions. Small RNA *rsmY* has demonstrated activation in the presence of mucin but decreased transcript levels under low oxygen conditions. Oxygen limitation activates T3SS and motility as shown previously (O'Callaghan et al., 2011) but exposure to mucin demonstrated activated biofilm formation. In CF lung environment both oxygen limitation and viscous mucous present together. Therefore we wanted to examine the effect on *exoS* expression when both mucin and anaerobic conditions were presented together. Thus, to examine the expression of *exoS* in such a scenario, PAK strain was cultured in an anaerobic chamber with an indicator in LB medium supplemented with 1% mucin and 100mM $KNO_3$. PAK strain in LB medium with 100mM $KNO_3$ was grown aerobically and was used as the control. As shown in the **Figure 36A and B** under anaerobic condition *exoS* transcription was activated however in the presence of mucin the expression was completely abolished. This is further confirmed by T3SS secretion assay **Figure 36C**. We wanted to confirm if this effect is mediated via the Gac-RsmA/Y/Z pathway. Thus, we examined the transcription of small RNAs in the presence of mucin under anaerobic conditions. For this *rsmY* was used as representative. The transcription of small RNAs *rsmY* was decreased in anaerobic conditions without mucin but activated at least 3-fold in the presence of mucin (**Figure 36D**). Thus, these results show that mucin and oxygen limitation act together to facilitate biofilm formation contrary to effects observed when studied independently.
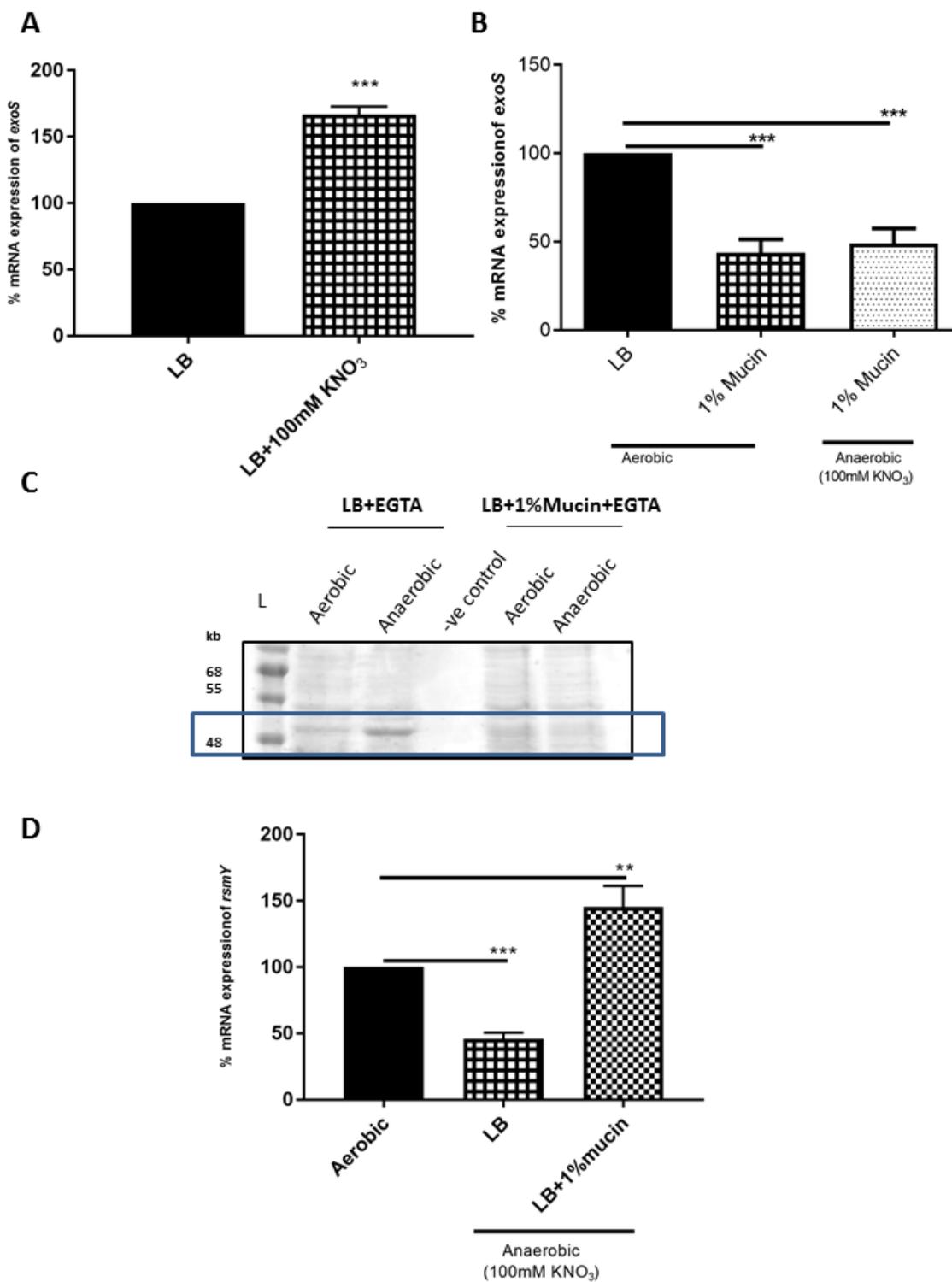
**Figure 36 Mucin and oxygen limitation together facilitate biofilm formation in *P*.**

*aeruginosa* **via the GacA/GacS-RetS-PA1611-RsmA/Y/Z pathway. A.** *exoS* expression under aerobic and anaerobic conditions at 12h. **B.** *exoS* expression under aerobic and anaerobic conditions in the presence of 1% mucin in LB medium. **C.** Secreted ExoS protein at 12 h under T3SS inducing conditions (LB+EGTA) in aerobic and anaerobic conditions with and without mucin. Secreted ExoS protein in the culture supernatants was analyzed by 12 % SDS-PAGE followed by staining with coomassie blue. Shown here are L-protein ladder, PAK in LB under aerobic conditions, PAK in LB medium under anaerobic conditions supplemented with 100mM $KNO_3$. Mucin was processed similarly to examine for any proteins and was used as negative control. Next two lanes show PAK in LB with 1% mucin grown aerobically and anaerobically with 100mM $KNO_3$. The location of the ExoS bands (49 kDa) is indicated by arrows. **D.** mRNA expression of *rsmY* under anaerobic and aerobic conditions with and without mucin respectively. Gene expression of both *exoS* and *rsmY* was normalized to the housekeeping gene *rpoD*. Under anaerobic growth conditions, medium was supplemented with 100mM $KNO_3$. For comparison PAK was cultured aerobically and anaerobically for 12h with and without 1% mucin. Data are presented as percent change relative to aerobic control. Data were analyzed using unpaired t-test or one-way ANOVA with Dunnett post-hoc test, NS $p > 0.05$, *$p < 0.05$, **$p < 0.01$ and ***$p < 0.001$, ****$p < 0.0001$.

**5.3.9 PA1611 plays a role in survival under anaerobic conditions in the presence of mucin**

Next, to examine the role of PA1611 in mucin under anoxic conditions, a coverslip biofilm formation assay was performed to study the biofilms formed and any difference in viability between wild type PAO1 and knockout PA1611 strain (ΔPA1611) in a PAO1 strain. Overnight cultures of PAO1 wild type and ΔPA1611 were inoculated in four groups of six well plates with coverslips. Aerobic and anaerobic, with and without mucin. Fresh M9 medium supplemented with 0.2% glucose were added to all the groups. For anaerobic culturing 100mM $KNO_3$ was added to the wells in the respective plates. Mucin was added at 1% concentrations to the wells of respective plates. After overnight culturing in aerobic and anaerobic conditions respectively, Biofilms were stained with Baclight live/dead stain for visualization. The biofilms were stained with SYTO9 (Live-green) and Propidium Iodide (dead-Red). As shown in the **Figure 37** PA1611 knockout demonstrated more dead cells under anaerobic conditions in presence of mucin as compared to aerobic controls. Thus, PA1611 may also play a role in viability under anoxic conditions. However, the exact role needs further studies. Further, it may also be noted that the biofilm appears a lot thicker in presence of mucin under anaerobic conditions as compared to aerobic controls.
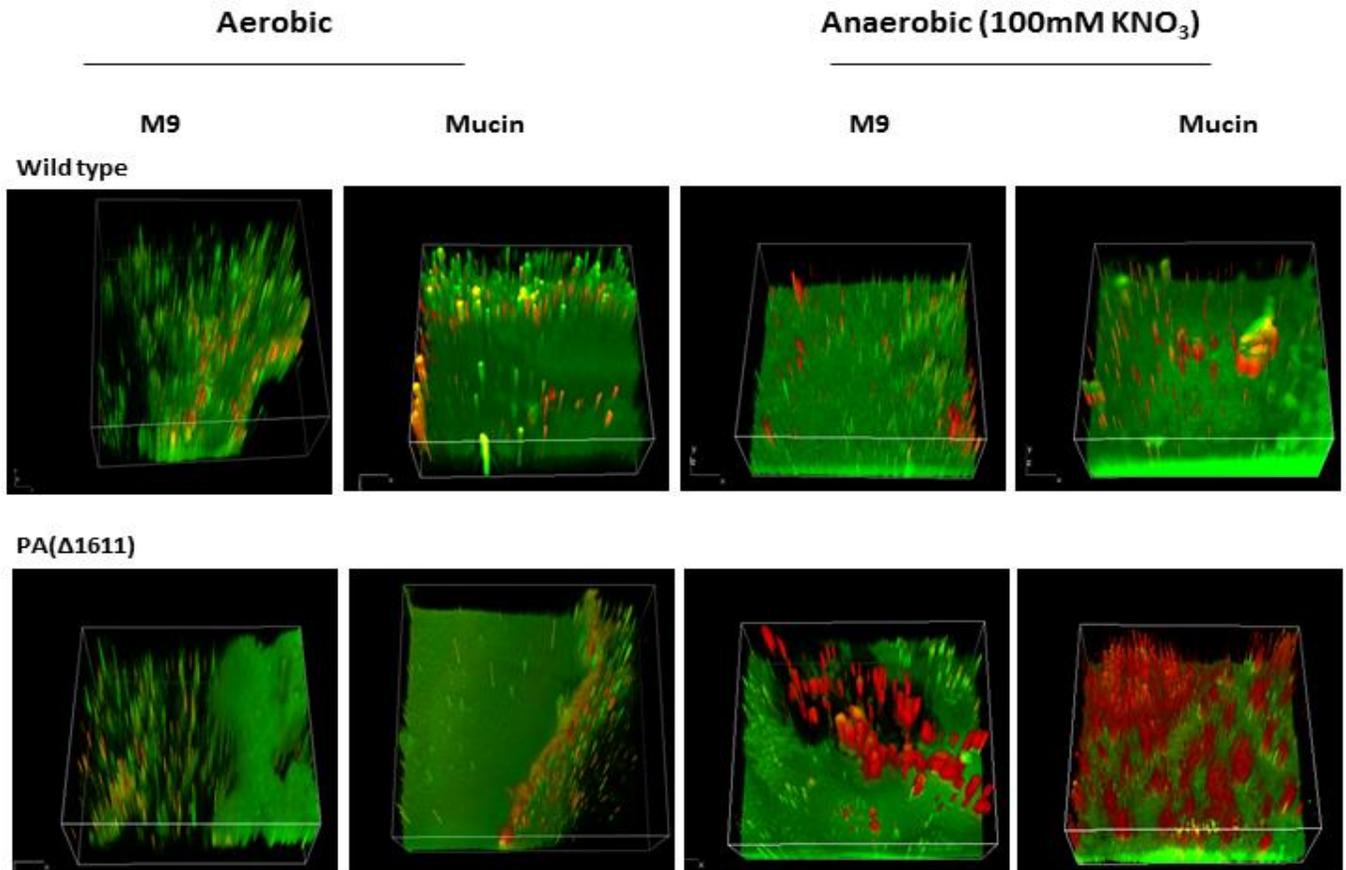
**Figure 37 PA1611 plays a role in survival under anoxic conditions in the presence of mucin.**

A live/dead assay for biofilm under anoxic conditions (right) as compared to aerobic (left) control in wild type PAO1 (top panels) and PA(ΔPA1611) in the presence of mucin as compared to that in M9 alone. Live cells are stained with SYTO-9 (green), and dead cells are stained with Propidium iodide (red). The top views are projected from a stack of 50 images taken at 1 μm intervals for a total of 50 μm. Experiments were repeated three times and representative images, processed at the same magnification, are shown aerobic control includes only M9 and anaerobic condition shows growth in M9 minimal medium with 100mM KNO$_3$ with or without 1% mucin.

**5.4 Discussion**

**5.4.1 PA1611 is key regulator of virulence in *P. aeruginosa***

PA1611 has been shown to be a key gene regulating biofilm formation and T3SS expression in *P. aeruginosa* (Bhagirath, et al., 2017; Kong et al., 2013). However, PA1611 demonstrated very low expression levels in *P. aeruginosa* PAO1. The environmental signals it responds to, in order to mediate chronic disease are yet unknown. Phenotype microarray comparison between a wild type PAO1, and a 1611 knockout strain of PAO1 demonstrated that ΔPA1611 strain was more sensitive to sodium salicylate as compared to the wild-type, however, this finding could not be validated in an independent culture assay with sodium salicylate. The ΔPA1611 strain was also found to be resistant to iron limitation (2,2 BIP) in PM assays. This was subsequently validated in an independent assay. Some of these discrepancies may be explained by the limitations of the PM assay. PMs are based on a redox assay in the bacteria in which the electron flow from the NADH reduce a tetrazolium dye, resulting in the irreversible formation of a purple color. The dye reduction or the color formation thus depends on the rate of electron flow through the respiratory chain and depends upon the conditions in each well of the plate. Results from PM are subject to experimental and biological noise. It is also known that the initial cell counts can significantly affect various growth parameter estimations from PM results (Borglin et al., 2012). Further, the proprietary nature of the plate contents in Biolog® plate makes precise determinations of inhibitory concentrations and media components very difficult. It is possible that the concentrations of added nutrients may be too low to be available to the target organism or in a form that is not easily utilized (Borglin et al., 2012). A quantitative polymerase chain reaction was performed to identify key genes that were differentially regulated in a PA1611 knockout mutant. Genes such as *rsmA*, *arr*, and *anr* were found to be upregulated, but other

genes such as *rhlR*, *wspR*, *vgrG*, *hcp1* were not found to be affected. Arr encodes for PDE that contain a conserved EAL domain which is involved in the c-di-GMP breakdown (Hengge, 2009). Low c-di-GMP levels are also associated with *retS* overexpression and activation of motility, T3SS, and suppression of T6SS (Moscoso et al., 2011). This finding is interesting and suggests the involvement of c-di-GMP with the GacS/GacA-RetS-PA1611-RsmA/Y/Z pathway. Previously we have shown that *cmpX*, a regulator for PA1611 function both via c-di-GMP and the Gac-RsmA/Y/Z pathway (Bhagirath, et al., 2017). The finding of overexpression of *arr* in a ΔPA1611 strain supports our previous findings. This was also further confirmed by measuring intracellular c-di-GMP levels indirectly. *cdrA* has been previously shown to reflect changes in intracellular levels of c-di-GMP (Rybtke et al., 2012) and was therefore used to compare c-di-GMP levels in wild type PAO1 and ΔPA1611. A PA1611 knockout showed lower levels of intracellular levels of c-di-GMP in alignment with our previous findings.

Anr (PA1544) has been shown to control transcriptional response to low oxygen in *P. aeruginosa* PAO1 (Ye et al., 1995). Activation of Anr in a PA1611 knockout mutant suggested a possible link to survival mechanism under oxygen-limited conditions. Given the central role of PA1611 in the pathogenesis of *P.aeruginosa* and yet low levels of expression under tested laboratory conditions, we wondered if PA1611 could be significant in environmental and clinical isolates. *P. aeruginosa* clinical isolates demonstrate the high genomic diversity, and hence the presence of PA1611 was first confirmed with PCR followed by measuring promoter activity assay in LB media. We tested the promoter activity of PA1611 in environmental strain PAK and clinical isolates PA082-PA096. All clinical isolates and PAK strain demonstrated significantly higher PA1611 promoter activity as compared to PAO1. *P. aeruginosa* environmental and CF isolates demonstrate a high frequency of mutation after long-term colonization in CF lungs

(Oliver et al., 2000). One example of an acquired mutation is the single-nucleotide polymorphisms (SNPs) in *mucA*, resulting in the overproduction of alginate (J. C. Boucher et al., 1997).  It can be speculated that PA1611 is repressed under normal conditions in strains such as PAO1 but is released from such control by a gene present on genomic islands in clinical or environmental strains. However further studies are needed to elucidate the regulation of PA1611 in PAO1. A key component of *P. aeruginosa* virulence is regulation of gene expression rather than the presence or absence of specific genes (Finnan et al., 2004). Given that no distinct phenotypic or genotypic profile has been found for CF clinical isolates further studies are needed to understand this differential gene expression for PA1611 between PAO1 and *P. aeruginosa* clinical isolates. The only conclusion that could be drawn at this stage is that given the high expression of PA1611 in a *P. aeruginosa* CF isolates and environmental strain PAK, PA1611 may be contributory to *P. aeruginosa* virulence in vivo. Investigation into factors that activate the expression of PA1611 may facilitate a better understanding of its specific role and involvement in key regulatory pathways in *P. aeruginosa*.

**5.4.2 PA1611 is involved in sensing complex signals and facilitating *P.  aeruginosa* survival in vivo**

It has been demonstrated that colonizing *P. aeruginosa* isolates are genotypic variants of their environmental counterparts (Hansen et al., 2012). Ecological factors in the CF lung environment shape *P. aeruginosa* gene regulation and virulence in a significant way. The identification of high levels of PA1611 expression in CF clinical isolates as compared to PAO1 prompted further investigation into triggers that might activate it.  To study PA1611 expression in conditions that mimic CF lung, the use of CF sputum obtained from a patient would be ideal, however; it carries a significant risk of introducing experimental variabilities such as clinical stage of disease at

which the sample was obtained or presence of antibiotics. Thus, a standard medium closely mimicking CF sputum and containing defined constituents was used (Fung et al., 2010). For studying expression, PAK strain was chosen since its genetic sequence is well known. In ASMDM medium T3SS effector gene *exoS* promoter activity was found to be significantly decreased. Since ASMDM consists of defined constituents, the *exoS* promoter activity was examined after removing every component of ASMDM. It was observed that the highest levels of *exoS* were obtained when mucin was removed from the medium. Thus, mucin was added at 1% concentration to examine the effect on *exoS* promoter activity, and it was observed that in the presence of mucin, *exoS* promoter activity was significantly diminished as compared to control. Mucin was added at different concentrations for this experiment. The greatest effect on gene expression with the lowest concentration of 1% and hence was chosen for downstream experiments. Levels of mucin in ASMDM and tested conditions have been kept at 1% (w/v). This result is in alignment with previous observation that mucin suppressed T3SS in *P. aeruginosa* in a concentration-dependent manner (Ohgita et al., 2013). Mucin is a key component of airways and is greatly compromised in CF. It has been reported that in CF the level of mucins is higher than 2% (w/v)(A. Boyd & Chakrabarty, 1995). It has been hypothesized that since epithelial mucin is negatively charged and viscous, they may affect T3SS needle rotation and effector secretion (Bansil & Turner, 2006).

Mucin is a high molecular weight complex glycoprotein, with multiple carbohydrate side chains. It has been previously shown that mucin activated biofilm formation, inhibited motility, aids in survival and facilitates antibiotic resistance in *P. aeruginosa* by activating *fliD*, (an adhesin)-mucin interaction (Landry et al., 2006). It was also observed that biofilm in mucin was significantly different from those in standard culture media in being more tightly packed and flat

181

matted appearance (Landry et al., 2006). These findings are in agreement with the observations in this study. Interestingly, the key players in the GacS/GacA-RetS-PA1611-RsmA/Y/Z were also found to be differentially regulated in the presence of mucin. PA1611and small RNAs RsmY and RsmZ were found to be activated in the presence of mucin which may also at least partially explain the activated biofilm formation. This result first highlights the effect of exogenous mucin on gene regulation via this key regulatory pathway. Apart from interaction and attachment, mucins also serve as a significant carbon source specifically under oxygen-limited conditions.

It has been shown that CF airways present the inhabiting bacteria with varying niches predominantly those with low-oxygen availability. Survival for *P. aeruginosa* under such low-oxygen conditions is dependent upon efficient de-nitrification. *P. aeruginosa* utilizes terminal electron acceptors, such as nitrates, nitrites and nitrous oxide as a substrate for growth. The CF airway mucus is rich in nitrates and forms a favorable niche to support the anoxic growth of *P. aeruginosa* (Worlitzsch et al., 2002). Under anaerobic conditions, it was observed that the levels of *exoS* were activated and small RNAs were decreased as compared to controls. However, Biofilm formation was enhanced, and a robust biofilm structure as compared to control was observable under anaerobic conditions. It has been shown that under anaerobic conditions, Anr/NarL pathway is activated in *P. aeruginosa* which facilitates the activation of T3SS master regulator ExsA to activate *exoS* secretion and negatively influences RsmY and Z levels (O'Callaghan et al., 2011). Further, it was also proposed that an *exsA* independent *aceA* negatively affected small RNAs to activate T3SS (Chung et al., 2013) or possibly by interaction with RetS. The observation of activated biofilm formation under anoxic conditions is not unique and has been made previously (Yoon et al., 2002). Outer membrane protein *oprF* has been

shown to be dramatically activated under anaerobic growth conditions (Yoon et al., 2002). Activated *oprF* allows for enhanced de-nitrification and is critical to *P. aeruginosa* survival under oxygen-limited conditions (Daniel J. Hassett et al., 2002; Yoon et al., 2002). Previously, we have observed that a transposon inserted in *cmpX* activated PA161. A *cmpX* mutant showed decreased expression of *oprF* (Bhagirath, et al., 2017). However, further studies are needed to determine the exact role of OprF in CmpX- GacS-GacA-RetS-PA1611-RsmA/Y/Z pathway.

Further, it has been shown that under low oxygen conditions, mucins facilitate alginate formation by *P. aeruginosa* to facilitate biofilm formation (Fung et al., 2010; Jain & Ohman, 1998). Iron is crucial to biofilm formation (Banin et al., 2005). A PM analysis (under aerobic conditions) demonstrated better survival of a PA1611 knockout mutant under Iron limited conditions (2,2 bipyridyl). PA1611 demonstrated activation under Iron limited conditions as well as enhanced siderophore production when overexpressed suggesting that it may have a role either directly or indirectly in facilitating biofilm by acquiring Iron. The exact pathway is unclear yet and needs elucidation. This study also shows that biofilm formation in the presence of mucin and oxygen limitation is mediated by the GacS/GacA-RetS-PA1611-RsmA/Y/Z pathway. This is first report highlighting sensing two key signals to mediate virulent phenotype in *P. aeruginosa*. This study also shows that PA1611 is critical to survival under oxygen-limited conditions specifically in the presence of mucin. The exact pathway for PA1611 mediated biofilm formation under anaerobic conditions requires further study, however; it may be hypothesized that in CF airways where oxygen and Iron are limited, and mucus is abundant may act as signals to activate PA1611 and facilitate biofilm formation via the GacS-A/RsmA/Y/Z pathway and support the survival of *P. aeruginosa*.

This study highlights the complexity of gene regulation for survival and persistence of *P.aeruginosa*. This study also emphasizes the significance of understanding inter-signaling pathway regulation of bacterial virulence as exemplified by the role of *cmpX* in c-di-GMP signaling and GacA/S-PA1611-RetS-RsmA/Y/Z pathway. Further investigation into complex signals affecting key regulators in *P. aeruginosa* is essential to inform newer and more specific therapeutic approaches.

# Chapter 6

## Conclusion and future directions

### 6.1 Conclusion

*P. aeruginosa* chronic infection is the most serious problem in CF lung disease. Exploring the pulmonary environment and physiological deviations in CF is valuable in understanding disease pathogenesis. Though we now recognize CF as a polymicrobial disease, better understanding of the CF lung disease requires investigating the CF airway microbiome, the interactions among the pathogens, the host, the environment and the resulting immune response. The growing knowledge on the complexity of CF airways and the emerging role of sinuses in bacterial persistence has opened up new targets for antimicrobial therapy and thus limiting the chronic infections. It is now understood that overshooting of inflammation in CF can support facultative anaerobes, such as *E. coli* and *P. aeruginosa* in inflamed respiratory tracts. Further investigation of bacterial pathogenicity and its regulatory systems, as well as the relationship between host responses and human microbiome, should provide novel approaches to control infections in CF. New techniques for enhancing mucociliary clearance, improving oxygen availability and restoring CFTR function will also bring CF patients more effective treatment options.

Approaches to managing *P. aeruginosa* chronic infection require a clear understanding of its pathogenic pathways and a clear mapping of intersecting pathways for virulence regulation. Current study informs advanced understanding of protein-protein interaction in a relatively novel regulatory pathway in *P. aeruginosa* as well as highlights the role of a conserved membrane protein in signaling. This study also demonstrates that though independent triggers may elicit a differential response in *P. aeruginosa* phenotypes, a combination of factors may elicit a completely different response. Environment extrinsic to colonizing pathogens in vivo present

multitude of factors in combination and the current study underlines the effect of simultaneous presentation of different factors in mediating bacterial virulence.

In conclusion, signaling in *P. aeruginosa* is far more complex than current knowledge encompasses. Signaling pathways function in unique ways to facilitate survival and pathogenicity thus more studies highlighting external factors in shaping virulence are needed. Understanding the interaction between host and the response of *P. aeruginosa* to those, are key to infection control and developing new therapeutic strategies.

## 6.2 Future directions

Under aerobic conditions, the expression of PA1611 is under control of PA1775. A transposon inserted in PA1775 activated PA1611. A PA1775 knockout mutant demonstrates decreased *oprF* levels. An *oprF* mutant demonstrates activated c-di-GMP levels and enhanced biofilm formation (Bhagirath, et al., 2017). Thus, it may be possible that activation of PA1611 may affect *oprF* levels and increase cellular c-di-GMP levels by activation of *pel* pathway. A PA1611 mutant demonstrated activated *arr*, a c-di-GMP phosphodiesterase and a PA1775 mutant demonstrated activated *wspR* a c-di-GMP synthase. Studies are needed to understand the effect of PA1611 knockout and over expression on intracellular c-di-GMP levels in both PAO1 and environmental strain PAK. Further, the signaling pathway between PA1611, *oprF* and *sigX* needs further studies.

PA1611 is well expressed in clinical isolates and PAK strain, however, its levels are undetectable in a PAO1 strain. Whole genome transposon studies are needed to identify regulators for PA1611 in PAK which may shed light on its regulation.

PA1775 has been annotated as a conserved small mechanosensor, however; the degree of conservation with *mscS* of *E. coli* is small. It also appears to respond to external osmotic changes as per preliminary studies. Its exact mechanosensory roles need to be elucidated by performing heterologous expression in *E. coli* followed by patch-clamp studies and osmotic survival assays. Further, the exact mechanism by which signal is intercepted, whether PA1775 first senses it or PA1611 perceives it first needs to be understood to determine hierarchy in signal transduction pathway.

Mucin and anaerobic conditions have demonstrated activated biofilm formation, based on current research, c-di-GMP and iron have key roles in activating biofilm formation, but the exact pathway is not well understood. Measuring intracellular c-di-GMP levels under aerobic and anoxic conditions as well as with and without mucin may help further understand the pathway for activated biofilm formation under these conditions. C-di-GMP has emerged as a key player with the GacS-A/RsmA/Y/Z pathway. PAK strain demonstrated activated PA1611 expression as compared to PAO1. To determine the c-di-GMP regulators for PA1611 a whole genome transposon mutagenesis needs to be performed to determine the different c-di-GMP enzymes involved in PA1611 regulation.

Detailed characterization of bacterial signal perception and regulatory pathways will add to the current pool of knowledge this may even allow the rational design of novel and specific therapeutic targets for the better management of infections and ensure better outcomes.

# References

Abou Alaiwa, M., Beer, A., Pezzulo, A., Launspach, J., Horan, R., Stoltz, D., . . . Zabner, J. (2014). Neonates with cystic fibrosis have a reduced nasal liquid pH; a small pilot study. *Journal of Cystic Fibrosis, 13*(4), 373-377. doi:10.1016/j.jcf.2013.12.006

Airola, M. V., Watts, K. J., & Crane, B. R. (2010). Identifying divergent HAMP domains and poly-HAMP chains. *Journal of Biological Chemistry, 285*(23), le7; author reply 1e8. doi:10.1074/jbc.L109.075721

Almblad, H., Harrison, J. J., Rybtke, M., Groizeleau, J., Givskov, M., Parsek, M. R., & Tolker-Nielsen, T. (2015). The cyclic AMP-Vfr signaling pathway in *Pseudomonas aeruginosa* Is Inhibited by cyclic Di-GMP. *Journal of Bacteriology, 197*(13), 2190-2200. doi:10.1128/jb.00193-15

Alrahman, M. A., & Yoon, S. S. (2017). Identification of essential genes of *Pseudomonas aeruginosa* for its growth in airway mucus. *The Journal of Microbiology, 55*(1), 68-74. doi:10.1007/s12275-017-6515-3

An, S., Wu, J., & Zhang, L. H. (2010). Modulation of *Pseudomonas aeruginosa* biofilm dispersal by a cyclic-di-GMP phosphodiesterase with a putative hypoxia-sensing domain. *Applied and Environmental Microbiology, 76*(24), 8160-8173. doi:10.1128/aem.01233-10

Ballard, S., & Inglis, S. (2004). Liquid secretion properties of airway submucosal glands. *The Journal of Physiology, 556*(Pt 1), 1-10. doi:10.1113/jphysiol.2003.052779

Ballard, S., Trout, L., Bebok, Z., Sorscher, E., & Crews, A. (1999). CFTR involvement in chloride, bicarbonate, and liquid secretion by airway submucosal glands. *American Journal of Physiology - Lung Cellular and Molecular Physiology, 277*(4 Pt 1), L694-699.

Banin, E., Vasil, M. L., & Greenberg, E. P. (2005). Iron and *Pseudomonas aeruginosa* biofilm formation. *Proceedings of the National Academy of Sciences of the United States of America, 102*(31), 11076.

Bansil, R., & Turner, B. S. (2006). Mucin structure, aggregation, physiological functions and biomedical applications. *Current Opinion in Colloid & Interface Science, 11*(2), 164-170. doi:doi.org/10.1016/j.cocis.2005.11.001

Baraquet, C., & Harwood, C. S. (2013). Cyclic diguanosine monophosphate represses bacterial flagella synthesis by interacting with the Walker A motif of the enhancer-binding protein FleQ. *Proceedings of the National Academy of Sciences of the United States of America, 110*(46), 18478-18483. doi:10.1073/pnas.1318972110

Barbieri, J. T., & Sun, J. (2004). *Pseudomonas aeruginosa* ExoS and ExoT. *Reviews of physiology, biochemistry and pharmacology, 152*, 79-92. doi:10.1007/s10254-004-0031-7

Barken, K. B., Pamp, S. J., Yang, L., Gjermansen, M., Bertrand, J. J., Klausen, M., . . . Tolker-Nielsen, T. (2008). Roles of type IV pili, flagellum-mediated motility and extracellular DNA in the formation of mature multicellular structures in *Pseudomonas aeruginosa* biofilms. *Environmental Microbiology, 10*(9), 2331-2343. doi:10.1111/j.1462-2920.2008.01658.x

Barr, H. L., Halliday, N., Cámara, M., Barrett, D. A., Williams, P., Forrester, D. L., . . . Fogarty, A. W. (2015). *Pseudomonas aeruginosa* & quorum sensing molecules correlate with clinical status in cystic fibrosis. *European Respiratory Journal, 46*(4), 1046.

Basbaum, C., Jany, B., & Finkbeiner, W. (1990). The serous cell. *Annual Review of Physiology, 52*(1), 97-113.

Basu Roy, A., & Sauer, K. (2014). Diguanylate cyclase NicD-based signalling mechanism of nutrient-induced dispersion by *Pseudomonas aeruginosa*. *Molecular Microbiology, 94*(4), 771-793. doi:10.1111/mmi.12802

Beatson, S. A., Whitchurch, C. B., Sargent, J. L., Levesque, R. C., & Mattick, J. S. (2002). Differential regulation of twitching motility and elastase production by Vfr in *Pseudomonas aeruginosa*. *Journal of Bacteriology, 184*(13), 3605-3613.

Becher, A., & Schweizer, H. P. (2000). Integration-proficient *Pseudomonas aeruginosa* vectors for isolation of single-copy chromosomal *lacZ* and *lux* gene fusions. *Biotechniques, 29*(5), 948-950, 952.

Benkert, P., Biasini, M., & Schwede, T. (2011). Toward the estimation of the absolute quality of individual protein structure models. *Bioinformatics, 27*(3), 343-350. doi:10.1093/bioinformatics/btq662

Berggård, T., Linse, S., & James, P. (2007). Methods for the detection and analysis of protein–protein interactions. *Proteomics, 7*(16), 2833-2842.

Berlutti, F., Morea, C., Battistoni, A., Sarli, S., Cipriani, P., Superti, F., . . . Valenti, P. (2005). Iron availability influences aggregation, biofilm, adhesion and invasion of *Pseudomonas aeruginosa* and *Burkholderia cenocepacia*. *International Journal of Immunopathology and Pharmacology, 18*(4), 661-670. doi:10.1177/039463200501800407

Bhagirath, A. Y., Li, Y., Somayajula, D., Dadashi, M., Badr, S., & Duan, K. (2016). Cystic fibrosis lung environment and *Pseudomonas aeruginosa* infection. *BMC Pulmonary Medicine, 16*(1), 174. doi:10.1186/s12890-016-0339-5

Bhagirath, A. Y., Pydi, S. P., Li, Y., Lin, C., Kong, W., Chelikani, P., & Duan, K. (2017). Characterization of the direct Interaction between hybrid sensor kinases PA1611 and RetS that

controls biofilm formation and the type III secretion system in *Pseudomonas aeruginosa*. *American Chemical Society infectious diseases, 3*(2), 162-175. doi:10.1021/acsinfecdis.6b00153

Bhagirath, A. Y., Somayajula, D., Li, Y., & Duan, K. (2017). CmpX affects virulence in *Pseudomonas aeruginosa* through the Gac/Rsm signaling pathway and by modulating c-di-GMP levels. *The Journal of membrane biology*. doi:10.1007/s00232-017-9994-6

Bielecki, P., Jensen, V., Schulze, W., Gödeke, J., Strehmel, J., Eckweiler, D., . . . Häussler, S. (2015). Cross talk between the response regulators PhoB and TctD allows for the integration of diverse environmental signals in *Pseudomonas aeruginosa*. *Nucleic Acids Research, 43*(13), 6413-6425. doi:10.1093/nar/gkv599

Bielecki, P., Komor, U., Bielecka, A., Musken, M., Puchalka, J., Pletz, M. W., . . . Haussler, S. (2013). Ex vivo transcriptional profiling reveals a common set of genes important for the adaptation of *Pseudomonas aeruginosa* to chronically infected host sites. *Environmental Microbiology, 15*(2), 570-587. doi:10.1111/1462-2920.12024

Bochner, B. R. (2009). Global phenotypic characterization of bacteria. *FEMS Microbiology Review, 33*(1), 191-205. doi:10.1111/j.1574-6976.2008.00149.x

Boles, B. R., Thoendel, M., & Singh, P. K. (2005). Rhamnolipids mediate detachment of *Pseudomonas aeruginosa* from biofilms. *Molecular Microbiology, 57*(5), 1210-1223. doi:10.1111/j.1365-2958.2005.04743.x

Booth, I. R., & Louis, P. (1999). Managing hypoosmotic stress: aquaporins and mechanosensitive channels in *Escherichia coli*. *Current Opinion in Microbiology, 2*(2), 166-169.

Bordi, C., Lamy, M. C., Ventre, I., Termine, E., Hachani, A., Fillet, S., . . . Filloux, A. (2010). Regulatory RNAs and the HptB/RetS signalling pathways fine-tune *Pseudomonas aeruginosa*

pathogenesis. *Molecular Microbiology, 76*(6), 1427-1443. doi:10.1111/j.1365-2958.2010.07146.x

Borglin, S., Joyner, D., DeAngelis, K. M., Khudyakov, J., D'haeseleer, P., Joachimiak, M. P., & Hazen, T. (2012). Application of phenotypic microarrays to environmental microbiology. *Current Opinion in Biotechnology, 23*(1), 41-48. doi:doi.org/10.1016/j.copbio.2011.12.006

Borlee, B. R., Goldman, A. D., Murakami, K., Samudrala, R., Wozniak, D. J., & Parsek, M. R. (2010). *Pseudomonas aeruginosa* uses a cyclic-di-GMP-regulated adhesin to reinforce the biofilm extracellular matrix. *Molecular Microbiology, 75*(4), 827-842. doi:10.1111/j.1365-2958.2009.06991.x

Borowitz, D. (2015). CFTR, bicarbonate, and the pathophysiology of cystic fibrosis. *Pediatric Pulmonology, 50 Suppl 40*, S24-S30. doi:10.1002/ppul.23247

Borriello, G., Werner, E., Roe, F., Kim, A., Ehrlich, G., & Stewart, P. (2004). Oxygen limitation contributes to antibiotic tolerance of *Pseudomonas aeruginosa* in biofilms. *Antimicrobial Agents and Chemotherapy, 48*(7), 2659-2664. doi:10.1128/AAC.48.7.2659-2664.2004

Boucher, J. C., Yu, H., Mudd, M. H., & Deretic, V. (1997). Mucoid *Pseudomonas aeruginosa* in cystic fibrosis: characterization of *muc* mutations in clinical isolates and analysis of clearance in a mouse model of respiratory infection. *Infection and Immunity, 65*(9), 3838-3846.

Boucher, R., Cotton, C., Gatzy, J., Knowles, M., & Yankaskas, J. (1988). Evidence for reduced $Cl^-$ and increased $Na^+$ permeability in cystic fibrosis human primary cell cultures. *The Journal of Physiology, 405*, 77-103.

Bouffartigues, E., Gicquel, G., Bazire, A., Bains, M., Maillot, O., Vieillard, J., . . . Chevalier, S. (2012). Transcription of the *oprF* gene of *Pseudomonas aeruginosa* is dependent mainly on the

*sigX* sigma factor and is sucrose induced. *Journal of Bacteriology, 194*(16), 4301-4311. doi:10.1128/jb.00509-12

Bouffartigues, E., Moscoso, J. A., Duchesne, R., Rosay, T., Fito-Boncompte, L., Gicquel, G., . . . Chevalier, S. (2015). The absence of the *Pseudomonas aeruginosa* OprF protein leads to increased biofilm formation through variation in c-di-GMP level. *Frontiers in Microbiology, 6*, 630. doi:10.3389/fmicb.2015.00630

Boutin, S., Graeber, S., Weitnauer, M., Panitz, J., Stahl, M., Clausznitzer, D., . . . Dalpke, A. (2015). Comparison of microbiomes from different niches of upper and lower airways in children and adolescents with cystic fibrosis. *PLoS One, 10*(1), e0116029. doi:10.1371/journal.pone.0116029

Boyd, A., & Chakrabarty, A. M. (1995). *Pseudomonas aeruginosa* biofilms: role of the alginate exopolysaccharide. *Journal of Industrial Microbiology, 15*(3), 162-168.

Boyd, C. D., & O'Toole, G. A. (2012). Second messenger regulation of biofilm formation: breakthroughs in understanding c-di-GMP effector systems. *Annual Review of Cell and Developmental Biology, 28*, 439-462. doi:10.1146/annurev-cellbio-101011-155705

Bratu, S., Landman, D., Gupta, J., & Quale, J. (2007). Role of AmpD, OprF and penicillin-binding proteins in beta-lactam resistance in clinical isolates of *Pseudomonas aeruginosa*. *Journal of Medical Microbiology, 56*(Pt 6), 809-814. doi:10.1099/jmm.0.47019-0

Brencic, A., & Lory, S. (2009). Determination of the regulon and identification of novel mRNA targets of *Pseudomonas aeruginosa* RsmA. *Molecular Microbiology, 72*(3), 612-632. doi:10.1111/j.1365-2958.2009.06670.x

Brencic, A., McFarland, K. A., McManus, H. R., Castang, S., Mogno, I., Dove, S. L., & Lory, S. (2009). The GacS/GacA signal transduction system of *Pseudomonas aeruginosa* acts exclusively

through its control over the transcription of the RsmY and RsmZ regulatory small RNAs. *Molecular Microbiology, 73*(3), 434-445. doi:10.1111/j.1365-2958.2009.06782.x

Brinkman, F. S., Schoofs, G., Hancock, R. E., & De Mot, R. (1999). Influence of a putative ECF sigma factor on expression of the major outer membrane protein, OprF, in *Pseudomonas aeruginosa* and *Pseudomonas fluorescens*. *Journal of Bacteriology, 181*(16), 4746-4754.

Brutinel, E. D., Vakulskas, C. A., Brady, K. M., & Yahr, T. L. (2008). Characterization of ExsA and of ExsA-dependent promoters required for expression of the *Pseudomonas aeruginosa* type III secretion system. *Molecular Microbiology, 68*(3), 657-671. doi:10.1111/j.1365-2958.2008.06179.x

Buelow, D. R., & Raivio, T. L. (2010). Three (and more) component regulatory systems - auxiliary regulators of bacterial histidine kinases. *Molecular Microbiology, 75*(3), 547-566. doi:10.1111/j.1365-2958.2009.06982.x

Burrowes, E., Baysse, C., Adams, C., & O'Gara, F. (2006). Influence of the regulatory protein RsmA on cellular functions in *Pseudomonas aeruginosa* PAO1, as revealed by transcriptome analysis. *Microbiology, 152*(Pt 2), 405-418. doi:10.1099/mic.0.28324-0

Chakraborty, R., Pydi, S. P., Gleim, S., Bhullar, R. P., Hwa, J., Dakshinamurti, S., & Chelikani, P. (2013). New insights into structural determinants for prostanoid thromboxane A2 receptor- and prostacyclin receptor-G protein coupling. *Molecular and Cellular Biology, 33*(2), 184-193. doi:10.1128/MCB.00725-12

Chambonnier, G., Roux, L., Redelberger, D., Fadel, F., Filloux, A., Sivaneson, M., . . . Bordi, C. (2016). The hybrid histidine kinase LadS forms a multicomponent signal transduction system with the GacS/GacA two-component system in *Pseudomonas aeruginosa*. *PLoS Genetics, 12*(5), e1006032. doi:10.1371/journal.pgen.1006032

Cheung, K. H., Leung, C. T., Leung, G. P., & Wong, P. Y. (2003). Synergistic effects of cystic fibrosis transmembrane conductance regulator and aquaporin-9 in the rat epididymis. *Reproductive Biology and Endocrinology, 68*(5), 1505-1510. doi:10.1095/biolreprod.102.010017 [pii]

Choi, K. H., Kumar, A., & Schweizer, H. P. (2006). A 10-min method for preparation of highly electrocompetent *Pseudomonas aeruginosa* cells: application for DNA fragment transfer between chromosomes and plasmid transformation. *Journal of Microbiological Methods, 64*(3), 391-397. doi:10.1016/j.mimet.2005.06.001

Chua, S. L., Sivakumar, K., Rybtke, M., Yuan, M., Andersen, J. B., Nielsen, T. E., . . . Yang, L. (2015). C-di-GMP regulates *Pseudomonas aeruginosa* stress response to tellurite during both planktonic and biofilm modes of growth. *Scientific Reports, 5*, 10052. doi:10.1038/srep10052

Chung, J. C., Rzhepishevska, O., Ramstedt, M., & Welch, M. (2013). Type III secretion system expression in oxygen-limited *Pseudomonas aeruginosa* cultures is stimulated by isocitrate lyase activity. *Open biology, 3*(1), 120131. doi:10.1098/rsob.120131

Ciofu, O., Mandsberg, L. F., Bjarnsholt, T., Wassermann, T., & Hoiby, N. (2010). Genetic adaptation of *Pseudomonas aeruginosa* during chronic lung infection of patients with cystic fibrosis: strong and weak mutators with heterogeneous genetic backgrounds emerge in *mucA* and/or *lasR* mutants. *Microbiology, 156*(Pt 4), 1108-1119. doi:10.1099/mic.0.033993-0

Clancy, J. P. (2016). Cystic fibrosis transmembrane conductance regulator function in airway smooth muscle. A novel role in cystic fibrosis airway obstruction. *American Journal of Respiratory and Critical Care Medicine, 193*(4), 352-353.

CLSI. (2012). *Methods for antimicrobial susceptibility testing of bacteria that grow aerobically. Approved Standard*. Clinical and Laboratory Standards Institute, 950 west valley road, suite 2500 Wayne, Pennsylvania, 19087,USA 2012.

Cornforth, D. M., Popat, R., McNally, L., Gurney, J., Scott-Phillips, T. C., Ivens, A., . . . Brown, S. P. (2014). Combinatorial quorum sensing allows bacteria to resolve their social and physical environment. *Proceedings of the National Academy of Sciences of the United States of America, 111*(11), 4280-4284. doi:10.1073/pnas.1319175111

Crawford, I., Maloney, P. C., Zeitlin, P. L., Guggino, W. B., Hyde, S. C., Turley, H., . . . Higgins, C. F. (1991). Immunocytochemical localization of the cystic fibrosis gene product CFTR. *Proceedings of the National Academy of Sciences of the United States of America, 88*(20), 9262-9266.

Csanády, L., Vergani, P., & Gadsby, D. C. (2010). Strict coupling between CFTR's catalytic cycle and gating of its Cl⁻ ion pore revealed by distributions of open channel burst durations. *Proceedings of the National Academy of Sciences, 107*(3), 1241-1246. doi:10.1073/pnas.0911061107

Cullen, L., & McClean, S. (2015). Bacterial adaptation during chronic respiratory infections. *Pathogens, 4*(1), 66-89. doi:10.3390/pathogens4010066

Dalton, J., Kalid, O., Schushan, M., Ben-Tal, N., & Villà-Freixa, J. (2012). New model of cystic fibrosis transmembrane conductance regulator proposes active channel-like conformation. *Journal of Chemical Information and Modeling, 52*(7), 1842-1853. doi:10.1021/ci2005884

Davies, D. G., Parsek, M. R., Pearson, J. P., Iglewski, B. H., Costerton, J. t., & Greenberg, E. (1998). The involvement of cell-to-cell signals in the development of a bacterial biofilm. *Science, 280*(5361), 295-298.

Davies, J. C., Ebdon, A.-M., & Orchard, C. (2014). Recent advances in the management of cystic fibrosis. *Archives of Disease in Childhood, 99*(11), 1033-1036. doi:10.1136/archdischild-2013-304400

Dawson, R., & Locher, K. (2006). Structure of a bacterial multidrug ABC transporter. *Nature, 443*(7108), 180-185. doi:10.1038/nature05155

Dewulf, J., Vermeulen, F., Wanyama, S., Thomas, M., Proesmans, M., Dupont, L., & De Boeck, K. (2015). Treatment burden in patients with at least one class IV or V CFTR mutation. *Pediatric Pulmonology*, n/a-n/a. doi:10.1002/ppul.23313

Deziel, E., Lepine, F., Milot, S., & Villemur, R. (2003). *rhlA* is required for the production of a novel biosurfactant promoting swarming motility in *Pseudomonas aeruginosa:* 3-(3-hydroxyalkanoyloxy) alkanoic acids (HAAs), the precursors of rhamnolipids. *Microbiology, 149*(8), 2005-2013.

Diaz, M., King, J., & Yahr, T. (2011). Intrinsic and extrinsic regulation of type III secretion gene expression in *Pseudomonas aeruginosa*. *Frontiers in Microbiology, 2*(89). doi:10.3389/fmicb.2011.00089

Ditta, G., Stanfield, S., Corbin, D., & Helinski, D. R. (1980). Broad host range DNA cloning system for gram-negative bacteria: construction of a gene bank of *Rhizobium meliloti*. *Proceedings of the National Academy of Sciences of the United States of America, 77*(12), 7347-7351.

Dove, S. L., & Hochschild, A. (2004). A bacterial two-hybrid system based on transcription activation. *Methods in Molecular Biology, 261*, 231-246. doi:10.1385/1-59259-762-9:231

Duan, K., Dammel, C., Stein, J., Rabin, H., & Surette, M. G. (2003). Modulation of *Pseudomonas aeruginosa* gene expression by host microflora through interspecies communication. *Molecular Microbiology, 50*(5), 1477-1491.

Dubois-Brissonnet, F., Trotier, E., & Briandet, R. (2016). The biofilm lifestyle involves an increase in bacterial membrane saturated fatty acids. *Frontiers in Microbiology, 7*, 1673. doi:10.3389/fmicb.2016.01673

Egan, M. E., Schwiebert, E. M., & Guggino, W. B. (1995). Differential expression of ORCC and CFTR induced by low temperature in CF airway epithelial cells. *American Journal of Physiology - Lung Cellular and Molecular Physiology, 268*(1 Pt 1), C243-251.

Engelhardt, J., Yankaskas, J., Ernst, S., Yang, Y., Marino, C., Boucher, R., . . . Wilson, J. (1992). Submucosal glands are the predominant site of CFTR expression in the human bronchus. *Nature Genetics, 2*(3), 240-248.

Fauvart, M., De Groote, V., & Michiels, J. (2011). Role of persister cells in chronic infections: clinical relevance and perspectives on anti-persister therapies. *Journal of Medical Microbiology, 60*(Pt 6), 699-709. doi:10.1099/jmm.0.030932-0

Favero, M. S., Carson, L. A., Bond, W. W., & Petersen, N. J. (1971). *Pseudomonas aeruginosa:* growth in distilled water from hospitals. *Science, 173*(3999), 836-838.

Ferrández, A., Hawkins, A. C., Summerfield, D. T., & Harwood, C. S. (2002). Cluster II *che* genes from *Pseudomonas aeruginosa* are required for an optimal chemotactic response. *Journal of Bacteriology, 184*(16), 4374-4383. doi:10.1128/jb.184.16.4374-4383.2002

Ferroni, A., Guillemot, D., Moumile, K., Bernede, C., Le Bourgeois, M., Waernessyckle, S., . . . Taddei, F. (2009). Effect of mutator *Pseudomonas aeruginosa* on antibiotic resistance

acquisition and respiratory function in cystic fibrosis. *Pediatric Pulmonology, 44*(8), 820-825. doi:10.1002/ppul.21076

Finnan, S., Morrissey, J. P., O'Gara, F., & Boyd, E. F. (2004). Genome diversity of *Pseudomonas aeruginosa* isolates from cystic fibrosis patients and the hospital environment. *Journal of Clinical Microbiology, 42*(12), 5783-5792. doi:10.1128/JCM.42.12.5783-5792.2004

Fischer, H., Illek, B., Sachs, L., Finkbeiner, W. E., & Widdicombe, J. H. (2010). CFTR and calcium-activated chloride channels in primary cultures of human airway gland cells of serous or mucous phenotype. *American Journal of Physiology. Lung Cellular and Molecular Physiology, 299*(4), L585-594. doi:10.1152/ajplung.00421.2009

Fito-Boncompte, L., Chapalain, A., Bouffartigues, E., Chaker, H., Lesouhaitier, O., Gicquel, G., . . . Chevalier, S. (2011). Full virulence of *Pseudomonas aeruginosa* requires OprF. *Infection and Immunity, 79*(3), 1176-1186. doi:10.1128/iai.00850-10

Fleming, A., & Young, M. (1940). The inhibitory action of potassium tellurite on coliform bacteria. *The Journal of Pathology, 51*(1), 29-35.

Flynn, J. M., Niccum, D., Dunitz, J. M., & Hunter, R. C. (2016). Evidence and role for bacterial mucin degradation in cystic fibrosis airway disease. *PLoS Pathogens, 12*(8), e1005846. doi:10.1371/journal.ppat.1005846

Fodor, A., Klem, E., Gilpin, D., Elborn, J., Boucher, R., Tunney, M., & Wolfgang, M. (2012). The adult cystic fibrosis airway microbiota is stable over time and infection type, and highly resilient to antibiotic treatment of exacerbations. *PLoS One, 7*(9), e45001. doi:10.1371/journal.pone.0045001

Frank, D. W. (1997). The exoenzyme S regulon of *Pseudomonas aeruginosa*. *Molecular Microbiology, 26*(4), 621-629.

Fraser, G. M., & Hughes, C. (1999). Swarming motility. *Current Opinion in Microbiology, 2*(6), 630-635.

Fung, C., Naughton, S., Turnbull, L., Tingpej, P., Rose, B., Arthur, J., . . . Manos, J. (2010). Gene expression of *Pseudomonas aeruginosa* in a mucin-containing synthetic growth medium mimicking cystic fibrosis lung sputum. *Journal of Medical Microbiology, 59*(Pt 9), 1089-1100. doi:10.1099/jmm.0.019984-0

Fuqua, W. C., Winans, S. C., & Greenberg, E. P. (1994). Quorum sensing in bacteria: the LuxR-LuxI family of cell density-responsive transcriptional regulators. *Journal of Bacteriology, 176*(2), 269-275.

Gabriel, S. E., Clarke, L. L., Boucher, R. C., & Stutts, M. J. (1993). CFTR and outward rectifying chloride channels are distinct proteins with a regulatory relationship. *Nature, 363*(6426), 263-268. doi:10.1038/363263a0

Galperin, M., & Nikolskaya, A. (2007). Identification of sensory and signal-transducing domains in two-component signaling systems. *Methods in Enzymology, 422*, 47-74. doi:10.1016/S0076-6879(06)22003-2

Gardner, S. G., Miller, J. B., Dean, T., Robinson, T., Erickson, M., Ridge, P. G., & McCleary, W. R. (2015). Genetic analysis, structural modeling, and direct coupling analysis suggest a mechanism for phosphate signaling in *Escherichia coli*. *BMC Genetics, 16 Suppl 2*, S2. doi:10.1186/1471-2156-16-S2-S2

Geisinger, E., & Isberg, R. R. (2017). Interplay between antibiotic resistance and virulence during disease promoted by multidrug-resistant bacteria. *The Journal of Infectious Diseases, 215*(suppl_1), S9-s17. doi:10.1093/infdis/jiw402

Gicquel, G., Bouffartigues, E., Bains, M., Oxaran, V., Rosay, T., Lesouhaitier, O., . . . Chevalier, S. (2013). The extra-cytoplasmic function sigma factor *sigX* modulates biofilm and virulence-related properties in *Pseudomonas aeruginosa*. *PLoS One, 8*(11), e80407. doi:10.1371/journal.pone.0080407

Gilbert, K. B., Kim, T. H., Gupta, R., Greenberg, E. P., & Schuster, M. (2009). Global position analysis of the *Pseudomonas aeruginosa* quorum-sensing transcription factor LasR. *Molecular Microbiology, 73*(6), 1072-1085.

Goodman, A. L., Kulasekara, B., Rietsch, A., Boyd, D., Smith, R. S., & Lory, S. (2004). A signaling network reciprocally regulates genes associated with acute infection and chronic persistence in *Pseudomonas aeruginosa*. *Developmental Cell, 7*(5), 745-754. doi:10.1016/j.devcel.2004.08.020

Goodman, A. L., Merighi, M., Hyodo, M., Ventre, I., Filloux, A., & Lory, S. (2009). Direct interaction between sensor kinase proteins mediates acute and chronic disease phenotypes in a bacterial pathogen. *Genes & Development, 23*(2), 249-259. doi:10.1101/gad.1739009

Govan, J. R., Brown, A. R., & Jones, A. M. (2007). Evolving epidemiology of *Pseudomonas aeruginosa* and the *Burkholderia cepacia* complex in cystic fibrosis lung infection. *Future microbiology, 2*(2), 153-164. doi:10.2217/17460913.2.2.153

Gronlund, A. (2004). Networking genetic regulation and neural computation: directed network topology and its effect on the dynamics. *Physical review. E, Statistical, nonlinear, and soft matter physics, 70*(6 Pt 1), 061908. doi:10.1103/PhysRevE.70.061908

Grosso-Becerra, M.-V., Santos-Medellín, C., González-Valdez, A., Méndez, J.-L., Delgado, G., Morales-Espinosa, R., . . . Soberón-Chávez, G. (2014). *Pseudomonas aeruginosa* clinical and

environmental isolates constitute a single population with high phenotypic diversity. *BMC Genomics, 15*(1), 318. doi:10.1186/1471-2164-15-318

Gupta, R. K., Setia, S., & Harjai, K. (2011). Expression of quorum sensing and virulence factors are interlinked in *Pseudomonas aeruginosa*: an in vitro approach. *American Journal of Biomedical Sciences, 3*(2), 116-125.

Gupta, S., Laskar, N., & Kadouri, D. E. (2016). Evaluating the effect of oxygen concentrations on antibiotic sensitivity, growth, and biofilm formation of human pathogens. *Microbiology Insights, 9*, 37-46. doi:10.4137/MBI.S40767

Guvener, Z. T., & Harwood, C. S. (2007). Subcellular location characteristics of the *Pseudomonas aeruginosa* GGDEF protein, WspR, indicate that it produces cyclic-di-GMP in response to growth on surfaces. *Molecular Microbiology, 66*(6), 1459-1473. doi:10.1111/j.1365-2958.2007.06008.x

Ha, D. G., & O'Toole, G. A. (2015). c-di-GMP and its effects on biofilm formation and dispersion: a *Pseudomonas aeruginosa* review. *Microbiology spectrum, 3*(2), Mb-0003-2014. doi:10.1128/microbiolspec.MB-0003-2014

Haley, C. L., Colmer-Hamood, J. A., & Hamood, A. N. (2012). Characterization of biofilm-like structures formed by *Pseudomonas aeruginosa* in a synthetic mucus medium. *BMC Microbiology, 12*(1), 181. doi:10.1186/1471-2180-12-181

Hansen, S. K., Rau, M. H., Johansen, H. K., Ciofu, O., Jelsbak, L., Yang, L., . . . Molin, S. (2012). Evolution and diversification of *Pseudomonas aeruginosa* in the paranasal sinuses of cystic fibrosis children have implications for chronic lung infection. *The ISME Journal, 6*(1), 31-45. doi:10.1038/ismej.2011.83

Harris, W., & Kirk, K. (2016). Ion channels and transporters of epithelia in health and disease. In K. L. Hamilton & D. C. Devor (Eds.), *CFTR and cystic fibrosis* (pp. 519-552). New York, NY: Springer New York.

Harshey, R. M. (1994). Bees aren't the only ones: swarming in gram-negative bacteria. *Molecular Microbiology, 13*(3), 389-394.

Hassett, D. J., Cuppoletti, J., Trapnell, B., Lymar, S. V., Rowe, J. J., Sun Yoon, S., . . . Ochsner, U. A. (2002). Anaerobic metabolism and quorum sensing by *Pseudomonas aeruginosa* biofilms in chronically infected cystic fibrosis airways: rethinking antibiotic treatment strategies and drug targets. *Advanced Drug Delivery Reviews, 54*(11), 1425-1443. doi:doi.org/10.1016/S0169-409X(02)00152-7

Hassett, D. J., Sutton, M. D., Schurr, M. J., Herr, A. B., Caldwell, C. C., & Matu, J. O. (2009). *Pseudomonas aeruginosa* hypoxic or anaerobic biofilm infections within cystic fibrosis airways. *Trends in Microbiology, 17*(3), 130-138. doi:10.1016/j.tim.2008.12.003

Hellingwerf, K. J., Postma, P. W., Tommassen, J., & Westerhoff, H. V. (1995). Signal transduction in bacteria: phospho-neural network(s) in *Escherichia coli*? *FEMS Microbiology Reviews, 16*(4), 309-321.

Hendrick, S. M., Mroz, M. S., Greene, C. M., Keely, S. J., & Harvey, B. J. (2014). Bile acids stimulate chloride secretion through CFTR and calcium-activated Cl$^-$ channels in Calu-3 airway epithelial cells. *American Journal of Physiology. Lung Cellular and Molecular Physiology, 307*(5), L407-418. doi:10.1152/ajplung.00352.2013

Hengge, R. (2009). Principles of c-di-GMP signalling in bacteria. *Nature Reviews Microbiology, 7*(4), 263-273. doi:10.1038/nrmicro2109

Hense, B. A., Kuttler, C., Muller, J., Rothballer, M., Hartmann, A., & Kreft, J. U. (2007). Does efficiency sensing unify diffusion and quorum sensing? *Nature Reviews Microbiology, 5*(3), 230-239. doi:10.1038/nrmicro1600

Heurlier, K., Williams, F., Heeb, S., Dormond, C., Pessi, G., Singer, D., . . . Haas, D. (2004). Positive control of swarming, rhamnolipid synthesis, and lipase production by the posttranscriptional RsmA/RsmZ system in *Pseudomonas aeruginosa* PAO1. *Journal of Bacteriology, 186*(10), 2936-2945.

Hickman, J. W., Tifrea, D. F., & Harwood, C. S. (2005). A chemosensory system that regulates biofilm formation through modulation of cyclic diguanylate levels. *Proceedings of the National Academy of Sciences of the United States of America, 102*(40), 14422-14427. doi:10.1073/pnas.0507170102

Hoang, T. T., Karkhoff-Schweizer, R. R., Kutchma, A. J., & Schweizer, H. P. (1998). A broad-host-range Flp-FRT recombination system for site-specific excision of chromosomally-located DNA sequences: application for isolation of unmarked *Pseudomonas aeruginosa* mutants. *Gene, 212*(1), 77-86.

Hoffman, L. R., Kulasekara, H. D., Emerson, J., Houston, L. S., Burns, J. L., Ramsey, B. W., & Miller, S. I. (2009). *Pseudomonas aeruginosa* lasR mutants are associated with cystic fibrosis lung disease progression. *Journal of Cystic Fibrosis, 8*(1), 66-70. doi:10.1016/j.jcf.2008.09.006

Hoffman, L. R., Richardson, A. R., Houston, L. S., Kulasekara, H. D., Martens-Habbena, W., Klausen, M., . . . Miller, S. I. (2010). Nutrient availability as a mechanism for selection of antibiotic tolerant *Pseudomonas aeruginosa* within the CF airway. *PLoS Pathogens, 6*(1), e1000712. doi:10.1371/journal.ppat.1000712

Hogardt, M., & Heesemann, J. (2013). Microevolution of *Pseudomonas aeruginosa* to a chronic pathogen of the cystic fibrosis lung. *Current Topics in Microbiology and Immunology, 358*, 91-118. doi:10.1007/82_2011_199

Hovey, A. K., & Frank, D. W. (1995). Analyses of the DNA-binding and transcriptional activation properties of ExsA, the transcriptional activator of the *Pseudomonas aeruginosa* exoenzyme S regulon. *Journal of Bacteriology, 177*(15), 4427-4436.

Hsing, W., & Silhavy, T. J. (1997). Function of conserved histidine-243 in phosphatase activity of EnvZ, the sensor for porin osmoregulation in *Escherichia coli*. *Journal of Bacteriology, 179*(11), 3729-3735.

Hsu, J.-L., Chen, H.-C., Peng, H.-L., & Chang, H.-Y. (2008). Characterization of the histidine-containing phosphotransfer protein B-mediated multistep phosphorelay system in *Pseudomonas aeruginosa* PAO1. *The Journal of Biological Chemistry, 283*(15), 9933-9944. doi:10.1074/jbc.M708836200

Huffnagle, G., & Dickson, R. (2015). The bacterial microbiota in inflammatory lung diseases. *Clinical Immunology, 159*(2), 177-182.

Huynh, T. N., Chen, L. L., & Stewart, V. (2015). Sensor-response regulator interactions in a cross-regulated signal transduction network. *Microbiology, 161*(7), 1504-1515. doi:10.1099/mic.0.000092

Hwang, T. C., & Sheppard, D. N. (2009). Gating of the CFTR Cl- channel by ATP-driven nucleotide-binding domain dimerisation. *Journal of Physiology (London), 587*(Pt 10), 2151-2161. doi:10.1113/jphysiol.2009.171595

Inglis, S., Corboz, M., Taylor, A., & Ballard, S. (1997). Effect of anion transport inhibition on mucus secretion by airway submucosal glands. *American Journal of Physiology - Lung Cellular and Molecular Physiology, 272*(2 Pt 1), L372-377.

Irie, Y., Starkey, M., Edwards, A. N., Wozniak, D. J., Romeo, T., & Parsek, M. R. (2010). *Pseudomonas aeruginosa* biofilm matrix polysaccharide Psl is regulated transcriptionally by RpoS and post-transcriptionally by RsmA. *Molecular Microbiology, 78*(1), 158-172. doi:10.1111/j.1365-2958.2010.07320.x

Jain, S., & Ohman, D. E. (1998). Deletion of *algK* in mucoid *Pseudomonas aeruginosa* blocks alginate polymer formation and results in uronic acid secretion. *Journal of Bacteriology, 180*(3), 634-641.

Ji, H. L., Chalfant, M. L., Jovov, B., Lockhart, J. P., Parker, S. B., Fuller, C. M., . . . Benos, D. J. (2000). The cytosolic termini of the beta- and gamma-ENaC subunits are involved in the functional interactions between cystic fibrosis transmembrane conductance regulator and epithelial sodium channel. *Journal of Biological Chemistry, 275*(36), 27947-27956.

Jin, F., Conrad, J. C., Gibiansky, M. L., & Wong, G. C. (2011). Bacteria use type-IV pili to slingshot on surfaces. *Proceedings of the National Academy of Sciences of the United States of America, 108*(31), 12617-12622. doi:10.1073/pnas.1105073108

Jing, X., Jaw, J., Robinson, H. H., & Schubot, F. D. (2010). Crystal structure and oligomeric state of the RetS signaling kinase sensory domain. *Proteins, 78*(7), 1631-1640. doi:10.1002/prot.22679

Johnson, D. A., Tetu, S. G., Phillippy, K., Chen, J., Ren, Q., & Paulsen, I. T. (2008). High-throughput phenotypic characterization of *Pseudomonas aeruginosa* membrane transport genes. *PLoS Genetics, 4*(10), e1000211. doi:10.1371/journal.pgen.1000211

Jolly, A., Takawira, D., Oke, O., Whiteside, S., Chang, S., Wen, E., . . . Fleiszig, S. (2015). *Pseudomonas aeruginosa*-induced bleb-niche formation in epithelial cells is independent of actinomyosin contraction and enhanced by loss of cystic fibrosis transmembrane-conductance regulator osmoregulatory function. *MBio, 6*(2), e02533-02514. doi:10.1128/mBio.02533-14

Jones , A. K., Fulcher, N. B., Balzer, G. J., Urbanowski, M. L., Pritchett, C. L., Schurr, M. J., . . . Wolfgang, M. C. (2010). Activation of the *Pseudomonas aeruginosa* AlgU regulon through *mucA* mutation Inhibits cyclic AMP/Vfr signaling. *Journal of Bacteriology, 192*(21), 5709-5717. doi:10.1128/jb.00526-10

Joo, N., Saenz, Y., Krouse, M., & Wine, J. (2002). Mucus secretion from single submucosal glands of Pig. Stimulation by carbachol and vasoactive intestinal peptide. *The Journal of Biological Chemistry, 277*(31), 28167-28175. doi:10.1074/jbc.M202712200

Karna, S. L., Zogaj, X., Barker, J. R., Seshu, J., Dove, S. L., & Klose, K. E. (2010). A bacterial two-hybrid system that utilizes gateway cloning for rapid screening of protein-protein interactions. *Biotechniques, 49*(5), 831-833. doi:10.2144/000113539

Kay, E., Humair, B., Dénervaud, V., Riedel, K., Spahr, S., Eberl, L., . . . Haas, D. (2006). Two GacA-dependent small RNAs modulate the quorum-sensing response in *Pseudomonas aeruginosa*. *Journal of Bacteriology, 188*(16), 6026-6033.

Kearns, D. B., Robinson, J., & Shimkets, L. J. (2001). *Pseudomonas aeruginosa* exhibits directed twitching motility up phosphatidylethanolamine gradients. *Journal of Bacteriology, 183*(2), 763-767. doi:10.1128/jb.183.2.763-767.2001

Kloda, A., & Martinac, B. (2001). Structural and functional differences between two homologous mechanosensitive channels of *Methanococcus jannaschii*. *The EMBO journal, 20*(8), 1888-1896. doi:10.1093/emboj/20.8.1888

Köhler, T., Curty, L. K., Barja, F., van Delden, C., & Pechère, J.-C. (2000). Swarming of *Pseudomonas aeruginosa* Is dependent on cell-to-cell signaling and requires flagella and pili. *Journal of Bacteriology, 182*(21), 5990-5996.

Kong, W., Chen, L., Zhao, J., Shen, T., Surette, M. G., Shen, L., & Duan, K. (2013). Hybrid sensor kinase PA1611 in *Pseudomonas aeruginosa* regulates transitions between acute and chronic infection through direct interaction with RetS. *Molecular Microbiology, 88*(4), 784-797. doi:10.1111/mmi.12223

Koretke, K. K., Lupas, A. N., Warren, P. V., Rosenberg, M., & Brown, J. R. (2000). Evolution of two-component signal transduction. *Molecular Biology and Evolution, 17*(12), 1956-1970.

Krogh, A., Larsson, B., von Heijne, G., & Sonnhammer, E. L. (2001). Predicting transmembrane protein topology with a hidden Markov model: application to complete genomes. *Journal of Molecular Biology, 305*(3), 567-580. doi:10.1006/jmbi.2000.4315

Kuchma, S. L., Ballok, A. E., Merritt, J. H., Hammond, J. H., Lu, W., Rabinowitz, J. D., & O'Toole, G. A. (2010). Cyclic-di-GMP-mediated repression of swarming motility by *Pseudomonas aeruginosa:* the *pilY1* gene and its impact on surface-associated behaviors. *Journal of Bacteriology, 192*(12), 2950-2964. doi:10.1128/jb.01642-09

Kuchma, S. L., Delalez, N. J., Filkins, L. M., Snavely, E. A., Armitage, J. P., & O'Toole, G. A. (2015). Cyclic di-GMP-mediated repression of swarming motility by *Pseudomonas aeruginosa* PA14 requires the MotAB stator. *Journal of Bacteriology, 197*(3), 420-430. doi:10.1128/jb.02130-14

Kulasakara, H., Lee, V., Brencic, A., Liberati, N., Urbach, J., Miyata, S., . . . Lory, S. (2006). Analysis of *Pseudomonas aeruginosa* diguanylate cyclases and phosphodiesterases reveals a role

for bis-(3'-5')-cyclic-GMP in virulence. *Proceedings of the National Academy of Sciences of the United States of America, 103*(8), 2839-2844. doi:10.1073/pnas.0511090103

Lai, S., Wang, Y., Wirtz, D., & Hanes, J. (2009). Micro and macrorheology of mucus. *Advanced Drug Delivery Reviews, 61*(2), 86-100. doi:10.1016/j.addr.2008.09.012

Lambiase, A., Catania, M. R., & Rossano, F. (2010). Anaerobic bacteria infection in cystic fibrosis airway disease. *New Microbiologica, 33*(3), 185-194.

Lamblin, G., Degroote, S., Perini, J., Delmotte, P., Scharfman, A., Davril, M., . . . Rousse, P. (2001). Human airway mucin glycosylation: a combinatory of carbohydrate determinants which vary in cystic fibrosis. *Glycoconjugate Journal, 18*(9), 661-684.

Landry, R. M., An, D., Hupp, J. T., Singh, P. K., & Parsek, M. R. (2006). Mucin-*Pseudomonas aeruginosa* interactions promote biofilm formation and antibiotic resistance. *Molecular Microbiology, 59*(1), 142-151. doi:10.1111/j.1365-2958.2005.04941.x

Lapouge, K., Schubert, M., Allain, F. H., & Haas, D. (2008). Gac/Rsm signal transduction pathway of gamma-proteobacteria: from RNA recognition to regulation of social behaviour. *Molecular Microbiology, 67*(2), 241-253. doi:10.1111/j.1365-2958.2007.06042.x

Larkin, M. A., Blackshields, G., Brown, N. P., Chenna, R., McGettigan, P. A., McWilliam, H., . . . Higgins, D. G. (2007). Clustal W and Clustal X version 2.0. *Bioinformatics, 23*(21), 2947-2948. doi:10.1093/bioinformatics/btm404

Laskowski, M. A., Osborn, E., & Kazmierczak, B. I. (2004). A novel sensor kinase-response regulator hybrid regulates type III secretion and is required for virulence in *Pseudomonas aeruginosa. Molecular Microbiology, 54*(4), 1090-1103. doi:10.1111/j.1365-2958.2004.04331.x

Lee, J., Wu, J., Deng, Y., Wang, J., Wang, C., Wang, J., . . . Zhang, L. H. (2013). A cell-cell communication signal integrates quorum sensing and stress response. *Nature Chemical Biology, 9*(5), 339-343. doi:10.1038/nchembio.1225

Lee, V. T., Matewish, J. M., Kessler, J. L., Hyodo, M., Hayakawa, Y., & Lory, S. (2007). A cyclic-di-GMP receptor required for bacterial exopolysaccharide production. *Molecular Microbiology, 65*(6), 1474-1484. doi:10.1111/j.1365-2958.2007.05879.x

Leeper-Woodford, S., & Detmer, K. (1999). Acute hypoxia increases alveolar macrophage tumor necrosis factor activity and alters NF-kappaB expression. *American Journal of Physiology - Lung Cellular and Molecular Physiology, 276*(6 Pt 1), L909-916.

Leroy, C., Prive, A., Bourret, J. C., Berthiaume, Y., Ferraro, P., & Brochiero, E. (2006). Regulation of ENaC and CFTR expression with K+ channel modulators and effect on fluid absorption across alveolar epithelial cells. *American Journal of Physiology. Lung Cellular and Molecular Physiology, 291*(6), L1207-1219. doi:10.1152/ajplung.00376.2005

Levina, N., Totemeyer, S., Stokes, N. R., Louis, P., Jones, M. A., & Booth, I. R. (1999). Protection of *Escherichia coli* cells against extreme turgor by activation of MscS and MscL mechanosensitive channels: identification of genes required for MscS activity. *EMBO Journal, 18*(7), 1730-1737. doi:10.1093/emboj/18.7.1730

Lewis, H. A., Zhao, X., Wang, C., Sauder, J. M., Rooney, I., Noland, B. W., . . . Emtage, S. (2005). Impact of the deltaF508 mutation in first nucleotide-binding domain of human cystic fibrosis transmembrane conductance regulator on domain folding and structure. *Journal of Biological Chemistry, 280*(2), 1346-1353. doi:10.1074/jbc.M410968200

Lewis, K. (2010). Persister cells. *Annual Review of Microbiology, 64*, 357-372. doi:10.1146/annurev.micro.112408.134306

Lewis, K. (2012). Persister cells: molecular mechanisms related to antibiotic tolerance. *Handbook of Experimental Pharmacology*(211), 121-133. doi:10.1007/978-3-642-28951-4_8

Li, K., Yang, G., Debru, A. B., Li, P., Zong, L., Li, P., . . . Bao, Q. (2017). SuhB regulates the motile-sessile switch in *Pseudomonas aeruginosa* through the Gac/Rsm pathway and c-di-GMP signaling. *Frontiers in Microbiology, 8*, 1045. doi:10.3389/fmicb.2017.01045

Li, L., Wang, Q., Zhang, H., Yang, M., Khan, M. I., & Zhou, X. (2016). Sensor histidine kinase is a beta-lactam receptor and induces resistance to beta-lactam antibiotics. *Proceedings of the National Academy of Sciences of the United States of America, 113*(6), 1648-1653. doi:10.1073/pnas.1520300113

Lillehoj, E. P., Kato, K., Lu, W., & Kim, K. C. (2013). Cellular and molecular biology of airway mucins. *International review of cell and molecular biology, 303*, 139-202. doi:10.1016/b978-0-12-407697-6.00004-0

Long, F., Williams, R., & Castile, R. (2004). Structural airway abnormalities in infants and young children with cystic fibrosis. *The Journal of Pediatrics, 144*(2), 154-161. doi:10.1016/j.jpeds.2003.09.026

López-Causapé, C., Rojo-Molinero, E., Macià, M., & Oliver, A. (2015). The problems of antibiotic resistance in cystic fibrosis and solutions. *Expert Review of Respiratory Medicine, 9*(1), 73-88.

Lovell, S. C., Davis, I. W., Arendall, W. B., 3rd, de Bakker, P. I., Word, J. M., Prisant, M. G., . . . Richardson, D. C. (2003). Structure validation by C alpha geometry: phi,psi and Cbeta deviation. *Proteins, 50*(3), 437-450. doi:10.1002/prot.10286

Lu, M., Leng, Q., Egan, M., Caplan, M., Boulpaep, E., Giebisch, G., & Hebert, S. (2006). CFTR is required for PKA-regulated ATP sensitivity of Kir1.1 potassium channels in mouse kidney. *Journal of Clinical Investigation, 116*(3), 797-807. doi:10.1172/JCI26961

Ma, S., Wozniak, D., & Ohman, D. (1997). Identification of the histidine protein kinase KinB in *Pseudomonas aeruginosa* and its phosphorylation of the alginate regulator AlgB. *The Journal of Biological Chemistry, 272*(29), 17952-17960.

Marsden, A. E., Intile, P. J., Schulmeyer, K. H., Simmons-Patterson, E. R., Urbanowski, M. L., Wolfgang, M. C., & Yahr, T. L. (2016). *vfr* directly activates *exsA* transcription to regulate expression of the *Pseudomonas aeruginosa* type III secretion system. *Journal of Bacteriology, 198*(9), 1442-1450. doi:10.1128/jb.00049-16

Matamouros, S., Hager, K. R., & Miller, S. I. (2015). HAMP domain rotation and tilting movements associated with signal transduction in the PhoQ sensor kinase. *MBio, 6*(3), e00616-00615. doi:10.1128/mBio.00616-15

Mathee, K., Narasimhan, G., Valdes, C., Qiu, X., Matewish, J. M., Koehrsen, M., . . . Lory, S. (2008). Dynamics of *Pseudomonas aeruginosa* genome evolution. *Proceedings of the National Academy of Sciences, 105*(8), 3100.

Matsushika, A., & Mizuno, T. (1998). Mutational analysis of the histidine-containing phosphotransfer (HPt) signaling domain of the ArcB sensor in *Escherichia coli*. *Bioscience, Biotechnology, and Biochemistry, 62*(11), 2236-2238.

McCarthy, R. R., Valentini, M., & Filloux, A. (2017). Contribution of cyclic di-GMP in the control of type III and type VI secretion in *Pseudomonas aeruginosa*. *Methods in Molecular Biology, 1657*, 213-224. doi:10.1007/978-1-4939-7240-1_17

McShane, D., Davies, J., Davies, M., Bush, A., Geddes, D., & Alton, E. (2003). Airway surface pH in subjects with cystic fibrosis. *European Respiratory Journal, 21*(1), 37-42.

Merighi, M., Lee, V. T., Hyodo, M., Hayakawa, Y., & Lory, S. (2007). The second messenger bis-(3'-5')-cyclic-GMP and its PilZ domain-containing receptor Alg44 are required for alginate biosynthesis in *Pseudomonas aeruginosa*. *Molecular Microbiology, 65*(4), 876-895. doi:10.1111/j.1365-2958.2007.05817.x

Meyerholz, D., Stoltz, D., Namati, E., Ramachandran, S., Pezzulo, A., Smith, A., . . . Welsh, M. (2010). Loss of cystic fibrosis transmembrane conductance regulator function produces abnormalities in tracheal development in neonatal pigs and young children. *American Journal of Respiratory and Critical Care Medicine, 182*(10), 1251-1261. doi:10.1164/rccm.201004-0643OC

Meyrick, B., & Reid, L. (1970). Ultrastructure of cells in the human bronchial submucosal glands. *Journal of Anatomy, 107*(Pt 2), 281.

Meyrick, B., Sturgess, J., & Reid, L. (1969). A reconstruction of the duct system and secretory tubules of the human bronchial submucosal gland. *Thorax, 24*(6), 729-736.

Mitchell, S. L., Ismail, A. M., Kenrick, S. A., & Camilli, A. (2015). The VieB auxiliary protein negatively regulates the VieSA signal transduction system in *Vibrio cholerae*. *BMC Microbiol, 15*, 59. doi:10.1186/s12866-015-0387-7

Molinski, S. V., Ahmadi, S., Hung, M., & Bear, C. E. (2015). Facilitating structure-function studies of CFTR modulator sites with efficiencies in mutagenesis and functional screening. *Journal of Biomolecular Screening*. doi:10.1177/1087057115605834

Montaudon, M., Berger, P., Cangini-Sacher, A., de Dietrich, G., Tunon-de-Lara, J., Marthan, R., & Laurent, F. (2007). Bronchial measurement with three-dimensional quantitative thin-section CT in patients with cystic fibrosis. *Radiology, 242*(2), 573-581. doi:10.1148/radiol.2422060030

Mornon, J. P., Lehn, P., & Callebaut, I. (2009). Molecular models of the open and closed states of the whole human CFTR protein. *Cellular and Molecular Life Sciences, 66*(21), 3469-3486. doi:10.1007/s00018-009-0133-0

Morrison, T. B., & Parkinson, J. S. (1994). Liberation of an interaction domain from the phosphotransfer region of CheA, a signaling kinase of *Escherichia coli*. *Proceedings of the National Academy of Sciences of the United States of America, 91*(12), 5485-5489.

Moscoso, J. A., Jaeger, T., Valentini, M., Hui, K., Jenal, U., & Filloux, A. (2014). The diguanylate cyclase SadC is a central player in Gac/Rsm-mediated biofilm formation in *Pseudomonas aeruginosa*. *Journal of Bacteriology, 196*(23), 4081-4088. doi:10.1128/jb.01850-14

Moscoso, J. A., Mikkelsen, H., Heeb, S., Williams, P., & Filloux, A. (2011). The *Pseudomonas aeruginosa* sensor RetS switches type III and type VI secretion via c-di-GMP signalling. *Environmental Microbiology, 13*(12), 3128-3138. doi:10.1111/j.1462-2920.2011.02595.x

Motley, S. T., & Lory, S. (1999). Functional characterization of a serine/threonine protein kinase of *Pseudomonas aeruginosa*. *Infection and Immunity, 67*(10), 5386-5394.

Mougel, C., & Zhulin, I. (2001). CHASE: an extracellular sensing domain common to transmembrane receptors from prokaryotes, lower eukaryotes and plants. *Trends in Biochemical Sciences, 26*(10), 582-584. doi:dx.doi.org/10.1016/S0968-0004(01)01969-7

Mourey, L., Da Re, S., Pedelacq, J., Tolstykh, T., Faurie, C., Guillet, V., . . . Samama, J. (2001). Crystal structure of the CheA histidine phosphotransfer domain that mediates response regulator

phosphorylation in bacterial chemotaxis. *The Journal of Biological Chemistry, 276*(33), 31074-31082. doi:10.1074/jbc.M101943200

Murray, T. S., Egan, M., & Kazmierczak, B. I. (2007). *Pseudomonas aeruginosa* chronic colonization in cystic fibrosis patients. *Current opinion in pediatrics, 19*(1), 83-88. doi:10.1097/MOP.0b013e3280123a5d

Nagel, G., Szellas, T., Riordan, J. R., Friedrich, T., & Hartung, K. (2001). Non-specific activation of the epithelial sodium channel by the CFTR chloride channel. *EMBO Reports, 2*(3), 249-254. doi:10.1093/embo-reports/kve045

Navarro-Arias, M. J., Dementhon, K., Defosse, T. A., Foureau, E., Courdavault, V., Clastre, M., . . . Papon, N. (2017). Group X hybrid histidine kinase Chk1 is dispensable for stress adaptation, host–pathogen interactions and virulence in the opportunistic yeast *Candida guilliermondii*. *Research in Microbiology, 168*(7), 644-654. doi:doi.org/10.1016/j.resmic.2017.04.009

Nieto, J. M., Madrid, C., Miquelay, E., Parra, J. L., Rodríguez, S., & Juárez, A. (2002). Evidence for direct protein-protein Interaction between members of the Enterobacterial Hha/YmoA and H-NS families of proteins. *Journal of Bacteriology, 184*(3), 629-635. doi:10.1128/jb.184.3.629-635.2002

Nikolskaya, A., & Galperin, M. (2002). A novel type of conserved DNA-binding domain in the transcriptional regulators of the AlgR/AgrA/LytR family. *Nucleic Acids Research, 30*(11), 2453-2459.

Norsworthy, A. N., & Visick, K. L. (2015). Signaling between two interacting sensor kinases promotes biofilms and colonization by a bacterial symbiont. *Molecular Microbiology, 96*(2), 233-248. doi:10.1111/mmi.12932

O'Callaghan, J., Reen, F. J., Adams, C., & O'Gara, F. (2011). Low oxygen induces the type III secretion system in *Pseudomonas aeruginosa* via modulation of the small RNAs RsmZ and RsmY. *Microbiology, 157*(Pt 12), 3417-3428. doi:10.1099/mic.0.052050-0

O'Toole, G. A., & Kolter, R. (1998). Initiation of biofilm formation in *Pseudomonas fluorescens* WCS365 proceeds via multiple, convergent signalling pathways: a genetic analysis. *Molecular Microbiology, 28*(3), 449-461.

Ohgita, T., Hayashi, N., Gotoh, N., & Kogure, K. (2013). Suppression of type III effector secretion by polymers. *Open Biology, 3*(12), 130133. doi:10.1098/rsob.130133

Ohta, N., & Newton, A. (2003). The core dimerization domains of histidine kinases contain recognition specificity for the cognate response regulator. *Journal of Bacteriology, 185*(15), 4424-4431. doi:10.1128/JB.185.15.4424-4431.2003

Oliver, A. (2010). Mutators in cystic fibrosis chronic lung infection: Prevalence, mechanisms, and consequences for antimicrobial therapy. *International Journal of Medical Microbiology, 300*(8), 563-572. doi:10.1016/j.ijmm.2010.08.009

Oliver, A., Canton, R., Campo, P., Baquero, F., & Blazquez, J. (2000). High frequency of hypermutable *Pseudomonas aeruginosa* in cystic fibrosis lung infection. *Science, 288*(5469), 1251-1254.

Oliver, A., & Mena, A. (2010). Bacterial hypermutation in cystic fibrosis, not only for antibiotic resistance. *Clinical Microbiology and Infection, 16*(7), 798-808. doi:10.1111/j.1469-0691.2010.03250.x

Park, S. H., Butcher, B. G., Anderson, Z., Pellegrini, N., Bao, Z., D'Amico, K., & Filiatrault, M. J. (2013). Analysis of the small RNA P16/RgsA in the plant pathogen *Pseudomonas syringae* pv.

tomato strain DC3000. *Microbiology (Reading, England), 159*(Pt 2), 296-306. doi:10.1099/mic.0.063826-0

Parkins, M. D., Ceri, H., & Storey, D. G. (2001). *Pseudomonas aeruginosa* GacA, a factor in multihost virulence, is also essential for biofilm formation. *Molecular Microbiology, 40*(5), 1215-1226.

Pena-Sandoval, G. R., Kwon, O., & Georgellis, D. (2005). Requirement of the receiver and phosphotransfer domains of ArcB for efficient dephosphorylation of phosphorylated ArcA in vivo. *Journal of Bacteriology, 187*(9), 3267-3272. doi:10.1128/JB.187.9.3267-3272.2005

Pessi, G., Williams, F., Hindle, Z., Heurlier, K., Holden, M. T., Cámara, M., . . . William, P. (2002). The global posttranscriptional regulator RsmA modulates production of virulence determinants and N-acylhomoserine lactones in *Pseudomonas aeruginosa*. *Journal of Bacteriology, 184*(1), 335.

Petrova, O. E., Gupta, K., Liao, J., Goodwine, J. S., & Sauer, K. (2017). Divide and conquer: the *Pseudomonas aeruginosa* two-component hybrid SagS enables biofilm formation and recalcitrance of biofilm cells to antimicrobial agents via distinct regulatory circuits. *Environmental Microbiology, 19*(5), 2005-2024. doi:10.1111/1462-2920.13719

Pezzulo, A., Tang, X., Hoegger, M., Alaiwa, M., Ramachandran, S., Moninger, T., . . . Zabner, J. (2012). Reduced airway surface pH impairs bacterial killing in the porcine cystic fibrosis lung. *Nature, 487*(7405), 109-113. doi:10.1038/nature11130

Pier, G., Grout, M., & Zaidi, T. (1997). Cystic fibrosis transmembrane conductance regulator is an epithelial cell receptor for clearance of *Pseudomonas aeruginosa* from the lung. *Proceedings of the National Academy of Sciences of the United States of America, 94*(22), 12088-12093.

Pierce, B. G., Hourai, Y., & Weng, Z. (2011). Accelerating protein docking in ZDOCK using an advanced 3D convolution library. *PLoS One, 6*(9), e24657. doi:10.1371/journal.pone.0024657

Poole, K., Neshat, S., Krebes, K., & Heinrichs, D. E. (1993). Cloning and nucleotide sequence analysis of the ferripyoverdine receptor gene *fpvA* of *Pseudomonas aeruginosa*. *Journal of Bacteriology, 175*(15), 4597-4604.

Qadri, Y. J., Cormet-Boyaka, E., Benos, D. J., & Berdiev, B. K. (2011). CFTR regulation of epithelial sodium channel. *Methods in Molecular Biology, 742*, 35-50. doi:10.1007/978-1-61779-120-8_3

Quinn, R., Lim, Y., Maughan, H., Conrad, D., Rohwer, F., & Whiteson, K. (2014). Biogeochemical forces shape the composition and physiology of polymicrobial communities in the cystic fibrosis lung. *MBio, 5*(2), e00956-00913.

Rajagopala, S. V., Sikorski, P., Kumar, A., Mosca, R., Vlasblom, J., Arnold, R., . . . Uetz, P. (2014). The binary protein-protein interaction landscape of *Escherichia coli*. *Nature Biotechnology, 32*(3), 285-290. doi:10.1038/nbt.2831

Rashid, M. H., & Kornberg, A. (2000). Inorganic polyphosphate is needed for swimming, swarming, and twitching motilities of *Pseudomonas aeruginosa*. *Proceedings of the National Academy of Sciences, USA, 97*(9), 4885-4890. doi:10.1073/pnas.060030097

Rawling, E. G., Brinkman, F. S., & Hancock, R. E. (1998). Roles of the carboxy-terminal half of *Pseudomonas aeruginosa* major outer membrane protein OprF in cell shape, growth in low-osmolarity medium, and peptidoglycan association. *Journal of Bacteriology, 180*(14), 3556-3562.

Redfield, R. J. (2002). Is quorum sensing a side effect of diffusion sensing? *Trends in Microbiology, 10*(8), 365-370.

Reimmann, C., Beyeler, M., Latifi, A., Winteler, H., Foglino, M., Lazdunski, A., & Haas, D. (1997). The global activator GacA of *Pseudomonas aeruginosa* PAO positively controls the production of the autoinducer N-butyryl-homoserine lactone and the formation of the virulence factors pyocyanin, cyanide, and lipase. *Molecular Microbiology, 24*(2), 309-319.

Rodrigue, A., Quentin, Y., Lazdunski, A., Mejean, V., & Foglino, M. (2000). Two-component systems in *Pseudomonas aeruginosa*: why so many? *Trends in Microbiology, 8*(11), 498-504.

Romling, U., Galperin, M. Y., & Gomelsky, M. (2013). Cyclic di-GMP: the first 25 years of a universal bacterial second messenger. *Microbiology and Molecular Biology Reviews, 77*(1), 1-52. doi:10.1128/mmbr.00043-12

Rosenthal, V. D., Al-Abdely, H. M., El-Kholy, A. A., AlKhawaja, S. A. A., Leblebicioglu, H., Mehta, Y., . . . Kushner-Davalos, L. (2016). International nosocomial infection control consortium report, data summary of 50 countries for 2010-2015: device-associated module. *American Journal of Infection Control, 44*(12), 1495-1504. doi:10.1016/j.ajic.2016.08.007

Rybtke, M. T., Borlee, B. R., Murakami, K., Irie, Y., Hentzer, M., Nielsen, T. E., . . . Tolker-Nielsen, T. (2012). Fluorescence-based reporter for gauging cyclic di-GMP levels in *Pseudomonas aeruginosa*. *Applied and Environmental Microbiology, 78*(15), 5060-5069. doi:10.1128/aem.00414-12

Sadikot, R. T., Blackwell, T. S., Christman, J. W., & Prince, A. S. (2005). Pathogen-host interactions in *Pseudomonas aeruginosa* pneumonia. *American Journal of Respiratory and Critical Care Medicine, 171*(11), 1209-1223. doi:10.1164/rccm.200408-1044SO

Sakuragi, Y., & Kolter, R. (2007). Quorum-sensing regulation of the biofilm matrix genes (pel) of *Pseudomonas aeruginosa. Journal of Bacteriology, 189*(14), 5383-5386.

Sánchez, P., Linares, J. F., Ruiz-Díez, B., Campanario, E., Navas, A., Baquero, F., & Martínez, J. L. (2002). Fitness of in vitro selected *Pseudomonas aeruginosa nalB* and *nfxB* multidrug resistant mutants. *Journal of Antimicrobial Chemotherapy, 50*(5), 657-664. doi:10.1093/jac/dkf185

Sanders, D. B., Bittner, R. C., Rosenfeld, M., Hoffman, L. R., Redding, G. J., & Goss, C. H. (2010). Failure to recover to baseline pulmonary function after cystic fibrosis pulmonary exacerbation. *American Journal of Respiratory and Critical Care Medicine, 182*(5), 627-632. doi:10.1164/rccm.200909-1421OC

Sato, H., & Frank, D. W. (2004). ExoU is a potent intracellular phospholipase. *Molecular Microbiology, 53*(5), 1279-1290. doi:10.1111/j.1365-2958.2004.04194.x

Sawicki, G. S., Ren, C. L., Konstan, M. W., Millar, S. J., Pasta, D. J., & Quittner, A. L. (2013). Treatment complexity in cystic fibrosis: Trends over time and associations with site-specific outcomes. *Journal of Cystic Fibrosis, 12*(5), 461-467. doi:doi.org/10.1016/j.jcf.2012.12.009

Schaller, G. E., Shiu, S. H., & Armitage, J. P. (2011). Two-component systems and their co-option for eukaryotic signal transduction. *Current Biology, 21*(9), R320-330. doi:10.1016/j.cub.2011.02.045

Schobert, M., & Jahn, D. (2010). Anaerobic physiology of *Pseudomonas aeruginosa* in the cystic fibrosis lung. *International Journal of Medical Microbiology, 300*. doi:10.1016/j.ijmm.2010.08.007

Schuster, M., & Greenberg, E. P. (2006). A network of networks: quorum-sensing gene regulation in *Pseudomonas aeruginosa*. *International Journal of Medical Microbiology, 296*(2-3), 73-81. doi:10.1016/j.ijmm.2006.01.036

Scotet, V., Duguépéroux, I., Saliou, P., Rault, G., Roussey, M., Audrézet, M.-P., & Férec, C. (2012). Evidence for decline in the incidence of cystic fibrosis: a 35-year observational study in Brittany, France. *Orphanet Journal of Rare Diseases, 7*, 14-14. doi:10.1186/1750-1172-7-14

Serohijos, A. W., Hegedus, T., Aleksandrov, A. A., He, L., Cui, L., Dokholyan, N. V., & Riordan, J. R. (2008). Phenylalanine-508 mediates a cytoplasmic-membrane domain contact in the CFTR 3D structure crucial to assembly and channel function. *Proceedings of the National Academy of Sciences of the United States of America, 105*(9), 3256-3261. doi:10.1073/pnas.0800254105

Shah, V., Meyerholz, D., Tang, X., Reznikov, L., Abou Alaiwa, M., Ernst, S., . . . Welsh, M. (2016). Airway acidification initiates host defense abnormalities in cystic fibrosis mice. *Science, 351*(6272), 503-507. doi:10.1126/science.aad5589

Silby, M. W., Winstanley, C., Godfrey, S. A., Levy, S. B., & Jackson, R. W. (2011). Pseudomonas genomes: diverse and adaptable. *FEMS Microbiology Reviews, 35*(4), 652-680. doi:10.1111/j.1574-6976.2011.00269.x

Simon, R., Priefer, U., & Puhler, A. (1983). A Broad Host Range Mobilization System for *In Vivo* Genetic Engineering: Transposon Mutagenesis in Gram Negative Bacteria. *Nature Biotechnology, 1*(9), 784-791.

Sosnay, P. R., Siklosi, K. R., Van Goor, F., Kaniecki, K., Yu, H., Sharma, N., . . . Cutting, G. R. (2013). Defining the disease liability of variants in the cystic fibrosis transmembrane conductance regulator gene. *Nature Genetics, 45*(10), 1160-1167. doi:10.1038/ng.2745

Sriramulu, D. D., Lunsdorf, H., Lam, J. S., & Romling, U. (2005). Microcolony formation: a novel biofilm model of *Pseudomonas aeruginosa* for the cystic fibrosis lung. *Journal of Medical Microbiology, 54*. doi:10.1099/jmm.0.45969-0

Starkey, M., Hickman, J. H., Ma, L., Zhang, N., De Long, S., Hinz, A., . . . Parsek, M. R. (2009). *Pseudomonas aeruginosa* rugose small-colony variants have adaptations that likely promote persistence in the cystic fibrosis lung. *Journal of Bacteriology, 191*(11), 3492-3503. doi:10.1128/jb.00119-09

Stigliani, M., Manniello, M., Zegarra-Moran, O., Galietta, L., Minicucci, L., Casciaro, R., . . . Del Gaudio, P. (2016). Rheological properties of cystic fibrosis bronchial secretion and *in vitro* drug permeation study: the effect of sodium bicarbonate. *Journal of Aerosol Medicine and Pulmonary Drug Delivery, 29*(4), 337-345.

Stover, C. K., Pham, X. Q., Erwin, A. L., Mizoguchi, S. D., Warrener, P., Hickey, M. J., . . . Olson, M. V. (2000). Complete genome sequence of *Pseudomonas aeruginosa* PAO1, an opportunistic pathogen. *Nature, 406*(6799), 959-964. doi:10.1038/35023079

Tang, X., Ostedgaard, L., Hoegger, M., Moninger, T., Karp, P., McMenimen, J., . . . Welsh, M. (2016). Acidic pH increases airway surface liquid viscosity in cystic fibrosis. *The Journal of Clinical Investigation, 126*(3), 879-891. doi:10.1172/JCI83922

Tapparel, C., Monod, A., & Kelley, W. (2006). The DNA-binding domain of the *Escherichia coli* CpxR two-component response regulator is constitutively active and cannot be fully attenuated by fused adjacent heterologous regulatory domains. *Microbiology, 152*(2), 431-441. doi:doi:10.1099/mic.0.28538-0

Toutain, C. M., Caizza, N. C., Zegans, M. E., & O'Toole, G. A. (2007). Roles for flagellar stators in biofilm formation by *Pseudomonas aeruginosa*. *Research in Microbiology, 158*(5), 471-477. doi:10.1016/j.resmic.2007.04.001

Trout, L., Gatzy, J., & Ballard, S. (1998). Acetylcholine-induced liquid secretion by bronchial epithelium: role of Cl⁻ and HCO3⁻ transport. *American Journal of Physiology - Lung Cellular and Molecular Physiology, 275*(6 Pt 1), L1095-1099.

Tunney, M. M., Field, T. R., Moriarty, T. F., Patrick, S., Doering, G., Muhlebach, M. S., . . . Elborn, J. S. (2008). Detection of anaerobic bacteria in high numbers in sputum from patients with cystic fibrosis. *American Journal of Respiratory and Critical Care Medicine, 177*(9), 995-1001. doi:10.1164/rccm.200708-1151OC

Ueda, A., & Wood, T. K. (2009). Connecting quorum sensing, c-di-GMP, Pel polysaccharide, and biofilm formation in *Pseudomonas aeruginosa* through tyrosine phosphatase TpbA (PA3885). *PLoS Pathogens, 5*(6), e1000483. doi:10.1371/journal.ppat.1000483

Urbanowski, M. L., Brutinel, E. D., & Yahr, T. L. (2007). Translocation of ExsE into Chinese hamster ovary cells is required for transcriptional induction of the *Pseudomonas aeruginosa* type III secretion system. *Infection and Immunity, 75*(9), 4432-4439. doi:10.1128/IAI.00664-07

Valentini, M., & Filloux, A. (2016). Biofilms and Cyclic di-GMP (c-di-GMP) Signaling: Lessons from *Pseudomonas aeruginosa* and other bacteria. *Journal of Biological Chemistry, 291*(24), 12547-12555. doi:10.1074/jbc.R115.711507

Vallis, A. J., Yahr, T. L., Barbieri, J. T., & Frank, D. W. (1999). Regulation of ExoS production and secretion by *Pseudomonas aeruginosa* in response to tissue culture conditions. *Infection and Immunity, 67*(2), 914-920.

Vasse, M., Noble, R. J., Akhmetzhanov, A. R., Torres-Barceló, C., Gurney, J., Benateau, S., . . . Hochberg, M. E. (2017). Antibiotic stress selects against cooperation in the pathogenic bacterium *Pseudomonas aeruginosa*. *Proceedings of the National Academy of Sciences, 114*(3), 546-551. doi:10.1073/pnas.1612522114

Ventre, I., Ledgham, F., Prima, V., Lazdunski, A., Foglino, M., & Sturgis, J. N. (2003). Dimerization of the quorum sensing regulator RhlR: development of a method using EGFP fluorescence anisotropy. *Molecular Microbiology, 48*(1), 187-198.

Vergani, P., Lockless, S. W., Nairn, A. C., & Gadsby, D. C. (2005). CFTR channel opening by ATP-driven tight dimerization of its nucleotide-binding domains. *Nature, 433*(7028), 876-880. doi:10.1038/nature03313

Vincent, F., Round, A., Reynaud, A., Bordi, C., Filloux, A., & Bourne, Y. (2010). Distinct oligomeric forms of the *Pseudomonas aeruginosa* RetS sensor domain modulate accessibility to the ligand binding site. *Environmental Microbiology, 12*(6), 1775-1786. doi:10.1111/j.1462-2920.2010.02264.x

Von Mering, C., Krause, R., Snel, B., Cornell, M., Oliver, S. G., Fields, S., & Bork, P. (2002). Comparative assessment of large-scale data sets of protein–protein interactions. *Nature, 417*(6887), 399-403.

Wang, J., Haanes, K. A., & Novak, I. (2013). Purinergic regulation of CFTR and Ca(2+)-activated Cl(-) channels and K(+) channels in human pancreatic duct epithelium. *American journal of physiology. Cell physiology, 304*(7), C673-684. doi:10.1152/ajpcell.00196.2012

Warren, A., Boulianne-Larsen, C., Chandler, C., Chiotti, K., Kroll, E., Miller, S., . . . Rosenzweig, F. (2011). Genotypic and phenotypic variation in *Pseudomonas aeruginosa* reveals signatures of secondary infection and mutator activity in certain cystic fibrosis patients with chronic lung infections. *Infection and Immunity, 79*(12), 4802-4818. doi:10.1128/IAI.05282-11

Whelan, F., & Surette, M. (2015). Clinical insights into pulmonary exacerbations in cystic fibrosis from the microbiome. What are we missing? *Annals of the American Thoracic Society, 12 Suppl 2*, S207-211. doi:10.1513/AnnalsATS.201506-353AW

Whitchurch, C. B., Leech, A. J., Young, M. D., Kennedy, D., Sargent, J. L., Bertrand, J. J., . . . Mattick, J. S. (2004). Characterization of a complex chemosensory signal transduction system which controls twitching motility in *Pseudomonas aeruginosa*. *Molecular Microbiology, 52*(3), 873-893. doi:10.1111/j.1365-2958.2004.04026.x

Widdicombe, J., & Wine, J. (2015). Airway gland structure and function. *Physiological Reviews, 95*(4), 1241-1319. doi:10.1152/physrev.00039.2014

Wine, J., & Joo, N. (2004). Submucosal glands and airway defense. *Proceedings of the American Thoracic Society, 1*(1), 47-53. doi:10.1513/pats.2306015

Winsor, G. L., Griffiths, E. J., Lo, R., Dhillon, B. K., Shay, J. A., & Brinkman, F. S. (2016). Enhanced annotations and features for comparing thousands of *Pseudomonas* genomes in the *Pseudomonas* genome database. *Nucleic Acids Research, 44*(D1), D646-653. doi:10.1093/nar/gkv1227

Wise, A. A., Fang, F., Lin, Y.-H., He, F., Lynn, D. G., & Binns, A. N. (2010). The receiver domain of hybrid histidine kinase VirA: an enhancing factor for *vir* gene expression in *Agrobacterium tumefaciens*. *Journal of Bacteriology, 192*(6), 1534-1542. doi:10.1128/jb.01007-09

Woodruff, W. A., & Hancock, R. E. (1989). *Pseudomonas aeruginosa* outer membrane protein F: structural role and relationship to the *Escherichia coli* OmpA protein. *Journal of Bacteriology, 171*(6), 3304-3309.

Worlitzsch, D., Tarran, R., Ulrich, M., Schwab, U., Cekici, A., Meyer, K. C., . . . Döring, G. (2002). Effects of reduced mucus oxygen concentration in airway Pseudomonas infections of cystic fibrosis patients. *Journal of Clinical Investigation, 109*(3), 317-325. doi:10.1172/jci13870

Xie, R., Dong, X., Wong, C., Vallon, V., Tang, B., Sun, J., . . . Dong, H. (2014). Molecular mechanisms of calcium-sensing receptor-mediated calcium signaling in the modulation of epithelial ion transport and bicarbonate secretion. *Journal of Biological Chemistry, 289*(50), 34642-34653. doi:10.1074/jbc.M114.592774

Xu, Q., Porter, S. W., & West, A. H. (2003). The yeast Ypd1/Sln1 complex: insights into molecular recognition in two-component signaling systems. *Structure, 11*(12), 1569-1581.

Yahr, T. L., & Wolfgang, M. C. (2006). Transcriptional regulation of the *Pseudomonas aeruginosa* type III secretion system. *Molecular Microbiology, 62*(3), 631-640. doi:10.1111/j.1365-2958.2006.05412.x

Yang, S.-J., Bayer, A. S., Mishra, N. N., Meehl, M., Ledala, N., Yeaman, M. R., . . . Cheung, A. L. (2012). The *Staphylococcus aureus* two-component regulatory system, GraRS, senses and confers resistance to selected cationic antimicrobial peptides. *Infection and Immunity, 80*(1), 74-81. doi:10.1128/iai.05669-11

Ye, R. W., Haas, D., Ka, J. O., Krishnapillai, V., Zimmermann, A., Baird, C., & Tiedje, J. M. (1995). Anaerobic activation of the entire denitrification pathway in *Pseudomonas aeruginosa* requires Anr, an analog of Fnr. *Journal of Bacteriology, 177*(12), 3606-3609.

Yoon, S. S., Hennigan, R. F., Hilliard, G. M., Ochsner, U. A., Parvatiyar, K., Kamani, M. C., . . . Hassett, D. J. (2002). *Pseudomonas aeruginosa* anaerobic respiration in biofilms: relationships to cystic fibrosis pathogenesis. *Developmental Cell, 3*(4), 593-603.

Zhang, W., & Shi, L. (2005). Distribution and evolution of multiple-step phosphorelay in prokaryotes: lateral domain recruitment involved in the formation of hybrid-type histidine kinases. *Microbiology, 151*(7), 2159-2173.

Zhu, Y., Qin, L., Yoshida, T., & Inouye, M. (2000). Phosphatase activity of histidine kinase EnvZ without kinase catalytic domain. *Proceedings of the National Academy of Sciences of the United States of America, 97*(14), 7808-7813.